Investigating the molecular components that result in the activation of fumonisin B1-induced programmed cell death in Arabidopsis thaliana

HEATHER LOUISE GOODMAN

Investigating the molecular components that result in the activation of fumonisin B1-induced programmed cell death in *Arabidopsis thaliana*

Heather Louise Goodman

Submitted for the qualification of Doctor of Philosophy

Department of Biosciences, Durham University

March 2019

Contents

Abstract

Programmed cell death (PCD) is a gene expression-dependent cell suicide program invoked by plants for selective elimination of unwanted cells during adaptive responses to stress or during growth and organ development. The signalling processes and protein/gene networks controlling plant PCD are not fully understood. Various experimental systems have been used to study plant PCD. The Arabidopsis-fumonisin b1 (FB1) system was selected in this project for its applicability to both *in vitro* cell suspension cultures or detached leaf disc experiments and whole plant experiments. FB1 is a cell death-activating mycotoxin produced by the maize fungal pathogen *Fusarium verticillioides*. FB1-induced PCD in Arabidopsis is dependent on light and is regulated by the plant defence hormone, salicylic acid. FB1 triggers PCD in light-grown Arabidopsis cell cultures, while dark-grown cell cultures are immune. Furthermore, by removing dark-grown cells from their growth medium and incubating them in medium taken from light-grown cells compromised this immunity to FB1, even when these cells were incubated in the dark. This demonstrated that soluble factors secreted into the extracellular matrix control the light dependency of FB1-induced PCD in Arabidopsis. A screen to identify extracellular proteins secreted into the growth medium with a putative regulatory function on FB1-induced cell death was setup using Arabidopsis cell cultures grown either in the light or in the dark. Isobaric tags for relative and absolute quantification (iTRAQ) technology was used to identify proteins differentially expressed in response to light, with quantitative reverse transcription polymerase chain reaction (qRT-PCR) evaluating the effects of light on the transcriptional response of selected candidates to FB1 exposure. Amongst numerous proteins with an expression profile corresponding with what would be expected for a protein with a putative function in regulating PCD, Arabidopsis RIBONUCLEASE 1 (RNS1) was selected for further analysis. *RNS1* expression is activated by FB1 under light conditions and darkness suppresses this response. Consistent with a putative function in PCD, RNS1 overexpressing plants were more susceptible to FB1, while loss-of-function transfer-DNA insertional mutants (*rns1*) gained immunity to FB1. Furthermore, complementation with native, but catalytically inactive RNS1, mimicked the *rns1* mutant, and also gained immunity.

In addition to the relationship between FB1 and light regulation, another platform to stimulate plant cells into initiating PCD focused on the relationship between FB1 and extracellular ATP (eATP). During FB1 accumulation, a rapid depletion of eATP occurs, instigating a cascade of defence signalling. Using this antagonism to manipulate cell cultures, whole genome microarray analysis lead to the identification of a zinc-finger protein in the C2H2 transcription factor family, referred to as Extracellular ATP Responsive Protein 1 (EARP1). *EARP1* expression is activated by FB1 in cell cultures, and this response is inhibited by additional treatment of exogenous ATP. Loss-of-function transfer-DNA insertional mutant lines (*earp1*) showed a phenotype of reduced cell death in response to FB1 treatment. In order to determine the down-stream signalling components of the EARP1 transcription factor, another whole genome microarray analysis was devised to compare the genetic profile of *earp1* against the wild type, in response to FB1. The microarray identified EARP1 as a potential 'hub-gene', responsible for the regulation of over 70% of FB1-responsive genes. EARP1 will be a useful molecular tool to identify crucial regulatory genes of FB1-incduced PCD in Arabidopsis.

A final effort to hone in on key PCD-regulatory components used whole genome microarray analysis to develop a screen focusing on the antagonistic relationship between eATP and SA. SA is an important phytohormone for FB1-induced PCD, so much so that Arabidopsis lines that are unable to accumulate SA are incapable of activating PCD. The screen was successful in identifying SA-responsive genes with either a synergistic or antagonistic response upon the addition of exogenous ATP. Furthermore, the majority of selected candidates from the screen responded to FB1 treatments. In addition to identifying a number of FB1-responsive genes, a number of genes selected from the whole-genome analysis showed altered expression levels in loss-of-function transfer-DNA insertional mutants of ICS1. ICS1 is essential for the synthesis of SA via the ISOCHORISMATE SYNTHASE (ICS) pathway and this project has revealed that FB1-induced SA biosynthesis occurs via this pathway.

This PhD project has made great strides in elucidating the molecular mechanisms involved in FB1 signalling through the development of proteomic- and transcriptomic screens. Each screen has also contributed to an in-house database, which sets a foundation for future projects investigating PCD.

Acknowledgements

First, a big thank you to Stephen Chivasa for being a fantastic supervisor. Your support through the successful and hard times has finally helped me complete this project, I couldn't have got through it without you're guidance and positivity. Plus I now know the best thing for freshers' flu is hot lemon and honey!

Next, a big thanks to Colleen Turnbull, Sarah Smith and Johan Kroon, who have been so helpful in the lab over the years, Colleen's excellent organization in the lab has been incredibly helpful and I will expect high standards at my next location. Thank you Johan and Sarah for your scientific wisdom and your invaluable work prior to my project.

I am also extremely grateful to have had so much support from Helen Luke, Sarah Wilbourn and Jen Topping from the department. You're help and guidance has been greatly appreciated.

To my closest friends and confidents. Thank you Flora and Max for being there for me through thick and thin. Our lunchtime laughs made going back to the lab to tackle particularly difficult experiments so much easier. A huge thank you to Liam who has always put a big smile on my face when times were tough. To Nic B, Helen, Nic W and Jam; I couldn't have got through this PhD without some down time. As soon as that last experiment was finished and I needed to chill out, I knew I could count on all of you to meet up and help me de-stress with a cheeky beer. Also a big thank you to my oldest friends, Georgia and Alex, for all of the years you have supported me and believed in me.

Lastly, a huge thank you to my family who have supported me every day and never gave up on me. It's been a tough journey and I'm so happy I have completed it!

Funding

I am extremely thankful for the opportunity to study at Durham University, and for the funding that has been made available to support my project. The organizations that have funded my laboratory group and my project are highlighted below.

Declaration

This thesis is submitted to Durham University in support of my application for the degree of Doctor of Philosophy. It has been composed by myself and has not been submitted in any previous application for any degree.

The work presented has been produced by myself, unless stated otherwise.

- Heather Goodman

List of Figures

List of Tables

Abbreviations

1D	One-dimensional
2DE	2-Dimensional polyacrylamide gel electrophoresis
ABA	Ascisic acid
ABC	ATP Binding Cassette
ADP	Adenosine 5' diphosphate
AMP	Adenosine 5' monophosphate
AMP-PCP	Adenosine 5'-[(β,γ)-methyleno] triphosphate
APS	Ammonium persulphate
Arabidopsis	*Arabidopsis thaliana*
ATP	Adenosine 5'triphosphate
BLAST	Basic local alignment search tool
bp	Base pairs
BR	Brassinosteroid
BSA	Bovine Serum Albumin
cDNA	Complementary deoxyribonucleic acid
CHAPS	3-[(3-cholamidopropyl) dimethylammonio]-1-propanesulfonate
cm	Centimetre
Col-0	*Arabidopsis thaliana* ecotype Columbia-0
CyDye	Cyanine dye DAVID Database for Annotation and Visualization of Integrated Discovery
DiGE	Difference in-gel electrophoresis
DMF	Dimethylformamide
DMSO	Dimethylsulphoxide

dNTP	Deoxynucleoside triphosphate
DNA	Deoxyribonucleic acid
DTT	Dithiothreitol
ECM	Extracellular matrix
EDTA	Ethylenediaminetetra-acetic acid
eARP's	eATP-regulated proteins
eATP	Extracellular ATP
ET	Ethylene
ETI	Effector-triggered immunity
EtBr	Ethidium bromide
FB1	Fumonisin b1
g	Acceleration due to gravity
gDNA	Genomic DNA
GO	Gene Ontology
HCl	Hydrochloric acid
HR	Hypersensitive Response
IEF	Isoelectric focusing
IPG	Immobilised pH gradient
JA	Jasmonic acid
KB	Kilobases
KDa	Kilo daltons
KO	Knock-out
LB	Lysis buffer
M	Molar
MALDI-ToF	Matrix-assisted laser desorption ionisation time-of-flight
mg	Milligrams
ml	Millilitre
mm	Millimetre
mM	Millimolar
MOWSE	Molecular Weight Search
MQ	Milli-Q
mRNA	Messenger ribonucleic acid
MS	Mass spectrometry
MSMO	Murashig and Skoog basal salts with minimum organics
MS/MS	Tandem mass spectrometry
MTT	Methyl thiazolyl blue tetrazolium
MW	Molecular weight
n	Number of replicates
nahG	Salicylate hydroxylase gene expressing
nm	Nanometre
NO	Nitric oxide
NASC	Nottingham Arabidopsis Stock Centre
OD	Optical density
p	Significance value
PA	Phosphatidic acid
PAMP	Pathogen-associated molecular patterns
PCD	Programmed Cell Death
PCR	Polymerase chain reaction
pH	Hydrogen potential
pI	Isoelectric point

ppm	Parts per million
PR	Pathogenesis-related
PTI	PAMP-triggered immunity
RNA	Ribonucleic acid
ROS	Reactive Oxygen Species
RPM	Revolutions per minute
SA	Salicylic acid
SD	Standard deviation
SDS	Sodium dodecyl sulphate
SDS-PAGE	Sodium dodecyl sulphate polyacrylamide gel electrophoresis
SE	Standard error
qRT-PCR	Quantitative reverse-transcriptase coupled polymerase chain reaction
TAE	Tris-acetate EDTA
TAIR	The Arabidopsis Information Resource
TEMED	N,N,N',N'-tetramethylethylenediamine
TFA	Trifluor acetic acid
Tris	2-amino, 2-(hydroxymethyl) propane 1,3-diol
TSP	Total soluble protein
T-DNA	Transfer-DNA
UGP1	UDP-glucose pyrophosphorylase 1
UTR	Untranslated region of a coding mRNA
UV	Ultraviolet
v/v	Volume to volume
w/v	Weight to volume
W	Watts
µg	Micro grams
µl	Micro litre
µM	Micro molar
µS	Micro Siemens

1

Introduction

1.1. Preamble

Agricultural practices have dramatically changed in order to adapt to a demanding socio-economic climate post-World War II. Food and textiles productions have soared in response to new technologies, scientific R&D, and government policies favoring maximal production and low prices. The combinations of these socio-economic and scientific changes have been necessitated by an expanding global population. In May 2018, the world population was at 7.6 billion and current projections estimate that the 8 billion mark will be breached by 2025 (World Population Prospects, *United Nations*, 2018). Increased food production is urgently required to support an expanding global population

One way of increasing food production would be to increase the arable land area under cultivation, but this has environmental consequences affecting the diversity of flora and fauna. In fact, current global land area under cultivation is being threatened by the rising sea level, increased desertification, and the rise of salinity in some parts of the world (Zhang and Cai, 2011; Imeson, 2012). Therefore, the challenge of supplying adequate food to an increasing global population will require new technologies for yield increases on roughly the same land area under cultivation.

Present-day levels of crop yield are already being attenuated by both biotic and abiotic stresses, including drought, excessive heat, pests, and pathogens. The situation is bound to worsen given the predictions of climate change, which are characterized by extremes of weather and possible outbreaks of disease (WHO, Who.int. 2019). Currently, Crop yields are significantly reduced by pest and pathogen attack, with the total global potential loss varying from crop-to-crop, but in some years reaching devastating levels such as 50% in wheat and a staggering 80% in cotton (Oerke, 2006). Crop protection against pests and pathogens relies heavily on expensive synthetic chemicals which, when used in high quantities, pose a high risk of water and soil contamination. It is critical that new solutions are devised to

increase crop yield for food security whilst also reducing the use of environmentally harmful chemicals. A logical solution is to develop more resilient crops. Developing new crop varieties with undiminished yield under such circumstances requires a detailed understanding of the molecular events underpinning plant stress-adaptive responses.

My PhD project used a well-defined model system to understand how plants respond to stress. The experimental system utilizes a fungal pathogen-derived mycotoxin, which triggers a diverse range of responses in *Arabidopsis thaliana*. Depending on the concentration of the mycotoxin and environmental conditions, Arabidopsis responses may include activation of changes in gene expression, particularly defence genes, degradation of chlorophyll, and development of programmed cell death (PCD) (Desjardins *et al*., 1995; Gilchrist *et al*., 1995; Wang *et al*., 1996; Yoo *et al*., 1996; Gilchrist, 1997). One of the key goals was to use this system to understand the genetics of plant-pathogen interactions with the hope of translation to crops at a later stage.

While utility of this research in plant biotechnology for developing crops with increased resistance to plant diseases is obvious, the ability of the mycotoxin to activate PCD may provide useful benefits. Plant PCD is activated during plant development, pathogen defence and as an adaptive response to stressors such as drought, excessive light and other abiotic stresses, such as hypoxia (Armstrong *et al*., 1980; Rustérucci *et al.,* 2001; Gechev *et al*., 2006; Hameed *et al*., 2013; Karpinski *et al*., 2013; Chai *et al*., 2015). This has led to the hypothesis proposing the existence of a core PCD machinery shared by diverse processes, but probably differing in the early stages proximal to the primary stimulus. Thus, the second key goal of my research was to utilize the Arabidopsis-mycotoxin system to understand important components of plant PCD.

1.2. Plant-Pathogen interactions

Plants defend themselves from a variety of pathogenic microbes using a two-branched immune response system (Jones and Dangl. 2006). Initial perception of a pathogen occurs through recognition of widely conserved molecules, such as bacterial flagellin, bacterial elongation factors (Ef-Tu), the fungal cell wall polymer

known as chitin, etc. (Boller and Felix. 2009). These structural molecules are detected from pathogenic and non-pathogenic microbes. This first stage is referred to as PAMP-Triggered Immunity (PTI), with PAMP (Pathogen Associated Molecular Proteins) referring to the molecules detected by transmembrane Pattern Recognition Receptors (PRRs) of the host plant. PRRs are surface localized proteins which generally contain a ligand binding extracellular domain, which when bound initiates a cascade of defence responses such as ion fluxes, MAPK activation and ROS formation (Zipfel, 2009). The physiological responses induced by PTI activation include stomatal closure, salicylic acid (SA) accumulation and callose deposition (Brown *et al*., 1998; Gomez-Gomez *et al*., 1999). Examples of PRRs include Flagellin-Sensitive 2 (FLS2), Elongation Factor Receptor (EFR), Chitin Elicitor Receptor Kinase 1 (CERK1) and Lysm-Containing Receptor-Like Kinase 5 (LYK5) (Dunning *et al*., 2007; Zipfel *et al*., 2006; Kombrink *et al*., 2011; Cao *et al*., 2014).

PTI activates defence against a broad spectrum of microbes. However, some pathogens establish successful infection by evading the host cellular surveillance system or by secreting virulence factors, known as effectors, that actively supress PTI (Jones and Dangl, 2006). To evade the host basal defences, amino acid polymorphisms or post-translational modifications of PAMPs can result in the loss of PAMP recognition (Sun *et al*., 2006). A sophisticated mechanism to overcome PTI has been observed in bacteria. Many Gram-negative bacteria make use of the Type III Secretion System (T3SS) to subtly deliver effector proteins into the host cell. Effector molecules come in a variety of forms, including enzymes, hormones and toxins (Abramovitch *et al*., 2006). The T3SS system uses a needle-like, extracellular appendage to directly inject effectors into the host plant cells, bypassing the cell wall and plasma membrane (Diepold *et al*. 2014). Many pathogens without a T3SS, such as the mammalian pathogens *Escherichia coli* and *Yersinia,* are ultimately rendered avirulent. This demonstrates the importance of this particular type of delivery system in pathogenicity (Hueck, 1998). The T3SS system is assembled by proteins encoded by highly conserved genes throughout the bacterial kingdom (Tampakaki *et al*., 2004), indicating an early evolutionary step in the formation of the T3SS. Moreover, the T3SS genes are related to flagellar genes, indicating that the T3SS needle-like extracellular appendage most likely evolved from the flagellum (Fields 1994; Woestyn 1994; Gijsegem 1995). T3SS effectors commonly investigated come from

the model system *Pseudomonas syringae pv.* tomato (*Pst*). For example, the effectors AvrPto and AvrPtoB from *Pst* suppress the PTI response activated by the PRRs: FLS2 and CERK1. *Pst* uses the toxin coronatine (COR) as a virulence factor to suppress Jasmonic Acid (JA) signalling, associated with wounding and necrotrophic bacterial pathogens. Furthermore, the effectors, AvrRpt2 and AvrRpm1, from *Pst* target the COI-1 (CORONATINE INSENSITIVE1) pathway to enhance virulence, linking them with the COR toxin (Zhao *et al*., 2003; Brooks *et al*., 2005; Thines *et al*., 2007; Thilmony *et al*., 2006; Geng et al., 2016).

Although the T3SS is a well-studied model for effector secretion and bacterial pathogenesis, there are many pathogens that are able to overcome their host without this mechanism. Many fungal pathogens use effectors at the site of contact or produce an appressorium to invade host cells and release effectors in the process (Lo Presti *et al*., 2015). Viruses typically enter a cell through wounds, particularly through wound-damage created by pest species, such as aphids. They then move from cell to cell via plasmodesmata (Mandadi and Scholthof. 2013). Viruses can promote virulence through 'viral effectors', which are virus-encoded proteins that interfere with the host defence signalling to encourage virulence (Mandadi and Scholthof. 2013). Microbial pathogens use an immense arsenal to overcome their host plant defences, but the common strategy is avoiding or compromising host surveillance to promote infection.

If the effectors released by the pathogen are recognized by the host, the second branch of the immune system is activated, referred to as Effector-Triggered Immunity (ETI). A polymorphic nucleotide binding leucine rich repeat (NB-LRR) or an extracellular leucine rich repeat (eLRR) domain, of receptor proteins encoded by a compatible resistance (R) gene, recognises a specific effector. For example, the NB-LRR protein, RPM1 from Arabidopsis, specifically recognizes the effector AvrRpm1 from *Pst*. Recognition of the effector activates swift defence responses, characterised by accumulation of anti-microbial proteins and secondary metabolite defence products, such as phytoalexins, often accompanied by a hypersensitive response (HR) (Boyes *et al*., 1998). HR is a specific form of programmed cell death that terminates some of the infected plant cells at the site of infection, thereby preventing the spread of infection to distal tissues. If the host plant is able to

recognize the effector protein and initiate an ETI response, the pathogen is referred to as avirulent. If the host does not produce an R protein with the ability to recognize the effectors secreted by the pathogen, the host cannot activate an ETI response and will ultimately be invaded by the pathogen, this is referred to as a virulent pathogen. The interaction between pathogen and host is constantly evolving, with natural selection driving the pathogen to overcome ETI and the host to adapt their R protein specificities.

There is rarely direct contact between the R protein and its effector. Usually the R protein indirectly recognises the avirulent pathogen effector by monitoring the alterations of components within the host plant. For example the RPM1 plasma membrane bound NB-LRR protein, interacts with RIN4 (RPM1 interacting protein 4). When *Pst* injects the AvrRpm1 effector molecule into the host, the effector phosphorylates RIN4. The host R protein, RPM1, is activated by direct interaction with the modified RIN4 protein, resulting in ETI defence responses, including HR (Liu *et al*., 2011; Spoel and Dong, 2012).

Once a localized resistance to a pathogen has been achieved through HR, the host develops resistance in the distal tissues. This spread of resistance is referred to as Systemic Acquired Resistance (SAR). The effect of SAR is long-lasting and effective against a vast number of pathogens. SAR is achieved through elevated salicylic acid levels and the increased expression of a number of pathogenesis-related (PR) genes (Malamy *et al*., 1990).

The current understanding of the two-branched immune response has previously been simplified by Jones & Dangl (2006) as a four-phased 'Zig-zag' model, as demonstrated in Figure 1.1. The first phase highlights the detection of PAMPs via PRRs, triggering PTI. The second phase displays the production of effectors, with a successful pathogen producing effectors that are undetected by the host plant. Phase 3 shows an effector (highlighted in red) that is recognized by the hosts corresponding R protein (Avr-R). This in turn, initiates ETI, which increases the amplitude of defence above the threshold to trigger HR. Phase 4 represents the selective pressures on both pathogen and host to outwit one another. This may be in the form of producing either new or modified effectors, capable of suppressing ETI or remaining

undetetected by the host, or for the host to produce new NB-LRR alleles that can recognize the newly acquired effectors (Figure 1.1).

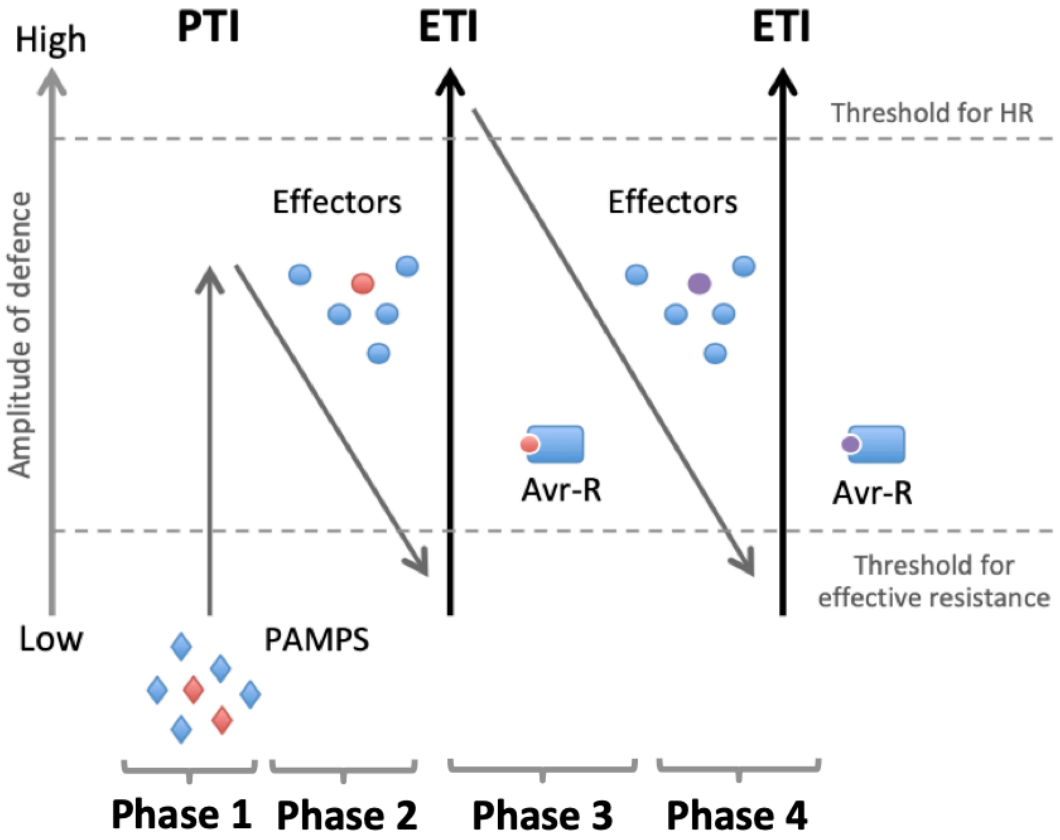

Figure 1.1 The Zig-zag model, representing the relationship between pathogen and plant host. Phase 1, Pathogen Associated Molecular Patterns (PAMPs) are identified Pattern Recognition Receptors (PRRs) by plant host, resulting in a PAMP-Triggered Immune (PTI) response. Phase 2, successful pathogens will deploy effector proteins to interfere with PTI and promote infection. Phase 3, one effector (red) is identified by the host plants resistance protein (Avr-R), this in turn initiates an Effector-Triggered Immune (ETI) response, with the amplitude of defence by-passing the threshold to initiate a Hypersentistve Response (HR). Phase 4, selective pressure on both host and pathogen requires modification of pathogenicity and defensive mechanisms. Pathogens will attain new effectors that can undergo ETI suppression, and the host will favour new Avr-R proteins that can recognize the newly acquired effectors and promote ETI. (Jones and Dangl, 2006).

1.3 Plant responses to wounding and damage

In many cases, pathogen entry into host cells is affected through wounds, such as those caused by herbivory, insect feeding, and other forms of mechanical damage. To combat pathogens utilising wounds for entry, plants have evolved a system to recognise Damage-Associated-Molecular-Patterns (DAMPs). Many DAMPs are nuclear or cytosolic components released from the host plant by damage inflicted during pathogen infection. DAMPs can also be in the form of hydrolytic enzymes released from the pathogen to gain access to the plant host (Abramovitch *et al*., 2006; Knogge, 1996; Boller and Felix, 2009). Examples of DAMPs include host structural components such as oligogalacturonides and cutin monomers (D'Ovidio *et al*., 2004; Kauss *et al*., 1999). Other DAMPs include the cleavage of precursor molecules such as PROPEP and SYSTEMIN (Huffaker *et al*., 2006; Bartels *et al*., 2013; Pearce *et al*., 1991).

Another DAMP that has recently come to light is extracellular ATP (eATP). Extracellular ATP has been shown to be a crucial intercellular signal and regulator of various cellular processes, including defensive intracellular signalling. Extracellular ATP defensive signalling results in the mobilisation of intracellular secondary messengers such as calcium, nitric oxide (NO) and reactive oxygen species (ROS) (Demidchik *et al*., 2009). Although eATP is a highly regulated signal in defence, the perforation of cells via pathogen infection, results in the damage-associated secretion of ATP into the ECM, where it can interact at the plasma membrane with receptors and alert the host of suspected damage and danger (Tanaka *et al*., 2014). Only a few DAMP-recognizing PRRs have been identified to date. PROPEP is cleaved to form the PEP DAMP molecule, which is recognized by PEP RECEPTOR1 and -2 (PEPR1 and -2). This particular DAMP PRR is structurally similar to FLS2. The SYSTEMIN DAMP receptor, SR160, from tomato (*Lycopersicon peruvianum*) is identical to the brassinosteroid hormone receptor from tomato (*Lycopersicon* esculentum), BRI1 (Montoya *et al*., 2002; Huffaker and Ryan, 2007; Yamaguchi *et al*., 2006; Krol *et al*., 2010; Scheer and Ryan, 2002). To date, only one eATP receptor has been identified, Does not Respond to Nucleotides 1 (DORN1) (Choi *et al*., 2014). Whether this receptor is the only receptor for eATP remains elusive.

1.4. Programmed cell death and the hypersensitive response

Programmed cell death (PCD) refers to the selective process of physically eliminating unwanted cells through an intracellular program (Ellis *et al*., 1991). The activation of PCD is required for a number of processes, including apoptosis and autophagy in mammalian cells, plus the previously mentioned hypersensitive response (HR) in plants. The process of apoptosis is a form of PCD occurring in multicellular organisms, which involves various cellular changes resulting in cell death including blebbing, cell shrinkage, nuclear and cytoplasm condensation, chromosomal DNA fragmentation and RNA decay (Levine *et al*., 1996; Ryerson and Heath. 1996; Mittler and Lam. 1995). The process of apoptosis can be used for developmental or defensive purposes. An example of tissue development in mammals is observed during embryo development, where fingers and toes are distinguished through the PCD of selected cells. In plants, this developmental process of PCD can be observed in the shaping of leaves to produce a unique pattern, with a drastic phenotype shown by the *Monstera* genus, characterized by the natural holes within their leaves.

In plants, there are two main classes of PCD; autolytic and non-autolytic PCD. The defining requirement of autolytic-PCD is the rapid cytoplasm clearance after tonoplast rupture. Non-autolytic can include tonoplast rupture but does not show the rapid clearance of cytoplasm (Van Doorn, 2011). Autolytic PCD often occurs through plant developmental processes and mild abiotic stress, whereas non-autolytic is associated with plant-pathogen interaction (Van Dorn, 2011). The non-autolytic form of PCD is mainly found in three scenarios. The first is the hypersensitive response (HR), the mechanism used by plants to prevent the spread of infection through rapid cell death of the local region surrounding the infection site. The second is the PCD resulting from the hijacking of the plants cell death response by necrotrophic pathogens. The third is the PCD that occurs during endosperm development in cereal seeds (Van Dorn, 2011).

My project is particularly interested in the molecular components regulating HR. HR coincides with the activation of ETI defence responses, resulting in rapid cell-death lesions at the site of infection and suppression of pathogen growth (Morel and Dangle. 1997; Heath. 2000). Once the pathogen is contained using HR, the host can

initiate SAR, in an attempt to 'immunize' the plant and prevent the use of the corrosive HR defensive strategy in the nearby future. A classic HR model system can be observed in Figure 1.2. Tobacco plants (*Nicotiana tabacum*) bearing the *N* gene from *Nicotiana glutinosa* are resistant to the tobacco mosaic virus (TMV). The resistance is shown by chimeric necrotic lesions associated with HR. Plants that lack the *N* gene do not activate a HR and are unable to contain TMV, resulting in subsequent systemic mosaic chlorosis (Lam *et al*., 2001; Dinesh-Kumar *et al*., 2000; Les Erickson *et al*., 1999).

Figure 1.2. A classic HR model system. Tobacco leaves (*Nicotiana tabacum* cv. Samsun (NN) were mock treated (left) or inoculated with TMV (right). The TMV inoculated leaf shows the necrotic lesions characteristic of HR, restricting the virus to infected regions only. (Lam *et al*., 2001).

It is difficult to determine the chronological order of the physiological events leading to a HR, as pathogen infections are non-synchronous. Chen and Heath (1991) attempted to characterize the cytological events occurring in cowpea upon infection by the biotrophic fungus *Uromyces vignae*. A three stage process was formulated: (i) The nucleus migrates to the site of fungal penetration and cytoplasmic streaming, (ii) cytoplasmic streaming diminishes, nucleus condenses, granules accumulate at the periphery of the cytoplasm and shrinkage of the protoplast commences, (iii) resulting in the collapse of the cytoplasm and ultimate death of the compromised cell (Chen

and Heath. 1991; Morel and Dangl. 1997). Video microscopy compiled by Freytag and colleagues (1994) has confirmed the timing of these events during the infection of potato by *Phytophthora infestans*. The entire process is completed in 46s, with 26s required for the collapse of the plant cell, and a further 20s for the death of the fungus. This rapid response also makes the detection of intermediate steps difficult to establish (Freytag *et al*.,1994).

1.5. Reactive oxygen species and PCD

The early events in plant response to biotic and abiotic stresses include an oxidative burst, which generates reactive oxygen species (ROS), and ion fluxes across the plasma membrane (Baker and Orlandi. 1995; Levine *et al*., 1994; May *et al*., 1996; Atkinson and Baker, 1989; Vranová *et al*., 2002). ROS are known to be toxic by-products of metabolic processes, and their regulation is tightly controlled by a network of antioxidant enzymes. The ability to control and regulate ROS allows these molecules to serve as a signal to control numerous biological responses. The generation of ROS occurs through the reduction of O_2, forming a superoxide ($O_2^{\bullet-}$) or hydroperoxide ($HO_2^{\bullet}$). These can be converted to the more stable hydrogen peroxide (H_2O_2) (Halliwell, 2006). Unlike $O_2^{\bullet-}$ or $HO_2^{\bullet}$, H_2O_2 has a longer half-life, allowing the molecule to migrate to various cellular compartments, and even signalling to neighboring cells (Henzler *et al*., 2000; Bienert *et al*., 2006). In addition to reacting with H_2O_2, $O_2^{\bullet-}$ can also react with nitric oxide radicals ($NO^{\bullet}$) to form peroxynitirite ($ONOO^-$), which is then protonated to peroxynitrous acid (ONOOH), a powerful oxidizing agent (Halliwell, 2006).

Several enzymes have been implicated in the production of ROS upon pathogen recognition. Plasma membrane NADPH oxidases and cell wall peroxidases are the two most likely sources (Grant *et al*., 2000; Bolwell *et al*., 2002). Mammalian neutrophils contain a NADPH oxidase, known as respiratory burst oxidase (RBO), which mediate microbial killing. The $gp91^{phox}$ subunit of this RBO is responsible for the generation of superoxide (Lambeth, 2004). Arabidopsis has 10 AtRBOH (Arabidopsis RBO homolog) genes that are homologous to the $gp91^{phox}$ subunit (Torres *et al*., 1998; Dangl and Jones, 2001). Each of these AtRBOH genes has Ca^{2+} binding EF-hands, which may account for the direct regulation of these oxidases by Ca^{2+} and the Ca^{2+} fluctuations preceding ROS formation (Keller *et al*., 1998). More

so, AtRBOH genes are transcriptionally up-regulated in response to pathogen or fungal elicitors (Yoshioka *et al*., 2003; Simon-Plas *et al*., 2002; Kawasaki *et al*., 1999). This is also shown across species with the silencing of NbRBOHA and NbRBOHB from *Nicotiana benthamiana* resulting in less ROS production and reduced resistance to *Phytophthora infestans* (Yoshioka *et al*., 2003). Arabidopsis antisense lines, lacking AtRBOHD and AtRBOHF showed that AtRBOHD is responsible for almost all of the ROS produced in response to avirulent bacteria or oomycete pathogens, and AtRBOHF is important in regulating HR (Torres *et al*., 2002). AtRBOHD and AtRBOHF have also been shown to be highly expressed in guard cells and vital for the regulation of stomatal-closure in response to ABA signaling (Kwak *et al*., 2003). There also appears to be functional cross-over among the AtRBOH family, with *atrbohD* and *atrbohF* loss-of-function mutants producing an accentuated response to ABA (Kwak *et al*., 2003). In contrast, though members of the AtRBOH family clearly show functional over-lapping, certain family members have been implicated in various other physiological functions, such as AtRBOHC, which appears to have a specific role in ROS signaling towards root hair development (Foreman *et al*., 2003). The AtRBOH family has been implicated in the production of apoplastic ROS, and NADPH oxidases appear to be the main enzymatic machinery responsible for the oxidative burst in response to pathogens. The precise structure and activation of these plant NADPH oxidases remains elusive (Torres and Dangl, 2005; Torres *et al*., 2006).

There are various sites and sources of ROS production. The location that generates the most ROS is the chloroplast during photosynthesis (Asada, 2006); followed by peroxisomes and glyoxysomes during photorespiration (del Rio *et al*., 2006), and mitochondrial respiration (Moller. 2001). Although the chloroplast produces the highest levels of ROS, the mitochondrial ROS are important regulators of various cellular processes, particularly that of stress adaptation and PCD (Robson and Vanlerberghe. 2002). As well as mitochondrial ROS, apoplastic ROS accumulation plays a pivotal role in the oxidative burst associated with the recognition of a pathogen, resulting in HR.

As well as pathogen-induced HR, various other stress stimuli activate oxidative stress, which is accompanied by the generation of ROS or impaired ROS

detoxification (Dat *et al*., 2000; Mittler *et al*., 2004). Examples of ROS-stimulating stresses include: extreme temperatures, drought, wounding, high-light, heavy-metal toxicity and fungal toxins (Dat *et al*., 2000; Gechev *et al*., 2004, 2006; Orozco-Cardenas *et al*., 2001; Diáz *et al*., 2001; Dietz *et al*., 1999; Shaw *et al*., 2004; Laloi *et al*., 2006). These stresses trigger cellular redox changes that serve as 'alarm' signals, which invoke corrective gene expression for stress adaptation. The transient or moderate elevations of ROS occurring as a 'warning signal' result in stress acclimation and primes the cells for greater protection against subsequent and more severe oxidative stress. This process has been observed by direct application of ROS or mild stresses, leading to transient ROS accumulation. This has been demonstrated in a number of studies, including the pretreatment of maize with H_2O_2 to establish seedling protection against chilling stress (Prasad *et al*., 1994). Further examples of H_2O_2 pretreatments have induced salt, high-light, heat and oxidative stress tolerance (Gechev *et al*., 2002, 2006; Karpinski *et al*., 1999; Lopez-Delgado *et al*., 1998). With regards to HR, ROS is an important signal molecule, activating PCD at the site of infection, limiting spread of cell death in uninfected cells surrounding the invaded zone, and triggering systemic acquired resistance (Alvarez *et al*., 1998; Torres *et al*., 2005).

1.6. Hormonal control of PCD

Plant hormone signaling is integral for the regulation of ROS-dependent cell death. There are three hormones that are particularly important for ROS regulation: salicylic acid (SA), ethylene (ET), jasmonic acid (JA) and abscisic acid (ABA). These hormones do not work independently, and in fact operate through a complex network of interactions. An arbitrary simplistic explaination of the roles of each hormone would be that (i) SA and ROS are continuously self-amplifying cell death, (ii) ET is required for the continuation of ROS production, and therefore maintaining cell death, and (iii) JA initiates the reduction in ROS and containment of the cell death to the localized area (Figure 1.3) (Overmyer *et al*., 2003). Finally, ABA has been shown to generate ROS accumulation in response to regulating stomatal closure (Garcia-Mata and Lamattina, 2001; Neill *et al*., 2002).

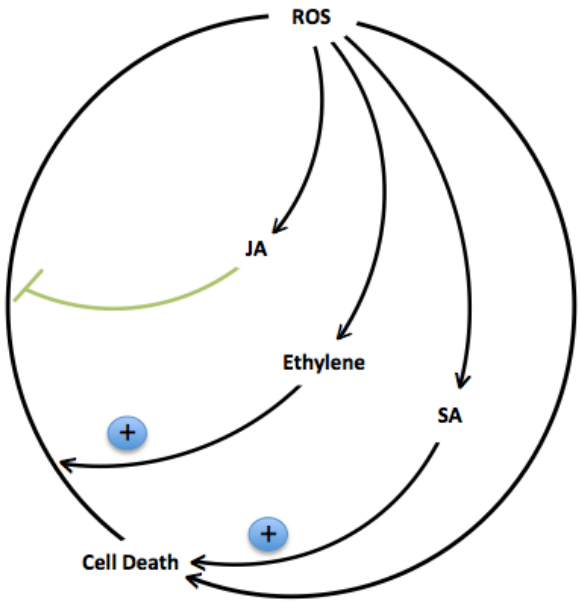

Figure 1.3. The hormonal regulation of cell death. Reactive oxygen species (ROS) and salicylic acid (SA) induce cell death. Ethylene amplifies ROS and promotes cell death and lesion spread. Jasmonic acid (JA) accumulation diminishes the promoting effect of ethylene and contains the cell death to the local area. (Overmyer *et al*., 2003).

1.6.1. Salicylic acid

SA is a hormone commonly associated with plant defence, particularly that of HR and SARs. The shikimate metabolic pathway synthesizes folates and aromatic amino acids (Herrmann and Weaver, 1999). Chorismate is produced through the shikimate pathway and utilized in plants to produce SA through two biosynthetic pathways (Figure 1.4). The most predominant is the ISOCHORISMATE SYNTHASE (ICS) pathway, which converts chorismate to isochorismate using ICS1 and ICS2. Isochorismate is then converted to SA using pyruvate lyase, however this last step still remains unclear (Serino *et al*., 1995; Wildermuth *et al*., 2001). The second pathway, referred to as the PAL pathway, converts chorismate through a number of steps to phenyalanine, and then to cinnamic acid using phenylalanine ammonia lyase enzymes (PAL1-4). Cinnamic acid is then converted to benzoic acid before forming SA (Klambt, 1962; Leon *et al*., 1995).

The ICS pathway, and particularly the ICS1 enzyme, is required for most of the SA produced in response to pathogens (Wildermuth *et al*., 2001). To date, only a handful of proteins have been shown to bind to the promoter of ICS1 and modulate SA accumulation. Three of these proteins promote expression: CBP6OG, SARD1 and WRKY28 (Van verk *et al*., 2011; Zhang *et al*., 2010). Two ethylene regulators, EIN3 and EIL1, restrict the expression of ICS1 (Chen *et al*., 2009).

With regards to the PAL pathway, BAH1 is an SA precursor downstream of PAL activity. Loss-of-function mutants of BAH1 reduce SA accumulation (Yaeno & Iba, 2008). This was also observed in ICS1 loss-of-function mutants; however, double mutants devoid of both BAH1 and ICS1 accumulated more SA than each of the independent mutants, which suggests potential cross-talk between the ICS and PAL pathways (Yaeno & Iba, 2008).

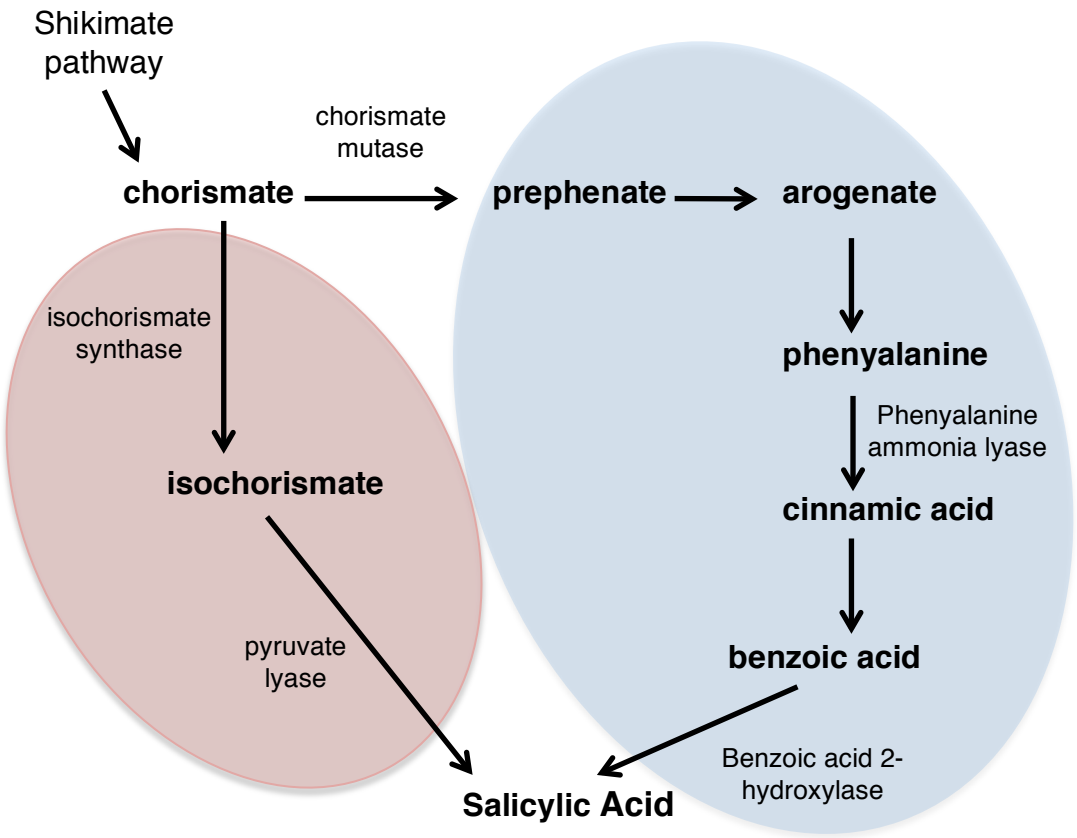

Figure 1.4. Pathway of Salicylic acid (SA) biosynthesis. The pink circle indicates the ICS pathway and the blue indicates the PAL pathway, each independently producing SA. Adaptation based on proposed pathway of SA biosynthesis by Ogawa *et al*. (2005).

Once SA has been synthesized, it interacts with NONEXPRESSOR OF PATHOGENESIS-RELATED (NPR) genes: NPR1, NPR3, and NPR4. There has been much debate as to how SA interacts with NPR genes to activate defence gene transcription. In 2012, two conflicting models were proposed (Fu *et al*., 2012; Wu *et al*., 2012). Fu and colleagues suggested that SA did not bind to NPR1, but bound to NPR3 and NPR4. This model suggests that under normal growth conditions NPR4 constantly removes most of the NPR1, by CULLIN3 mediated ubiquitination; preventing superfluous defence expression. Basal levels of SA are required to disrupt some of the NPR1-NPR4 interactions but not all, in order to maintain basal levels of NPR1. This was supported with genetic evidence through SA-deficient plants: eds5, ics1 and the NAhG transgenic line expressing an SA-degrading enzyme (Nawrath *et al*., 2002; Wildermuth *et al*., 2001; Gaffney *et al*., 1993). These lines are unable to maintain NPR1 homeostasis, resulting in enhanced disease resistance. Upon recognition of a pathogen, SA levels increase greatly at the site of infection, with a concentration gradient forming further from the infection site. SA binds with greater affinity to NPR4 than NPR3. NPR4-SA can no longer bind to NPR1, blocking the ubiquitination of NPR1. The stabilized NPR1 interacts with class II TGAs (TGA2, TGA5 and TGA6), and activates defence gene transcription (Zhang *et al*., 1999; Zander *et al*., 2014). With even higher concentrations of SA forming at the site of infection, NPR4 is completely saturated, allowing NPR3 to bind to SA. Unlike NPR4, the binding of SA to NPR3 allows the interaction of NPR3 and NPR1, mediating ubiquitination and degradation of NPR1 and ultimately activating cell death. SA levels diminish at a sufficient distance from the infection site, and no longer saturate NPR4. With sufficient numbers of NPR4 to bind to SA, NPR3-SA interactions rarely occur, stabilizing NPR1. This signals the reversal of cell death and general defence gene expression continues, protecting the tissue around the infected area but limiting the range of cell death (Fu *et al*., 2012).

In contrast to the findings of Fu *et al*. (2012), the second model proposed NPR1 to directly bind to SA with high affinity (Wu *et al*., 2012). Wu and colleagues proposed that SA binds to the C-terminal domain of NPR1, which releases it from autoinhibition by the N-terminal BTB-POZ domain, allowing the c-terminal end to interact with TGA proteins, and ultimately activate defence. This model does not propose that regulation of NPR1 is mediated by protein degradation, and that NPR3

and NPR4 are not ultimately required for full activation of defence gene expression (Wu *et al*., 2012).

The most recent work to directly address this conflict proposes that the degradation model of NPR1 by Fu and colleagues is likely to be incorrect, and the NPR1 activation model by Wu and colleagues is likely to be an incomplete proposal (Ding *et al*., 2018). Further genetic analysis of the NPR proteins discovered a conserved amino acid from the C-termini of all three NPR proteins. Mutating this conserved region of the C-terminal domain in NPR3 and NPR4 suppressed defence signaling, indicating a more crucial role for NPR3 and NPR4 than conceived by Wu *et al*. (Ding *et al*., 2018). The mutation was shown to almost eliminate SA binding with NPR4, indicating that NPR4 functions as a co-repressor of defence signaling in the absence of SA. Ding and colleagues proposed that SA binds with NPR4 and NPR3 directly to their c-terminal domains, releasing their suppression of defence gene promoters (Ding *et al*., 2018). With regards to NPR1, the new model suggests that under low SA, NPR3 and NPR4 suppress defence gene transcription, whilst NPR1 binds with the limited SA and maintains basal levels of transcription. Under high SA concentrations, more NPR1-SA interactions occur, increasing defence gene expression. Furthermore, SA binds to NPR3 and NPR4, releasing their suppression on defence gene promoters, increasing defence gene transcription even further (Ding *et al*., 2018). To summarize, the conformational change occurring upon SA binding with NPR1 actively promotes transcription, whereas the binding of SA to NPR3 or NPR4 relieves the repressive pressure of the NPR-induced genes (Figure 1.5) (Ding *et al*., 2018; Innes, 2018).

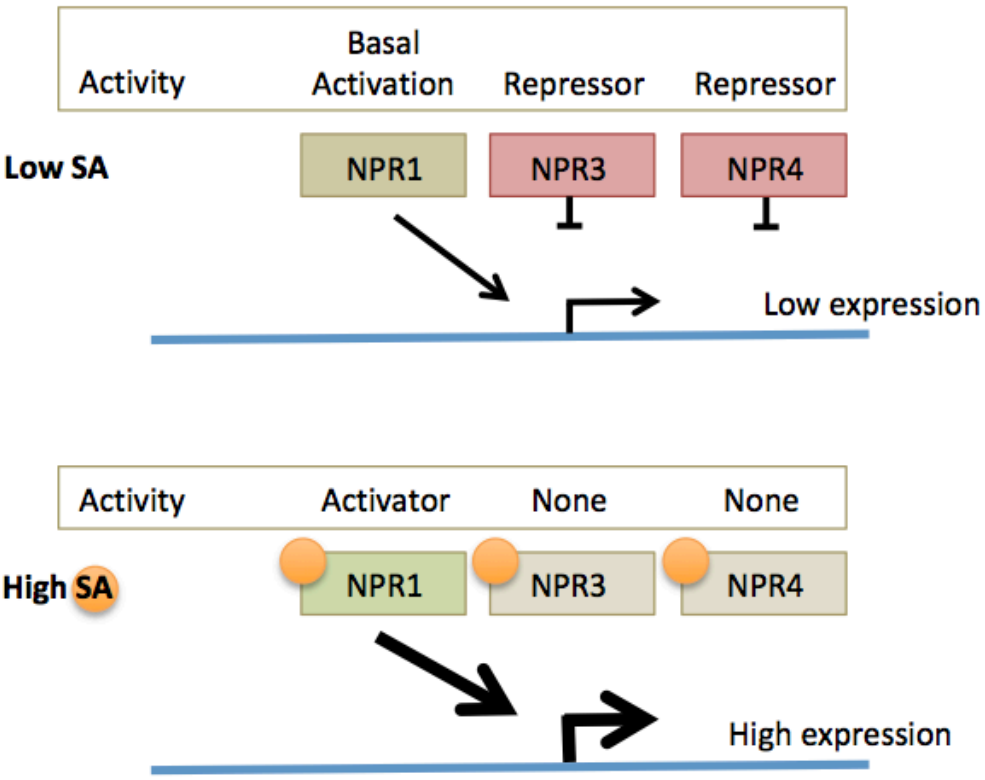

Figure 1.5. Regulation of gene expression through salicylic acid (SA) and NPR genes. Basal levels of SA interact with NPR1 to activate minimal gene expression, and maintain normal homeostatic levels of SA-induced gene expression. In the absence of SA, NPR3 and NPR4 function as transcriptional co-repressors of SA-induced gene expression. In the presence of high levels of SA, the binding of NPR1 to SA escalates, increasing gene expression. Greater concentrations of SA increase NPR3 and NPR4 binding to SA, releasing defence gene promoters from repression, allowing for further activation of SA-induced genes through NPR1 (Ding *et al*., 2018; Innes, 2018).

The biosynthesis of SA and the downstream signaling from SA accumulation includes a myriad of genes. The ability to detect and measure the abundance of these proteins or gene transcripts enables us to use these genes as genetic markers to quantify the SA accumulation under specific treatments. The most common genes regulated by SA are the PATHOGENESIS-RELATED (PR) genes, particularly PR1, PR2 and PR5. Mutants devoid of NPR1 fail to express PR1, PR2 and PR5, and show enhanced susceptibility to pathogen infection, even after SA treatments (Scott *et al*., 1994; Glazebrook *et al*., 1996; Shah *et al*., 1997; Zhang *et al*., 1999; Nawrath and Métraux, 1999).

Another genetic approach for investigating SA-induced gene expression is to detect the abundance of proteins upstream of the SA biosynthesis pathway and use mutants deprived of these proteins. Well-established mutants for this approach include the previously mentioned ICS1, which is crucial in the Isochorismate pathway of SA biosynthesis. Another protein that is crucial for SA signaling is PHYTOALEXIN DEFICIENT 4 (PAD4), which is responsible for synthesizing camalexin, an antimicrobial compound (Glazebrook *et al*., 1996). PAD4 also interacts directly with EDS1 (ENHANCED DISEASE SUSCEPTIBILITY 1). Twelve EDS proteins were identified by screening for enhanced susceptibility to the virulent strain of *Pseudomonas syringae* pv. *maculicola*. A number of *eds* mutations include alleles of *npr1* and *pad4* mutants (Glazebrook *et al*., 1994, 1996).

SA is a crucial hormone in plant defence, and specifically HR. As discussed, there are well-established SA-dependent pathways, however there are particular areas of SA-biosynthesis and SA-signaling that remain elusive. My project utilized chemical and genetic approaches to identify putative PCD-regulatory proteins responding to SA. An important point to note is that there are many plant hormones that are important in plant defence and HR. The four most important hormones in in plant defence are SA and JA, ET and ABA. The network of hormonal cross-talk and proteins involved in this process is complex and focusing on one hormone may shed some light on particular proteins responding to SA, but to develop a clear pathway which results in HR, may require further investigation in various other hormonal systems. Below I have briefly summarized the role of three other important hormones in plant immunity.

1.6.2. Further phytohormones influencing PCD

Unlike SA, which plays a crucial role in HR development, resistance to necrotrophic pathogens is largely dependent on the overlapping of JA, ET and ABA signaling pathways. JA-knockout mutants have shown to have increased susceptibility to a number of *Botrytis* species (Glazebrook, 2005; Van Baarlen *et al*., 2007), and *A. brassicicola* infected plants show an accumulation of JA and JA-induced genes (Van Wees *et al*., 2003). Similar experimentation has also implicated ET as regulator of defences against the nectrophic pathogens *F. oxysporum* (Berrocal-Lobo & Molina, 2004) and *S. sclerotiorum* (Guo & Stotz, 2007), with ET-insensitive mutants showing enhanced susceptibility to the pathogens. ABA is an important hormone in regulating defence responses towards oomycete infection and some necrotrophic fungi. The infection of Arabidopsis with *P.irregulare* initiates a rapid increase in ABA levels. Mutants impaired in ABA signaling show enhanced susceptibility to *A. brassicicola* and *L.maculans* (Kaliff *et al*., 2007; Flors *et al*., 2008). Although my project focuses on the role of SA and PCD, the complexity between the hormonal signaling pathways requires a fundamental understanding of the core signaling components for each hormonal system, which I have briefly summarized below.

Jasmonic Acid

Jasmonates (JA and other oxylipin derivatives) are synthesized in response to a large array of external stimuli, particularly wounding-response, and play a crucial role in plant development. JA itself is involved in plant defence against pathogens, insects and herbivory. The SA pathway is predominantly induced in response to biotrophic pathogens, whereas the JA pathway, in combination with ET, is generally induced by necrotrophic pathogens, and JA in combination with ABA responds to herbivorous insects (Penninckx *et al*., 1998; Glazebrook, 2005; Howe and Jander, 2008; Vos *et al*., 2013). JA and SA work antagonistically to regulate expression of PR-genes (Niki *et al*., 1998). JA initiates a cascade of signaling ultimately resulting in growth inhibition, increased trichome density, senescence, tendril coiling, flower development and leaf abscission (Yamane *et al*., 1980; Dathe *et al*., 1981; Ueda and

Kato, 1982; Traw and Bergelson, 2003; Yoshida *et al*., 2009; He *et al*., 2002; Falkenstein *et al*., 1991; Curtis, 1984).

The F-box protein COI1 is a key regulator of JA signaling (Xie *et al*., 1998). COI1 is a subunit of the Skp, Cullin, F-box containing complex (SCF^{COI1}), and upon JA binding to COI1, SCF^{COI1} targets JASMONATE ZIM (JAZ) transcriptional repressor proteins for degradation (Chini *et al*., 2007). The degradation of JAZ proteins alleviates the repression on the downstream transcription activators, ETHYLENE RESPONSE FACTOR 1 (ERF1) and OCTADECANOID-RESPONSIVE ARABIDOPSIS AP2/ERF59 (ORA59) (Lorenzo *et al*.,2003; Pré *et al*., 2008). JA signaling is regulated by an antagonistic relationship between ERF1 and MYC2, downstream from SCF^{COI1} (Van der Does *et al*., 2013). ERF1 activates the same genes that MYC2 suppresses, with ERF2 favoring a response to pathogens, and MYC2 favoring a response to wounding (Lorenzo *et al*., 2003)

SA and JA have been shown to work antagonistically of each other in an effort to direct plant defence signaling to overcome biotrophic or necrotrophic pathogens (Glazebrook *et al*., 2003; De Vos *et al*., 2005; Sato *et al*., 2010). SA prevents the accumulation of ORA59, inhibiting the JA signaling pathway downstream of the SCF^{COI1} complex. The mechanism by which SA targets ORA59 remains unclear (Van der Does *et al*., 2013). With regards to ERF1, SA mediates antagonism through a different mechanism. ERF1 and ORA59 activate transcription of the JA-responsive gene, PLANT DEFENSIN 1.2 (PDF1.2) (Zarei *et al*., 2011). SA induces GRX480, a member of a glutaredoxin family, through the NPR1 pathway. GRX480 disrupts JA signaling through the suppression of PDF1.2 (Figure 1.6) (Brown *et al*., 2003; Ndamukong *et al*., 2007).

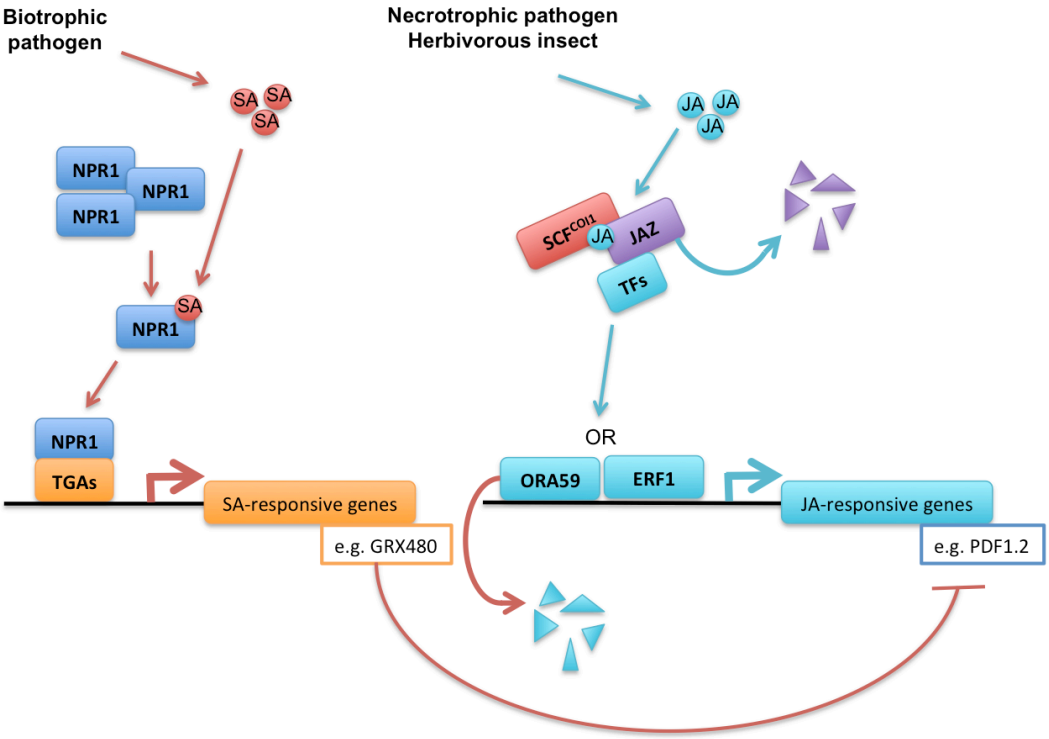

Figure 1.6. Model for SA/JA signaling interaction. Biotrophic pathogen infection results in accumulation of SA. SA binds NPR1, which interacts with TGA transcription factors and ultimately activates SA-responsive genes. Necrotrophic pathogen infection or wounding through insect herbivory results in the accumulation of JA. Binding of JA to the SCF^{COI1} complex leads to the degradation of JAZ proteins, releasing the repressive pressure on transcription factors such as ORA59 or ERF1, and activates JA-responsive gene transcription. SA regulation of the JA pathway occurs in two forms. SA targets ORA59 for degradation, but the mechanism remains elusive. SA induces expression of GRX480 which inhibits the JA-responsive gene PDF1.2. Figure built upon Van der Does *et al*. (2013) model.

Ethylene

ET is a gaseous hormone known for its role in senescence and ripening, but also plays a pivotal role in response to biotic and abiotic stresses. Five receptors located at the endoplasmic reticulum perceive ET, ETHYLENE RESPONSE 1 (ETR1), ETHYLENE RESPONSE SENSOR 1 (ERS1), ERS2, and ETHYLENE INSENSITIVE 4 (EIN4) (Hua and Meyerowitz, 1998). Without ET stimulation, these receptors activate CONSTITUTIVE TRIPLE RESPONSE 1 (CTR1), which phosphorylates and inactivates ETHYLENE INSENSITIVE 2 (EIN2) (Kieber *et al*., 1993; Clark *et al*., 1998; Alonso *et al*., 1999). ET binding inactivates the receptors, preventing phosphorylation of EIN2, resulting in the translocation of EIN2 to the nucleus where it stabilizes EIN3. EIN3 accumulates and activates various ethylene transcription factors, including, ETHYLENE RESPONSE FACTOR 1 (ERF1) which has been shown to also interact with JA signaling (An *et al*., 2010; Ju *et al*., 2012; Qiao *et al*., 2012; Solano *et al*., 1998; Lorenzo *et al*.,2003).

Abscisic Acid

ABA signaling is known for its role in various regulatory roles requiring the accumulation of ROS. ABA interacts with members of the PYR/PYL/RCAR family of receptors; when bound to these receptors, ABA creates a surface for protein phosphatases (PP2Cs) to bind (Ma *et al*., 2009; Park *et al*., 2009). The binding of PP2Cs prevents the autophosphorylation of the SnRK2 family of kinases (SNF1-RELATED PROTEIN KINASE). This prevents the activation ABA-RESPONSIVE ELEMENT BINDING FACTOR (ABF) bZIP transcription factors (Furihata *et al*., 2006; Yoshida *et al*., 2006a, 2006b). ABFs induce a number of defence-related genes, including OPEN STOMATA 1 (OTS1), FLS2, WRKY30, FLG22-INDUCED RECEPTOR –LIKE KINASE (FRK1) and NONHOST RESISTANCE TO P.S.PHASEOLICOLA 1 (NHO1) (Schroeder *et al*. 2001; Yoshida *et al*. 2002; de Torres-Zabala *et al*. 2009).

1.7. The role of light in PCD

Plants are required to continuously adapt to light abundance, quality, direction and duration, in order to gain the most favourable conditions. In response to biotic and abiotic stressors, plants rely heavily on the resources the plant is able to obtain. If there is a lack of water or nutrients in the soil, the plant needs to expend more energy promoting its root architecture in order to find those much-needed resources. In contrast, if shade-intolerant plants are not achieving enough sunlight interception due to competition from surrounding plants, energy will need to be transferred to the shoots and leaves. Whilst in this constant battle for maximal resources, plants need to fend off harmful insects and pathogens. In order to survive, plants must compromise defence in order to gain maximal resources when a threat is not imminent, but they also require the ability to shift this compromise towards defence as soon as a threat is detected.

With regards to plant immunity, recent genetic studies have contributed to the perception that light-dependency of plant defence is mediated by photoreceptor signalling (Roden and Ingle, 2009). Certain plant defence responses occur independently of light, such as camalexin and JA production (Zeier *et al*., 2004). Light regulation appears to play an essential role in SA-mediated defence signalling. The accumulation of SA following infection by various avirulent *Pseudomonas* strains has been shown to be light-dependent (Genoud *et al*., 2002; Zeier *et al*., 2004; Greibel and Zeier, 2008). However, infecting Arabidopsis ecotype Dijon-17 with turnip crinkle virus resulted in SA accumulation in the dark (Chandra-Shekara *et al*., 2006). This suggests that the light-dependency of SA accumulation may be pathogen specific (Roden and Ingle, 2009). Downstream SA-mediated defence responses are fundamentally regulated by light, particularly that of the HR. Infecting dark grown plants with avirulent or viral pathogens, results in reduced HR lesions or no HR response altogether (Mateo *et al*., 2004; Zeier *et al*., 2004; Chandra-Shekara *et al*., 2006; Griebel and Zeier, 2008). SA-mediated SAR response also appears to be light-dependent. Inoculating dark-grown plants with the avirulent *AvrRpm1* strain of *Pst* shows SAR to be completely abolished, whereas light grown plants show increased resistance to subsequent infections of virulent *Pst* (Zeier *et al*., 2004). This is not

surprising as the SA-induced systemic response occurs after HR as previously discussed; therefore if the HR response is light-dependent, the defective SAR response is to be likely the consequence of a substandard primary response to the pathogen.

Light regulation of gene expression is achieved through photoreceptors. Arabidopsis uses 13 known photoreceptors for light perception: phytochromes, cryptochromes, phototropins, ZEITLUPE (ZTL), and UVR8 (Butler *et al*., 1959; Quail, 1991, 1994; Furuya, 1993; Ahmad & Cashmore, 1993; Huala *et al*., 1997; Jarillo *et al*., 1998; Briggs and Christie, 2002; Christie *et al*., 1998, 1999; Kim *et al*., 2007; Brown *et al*., 2005; Rizzini *et al*., 2011). The mechanism behind light-dependent defence signalling has been the focus of many research groups, with phytochromes being at the centre of most studies. Phytochromes are possibly the most well characterised photoreceptors to date. There are 5 phytochromes in Arabidopsis (PHYA-E), which are responsible for monitoring the red to far-red region of the light spectrum (750-850nm) (Clack *et al*., 1994; Mathews and Sharrock, 1997). Exposure to red light converts the phytochrome to its active form (Pfr); and darkness or far-red light transforms the phytochrome back to its inactive form (Pr) (Figure 1.7.A). Pfr formation exposes a nuclear localization signal and induces translocation of the Phy protein from the cytosol to the nucleus, resulting in a cascade of signalling responses for light-regulated processes such as seed de-etiolation, shade avoidance, circadian regulation, stem and hypocotyl elongation (Smith, 1995; Smith *et al*., 1997; Quail *et al*., 1995; Mazzella *et al*., 1997; Botto *et al*., 1996).

Phytochrome signalling is initiated through direct interaction with Phytochrome Interacting Factors (PIFs). The first PIF protein identified was PIF3, isolated from a yeast two-hybrid screen, and shown to directly bind with the C-terminal domain of both PhyA and PhyB in Arabidopsis and rice. The PIF3 protein has a higher affinity to bind with the Pfr formation of the Phy proteins and shows preference to bind with PhyB (Zhu *et al*., 2000; Shimizu-Sato *et al*., 2002; Ni *et al*., 1999). Subsequently, further PIF proteins were identified through reverse-genetic approaches or sequence homology similarities (Huq and Quail, 2002; Huq *et al*., 2004; Khanna *et al*., 2004). All the PIFs identified are from the basic helix–loop–helix (bHLH) subfamily 15 of Arabidopsis, however not all these proteins interact with phytochromes, and are

therefore not PIFs. PIF proteins have been shown to interact with multiple Phy proteins to varying extents. PIF1, PIF3 and PIF6 have a strong affinity to PhyB, in comparison to PIF4 and PIF5 (Toledo-Ortiz *et al*., 2003; Duek and Fankhauser, 2005). In the presence of light, PIF3 and other related PIFs are rapidly degraded, and further investigation has shown that these PIF proteins act as negative regulators of phytochrome signalling. The light-dependent mechanism by which PIF proteins are degraded remains unknown, however it has been shown that PIF3 is phosphorylated and this process is dependent on the direct interaction with the active formation of PhyA and PhyB (Pfr) (Al-Sady *et al*., 2006). A possible model of pytochrome signalling is shown in Figure 1.7.B (Castillon *et al*., 2007). The model suggests that under dark conditions, PIFs are localized to the nucleus and are responsible for the negative regulation of photomorphogenesis through gene expression, particularly gibberellin responsive genes, which inhibit seed germination in the dark (Oh *et al*., 2007). Light induces photoconvertion of phytochromes to their active formation (Pfr) and are translocated to the nucleus from the cytosol. In the nucleus, the phytochromes directly interact with the PIFs. This induces the phosphorylation of the PIFs, and ubiquitin ligase targets the PIFs for degradation by the 26S proteasome. The removal of PIFs relieves the negative regulation of photomorphogenesis (Castillon *et al*., 2007).

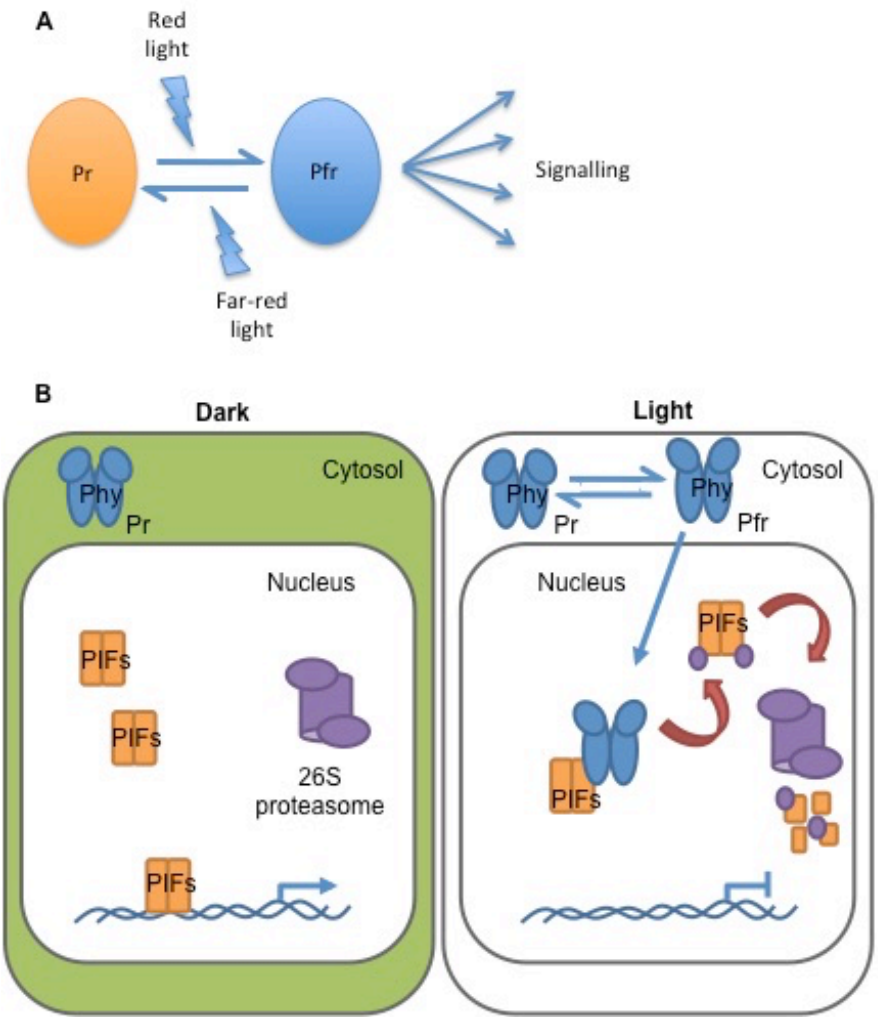

Figure 1.7. Phytochrome activation through red to far-red region of the light spectrum. A) Pr is the inactive form, initiated by far-red light. Pfr is the active form initiated by red light, which triggers light-dependent signalling. **B.** In its active form, phytochromes (Pfr) are translocated to the nucleus where they directly interact with PIFs. The PIFs are phosphorylated and targeted for degradation by the 26S proteasome. The removal of PIFs relieves the negative regulation of photomorphogenesis (Castillon *et al*., 2007).

PhyB is possibly the most characterised receptor of red/far-red end of the light spectrum (Whitelam & Smith. 1991; Robson *et al*., 1993) and use of PhyB deficient mutants has revealed a wide range of physiological disturbances, particularly within the SA signalling pathway. The absence of PhyB results in a reduction in pathogenesis-related (PR) gene expression upon SA treatment. This response is also seen in *phyA* mutants, however the response is stronger in *phyB* mutants (Wada *et al*., 2005). Both PhyA and Phyb have also been implicated in cell death regulation, wherein the protein PSI2 (PHYTOCHROME SIGNALING 2) negatively regulates both phytochromes A and B resulting in cell death (Genoud *et al*., 1998).

Phytochromes A and B have been linked with plant defence against bacterial pathogens, as *phyA phyB* double knock out mutants were shown to exhibit reduced HR and increased vulnerability to an avirulent *Pst* strain (AvrRpt2) (Genoud *et al*., 2002). However, this phenotype was not displayed when inoculated with *Pst AvrRpm1* or turnip crinkle virus; but SAR establishment was still compromised (Griebel and Zeier, 2008; Chandra-Shekara *et al*., 2006). Other plant photoreceptors, cyrptochromes and phototrophins do not appear to regulate light-dependent plant immunity (Gabriel and Zeier, 2008). Alongside phytochromes, there appears to be an alternative light-dependent regulatory role for plant defence in the chloroplast, relating to redox status, which was discussed earlier on in this chapter under ROS.

The downstream molecular components and pathway of PhyA and PhyB-mediated plant defence remain elusive, however Rusaczonek and colleagues have shown insight into common genes involved in UV-induced cell death (Rusaczonek *et al*., 2015). Exposure to UV is particularly harmful to photosystem II and the CO_2 assimilation process of photosynthesis (Ohinishi *et al*., 2005). UV is separated into three wavebands: UV-A (315-400nm), UV-B (280-315nm), and UV-C (200-280nm). It has been reported that UV-C induces PCD, and that mitochondria and ROS are important in this process (Gao *et al*., 2008). Rusaczonek's group showed that UV-C radiation enhanced cell death in the *phyB* mutant and *phyA phyB* double mutant. Along with ROS and SA accumulation experiments with the *phyB* mutants, it was demonstrated PhyB plays an important role in UV-C induced PCD, but this mechanism is independent, or with minor involvement, of H_2O_2 and SA signalling (Rusaczonek *et al*., 2015). Another development from this study was the role of

phytochromes in extinguishing excessive energy induced by UV on PSII. The study showed PhyB functions as a positive regulator of photochemical reactions in photosystem II (PSII). The study concluded by suggesting that PhyB and PhyA are important components of extinguishing excess energy and preventing subsequent PCD in response to a damaged photosynthetic electron transport chain (Rusaczonek *et al*., 2015)

Rusaczonek and colleagues also perfomred meta-analysis of gene expression data from *phyB, phyA* and WT plants. Transcriptomic data produced a list of 91 genes that responded to UV-C and showed altered regulation between *phy* mutants and the wildtype (Rusaczonek *et al*., 2015). Among the 91 genes, a few stand out. Two proteins involved in PSII protein complex are up-regulated by UV exposure in the WT, and then massively up-regulated even further by the two *phy* mutants (At3g08940 and At5g66570). This supports the concept that phyA and phyB are important components of UV detection or regulation by the PSII complex. Other interesting genes include two purple acid phosphatases that appear to be significantly down-regulated in the WT, and even further in the *phy* mutants. Two serine-type endopeptidases show massive down-regulation in the *phy* lines, which is much more subtle in the WT. There are many more interesting proteins among the 91 genes, and this will be an exceptional resource for research into light signalling.

1.8. Fumonisin B1 and PCD

Fumonisins are naturally occurring phytotoxic compounds produced by *Fusarium* fungi. The most prevalent fumonisins found in food are fumonisin B1 (FB1), FB2 and FB3. In animals, fumonisins can have harmful health effects and, although health affects in humans remain inconclusive, there is evidence to suggest high exposure may result in health issues such as cancers or birth defects (Gelderblom *et al*., 1988; Marasas *et al*., 2004). The crop with the highest accumulation of fumonisins is maize (Figure 1.8), followed to a lesser degree by wheat and other cereals. FB1 is particularly prevalent in maize, with warmer climates showing the highest exposures. Guatemala, Zimbabwe and China reported the highest exposures of FB1 to humans, with a maximum of 7700ng/kg body weight (bw) per day; a massive increase compared with the average exposure of FB1 and total fumonisns in

European countries, which was below 250ng/kg bw per day (World Health Organisation, 2018).

There are wide ranges of detrimental health affects in animals associated with fumonisins. FB1 shows particularly harmful effects on the liver and kidneys (Voss *et al*., 2001; Carlson *et al*., 2001; Bhandari *et al*., 2002). The fumonisin toxin can cause cancer following the disruption of fat metabolism, resulting in depletion of complex sphingolipids and accumulation of fats in the form of sphingoid bases and sphingoid base metabolites (Wang *et al*., 1991). Fumonisin immunotoxicity has been observed in pigs and mice at low oral doses, resulting in dampened immune response; however the significance of these data remains inconclusive (Colvin and Harrison, 1992; Becker *et al*., 1995; Abbès *et al*., 2016). Fumonisins are also possibly capable of mutagenicity, but again this remains inconclusive. With regards to birth defects, neural tube defects have been observed in mice (Gelineau-van Waes *et al*., 2005). Fumonisins have also been linked to leukoencephalomalacia (softening of brain tissue) in horses (Marasas *et al*., 1988). It is unlikely that the toxin acts directly as a neurotoxin in the brain, but it potentially disrupts vascular function. This has been supported with induction of pulmonary edema's in pigs (Colvin and Harrison, 1992; Casteel *et al*., 1994). The mechanism behind altering vascular function is likely the result of accumulating sphingoid bases and metabolites in the blood (World Health Organisation, 2018).

The effects of fumonisins in humans are less evident than in animals, however these results do contribute to the concern of cancers induced by fumonisins. No significant correlation has been associated in humans with regenerative cell proliferation in the liver and kidneys, leading to cancer in animals. A study has indicated that FB1 contamination of rice is linked with a higher risk of oesophageal cancer (Yoshizawa *et al*., 1994; Sun *et al*., 2007). Another study in Guatemala showed consumption of maize-based foods contaminated with fumonisin correlated with disrupted fat metabolism in women, and in animals this disruption resulted in carcinogenicity (Torres *et al*., 2014; Riley *et al*., 2015). Fumonisn consumption has also been linked with stunted growth in children and increased risk of neural tube defects in pregnant women (World Health Organisation, 2018). The evidence for fumonisin toxicity in

humans is correlative and scarce, with most studies unable to conclusively state that fumonisins are detrimental to human health. However, the potential health concerns are life-threatening and a major concern for communities with limited diversity of crop species and are dependent on few crops as a main source of nutrition. Methods for detecting, preventing and controlling fumonisins are needed and are currently a main focus for many research groups, national authorities and funding bodies.

Figure 1.8. Fumonisin contaminated maize (bottom). Control (top). (World Health Organisation, 2018).

1.8.1 Arabidopsis-Fumonisin B1 interaction, a model system to investigate PCD

Although fumonisins are a major concern for food security, fumonisin toxin interactions with plants are useful as a model system for studying pathogen-induced PCD. This area of research is beneficial, as it will also shed light on how fumonisin-producing fungal pathogens infect plants. Furthermore, such experimental systems may potentially shed light on how other forms of PCD processes occur, including biotic- and abiotic-induced cell death. FB1 from *Fusarium moniliforme* is predominantly used in plant PCD research. FB1 provokes an apoptotic-like form of PCD in plant and animal cell cultures (Tolleston *et al*., 1996; Wang *et al*., 1996; Yoo *et al*., 1996; Gilchrist, 1997). FB1 disrupts spingolipid biosynthesis likely through competitive inhibition of ceramide synthase (Wang *et al*., 1990; Abbas *et al*., 1994; Gilchrist *et al*., 1997; Yoo *et al*., 1996). Sphingolipids have a diverse array of physiological roles in many cellular processes, ranging from acting as an anchor for membrane proteins and as secondary messengers for the regulation of developmental

and defensive responses, including apoptosis (Futerman, 1995; Spiegel and Merrill, 1996).

Research investigating the molecular mechanism of FB1-induced PCD in plants was influenced greatly by Frederick Ausubel's laboratory group (Asai *et al*., 2000; Stone *et al*., 2000). Two papers were published from the group in 2000, and reported on the hormonal signaling required for FB1-induced PCD, and that this process was dependent on light.

1.8.2. FB1-induced lesion formation

Ausubel's group used Arabidopsis and tomato protoplasts and intact plants to determine the PCD profile of the FB1 toxin (Asai *et al*., 2000; Stone *et al*., 2000). Arabidopsis protoplasts treated with FB1 showed a dose-dependent reduction in cell viability. The cell death induced by FB1 was successfully suppressed by cordycepin and cycloheximide, inhibitors of transcription and translation, and by staurosporine, a protein kinase inhibitor (Stone *et al*., 2000). This result confirmed that the cell death occurring was not a necrotic process, but an activation of a controlled program that requires the plant's ability to produce proteins and activate metabolic processes (Asai *et al*., 2000). Intact Four-week old Arabidopsis plants treated with FB1 triggered a rapid cell death. After a week the infiltrated leaves were completely dead and small lesions had formed on distal tissue, indicating the FB1 had systemically spread (Asai *et al*., 2000; Stone *et al*., 2000). Previous studies have shown the light-dependence of cell death in response to various pathogens (Peever and Higgins, 1989), this was also reported for FB1. FB1-induced cell death in Arabidopsis was alleviated in the dark (Asai *et al*., 2000, Stone *et al*., 2000). FB1-induced cell death showed phenotypic and physiological features similar to that of avirulent bacterial-induced HR. Reactive oxygen intermediates (ROIs), callose and camalexin accumulation increased in FB1-induced cell death, similar to HR-inducing *Pseudomonas maculicola* AvrRpt2 strain (Asai *et al*., 2000). Further evidence to support the similarity of FB1-induced PCD to HR was shown by the fragmentation of nuclear DNA and disintegration of the nucleus (Stone *et al*., 2000). An interesting observation showed that in tomato, fully expanded leaves, in contrast to young rapidly expanding leaves, produced fewer lesions in response to AAL toxins, which are structurally related to fumonisins. This was also observed in protoplasts derived

from older Arabidopsis leaves (Asai *et al*., 2000), which suggests that older leaf tissue is less sensitive to FB1, or structurally similar toxins.

1.8.3. Defence-related genes and hormone signalling

Alongside phenotypic response of FB1, defence gene responses were evaluated. As previously stated, HR induction is concomitant with *PR* gene induction (Stintzi *et al*., 1993; van Loon and van Strein, 1999). FB1-induced cell death was accompanied with *PR* gene transcription; including *PR5, PR2* and *PR1*, which were previously mentioned as SA-induced *PR* genes (Stone *et al*., 2000; Scott *et al*., 1994; Glazebrook *et al*., 1996; Shah *et al*., 1997; Zhang *et al*., 1999; Nawrath and Métraux, 1999)

With the induction of *PR* genes and the similarity to pathogen-induced HR, Asai *et al*. (2000) attempted to determine if SA, JA or ET signaling was involved in the FB1-induced cell death pathway. Protoplasts obtained from Arabidopsis mutants, with disrupted signaling for each of the hormones, were treated with FB1. JA-insensitive mutant *jar1-1*, ET-insensitive mutant *etr1-1*, SA-depleted mutant *pad4-1*, and SA-depleted transgenic plant NahG were used (Staswick *et al*., 1992; Bleeker *et al*., 1988). All of the mutant lines showed less susceptibility to FB1 in comparison with the WT. In contrast, an NPR1 loss-of-function mutant showed similar susceptibility to the WT. NPR1 is required for SA-, JA- and ET-dependent defence responses, which suggests that FB1-induced cell death requires all three hormones upstream of NPR1 (Asai *et al*., 2000). This data concludes that identifying the molecular components upstream and downstream of SA, JA, and ET will help elucidate the signaling components of FB1-induced PCD. Once the pathway is determined, applying this knowledge to crop species and other HR-inducing pathogen systems will aid the development of increasing resistance of plants against toxigenic pathogens.

1.9. The role of extracellular ATP in PCD

Adenosine-5'-triphosphate (ATP) is an essential energy molecule within all living organisms. The energy-rich ATP molecule is a fundamental requirement in reactions of many metabolic processes. The available energy is released when the high-energy

gamma phosphate is hydrolysed to produce adenosine diphosphate (ADP) and an inorganic phosphate (P_i). The bulk of ATP synthesis occurs intracellularly via ATP synthase enzymes located in the mitochondria and chloroplasts. Energy is released when a gradient of protons passes through the ATP synthase complex and drives the production of ATP from ADP and P_i (Lardy and Wellman, 1952). After synthesis, ATP is transported to different compartments of the cell, depending on the demand for chemical energy. ATP plays a critical role in many intracellular functions that demand energy, such as respiration (Lardy and Wellman, 1952), photosynthesis (Horton, 1989), and muscular contraction (Gordon, 1986).

1.9.1. Extracellular ATP

As well as being a vital molecule within the cell, ATP is also found outside the cell where it plays a role in cell signaling. This extracellular ATP (eATP) originates in the cytosol and is secreted to the ECM by a number of mechanisms such as exocytosis (Schweitzer, 1987), efflux via anion channels (Dutta *et al*., 2002) and export via ABC transporter proteins (Thomas *et al*., 2000). An Arabidopsis protein was identified, PM-ANT1, which mediates the transport of ATP across the plasma membrane into the apoplast (Rieder and Neuhaus, 2011). Mutant pollen grains in which expression of this protein is disrupted have decreased eATP levels and increased intracellular ATP levels, and mutant plants have reduced silique length and diminished seed yield (Reider and Neuhaus. 2011). PM-ANT1 is a plasma membrane ATP exporter active during pollen maturation (Reider and Neuhaus. 2011).

The acceptance of ATP as an extracellular signal in both animals and plants has been quite controversial as it was unclear as to why cells would release such an important energy-rich molecule outside of the cell. However, the identification of mammalian eATP receptors was a turning point in recognizing eATP as an authentic signalling molecule. In animals, eATP signals across the plasma membrane by binding to P2 purinoceptors (Khakh and North, 2006). P2 receptors are divided into two sub-families, P2X and P2Y purinoreceptors (Kennedy *et al*., 1985). P2X are ionotropic ligand-gated cation channel receptors which, when bound to ATP, provide Ca^{2+} passage across the plasma membrane (Brake *et al*., 1994). P2Y are metabotropic G-

protein-coupled receptors that have two sub- groups; one uses G-proteins to activate phospholipase C/inositol triphosphate ($InsP_3$) endoplasmic reticulum C^{2+}-release pathway, and another sub-group that uses G-proteins to inhibit adenylyl cyclase and modulate ion channels (Abbracchio and Burnstock, 1994). P2 receptors have many roles, including cell proliferation, growth, cell death, platelet aggregation, wound healing, and immune response (Burnstock, 2001).

1.9.2. Identification of a plant eATP receptor

Until recently, a receptor for eATP at the cell surface in plants remained elusive. However, a recent study by Choi *et al* (2014) identified the first plant receptor for eATP. DORN1 (Does Not Respond to Nucleotides-1) binds ATP with a high affinity and initiates ATP-induced calcium influx into the cytosol (Choi *et al*., 2014). The eATP receptor was identified in a forward genetic screen to isolate *Arabidopsis thaliana* mutants in which ATP treatment was unable to activate Ca^{2+} influx. Two mutant lines, *dorn1-1* and *dorn1-2,* were deficient in the cytoplasmic calcium response to addition of exogenous ATP. The mutation in *dorn1-1* and *dorn1-2* is due to a point mutation in the gene that encodes a lectin receptor kinase-I.9 (LecRK-I.9) protein. The same phenotype was obtained with a transferred DNA (T-DNA) insertion mutant, *dorn1-3*. Complementation of *dorn1*-3 mutant by ectopic expression of the wildtype LecRK-I.9 gene re-establishes normal Ca^{2+} influx (Choi *et al*., 2014). The *dorn1* mutants clearly showed a defect in calcium response specifically to exogenous ATP; however, they did not show calcium responses that differed to the wildtype when subjected to other treatments that trigger calcium influx (Choi *et al*., 2014). This in turn shows that DORN1 encodes a receptor that is specifically responsive to ATP treatments (Choi *et al*., 2014).

The DORN1 protein has an intracellular kinase domain, a transmembrane domain, and an extracellular lectin-binding domain. Choi *et al* (2014) used an *in vitro* kinase assay to demonstrate that the kinase domain is completely inactive in the mutant lines. However, in experiments to cross-link the recombinant extracellular lectin-binding domain with biotinylated 8-azido-ATP, co-incubation with unlabelled ATP abolished the biotinylation of DORN1. This confirmed that DORN1 binds eATP at the cell surface via the extracellular lectin-binding domain. The binding of eATP at

the lectin- binding domain is an interesting revelation as these domains typically bind carbohydrates. This lectin- binding domain however, does not contain the conserved Ca^{2+} and Mg^{2+} binding residues that are required for monosaccharide binding (Hervé *et al*., 1999). In conclusion, Choi *et al* (2014) have identified a receptor at the cell surface that binds eATP, which in turn results in the inactivation of the intracellular kinase domain.

1.9.3. Secondary messengers in eATP signalling

Various secondary messenger molecules mediate eATP signalling in plants. The perception of eATP at the plasma membrane activates a Ca^{2+} influx into the cytosol (Tanaka *et al*. 2010), and this is dependent on eATP binding to the DORN1 receptor (Choi *et al*., 2014). Closely linked with Ca^{2+} influx is the production of a number of other secondary messengers such as phosphatidic acid (PA) (Testerink and Munnik, 2005), nitric oxide (NO) (Durner *et al*., 1998) and reactive oxygen species (ROS) (Demidchik *et al*., 2009). Previous pharmacological studies have given evidence for the generation of ROS to be both upstream (Demidchik *et al*., 2009) and downstream (Song *et al*. 2006. Wu *et al*. 2008) of Ca^{2+} influx; the production of ROS is also concurrently linked with the biosynthesis of NO (Reichler *et al*. 2009, Tonón *et al*. 2010, Wu and Wu. 2008, Foresi *et al*. 2007). Ca^{2+} antagonists stop the accumulation of NO, via ATP, yet ATP-mediated Ca^{2+} influx is cancelled by NO scavengers (Wu and Wu. 2008). It clearly shows that the mechanisms behind the production of secondary messengers are not simple linear pathways.

Although the pathway of secondary messengers appear to be complex, many research groups have tried to determine the pathway in various experimental systems; for example Laxalt *et al*. (2007) has provided evidence for the role of PA and NO in tomato cell culture responses to eATP. eATP increases PA levels by activating phospholipase D (PLD) and phospholipase C (PLC) pathways, with diacylglycerol kinase (DGK) (Laxalt *et al*., 2007). In animals, NO production is induced by eATP downstream of PLC activation (Clementi. 1998) However, Laxalt *et al* (2007) showed NO production in plants to be upstream of the defence response of PA formation. In plants, NO regulates PA formation via activation of the PLC/DGK pathway; this however, is independent of PLD. Treatment with inhibitors of PLC resulted in the reduction of ROS production, yet NO levels remained

unaffected. This shows that NO formation is upstream of PA production, yet ROS generation remains downstream (Laxalt *et al*., 2007).

Demidchik *et al* (2009) using *Arabidopsis thaliana,* showed that plant eATP activates a plasma membrane NADPH oxidase, AtRBOHC, to produce ROS. However, unlike Laxalt *et al* (2007), Demidchik *et al* state that AtRBOHC is the major contributor of eATP-mediated ROS formation, which results in the influx of Ca^{2+} into the cell. This study suggests that Ca^{2+} influx is downstream of ROS production, rather than Ca^{2+} initiating the production of secondary messengers (Demidchik *et al*., 2009).

1.9.4. eATP is required for cell viability

A link between eATP and cell death was made in several papers published by a Durham University group working on eATP. The central evidence constituting this link was the observation that bacterial pathogens capable of inducing defence gene expression and cell death activate a dramatic collapse of eATP levels *in planta*, while mutant bacterial strains incapable of activating defence genes and cell death fail to do so (Chivasa *et al*., 2009). Moreover, elicitor compounds that activate disease resistance and cell death in tobacco also reduce the amount of eATP in treated leaves (Chivasa *et al*., 2010).

In order to explore this link further, an experimental system to manipulate the amount of eATP available for cell signaling was developed (Chivasa *et al*., 2005). This system relied on reducing or increasing the amount of eATP and monitoring the plant's defence systems against pathogen attack. The system consisted of ATP sequestering enzymes directly applied to the apoplast. For example, apyrase which degrades ATP and ADP to AMP and P_i can be infiltrated into the apoplast to deplete endogenous eATP (Chivasa *et al*., 2005). Similarly a glucose-hexokinase mixture applied in the ECM breaks down ATP (Chivasa *et al*., 2005). Infiltration of exogenous ATP raises the level of endogenous eATP, while supplying the non-hydrolysable analogue of ATP, β,γ- methyleneadenosine 5'-triphosphate (AMP-PCP), results in the inhibition of ATP cleavage in the ECM (Chivasa *et al*., 2005). Because of the high molecular charge precluding membrane diffusion, both exogenous ATP and AMP-PCP should be limited to the ECM.

An unexpected outcome of plant treatments with the reagents that interfere with eATP utilization was the onset of cell death. This cell death response mimicked pathogen-induced HR and is dependent on light (Chivasa *et al*., 2005; Chivasa *et al*., 2009). Chivasa *et al* (2009) showed that tobacco plants grown at a light intensity of ~100μmol m^{-2} sec^{-1} and treated with AMP- PCP, did not die, though equivalent plants grown at ~200μmol m^{-2} sec^{-1} were extremely sensitive to AMP-PCP treatments and programmed cell death was induced. Furthermore, when the plants were grown at a low light intensity and were moved to high light conditions, the plants remained insensitive to eATP removal treatments; however, plants grown under high light conditions retained their sensitivity when moved to low light conditions The findings of this experiment indicated that light conditions during growth can be used to manipulate the cell death response to AMP-PCP treatments (Chivasa *et al*., 2009).

1.9.5. eATP regulation of pathogen-induced HR

After establishing that eATP regulated cell viability, the next stage for Chivasa and colleagues was to determine if eATP invoked cell death upon stimulation with a pathogen or the pathogen-derived chemical, FB1. Arabidopsis cultures spiked with [^{32}P]ATP were treated with 1μM of FB1. A rapid depletion of ATP occurred in the cell medium and by 40h, labelled ATP was undetectable (Chivasa *et al*., 2005). Examining the integrity of the cells within the cultures through evans blue staining showed that the depletion of eATP preceded the onset of FB1-induced cell death. This implies that eATP regulation occurs in the ECM, and is not altered by leakage of intracellular components post-cell death (Chivasa *et al*., 2005). Building upon the results from this experiment, treatments of exogenous ATP after FB1 treatments were able to rescue the cells from cell death up until 40h, after 48h the cells had gone past the point of rescuing, even before the physical symptoms of cell death occurred. This suggests that between 40- and 48h there is an irreversible switch that commits to cell death (Chivasa *et al*., 2005). These results were also mimicked in intact plant tissue (Chivasa *et al*., 2005).

In conclusion, Chivasa and colleagues showed that eATP acts as a negative regulator of cell death, and this mechanism is a controlled process rather than a necrotic phenotype of pathogen disease (Chivasa *et al*., 2005, 2009).

1.10. Aims and objectives

The objective for my PhD project is to device a number of methods to screen for putative proteins involved in the regulation of PCD. Using the cell death-inducing mechanism of FB1 as a focal point; I will identify FB1-responsive genes and, using reverse genetics, determine whether the screens have successfully identified PCD-regulatory proteins.

2
Materials and Methods

2.1. Materials

2.1.1. Chemicals and solutions

Name (Supplier)

1-napthaleneacetic acid (Sigma-Aldrich)
Acetone (Fisher Scientific)
Acrylamide/Bis 37:5:1(BioRad)
Agar Bacteriological (Oxoid)
Agarose (Bioline)
Ammonium persulfate APS (Thermo Scientific)
Bromophenol Blue (BioRad)
Citric Acid (Sigma-Aldrich)
Coomassie (Sigma-Aldrich)
Di-Potassium hydrogen orthophosphate (BDH)
Ethanol
Ethidium bromide (Sigma-Aldrich)
Ethylenediaminetetraacetic acid EDTA (Sigma-Aldrich)
Fumonisin-B1 (Sigma-Aldrich)
Glacial Acetic Acid (Fisher Scientific)
Glycerol (Fisher Scientific)
Hydrochloric acid, 35-38% (Sigma-Aldrich)
Kinetin (Sigma-Aldrich)
Glufosinate-ammonium [BASTA] (AgChem Access)
Methanol (VWR)
MOPs (Sigma-Aldrich)
Murashige & Skoog medium, Basal salt mixture [MSMO] (Duchefa Biochemie)
Orange G (Sigma-Aldrich)
Potassium Chloride (Fisher Scientific)
Propan-2-ol [Isopropanol] (Fisher Scientific)
Salicylic acid (Sigma-Aldrich)
Sodium Chloride (VWR)
Sodium dodecyl sulfate, SDS (Sigma-Aldrich)

SYPRO (invitrogen)
Sucrose (Sigma-Aldrich)
TEMED (BDH, Sigma-Aldrich)
Toludine blue (Sigma-Aldrich)
Torulopsis utilis RNA (torula yeast RNA) (Sigma-Aldrich)
Tris (Apollo Scientific Ltd.)
Trypsin Gold, Mass Spectrometry Grade (Promega)
Tryptone (Formedium)
Yeast extract (Oxoid)

2.1.2. Plant lines

Table 2.1. *Arabidopsis thaliana* plant lines

Name	*Ecotype*	*Gene (AGI)*	*Type*	*Original source*	*Identification*
Col-0	Columbia	-	Wild-type	Lab stock	-
Ler	Landsberg ercta	-	Wild-type	Lab stock	-
Ws	Wassileweskija	-	Wild-type	Lab stock	-
Arabidopsis thaliana mutant plant lines					
Name	Ecotype	Gene	Type	Original source	Identification
phyb.1	Columbia	At2g18790	T-DNA insertion	NASC	SALK_022035
phyb.2	Columbia	At2g18790	T-DNA insertion	NASC	SALK_069700
rns1.1	Wassileweskija	At2g02990	T-DNA insertion	INRA	FLAG_566AO8
rns1.2	Columbia	At2g02990	T-DNA insertion	NASC	SALK_087165
rns1.3	Columbia	At2g02990	T-DNA insertion	GABI-Kat	GABI_760D11
asRNS1	Columbia	At2g02990	Antisense	Pamela Green Lab group (Bariola et al., 1999)	
dorn1.1	Columbia	At5g60300	T-DNA insertion	NASC	SALK_042209

dorn1.2	Columbia	At5g60300	T-DNA insertion	NASC	SALK_024581
earp1.1	Columbia	At1g49900	T-DNA insertion	NASC	SALK_070432
earp1.2	Columbia	At1g49900	T-DNA insertion	NASC	SALK_100396
sid2	Columbia	At1g74710	T-DNA insertion	NASC	SALK_088254

2.2 Plant growth

2.2.1. Growth

Soil (Levington Advance Seed & Modular F2S) was sterilized at 120°C for 20 minutes to remove pests. *Arabidopsis thaliana* seeds were grown in nurseries for one week before individual seedlings were transferred to individual pots. The plants were grown under long day conditions 16-hour light (22°C) (100-120 μmol.s-1.m-2), 8 hours dark (15°C). Experiments on Arabidopsis were conducted at 4-5 weeks, prior to bolting.

2.2.2. Arabidopsis cell suspension cultures

Culture media consisted of 3% (w/v) sucrose, 0.443% (w/v) MSMO, 0.05% (w/v) 1-napthaleneacetic acid and 0.05% (w/v) kinetin. The pH was adjusted to 5.7 with KOH. 100mL of medium was transferred to 250mL conical flasks, sealed with 4 layers of aluminium foil, and autoclaved at 120°C for 20 minutes.

Arabidopsis thaliana cell suspension cultures were grown in 100mL of cell suspension medium in a sterile 250mL conical flasks. The flasks were kept shaking (60 RPM) at 22°C in either constant darkness, or under a photoperiod of 16 hours at 100μmol.s^{-1}.m^{-2}. Fresh cultures were created every seven days under sterile conditions by subbing 10mL of the previous week culture to fresh Arabidopsis cell suspension culture medium, and were ready for experiments three days post-sub-culturing.

Prior to experimentation the cell density can be adjusted by pipetting 1mL of suspended cell culture into pre-weighed eppendorfs. The culture media was siphoned

off through pipetting with a fine tip (200µL). Three replicated eppendorfs provided an average weight of the cells within the flask and can be appropriately adjusted to the required percentage density of cells within fresh culture media.

2.3. Plant and cell culture treatments

2.3.1. Preparation of FB1 stock solutions

FB1 was ordered in 5mg powdered form, and re-suspended in 70% methanol to produce stock solutions of 1mM FB1. FB1 stock solutions were stored at -20°C for several months.

2.3.2. FB1 leaf injections

1mM FB1 stock solution was diluted with MQ water to a concentration of 2.5-5µM, depending on the experiment. The working solution of FB1 was directly infiltrated into the apoplast of attached leaves from the abaxial surface using a needleless 1mL syringe. Treated leaves were marked with a non-toxic coloured marker and symptoms were left to develop. Symptom development was monitored every 24 hours, with the characteristic cell death patches becoming visible at around 3 days after injecting with a FB1 concentration of 3µM. Photographs were taken when symptoms had sufficiently progressed.

2.3.3. FB1 cell death conductivity assay

An FB1 solution of 5µM was injected into leaves (see 2.3.2) and leaf discs of 8mm in diameter were cored from the injected leaves. The leaf discs were floated on 9mL of a 5µM FB1 solution in small petri dishes. Ten leaf discs from ten individual plants were added to each petri dish, and replicated five times. During the process of leaf coring, the floating leaf discs were quickly incubated in the dark and exposure to the light was kept to a minimum during the set-up. Once all of the replicated petri dishes were completed, the dishes were subjected to total darkness for roughly 48 hours and removed from the dark incubation in the morning in order to expose the leaf discs to as much light within the first 24 hours upon light exposure. To determine the amount of electrolyte leakage from dying cells, conductivity measurements were taken every

24 hours after light exposure using a hand held EC meter (HI-98311 EC, TDS and Temperature Tester, Low Range; HANNA instrument®).

2.3.4. FB1 cell culture treatment

Working stock solutions of 50µM FB1 were prepared from 1mM stock solutions and filter sterilized using a 0.2µM size syringe filter (VWR). Treatments of 1µM FB1 were added to 30mL flasks of 5% (w/v) density cell suspension culture.

2.3.5. Adenosine triphosphate (ATP) and salicylic acid (SA) cell culture treatment

Stock solutions of 100mM ATP and 100mM SA were prepared fresh. Each solution was filter sterilized using a 0.2µM syringe filter (VWR). A final concentration of 400µM ATP and 200µM SA were used for cell culture treatments.

2.3.6. MTT (3-[4,5-dimethylthiazol-2-yl]-2,5 diphenyl tetrazolium bromide) cell death assay

The MTT assay is a colorimetric method to measure the activity of reductase enzymes that reduces yellow MTT into dark blue formazan crystals. This occurs in the presence of viable mitochondria and can be used as a cell viability assay. Cell cultures that were grown in light or dark conditions, were corrected to a 5% density in 40mL flasks. The cells were left to settle at the bottom of the flasks and the culture media was siphoned off using a fine pipette. Three replicate flasks were used for each of the following treatments:

- Light grown cells and culture filtrate from light conditions, treated with 1µM FB1
- Dark grown cells and culture filtrate from dark conditions, treated with 1µM FB1
- Dark grown cells and culture filtrate from light conditions, treated with 1µM FB1

The equivalent treatments were replicated with the replacement of FB1 with MQ water. After 9 days, 500mg of MTT was added to each of the flasks and left to incubate for 1 hour at room temperature. After the incubation, roughly 200µl of suspended cells were taken and transferred from each flask using a cut tip, and placed in the well lids of a 96-well plate to be photographed.

2.3.7. Lactophenol blue staining

Visualisation of dead cells using lactophenol blue staining was performed on four-week-old Arabidopsis plants. Leaf discs of 8mm diameter were cored from Arabidopsis leaves and floated on 3μM FB1 solution. The leaf discs were incubated in the dark for 48 hours before being introduced to a 16 h-photoperiod. To visualize the FB1-induced cell death, leaf discs were taken every 24 hours from the beginning of the experiment up until 96 hours. Leaf discs were fixed in 3mL of lactophenol [9% (w/v) phenol, 9% (v/v) glycerol, 9% (v/v) lactic acid, 73% (v/v) ethanol] overnight at 37ºC in a bijou bottle. They were then incubated in fresh lactophenol saturated with Evans Blue dye at 37ºC until all the tissue absorbed the dye. Stained leaf discs were then distained in chloral hydrate (250% w/v) in MQ water at 37ºC until background staining was minimal. Leaf discs were observed using a Zeiss Axioskop compound microscope using a x20 objective (Carl Zeiss, Cambridge, UK), and imaged using a QImaging Retiga-2000r camera (Photometrics, Marlow, UK).

2.4. Nucleic acid

2.4.1. RNA extraction

Frozen leaf tissue was ground to a fine powder with a pre-chilled pestle and mortar. Sigma-Aldrich Spectrum™ Plant Total RNA Kit was used to extract RNA as per manufacturer's recommendations. RNA was quantified by measuring absorbance at wavelengths of 260 and 280 nm using a Thermo Scientific NanoDrop™1000 Spectrophotometer.

2.4.2. RNA quantification and integrity check

Electrophoresis was used to separate RNA samples. 1.2% (w/v) high purity agarose (Bioline, London, UK) gels were made up with 3-(N-morpholino)propanesulfonic acid (MOPS) buffer [4.18% (w/v) MOPS, 20 mM sodium acetate, 10mM EDTA, pH 7 adjusted with 2 M NaOH]. 1μg of total RNA was mixed with 5μL of RNA loading buffer (50% (v/v) formamide, 17.5% formaldehyde, and 100 μg Ethidium Bromide (EtBr) in 1:2 dilution of MOPS buffer) for 15 minutes at 55ºC to allow the EtBr to bind to the RNA. The samples were separated using a dedicated gel tank, washed

with 2% SDS overnight, at constant 100 V for 20 minutes to allow proper separation of RNA bands. 28S and 18S ribosomal RNA bands were visualized on the gel using a UV transilluminator and used as a quality control for RNA degradation. Gels were photographed with a UVP Bioimaging systems 55+2 camera and images printed using a Mitsubishi P93 thermal printer (Mitsubishi) on high-density paper. RNA samples that showed no significant degradation on gel were used for reverse transcription.

2.4.3. cDNA synthesis

cDNA synthesis was performed using the GoScript™ kit (Promega, Madison, WI, USA) according to the manufacturers recommendations. For each sample, 2 µg of total plant RNA were mixed with 0.5 µg of oligo $(dT)_{15}$ and to a final volume of 5 µL with MQ water. The mix was incubated for 5 minutes at 65ºC to allow the oligo $(dT)_{15}$ to bind to the poly-A tails of the messenger RNA and to destroy RNA secondary structure. The samples were then placed on ice for 1 minute to prevent secondary structures reforming and spun down to remove condensation droplets before adding 4 µL of 5X GoScript™, 2.2mM MgCl2, 0.5mM PCR nucleotide mix, 20 units of RNasin (Promega Ltd., Madison, WI, USA) to a final volume of 20 µL. The samples were gently mixed with a pipette. The reaction was heated at an annealing temperature of 25ºC for 5 minutes before entering an extension phase at 42ºC for 1 hour, and terminated at 70ºC for 15 minutes. cDNA samples were stored at -20ºC.

2.4.4. Reverse transcriptase (RT)-PCR

PCR reactions were prepared using the BioTaq DNA Polymerase kit (Bioline, London, UK). PCR mixtures were prepared on ice using 200 µL thin walled flat cap PCR tubes. Each reaction consisted of 2 µL of cDNA template (1:3 dilution) in Taq polymerase buffer [16 mM $(NH_4)_2SO_4$, 67 mM Tris-HCl (pH 8.8 at 25ºC), 0.01% stabilizer] containing 1Unit of BioTaq, 1.5 mM $MgCl_2$, 0.2 µM of each primer and 0.2 mM of each dNTP. The final volume was made up to 50 µL with MQ water. Reactions were carried out on a G-Storm Thermal Cycler GS1 (GRI, Essex) with a heated lid at 111 ºC. Samples were heated at 94ºC for one minute prior to cycling to disrupt any unspecific binding that might have occured. Each cycle typically

consisted of 40 seconds denaturation at 94ºC followed by annealing, at 56-62ºC, for 40 seconds and elongation at 72ºC for 1 minute. A final elongation step at 72ºC was carried out for 5 minutes and reactions left on hold at 4ºC until analysed by gel electrophoresis.

Reaction Mix	µl
10X PCR Buffer	5
50mM $MgCl_2$	1.5
10mM dNTPs	1
Taq Polymerase	0.2
10µM Forward Primer	1
10µM Reverse Primer	1
cDNA (1:3 dilution)	2
H_2O	38

2.4.5. Direct DNA PCR

For genotyping of individual Arabidopsis SALK homozygous KO plants and segregation analysis of heterozygous lines the Phire Plant Direct PCR kit (Thermo Scientific, Massachusetts, USA) was used according to the manufacturer's instructions. 5 mm leaf disk was manually ground in 100 µL of the kit buffer. The resulting solution was directly added to PCR mix Primers were confirmed on wild-type genomic DNA with a gradient across the heat cycler for the annealing step. The PCR mix was setup as follows:

Reaction Mix	µL
Arabidopsis gDNA	5
10µM Forward Primer	0.4
10µM Reverse Primer	0.4
Sensifast	10
H_20	4.2

Once the optimal annealing temperature was determined, the specificity of the primers was confirmed using genomic DNA from homozygous T-DNA insertion lines alongside wild-type positive control template.

2.4.6. Primer design strategy

PCR primers were designed to gene targets using the NCBI primer BLAST sequence analysis web software available from the National Centre for Biotechnology Information (NCBI; http://www.ncbi.nlm.nih.gov/tools/primer-blast/). This software uses a combination of Primer3 primer design software (Rozen and Skaletsky 2000) and BLAST in order to identify specific primers in the template sequence that don't amplify unintended sequences in the genome or transcriptome of the organism being used. Only primer pairs amplifying the intended product were selected. The input sequence was the full-length genomic DNA sequence or full-length mRNA sequence of the gene of interest. The default parameters were used when designing primers for gDNA and cDNA amplification except for cDNA primers intended to ensure specificity to cDNA template over possible gDNA contaminants, these primers were required to span and exon-exon junction. If no suitable exon-exon junction primer set was available then the default setting was used.

Primers were synthesized by Information DNA Technologies (IDT, Iowa, USA). Upon delivery, primers were re-suspended in sterile distilled water to a concentration of 100 µmol /mL and stored at 20ºC. Primers used in this work are listed in Appendix 3.

2.4.7. Gel electrophoresis

DNA samples were analysed by agarose gel electrophoresis. High purity agarose (Bioline, London, UK) was dissolved in TAE buffer (40 mM Tris-acetate, 1 mM EDTA) to a final concentration of 0.8-3.5% (w/v). Agarose percentage used varied depending on the expected size of fragments. The intercalating dye ethidium bromide was added to the final concentration of 0.5 µg/mL. A total of 10 µL PCR product was mixed with 1.5 µL of Orange G DNA loading buffer [3% (v/v) glycerol 0.2% (w/v) Orange G] before loading into the agarose gel and the electrophoresis was run at 100 V. DNA molecular marker HyperLadder I (200 to 10,000 bp) or Hyperladder

V (25 to 500 bp) were used to confirm the size of the target PCR product. Resolved DNA bands were visualized under UV light (UVB, λ=300 nm) using a UV transilluminator.

2.4.8. Quantitative Real-time PCR (qRT-PCR)

Quantitative PCR primers were designed to gene targets using the NCBI primer BLAST (Geer *et al*., 2010) and primer annealing was tested using gradient PCR. Relative expression was compared between genotypes and treatments using target primers and primers to the housekeeping gene *ACTIN2* (At3g18780) and EIF4A (At3g13920) for normalization. Bioline Sensifast™ SYBR® No-ROX One-Step Kit was used in conjunction with Qiagen Rotor- Gene® Q. Each biological sample was replicated three times and pooled, then split into three identical technical replicates. REST 2009. Qiagen software was used for analysis (Pfaffl, 2001; Pfaffl *et al*., 2002).

Reaction Mix	µL
Arabidopsis gDNA	5
10µM Forward Primer	0.4
10µM Reverse Primer	0.4
Sensifast	10
H_20	4.2

2.5. Protein

2.5.1. Protein extraction of cell cultures

Treated cells were filtered in 2 layers of Miracloth (Merk, Nottingham, UK) and culture filtrate (CF) was retained for analysis of secreted proteins. The cells were re-suspended in 20 mL of cold (4°C) Tris/EDTA buffer (10 mM Tris base, 1 mM EDTA, pH 8.0 adjusted with HCl concentrated) and homogenised using a 4°C water bath cooled French Press (Constant systems Ltd., Warwick, UK) by passing the sample 2 times under 24,200 PSIs of pressure. Homogenate was centrifuged at 20,000 g for 30 minutes at 4°C to remove cell debris. The supernatant was centrifuged at 100,000 g for 1 hour at 4°C to separate the microsomal fraction (green pellet) from the Total Soluble Protein (TSP) fraction (supernatant). The CF was

retained in 50 mL falcon tubes and cold (4°C) 100% acetone added to roughly a ratio 1:4. The samples were stored at -20°C overnight.

2.5.2. TSP and CF protein extraction

The supernatant (TSP) was precipitated in 80% acetone overnight at -20°C. The resulting protein pellet was washed twice with 80% acetone and once in 100% acetone. The final pellet was re-suspended in lysis buffer (LB; 9 M urea, 2 M thiourea, 4% w/v CHAPS, 30 mM Tris-HCl, pH 8.8) by mixing in an orbital shaker (180 RPM) overnight. Protein samples were quantified by the modified Bradford method and stored at -20°C for long-term storage. The same process was applied to the CF.

2.5.3. Protein quantification (Bradford assay)

A modification to the standard Bradford assay, developed by Ramagli (Ramagli *et al*., 1985) was used to allow the use of this assay on samples containing carrier ampholytes and thiol containing compounds that would interfere with the standard assay. The calibration curve was made by making Bovine Serum Albumin (BSA) dilutions in LB ranging from 1-10 µg. To each sample, the required volume of BSA in LB was mixed with 10 µl of 0.1 N HCl and the volume made up to 100 µL with MQ water, taking care that the same volume of LB used for the highest BSA concentrations was also present in the lower concentrations. All protein samples were pelleted on a benchtop centrifuge before 2 µL of each sample was measured in triplicate. Calibration and sample solutions were mixed with 900 µL of Protein Assay Dye Reagent concentrate (Bio-Rad Laboratories Ltd, Hemel Hempstead, UK) 1:4 diluted with MQ water. Proper mixing was insured by vortexing the cuvette. After 5 minutes of incubation at room temperature, the absorbance at 595 nm was recorded using an Ultrospec 1100 pro spectrophotometer (GE Healthcare, Amersham, UK). Protein concentration was calculated using Microsoft Excel by plotting the absorbance values in a scatter graph where the Y-axis represents the absorbance measured and the X-axis the protein concentration being estimated (Figure 2.1). The calibration line should have R2 over 0.985 to be suitable for proteomic studies (Bio-Rad 2D-DiGE manual). A new calibration curve was made

for every set of samples to be quantified to take into account day-day variations of the reagents, temperature, etc.

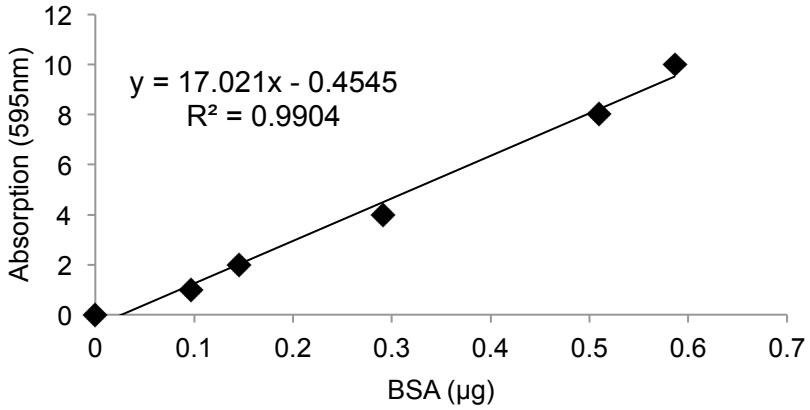

Figure 2.1. Typical Bradford calibration curve using BSA.

2.5.4. SDS PAGE

Separation of proteins based on their molecular weight was performed by sodium dodecyl sulphate polyacrylamide gel electrophoresis (SDS-PAGE) as outlined by Laemmli (Laemmli 1970).

Gel casting

1D SDS-PAGE analysis of protein samples was performed using a Bio-Rad's Mini Protean II vertical gel apparatus (Bio-Rad Laboratories Ltd.). Glass plates were cleaned with 70% (v/v) ethanol prior to use to remove contaminating protein or residual acrylamide. Gels were 0.75 mm thick and consisted of a stacking gel on top of a resolving gel. The stacking gel ensures the proteins enter the resolving gel at the same time while the resolving gel separates the proteins based on their molecular weight. Resolving gel contained 12% (w/v) acrylamide (acrylamide:bis-acrylamide 37.5:1) (Bio-Rad Laboratories Ltd.), 375 mM Tris HCl pH 8.8, 0.1% (w/v) SDS, 0.05% (w/v) APS (Bio-Rad Laboratories Ltd.), and 0.02% (v/v) TEMED (Bio-Rad Laboratories Ltd.). The resolving gel was immediately poured into the glass plates taking care not to trap air bubbles. Gels were covered with water saturated butan-1-ol and allowed to allow polymerization, then was washed away. The stacking gel [5% (w/v) acrylamide, 125 mM Tris-HCl pH 6.8, 0.05% (w/v) APS and 0.04% (v/v) TEMED] was poured on top of the resolving gel. A minimum thickness of stacking

gel between the bottom of the wells and the beginning of the resolving gel was 5 mm.

Protein sample preparation and gel loading

The SDS-PAGE gels were placed in an electrophoresis tank with SDS running buffer [25 mM Tris-HCl, 190 mM glycine, 0.1% (w/v) SDS]. A concentration of 50µg of protein sample, suspended in LB, was mixed with 5X loading buffer [10% (w/v) SDS, 5% (w/v) DTT (Melford Laboratories Ltd., Ipswich, UK), 0.05% (w/v) bromophenol blue, 0.312 M Tris-HCl pH 6.8, 50% (v/v) glycerol] resulting in 1X loading buffer concentration mix in a volume of up to 25 µL. The mixture was then boiled for 5 minutes to ensure complete breakage of disulfide bonds. The samples were loaded into separate wells and an SDS7 marker set was used in each gel for protein band size estimation purposes.

1D gel electrophoresis

Electrophoresis was carried out at room temperature at 100 V for 15 minutes, to allow the proteins to enter the resolving gel, followed by 120 V until the bromophenol blue dye front reached the bottom of the gel. Gels were then stained with coomassie brilliant blue R-250 or SYPRO Ruby (Genomic Solutions Ltd, Huntingdon, UK) for protein visualization.

2.5.5. RNase activity assay

Preparation of protein extracts

The RNase activity assay was performed on four-week-old Arabidopsis plants. Leaves were taken from the plants foil wrapped and snap frozen to prevent changes in RNase expression in response to wounding. The leaf tissue was homogenized at room temperature in extraction buffer (150mM citric acid-Na2HPO4, pH3, 0.1mM PMSF) at a ratio of 100mg tissue: 10µL extraction buffer. Homogenate was centrifuged at 20,000 g for 30 minutes at 4°C to remove cell debris. Supernatant was quantified by the modified Bradford method and stored at -20°C for long-term storage.

Gel casting

Gel preparation followed the same protocol as One-dimensional SDS-PAGE gels with minor modifications to the stacking and separating mixtures:

Separating gel:

11.3% [w/v] acrylamide, and 0.3%[w/v] N',N'-methlyene-bis-acrylamide, 0.46M Tris (pH9), 2.4mg/mL *Torulopsis utilis* RNA, 0.08% [w/v] N',N',N',N'-tetramethyl-ethylenediamine and 0.8% [w/v] ammonium persulfate.

Stacking gel:

4.5% [w/v] acrylamide, and 0.12%[w/v] N',N'-methlyene-bis-acrylamide, 0.063M Tris (pH9), 0.08% [w/v] N',N',N',N'-tetramethyl-ethylenediamine and 0.8% [w/v] ammonium persulfate.

Electrophoresis and activity staining

Equal volume of 2X sample-loading buffer (2%[w/v] SDS, 10% [w/v] glycerol, and 0.025% [w/v] bromophenol blue in 50mM Tris-HCl buffer, pH6.8) added to 50µg of protein sample before electrophoresis. Unlike the standard SDS PAGE, the samples are not boiled, which ensures that the RNase proteins remain functional and intact. The separating gel and stacking gel were run at a constant current of 1.7mA/cm in running buffer (1.4% [w/v] glycine, 27.5mM Tris, and 0.1% [w/v] SDS). SDS was washed from the gels with two 10-minute treatments of 25% [w/v] isopropanol in 0.01M Tris-HCl buffer. A further two 10 minute washes with 0.01M Tris-HCl to remove isopropanol. The gel was then incubated in a Techne Hybridiser HB-1 chamber at 51°C for 50 minutes in 0.1M Tris-HCl buffer. After the incubation phase the gels were washed in 0.01mM Tris-HCl spiked with 2M $ZnCl_2$, before staining for 10 minutes in 0.01mM Tris-HCl with an additional 0.2% [w/v] toluidine blue O. Gels were de- stained with 0.01mM Tris-HCl until white bands, indicating RNAse activity, showed through. Photographs were taken on a MiniSun LED graphics pad.

2.5.6. 2-dimensional gel electrophoresis (2DE)

Preparation of CyDyes

CyDye DiGE fluor minimal dyes (GE Healthcare, Amersham, UK) were reconstituted from their supplied dry form using unopened high quality dimethylformamide (DMF) anhydrous (≥ 99.8% pure. Unopened CyDye vials were removed from the -20ºC freezer and allowed to equilibrate at room temperature for at least 5 minutes prior to opening. The contents of each vial were centrifuged at 13,000 g for 5 minutes prior to opening and resuspended in 10 µl of DMF to obtain the primary stock solution (1 nmol/µl), which is stable at -20ºC for at least 4 weeks. The working stock was obtained by further diluting the primary stock to 400 pmol/µl in DMF.

Protein CyDye labelling

All labelling reactions with CyDyes were done using the recommended ratio of 400pmol dye/50 µg protein. A total of 50 µg of each sample was labelled in a final volume of 140 µl. A pooled standard was obtained by mixing 50 µg of all the samples in the experiment. The labelling reaction was carried out in 500 µL eppendorfs at 4ºC, in the dark, inside an ice bath. Reaction was started with the addition of 1 µL of working stock dye, vortexed and was left incubating in the ice bath in the dark for 30 minutes. 1 µl of 10 mM lysine was added to stop the reaction by quenching un-reacted dye, after which the tubes were left for a further 10 minutes on ice. Tubes containing labelled protein were stored at 20ºC.

DiGE sample mixing and large format 2DE of DiGE analytical gels

Sample mixture consisted of 12.5 µg of the Cy3- and Cy5-labelled protein samples, making up a total loading of 37.5 µg of protein per gel. The mixture was made up to 70 µL with blue LB [9 M urea, 2 M thiourea, 4% (w/v) CHAPS, 0.05% (w/v) bromophenol blue]

Large format gels

Large format gels were cast in 26 x 20 x 1 cm low fluorescence glass cassettes, using the a2DE Optimizer (nextgensciences Ltd, Alconbury, UK). Prior to gel casting, glass plates were scrubbed and then soaked for 1 hour in 1% (v/v) Decon (Decon Laboratories Limited, Sussex, UK), rinsed with MQ water, soaked in 1% HCl (v/v) for 1 hour and then thoroughly rinsed with MQ water. Clean plates were air dried, protected from dust then assembled into cassettes and place inside the nextgenautocast tank (nextgensciences Ltd, Alconbury, UK), each separated from each other by a thin plastic spacer. The a2DE Optimizer supervisor software (version 1.4.0.27313) was used for automated gel casting. A custom program was created for casting gradient gels using a commercial kit supplied by the same company. The gels were then overlaid with 1 mL of isopropanol and left to polymerize until the following day. The acrylamide gradient generated on the gels was linear from 10% to 15% with a rapid increase in concentration close to the end of the gel (hook).

Protein loading by anodic cup

Rehydration of 24 cm pH 4-7 IPG strips (GE Healthcare, Amersham, UK) was performed. A total volume of 450 µl rehydration solution [1% (m/v) fresh DTT, 1% (v/v) of relevant IPG ampholite buffer and 0.002% (w/v) bromophenol blue in LB] was used to rehydrate the strips for 12-24 hours. Rehydrated strips were then transferred gel side up to clean individual ceramic Ettan IPGphor strip holders (GE Healthcare, Amersham, UK) with the acidic end at the anode. Strips were then completely covered in paraffin oil to prevent dehydration. Protein samples were centrifuged at 16,000 g for 5 minutes prior to loading to remove insoluble material. A total volume of 70 µl containing the protein sample in rehydration solution was loaded by pipetting under the paraffin oil.

Large format first dimension isoelectric focusing

Rehydrated IPG strips with the protein samples loaded in the cup were focused in an Ettan IPGphor unit using fixed a setting of 50 µA per strip at constant 20°C. IPG

strips were focused to 70,000 V.hr-1 in order to achieve optimal focusing. A longer V.hr-1 count could result in over-focusing and poor spot separation. Gradient steps allow salts to gradually enter the electrode wicks and proteins to enter the strip from the cup.

IPG strip equilibration

Immediately after IEF completion, strips were removed from the strip holders and carefully rinsed with MQ water to remove excess paraffin oil. Next, they were placed inside large cylindrical equilibration tubes. Strips were equilibrated in 5 mL of equilibration buffer [6 M urea, 30% (v/v) glycerol, 2% (w/v) SDS, 50 mM Tris-HCl pH 8.8, 0.002% (w/v) bromophenol blue] containing 1% (w/v) DTT for 15 minutes at room temperature. The strips were further equilibrated in buffer containing 4.8% (w/v) iodoacetamide for a further 15 minutes.

Second dimension large format SDS-PAGE

Large format 2D gradient gels were rinsed with MQ water and the IPG strips were laid onto the resolving gel. IPG strips were then overlaid with a warm agarose sealing solution [0.5% (w/v) agarose, 0.002% (w/v) bromophenol blue]. Second dimension electrophoresis was performed using the Ettan DALTtwelve vertical electrophoresis system (GE Healthcare, Amersham, UK), at 5 W per gel for 30 minutes followed by 17 W per gel until the bromophenol blue dye front reached the bottom of the gels at 25°C. A typical run lasted 5 hours.

Imaging using the Typhoon 9400 variable mode imager

SYPRO stained and DiGE protein gels were scanned with the Typhoon 9400 Variable Mode Imager (Amersham Biosciences). DiGE analytical gels were imaged inside their respective glass cassettes immediately after 2DE finished in fluorescent mode, normal sensitivity at the + 3 mm focal plane and using the appropriate combination of laser/filter for each of the CyDyes. They were held in place by Ettan Dalt gel holders during each scan. Each gel was prescanned once for each CyDye at

a low resolution (pixel size 500 μM) to adjust PMT settings so that the most abundant protein spot had a signal intensity close to 70,000 AU, in a maximum linear dynamic range of 100,000 AU. This PMT value was used in the final scan at high resolution (pixel size 100 μM). 1D gels were imaged directly on the platen. SYPRO gels were scanned in fluorescence mode, normal sensitivity, on the platen focal plane using the Cy3 laser/filter settings.

2.5.7. Isobaric tags for relative and absolute quantitation (iTRAQ)

Refer to 2.5.2 for culture filtrate protein extraction

Trypsin Gold digest

After samples had been successfully quantified (refer to 2.5.3) 5uL of 1.5M Tris-HCl pH8.8 was added to 15uG of sample. 800uL 100% acetone was added, vortexed and incubated at room temperature for 20 minutes. The mixture was centrifuged at 10,000 x g for 10 minutes and the supernatant was removed. The pellet was washed with 800uL 80% Acetone, then vortexed, and centrifuged (10,000 x g) for 10 minutes and the supernatant was removed again. This wash step was repeated for a third time however the supernatant was not removed on the final wash. 5uL 2% SDS denaturant was added and was incubated at room temperature for 1 hour. After 1 hour, 95uL of dissolution buffer was added and then was left to shake on a vortex mixer for 20 minute at room temperature. The samples were then centrifuged at 9,000 x g for 5 minutes then 2uL of reducing agent was added, followed by a further incubation step of 60C for 1 hour. 1uL of blocking reagent was then added and left to incubate at room temperature for 10 minutes. 10uL of 0.5ug/uL Trypsin Gold was then added and incubated at 37C overnight. The samples were freeze-dried the following day. The proceeding stages were performed by in-house proteomic laboratory at Durham University.

iTRAQ Sample Clean-up

Samples were cleaned-up using HILIC SPE cartridges (PolyLC Inc.), containing 300 mg of 12µm polyhydroxyethyl-A, to remove unincorporated label and buffer salts. The cartridges were equilibrated by sequential addition of 4 x 3 mL releasing solution (5% ACN, 30 mM ammonium formate pH 3.0) followed by 4 x 3 mL binding solution (85% ACN, 30 mM ammonium formate pH 3.0). The dried iTRAQ-labelled peptide residue was dissolved in 75 µL of 3% acetonitrile (ACN), 0.1% formic acid (FA) followed by 150 µL of 0.3 M ammonium formate, pH 3. The pH of the mixture was checked and adjusted to 3.0 using trifluoroacetic acid (TFA) if necessary. After clarifying by centrifugation (10,000 x g, 10 mins), the samples were mixed with 1275 µL ACN. The resulting 1.5 mL sample was added to the SPE cartridge and the flow-through retained and passed through a second time. The column was then washed twice with 2 mL binding solution. Finally, the peptides were eluted with 2 x 1 mL releasing solution. The eluate was freeze-dried and re-suspended in 3% ACN, 0.1% formic acid for liquid chromatography-mass spectrometry (LC-MS).

LC-MS Analysis

LC-MS analysis was performed using a TripleTOF 6600 mass spectrometer (Sciex) linked to an Eksigent 425 LC system via a Sciex Nanospray III source. Peptides originating from 5µg protein were used for each LC-MS run and chromatographic separations of peptides used a trap and elute method. Samples were loaded and washed on a Triart C18 guard column 1/32", 5 µm, 5 x 0.5 mm (YMC) acting as a trap, and online separation of peptides performed over 87 mins on a TriArt C18 1/32", 3 µm, 150 x 0.3 mm column (YMC) at a flow rate of 5 µL/min. Buffer A was 0.1% FA in water and buffer B 0.1% FA in ACN. Sequential linear gradients of 3 to 5% B over 2 minutes, 5 to 30% B over 66 minutes, 30 to 35% B over 5 minutes and 35 to 80% B over 2 minutes were followed by a 3 min column wash in 80% B. Return to 3% B was over 1 min before column re-equilibration for 8 minutes. Data-dependent top-30 MS-MS acquisition, with collision energy adjusted for iTRAQ-labelled peptides, was started immediately upon gradient initiation and was for 85

min. Throughout this period, precursor-ion scans (400 to 1600 m/z) of 250 ms enabled selection of up to 30 multiply-charged ions (>500 cps) for CID fragmentation and MS/MS spectrum acquisition (m/z 100-1500) for 50 ms. The cycle time was 1.8 sec and a rolling precursor exclusion of 15 sec was applied to limit multiple fragmentation of the same peptide. Analyst TF 1.7.1 instrument control and data processing software (AB Sciex) was used to acquire spectrometer data.

Mass Spectra Data Analysis

Protein identification and relative quantification was performed by processing the raw .wiff data-files against relevant databases using ProteinPilot™ 5.0.1 version 4895 software, incorporating the Paragon™ Algorithm 5.0.1.0.4874, (AB Sciex). An iTRAQ 8-plex (peptide-labelled) Paragon method, for tryptic peptides with iodoacetamide cys-modification and data acquired on a TripleTOF 6600 spectrometer, was used. Label bias-correction was activated in this, the 'Thorough ID' and 'Run False Discovery Rate Analysis' options were selected, and the Detected Protein Threshold was set at 0.05 (10%) [Unused ProtScore (conf)]. Peptide and protein tables were exported from ProteinPilot for subsequent manual data-handling and filtering.

2.6. Software packages

REST 2009 (Qiagen) (Pfaffl, 2001; Pfaffl *et al*., 2002)

Genevestigator (Zimmermann *et al*., 2004; Grennan, 2006; Hruz *et al*., 2008)

Qiagen Rotorgene Q Version 1.7 © 1990-1999 Info-ZIP Pty. Ltd.

2.7. Internet services

The Arabidopsis Information Resource (TAIR). 2018 (https://www.Arabidopsis.org/servlets/TairObject?id=29349&type=locus)

SignalP 4.1 Server. 2018. (http://www.cbs.dtu.dk/services/SignalP/) (Nielsen, 2017)

TMHMM Server, V.2.0. 2018 (http://www.cbs.dtu.dk/services/TMHMM/) (Sonnhammer *et al*., 1998; Krogh *et al*., 2001)

Agilent 101: Intro to Microarrays & Genomics. 2019. (https://www.agilent.com/labs/features/2011_101_microarray.html)

AgriGO (bioinfo.cau.edu.cn/agriGO. 2018) (Du *et al*., 2010; Tian *et al*., 2017).

MapMan 3.0.0. 2018. (https://mapman.gabipd.org/) (Usadel *et al*., 2009)

3

Developing a screen to identify putative cell death-regulatory proteins

3.1. Introduction

Light is a key regulatory component of many cellular processes in plants. In particular, light has a profound effect on plant immunity and the activation of defence responses (Roden and Ingle, 2009). Work in this chapter built on previous research showing that light is a powerful regulator of PCD (Brodersen *et al*., 2002; Genoud *et al*., 2002; Karpinski *et al*., 2003; Mateo *et al*., 2004; Zeier *et al*., 2004; Chandra-Shekara *et al*., 2006; Griebel and Zeier, 2008). Fumonisin B1 (FB1)-induced cell death is blocked by dark-incubation in both Arabidopsis leaves (Stone *et al*., 2000) and in leaf-derived protoplasts (Asai *et al*., 2000). This provides an opportunity to use light and FB1 as tools to develop a screen to identify genes/proteins that regulate plant cell death. Arabidopsis cell suspension cultures are an ideal *in vitro* system for developing such a screen. They grow rapidly to produce a homogenous suspension of log phase cells in 3-5 days and they respond to FB1 just like whole plants (Chivasa *et al*., 2005). Because they are provided with sucrose, they can grow in complete darkness as cream-coloured cells or in a 16 hour-photoperiod as green cells with chlorophyll (Figure 3.1A), enabling the light effects to be evaluated.

3.2. Factors secreted into the ECM regulate FB1-induced cell death

The effects of light on FB1-induced cell death in Arabidopsis cell suspension cultures were investigated using the MTT (3-[4,5-dimethylthiazol-2-yl]-2,5 diphenyl tetrazolium bromide) assay. MTT tetrazolium salts are commonly used for evaluating the cytotoxicity of various drugs/compounds using cell cultures (Mosmann, 1983). The MTT reagent is originally pale yellow in colour and is taken up by cells and converted into the dark blue formazan by mitochondrial enzymes of living cells. If the cells are dead, the colour will remain pale yellow.

When incubated with MTT in the absence of FB1, both light- and dark-grown cell cultures are able to metabolise the MTT solution and produce the purple pigment

(Figure 3.1B). This indicates that the cells are alive. However, after treatment with 1μM FB1 for 3 days, the cell cultures respond differently, depending on the presence or absence of light. Under light conditions, FB1 treated cell cultures are unable to convert MTT to the purple pigment, while equivalent control cell cultures turn purple. This confirms that under light conditions, FB1 stimulates cell death of Arabidopsis cultures. However, under complete darkness, the FB1-treated cell cultures produce the purple pigment upon addition of MTT, indicating that cell death has been blocked (Figure 3.1.B). These results show that FB1-induced death in cell suspension cultures is also regulated by light as seen in whole plants.

In a cell suspension culture, metabolites and proteins secreted to the extracellular matrix accumulate in the growth medium and they are easily harvested by simple filtration and subsequent concentration steps. Thus, cell cultures provide an excellent system to investigate the influence of secreted metabolites on physiological responses. Therefore, I investigated the effects of secreted factors in the ECM on light-dependent, FB1-induced PCD. The plant ECM consists of the external surface of the plasma membrane, the cell wall, and the mobile apoplastic fluid, which contains dissolved metabolites and macromolecules. In cell cultures, the mobile phase equivalent is the growth medium, commonly known as the culture filtrate (CF) as it can be separated from the culture by filtration.

To evaluate the effects of secreted molecules on PCD, the CF of dark-grown cell cultures was removed and replaced with CF from light-grown cell cultures prior to FB1 treatment. The dark-grown cells, now swimming in CF from light-grown cells, were then treated with FB1 and incubated in complete darkness, which normally suppresses cell death. Evaluation of these cells using the MTT assay revealed that dark-incubation failed to protect these cells from FB1 toxicity (Figure 3.1.B). The entirety of these results not only confirms that light regulates FB1-induced PCD, but also provides new crucial evidence that light controls this cell death via regulation of secreted factors in the soluble phase of the ECM. The ECM contains diverse molecules and metabolites, such as proteins, lipids, carbohydrates, and inorganic molecules and ions. However, the identity of these molecules or metabolites will require further analysis. Therefore, a systematic investigation of the light-regulated components of the soluble phase of the ECM could provide useful insights into PCD

signalling. The results obtained in this section can be used to develop an invaluable screen to identify putative PCD-regulatory factors.

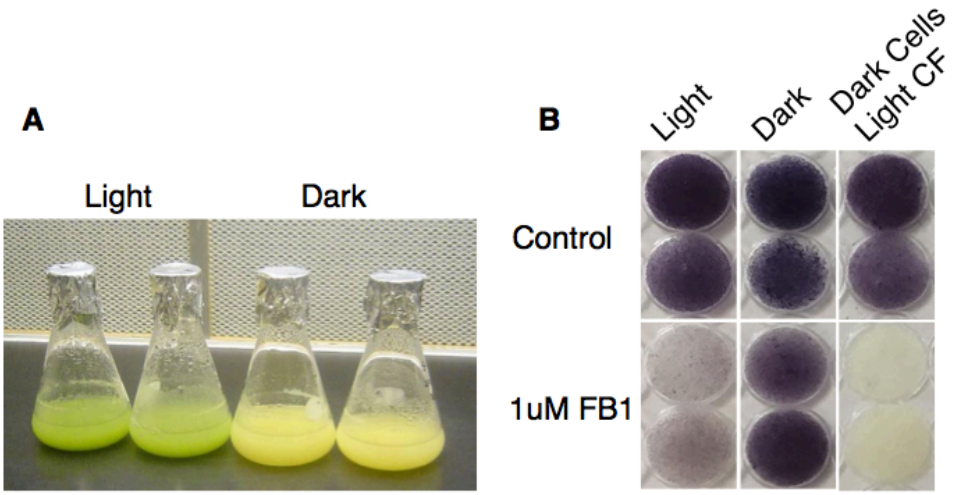

Figure 3.1. Response of Arabidopsis cell cultures to FB1. **A**) Appearance of light-grown (green) and dark-grown (yellowish-cream) Arabidopsis cell cultures. **B**) Cell cultures were mock- or FB1-treated and, after addition of MTT solution, a lawn of cells was pipetted into wells of 96-well plates for photographing. Top row shows viable control cell cultures (purple in colour) without FB1 treatments. The bottom row shows viability of FB1-treated cell cultures. Light-grown cells are dead while dark-grown cells are resistant to FB1. Dark-grown cells incubated with culture filtrate from light-grown cells become sensitive to FB1 and are dead.

3.3. A screen to identify light-dependent ECM factors regulating cell death

After providing evidence that factors secreted into the ECM play a pivotal role in light-regulated FB1 toxicity, I proposed a screen for use in identifying these factors (Figure 3.2). The screen has 2 stages as follows: (i) Stage 1 involves growth of Arabidopsis Landsberg *erecta* (L*er*) cell cultures, in either light or dark conditions, for harvesting the culture filtrate. High throughput mass spectrometric methods can be used to identify molecules with quantitative differences between the two growth conditions. Metabolomics and proteomics are ideal for such an unbiased analysis. In this thesis, Stage 1 focused entirely on the protein identification, with no attempt made at metabolomics analysis. (ii) Stage 2 then evaluates the relative expression of proteins identified in the culture filtrate of dark-grown versus light-grown

Arabidopsis cells. Candidates are then screened on the basis that their expression must be different between the 2 growth conditions. Stage 2 filters the putative candidates identified in stage 1 down to a small number of candidate genes that could be evaluated using further experiments, such as the use of genetic mutants or pharmacological agonists/antagonistic compounds, as appropriate.

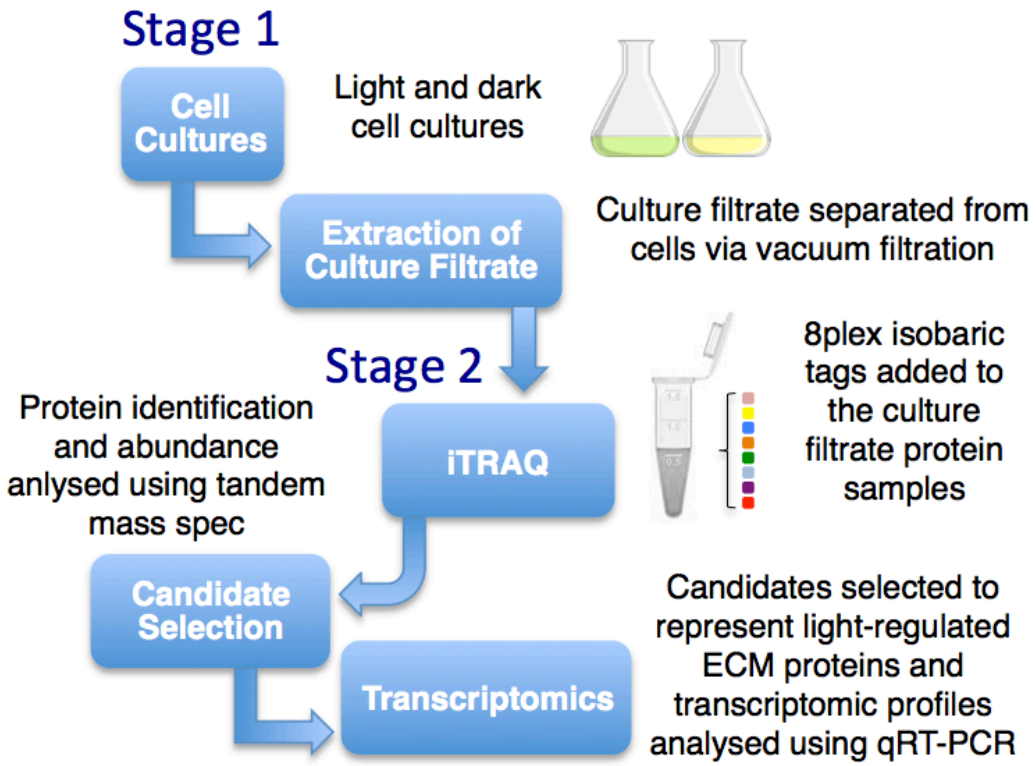

Figure 3.2. Schematic diagram of a screen developed to identify light-dependent ECM factors regulating cell death. Stage 1 includes the extraction of proteins secreted into the culture filtrate of light and dark grown cell cultures. Protein identification and quantification of protein response to light are evaluated using isobaric tag for relative and absolute quantitation (iTRAQ). Stage 2 involves analysis of the proteins identified that respond to light and dark conditions. The identified proteins were filtered down to a list of proteins showing differential abundance between light and dark growth conditions. A selection of genes from the analysis were used to validate the iTRAQ through qRT-PCR analysis of cell cultures subjected to light and dark conditions.

3.4. Arabidopsis light-regulated ECM proteins

To screen for candidates involved in regulating FB1-induced PCD, this thesis focused on the protein components as explained above. In addition to screening for putative cell death-regulatory proteins, this part of the project was also aimed at expanding the in-house database of Arabidopsis ECM proteins experimentally verified by mass spectrometry. Previous analyses from the group have used a less sensitive older generation mass spectrometer, while in this thesis, access to a newer machine with much higher sensitivity was available.

After 5 days of growth in light or dark conditions, cells were separated from the growth medium and total soluble proteins (TSP) were extracted from the cells, while secreted proteins were recovered from the CF via precipitation. The protein fractions were resolved by SDS-PAGE and stained with Sypro ruby. As expected, the protein profiles revealed massive differences between TSP and CF samples (Figure 3.3). With the limited resolution of one-dimension gels, there were no apparent differences between the TSP profiles of light- and dark-grown cells. The sheer number of proteins in the TSP may mask the differences in protein abundance between the light and dark protein samples in one-dimensional gels. The CF samples, however, had very different profiles between light and dark growth conditions, with very distinct bands appearing uniquely or more abundantly in either the dark-incubated or light-incubated samples (Figure 3.3). The dark-incubated samples had a profile with an overall higher abundance of small molecular weight proteins found towards the bottom of the gel (Figure 3.3).

The light and dark CF samples were labelled with fluorescent Cy3 and Cy5 dyes, respectively, and mixed before further analysis using 2-dimensional gel electrophoresis (2DE). In comparison to SDS-PAGE, 2DE has far superior protein resolution capability. The spectrally distinct fluorophores used to label the samples enable multiplexing and running the samples in the same gel. At the end of the run, the gel imager acquires the Cy3 image and the Cy5 image, with the imaging software generating an overlay of these two images (Figure 3.4). The software was used to assign a pseudo green colour and a pseudo red colour to the Cy3 and Cy5 images, respectively. Proteins with equal abundance between the 2 samples should appear yellow in the overlay image, while any spots appearing green or red are differentially

expressed between the two samples. As can be clearly seen in the overlay gel image, there are a number of protein spots that show differing expression in response to light and dark conditions (Figure 3.4). Green protein spots have higher abundance in dark-grown cell cultures when compared with light-grown cultures, and the reverse is true for red protein spots. Taken together, both SDS-PAGE and 2DE results highlight secreted protein differences between light and dark growth conditions. This also shows that, even under no PCD stimulation, secreted proteins in the ECM are responsive to light. This may be an important observation for not only studies in light-regulated PCD, but also other plant responses that are regulated by light. Overall, the results confirm that light regulates the abundance of some proteins found in the soluble phase of the ECM. These proteins are potential candidates with a putative role in regulating FB1-induced cell death.

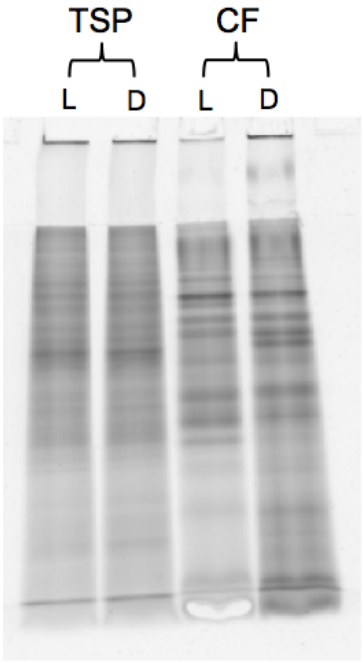

Figure 3.3. SDS-PAGE of Arabidopsis cell culture proteins. 50µg of Total Soluble Protein (TSP) and Culture Filtrate protein (CF), from cultures grown in light (L) or darkness (D) were separated by SDS-PAGE on 12% acrylamide gels and stained with Sypro Ruby.

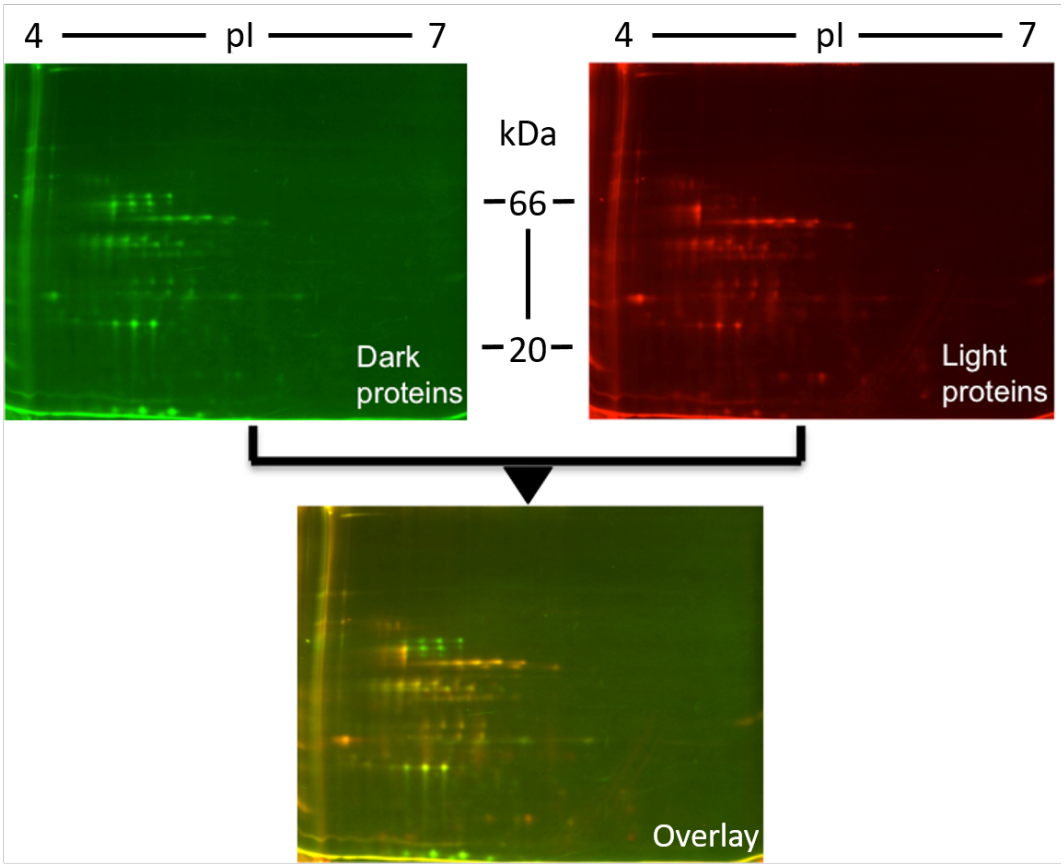

Figure 3.4. 2D profiles of Arabidopsis CF protein. 50µg of Cy3-labelled CF protein from dark-grown cultures and 50µg of Cy5-labelled CF protein from light-grown cultures were mixed and co-separated with 2DE. The Cy3 and Cy5 images are displayed separately, with the overlay of the two showing qualitative differences in the expression level of some of these proteins (green or red in colour).

3.5. Protein analysis using isobaric tags for relative and absolute quantitation

In the preceding section, SDS-PAGE and 2DE revealed qualitative differences in the abundance of secreted proteins from light-grown versus dark-grown cell cultures. In this section, iTRAQ analysis was used to identify all the culture filtrate proteins and to quantify their response to light. Only those proteins showing a strong response to light stimulation would be selected as potential candidates with a putative regulatory role in Arabidopsis response to FB1.

Inoculum from 1-week-old Arabidopsis cell suspension cultures was sub-cultured into fresh growth medium at 10-fold dilution and grown under light or dark conditions. Three days later, the cell density of cultures was standardised across 4 replicates each of light- or dark-grown cells and left to grow for a further 2 days before sample processing. Previous lab optimisation has shown 5 days to be a suitable time for extraction of cells, as the cells are growing within the logarithmic phase. The CF was separated from the cells and CF proteins isolated as described in the methods. The protein samples were labelled with iTRAQ reagents and analysed by mass spectrometry (MS). A total of 363 proteins were identified in the soluble phase of the ECM. This list was condensed to 321 proteins by removing proteins where only one peptide was sequenced; a stringency of a minimum of 2 peptides was applied to reduce the likelihood of incorrect protein identifications. The list was further reduced to 306 proteins by removing proteins with a protein score less than 1.3, which is equivalent to 95% certainty that these proteins have been correctly matched with the sequenced peptides.

Previous ECM protein analyses in the group identified varying numbers of proteins. A total of four MS analysis experiments were conducted during my project (three of which I ran). While previous protein identifications were conducted on the QStar Pulsar-i, a hybrid quadrapole Time-Of-Flight mass spectrometer (Applied Biosystems, Foster City, USA), the iTRAQ data presented in this thesis was run on a new and more sensitive mass spectrometer, TripleTOF 6600 (AB Sciex^{TM}, Warrington, United Kingdom), which appears to have identified more proteins in the ECM. However, after careful examination of all proteins identified in each of the four MS runs, it was clear that each run identified a number of unique proteins. Therefore, the proteins identified in this thesis add to the growing list of plant ECM

proteins, experimentally verified to be expressed in rapidly growing cell cultures. I created an in-house database of all Arabidopsis ECM proteins identified from all runs and indicate which runs identified which proteins. It is likely that proteins identified across all four runs are highly abundant in the ECM, and candidates identified in one or two of the runs are likely to be lower abundance proteins.

Of the 306 positively identified proteins, the abundance of 172 proteins was significantly different ($p < 0.05$) between light-grown and dark-grown cultures (Appendix 1). The highest differences in protein expression between light- and dark-incubated cultures were over 2-fold. While statistically significant, some of the changes were very modest, being as low as 1.042-fold change. Whether these small changes translate to significant biochemical or physiological responses will require detailed analyses in the future. Overall, these results show that light has a very broad impact on the ECM proteome. The top 25 extracellular proteins are shown in Table 3.1 and Table 3.2, showing either a higher level of expression in response to light conditions when compared to the dark, or those expressed at lower levels in response to light. The proteins showing the highest response to light are interesting candidates for further investigation into light-dependent physiological functions.

Table 3.1. The top 25 extracellular Arabidopsis proteins from cell cultures expressed at higher levels under light growth conditions, compared to dark conditions.

AGI[a]	Symbol[b]	Name	Ratio[c]	*p*-value[d]
At5g19100	-	Eukaryotic aspartyl protease family protein	2.2	0.000349463
At3g08030	-	DNA-directed RNA polymerase subunit beta	2.1	5.77295E-05
At5g44130	FLA13	Fasciclin-like arabinogalactan protein 13	1.9	5.03353E-06
At1g15270	-	Translation machinery associated TMA7	1.8	3.08843E-05
At5g64120	PRX71	Peroxidase 71	1.8	1.74438E-05
At5g44390	BBE25	Berberine bridge enzyme-like 25	1.8	0.000101448
At1g49750	-	Leucine-rich repeat (LRR) family protein	1.8	0.000245444
At2g13820	XYP2	Non-specific lipid-transfer protein-like protein	1.81	0.014575722
At5g07030	-	Aspartyl protease family protein	1.7	2.28589E-05
At4g12910	SCPL20	Serine carboxypeptidase-like 20	1.6	2.50009E-06
At1g44130	-	Aspartyl protease family protein	1.6	0.000145291
At1g71380	CEL3	Endoglucanase 9	1.6	1.55991E-05
At1g03870	FLA9	Fasciclin-like arabinogalactan protein	1.6	5.23683E-05
At2g47010	-	Calcium/calcium/calmodulin-dependent Serine/Threonine-kinase	1.6	1.1389E-06
At3g54400	-	Eukaryotic aspartyl protease family protein	1.6	0.001524925
At3g45970	EXPL1	Expansin-like A1	1.6	9.0579E-06
At3g18280	TED4	Bifunctional inhibitor/lipid-transfer protein/seed storage 2S albumin superfamily protein jn	1.6	0.00422342
At3g45600	TET3	Tetraspanin-3	1.6	4.4027E-05
At5g06870	PGIP2	Polygalacturonase inhibitor 2	1.6	0.001175409
At5g64570	BXL4 XYL4	Beta-D-xylosidase 4	1.5	1.06726E-06
At3g61820	-	Eukaryotic aspartyl protease family protein	1.5	0.000735512
At5g05340	PRX52	Peroxidase 52	1.5	0.006986927
At1g64760	ZET	Glucan endo-1,3-beta-glucosidase 8	1.4	5.1484E-07
At2g46880	PAP14	Probable inactive purple acid phosphatase 14	1.4	1.06413E-05
At5g08380	AGAL1	Alpha-galactosidase 1	1.4	1.01887E-06

[a]AGI (Arabidopsis Genome Initiative, 2000) code
[b]Gene symbol used in NCBI database
[c]Ratio of dark/light protein abundance, which represents the fold changes
[d]Probability value for the comparison of means using Student's t-test.

Table 3.2. The top 25 extracellular Arabidopsis proteins from cell cultures expressed at lower levels under light growth conditions, compared to dark conditions.

AGI[a]	Symbol[b]	Name	Ratio[c]	*p*-value[d]
At1g78850	MBL1	Curculin-like (Mannose-binding) lectin family protein	-2.3	1.50238E-07
At4g12880	ENODL19	Early nodulin-like protein 19	-2.1	5.11597E-06
At2g02990	RNS1	Ribonuclease 1	-2.1	5.14536E-05
At3g22800	-	Leucine-rich repeat extensin-like protein 6	-2.0	2.39566E-07
At2g16060	GLB1 HB1	Non-symbiotic hemoglobin 1	-1.9	4.21958E-06
At1g03220	-	Aspartyl protease-like protein	-1.9	4.90972E-05
At3g15356	FLA1	Legume lectin family protein	-1.7	1.55532E-05
At2g47320	-	Peptidyl-prolyl cis-trans isomerase CYP21-3, mitochondrial	-1.6	1.22625E-06
At1g68290	BFN2 ENDO2	Endonuclease 2	-1.6	0.000156619
At1g19730	ATH4	Thioredoxin H4	-1.5	0.033993465
At4g25900	-	Aldose 1-epimerase family protein	-1.5	2.23717E-05
At1g03820	-	E6-like protein	-1.5	0.005873653
At3g12700	NANA	Chloroplast nucleoid DNA binding protein-like	-1.4	9.01804E-05
At3g62060	PAE6	Pectin acetylesterase 6	-1.4	0.011757982
At1g03230	-	Aspartyl protease-like protein	-1.4	0.000200765
At3g45010	SCPL48	Serine carboxypeptidase-like 48	-1.4	2.117E-05
At4g22730	-	Leucine-rich repeat protein kinase family protein	-1.4	0.001765767
At2g19780	-	Leucine-rich repeat-containing protein	-1.4	0.00762521
At5g15650	RGP2	UDP-arabinopyranose mutase 2	-1.4	0.003297802
At5g41870	-	Pectin lyase-like superfamily protein	-1.4	3.71666E-05
At4g29360	-	Glucan endo-1,3-beta-glucosidase 12	-1.4	1.86262E-05
At5g19120	-	Eukaryotic aspartyl protease family protein	-1.3	1.68012E-05
At2g22420	PER17	Peroxidase 17	-1.3	3.85606E-05
At1g07890	APX1	L-ascorbate peroxidase 1, cytosolic	-1.3	0.023385639
At2g17120	LYM2	LysM domain-containing GPI-anchored protein 2	-1.3	0.000124648

[a]AGI (Arabidopsis Genome Initiative, 2000) code and gene symbol
[b]Gene symbol used in NCBI database
[c]Ratio of dark/light protein abundance, which represents the fold changes
[d]Probability value for the comparison of means using Student's t-test.

AgriGO (bioinfo.cau.edu.cn/agriGO. 2018; Du *et al*., 2010; Tian *et al*., 2017) was used to run a Gene Ontology (GO) analysis of the 172 differentially expressed proteins identified via iTRAQ. The proteins were split into high expression and low expression lists, which consisted of roughly the same number of proteins, and analysed separately. AgriGO categorized the proteins identified into biological process and functional groups (Figures 3.5-3.6). The input list for proteins highly expressed and those with lower expression levels have representatives in most molecular process classes, which indicates a high diversity of proteins in the soluble phase of the ECM. A large proportion of proteins identified were assigned to known metabolic processes, particularly carbohydrate and protein metabolism (Figure 3.5). Also a high percentage of proteins have catalytic or hydrolase activity (Figure 3.6). Generally, there is little difference between proteins showing higher expression and lower expression in response to light for both biological process and function; however proteins with higher expression under light conditions appear to have a significant proportion of proteins that have a defensive and developmental response, which is not represented in the list of proteins with lower expression (Figure 3.5). From analysing the AgriGO data, one can predict that proteins with a putative role in PCD will have higher expression levels in response to light as PCD is not only specific to defence response, but also plant development and appendage assembly.

As well as GO analysis, I manually categorized the 172 proteins into protein family/functional groups via gene descriptions provided in the NCBI gene database. The gene descriptions in some cases were rather vague but I managed to distinguish protein families that were highly represented in the iTRAQ dataset. The most abundant class of proteins are shown in Table 3.2. Aspartyl proteases were the most abundantly identified proteins, with a total of 15 genes belonging to this protein family. Further condensing the iTRAQ list using a 1.5 fold-change threshold reduced the proteins to a total of 30. Of these 30 proteins, 5 are aspartyl proteases, indicating that aspartyl proteases are not only highly represented within the 172 identified ECM proteins, but also among the most differentially expressed proteins in response to light. Peroxidases and proteins encoding a leucine-rich repeat (LRR) motif were the next most abundant protein families in the iTRAQ dataset, each with 8 representative proteins. Further abundant protein families include: glucosidases; berberine-bridge enzyme-like proteins; SKU5-similar proteins; Flasciclin-like proteins;

galactosidases; pectinases; etc (Table 2). Almost all of the protein families contain proteins up-regulated in response to light, and also proteins which are down-regulated in response to light. The only abundant family with proteins specifically showing higher expression in response to light was the Late Embryogeneis Abundant (LEA) protein family, with 4 members identified. There was also only one protein family with proteins specifically down-regulated in response to light, which was thioredoxin reductase proteins with 3 representative proteins identified.

Prior to analysing the iTRAQ dataset, I expected that protein families with a number of family members identified within the iTRAQ would most likely respond to light in a similar way, and most likely provide a similar function. This expectation was not supported by the results. This implies that further investigation into selected candidates from these protein families may be useful, but cannot predetermine the response of other members of the protein families.

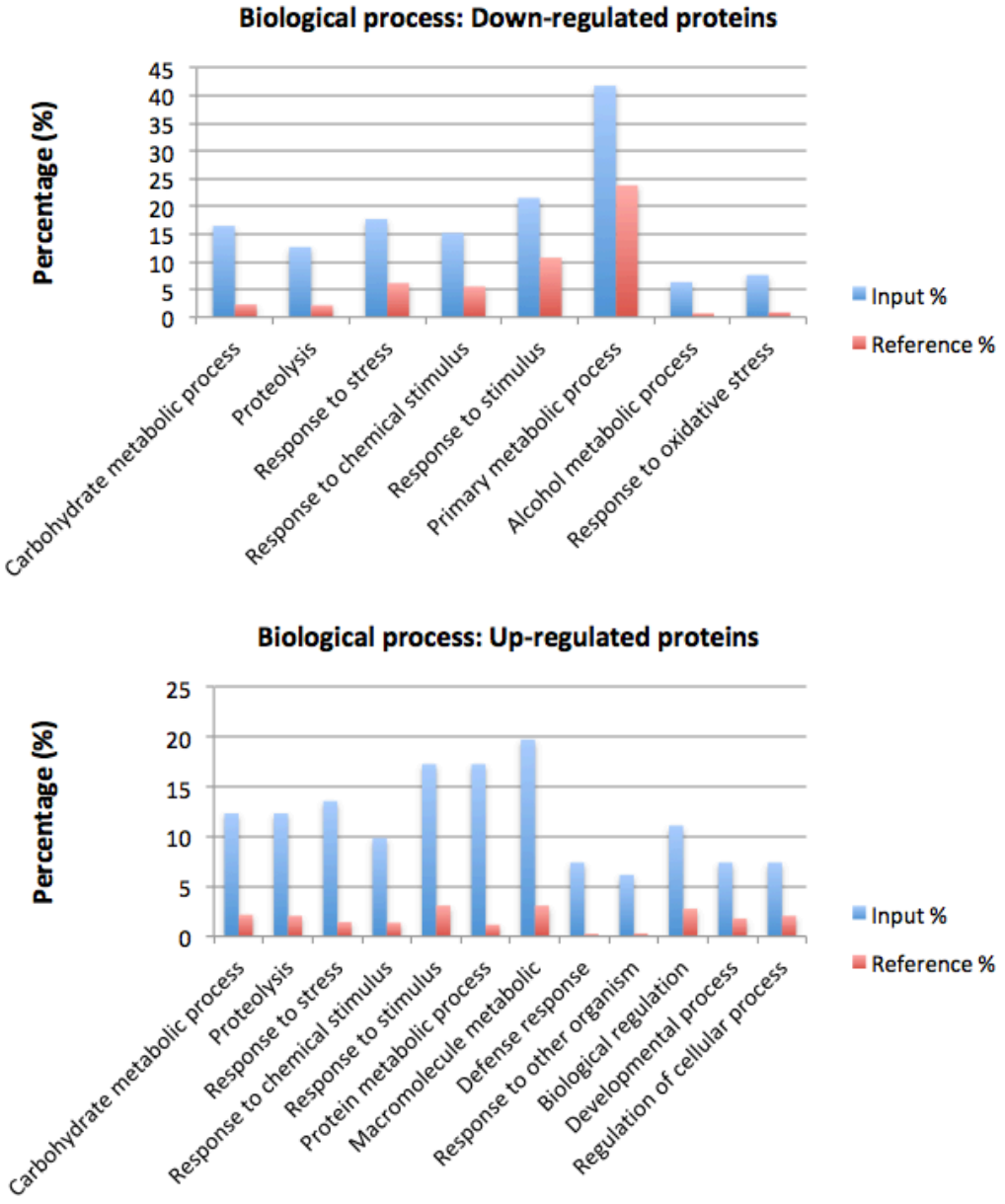

Figure 3.5. Biological process GO analysis. Percentage of proteins from the iTRAQ dataset (Input %) compared with the *Arabidopsis thaliana* genome (Reference %) and categorized into biological processes. **A)** The biological processes particularly enriched for proteins that show lower expression in response to light. **B)** The biological processes particularly enriched for proteins that show higher expression in response to light.

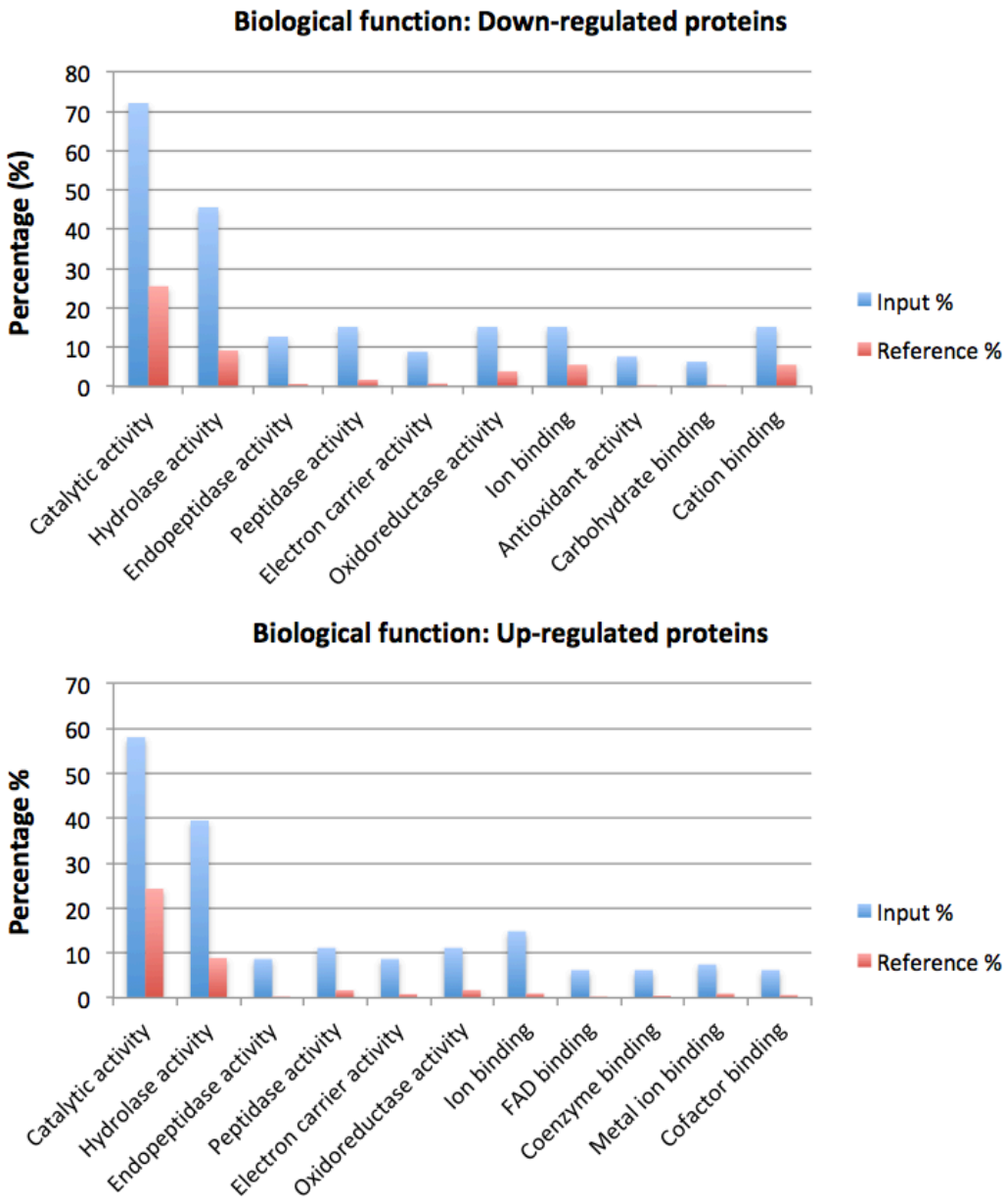

Figure 3.6. Biological function GO analysis. Percentage of proteins from the iTRAQ dataset (Input %) compared with the *Arabidopsis thaliana* genome (Reference %) and categorized into biological function. **A)** The biological function particularly enriched for proteins that show lower expression in response to light. **B)** The biological function particularly enriched for proteins that show higher expression in response to light.

Table 3.3. Abundant protein families within the iTRAQ

Protein family	*AGI*[a]		*Total No. identified*[d]	*Total number identified (>1.5 fold change)*[e]
	Up-regulated[b]	*Down-regulated*[c]		
Aspartyl protease	At5g19100 At5g07030 At1g44130 At3g54400 At3g61820 At2g17760 At1g65240	At1g05840, At3g52500, At1g79720, At3g18490, At5g19120, At1g03230, At1g03220	15	5
Peroxidase	At5g64120 At5g05340 At5g06720 At4g11600	At2g37130, At5g17820, At1g07890, At2g22420	8	1
Leucine-rich repeat family	At1g49750 At3g12145 At5g23400	At3g24480, At5g21090, At2g19780, At4g22730, At3g22800	8	2
Glucosidase	At1g64760 At5g58090 At4g34480 At4g31140	At2g44450, At3g02740, At4g29360	7	0
Berberine bridge enzyme-like	At5g44390 At4g20840 At4g20830 At4g20860	At5g44400, At5g44380	6	1
SKU5 similar	At1g41830 At4g22010 At5g66920 At4g25240 At5g48450	At4g12420	6	0
Flasciclin-like	At5g44130 At1g03870 g45470 At4g12700	At3g15356	5	3
Galactosidase	At5g08380 At2g28470 At3g13750	At3g26380, At4g36360	5	0
Pectinases	At3g49220 At4g19410 At4g23820	At5g41870, At3g62060	5	0
Late embryogenesis abundant family	At3g54200 At2g27260, At3g52470, At2g01080	-	4	0
Xylosidase	At5g64570, At1g78060, At1g68560	At5g10560	4	1
Serine carboxypeptidase-like	At4g12910, At5g42240	At5g08260, At3g45010	4	1

O-Glycosyl hydrolase	At5g55180	At3g07320, At2g05790, At5g13980	4	0
Isomerase	At4g34870, At4g38740	At2g47320	3	1
Purple acid phosphatase	At2g46880	At4g24890, At1g13750	3	0
Xyloglucan endotransglucosylase	At2g06850	At4g37800, AT4G03210	3	0
Early nodulin	AT4G31840	At5g25090, At4g12880	3	1
Thioredoxin reductase	-	At2g17420, At5g42980, At1g19730	3	0

[a] AGI (Arabidopsis Genome Initiative, 2000) code for the
[b] Proteins up-regulated in response to light
[c] Proteins down-regulated in response to light
[d]Total number of genes identified for each protein family
[e]Total number of genes identified for each protein family with at least a 1.5 fold change (Log2)

3.6. Effects of light on gene expression of selected candidates

Differentially expressed proteins identified by iTRAQ are potential candidates regulating FB1-induced cell death. Because iTRAQ is a very expensive technology, further steps to filter the iTRAQ dataset utilised analysis of gene expression with quantitative reverse transcription PCR (qRT-PCR). In the first instance, I was interested in comparing relative gene expression in light-grown versus dark-grown cells and comparing this to iTRAQ protein expression data. This would identify candidates with positive correlation of gene expression and protein expression. These candidates could then be further analysed for response to FB1 treatment using the cheaper route of gene expression analysis incorporating multiple time-points. Such experiments would be more informative when compared to a single-point iTRAQ experiment.

From the 172 differentially expressed proteins (Appendix 1), 13 candidates were selected based on fold-change, recurring protein families, and general interest from our Research Group (Table 3.3). Before progressing experimentally with these candidates, I conducted sequence analysis to determine if they are predicted to be secreted to the ECM via the classical eukaryotic secretory pathway. The amino acid sequence for each protein was analysed for the presence of a signal peptide, transmembrane domains, and a HDEL/KDEL motif. The signal peptide is located at

the N-terminus of the amino acid sequence, and is about 16-30 amino acids long. The presence of a signal peptide indicates that the protein is destined to the secretory pathway, though this will include membrane-bound proteins and proteins localised to particular organelles (e.g. endoplasmic reticulum, golgi, etc.) (Gierasch, 1989; von Heijne, 1990; Rapoport, 1992; Bendtsen *et al*., 2004; Petersen *et al*., 2011). SignalP 4.0, an online signal peptide prediction tool (Nielsen, 1999) was used for amino acid sequence analysis. After confirming that all of the selected candidates contained a signal peptide, I manually searched for HDEL or KDEL motifs in the amino acid sequences. By default, proteins containing a signal peptide will be automatically targeted to the secretory pathway, however the final destination of the protein is determined by the presence/absence of a sorting signal, such as a HDEL or KDEL motif, which retains the protein in the ER or Golgi complex or directs it to the vacuole (Munro and Pelham, 1987; Pelham *et al*., 1990; Napier *et al*., 1992; Denecke *et al*., 1992). None of the candidates contained HDEL or KDEL motifs, which confirmed that the proteins were secreted to the ECM.

Table 3.4. Candidate proteins selected from the iTRAQ data for further analysis.

AGI[a]	*Gene symbol/ Name*[b]	*Fold change*[c]	*P-value*[d]	*Signal peptide*[e]	*TMD*[f]	*H/K DEL*[g]
At5g44130	FLA13: Fasciclin-like arabinogalactan protein 13	1.918	5.03E-06	Yes	No	No
At5g64120	PRX71: Peroxidase 71	1.835	1.74E-05	Yes	No	No
At5g07030	Aspartyl protease family protein	1.694	2.29E-05	Yes	No	No
At1g03870	FLA9: Fasciclin-like arabinogalactan protein 9	1.628	5.24E-05	Yes	No	No
At3g61820	Eukaryotic aspartyl protease family protein	1.514	7.36E-04	Yes	No	No
At5g05340	PRX52: Peroxidase 52	1.478	7.00E-03	Yes	No	No
At5g20950	BGLC1: Beta-D-glucan exohydrolase-like protein	1.31	3.30E-03	Yes	No	No
At5g58090	Glucan endo-1,3-beta-glucosidase 6	1.262	8.84E-06	Yes	No	No
At4g34180	CYC1: CYCLASE1	-1.099	0.015	Yes	No	No
At1g30600	SBT2.1: Subtilisin-like protease SBT2.1	-1.122	0.017	Yes	No	No
At3g23450	Transmembrane protein	-1.132	0.037	Yes	Yes	No
At1g68290	BFN2/ENDO2: Endonuclease 2	-1.632	1.56E-04	Yes	No	No
At2g02990	RNS1: Ribonuclease 1	-2.102	5.14E-05	Yes	No	No

[a]AGI (Arabidopsis Genome Initiative, 2000) code and gene symbol
[b]Gene symbol and name used in NCBI database
[c]Ratio of dark/light protein abundance, which represents the fold changes
[d]Probability value for the comparison of means using Student's t-test.
[e]Presence of a signal peptide
[f]Presence of transmembrane domains
[g]Presence of a HDEL or KDEL motif

A similar method to identifying signal peptides was also used to predict the presence and location of transmembrane domains in the amino acid sequence, using the TMHMM 2.0 tool (Krogh *et al*. 2001). All of the selected candidates showed no transmembrane domain sequences, which confirms that once secreted, the proteins are not bound to the cell surface. Overall, the proteins contained a signal peptide, which targets the protein to the ECM. There are no H/KDEL motifs to retain the proteins to the ER, and no transmembrane domains; therefore the proteins are not bound to the cell surface, but exist freely in the ECM.

Three groups of proteins were taken forward for further analysis. The first group consisted of the 13 candidates selected by the filter as described above. The second group consisted of 4 proteins excluded by the filter because they are not responsive to light, but were selected to serve as negative controls. All proteins in the control group (BCB, DGR2, At3g45160 and At1g20030) have a signal peptide, no transmembrane domain, and no endoplasmic-retention motif in their protein sequence - this confirms ECM localisation (Table 3.4). These proteins could reveal if the screen excluded some useful candidates that should have been included in this analysis. The third group consists of 3 proteins not identified in any of the ECM protein fractions analysed by our group. They were selected from ongoing PCD investigation within our research group. All 3 proteins (BGLU46, BGLU31 and At3g22600) are similarly targeted for ECM localisation (Table 3.4), though failure to detect then by mass spectrometric analysis could indicate extremely low abundance or insolubilisation into the cell wall. Therefore, a total of 20 proteins across these 3 groups were taken for further analysis.

Table 3.5 Candidate proteins that were not identified in the iTRAQ, but are located in the soluble phase of the ECM.

AGI[a]	*Gene symbol*[b]	*Name*	*Signal peptide*[c]	*TMD*[d]	*HDEL*[e]
AT5G20230	BCB	Blue-copper-binding protein	Yes	No	No
AT1G61820	BGLU46	Beta glucosidase 46	Yes	No	No
AT5G24540	BGLU31	Beta glucosidase 31	Yes	No	No
AT3G22600	-	Bifunctional inhibitor/lipid-transfer protein/seed storage 2S albumin superfamily protein	Yes	No	No
AT5G25460	DGR2	Transmembrane protein, putative	Yes	No	No
AT3G45160	-	Putative membrane lipoprotein	Yes	No	No
AT1G20030	-	Pathogenesis-related thaumatin superfamily protein	Yes	No	No

[a]AGI (Arabidopsis Genome Initiative, 2000) code and gene symbol
[b]Gene name used in NCBI database
[c]Presence of a signal peptide
[d]Presence of a transmembrane domains
[e]Presence of a HDEL or KDEL motif

Dark-grown and light-grown Arabidopsis cell cultures were harvested 3 days after sub-culturing for RNA extraction and qRT-PCR analysis. Results of transcript abundance revealed the following trends within each protein group as follows:

(i) The 13 candidate proteins selected by the filter - For a majority of these candidate proteins, there was a positive correlation between gene expression and the proteomics data. Thus, *RNS1, BFN2, At3g23450, CYC1* and *BGCL1* were expressed at lower levels in response to light at both protein and RNA levels, while *PRX71, At5g07030, At3g61820* and *PRX52* were transcriptionally and translationally expressed at higher levels in response to light (Figure 3.7). However, the remaining candidates either showed the opposite response (*FLA13* and *FLA9*) at protein versus RNA levels, or showed no significant response to light (*SBT2.1* and *At5g58090*) at the RNA level (Figure 3.7). An explanation for this is that post-translational regulatory control may activate changes of protein abundance, without the need for activation of gene expression at the transcript level. This serves as a caution for studies that entirely rely on gene expression data without checking proteome data.

(ii) The 4 negative control proteins - BCB, DGR2 and At3g45160 were identified by the iTRAQ, but did not significantly respond to light at the protein level. Gene expression analysis revealed that these genes also do not respond to light at the transcript level (Figure 3.8). At1g20030 significantly responded to light at the transcription level, although the relative fold change was marginal (Figure 3.8), which may explain why it was not identified in the iTRAQ. Overall, these control proteins show the robustness of the screen in excluding these candidates.

(iii) The 3 proteins not identified in the ECM protein fractions – Expression of BGLU46, BGLU31 and At3g22600 genes significantly responded to light at the transcription level (Figure 3.8). This indicates a limitation of the screen developed here – that proteins not highly abundant in the ECM fractions and missed by mass spectrometric identification will not be identified by the screen. However, this affects almost all screens developed for any biological application

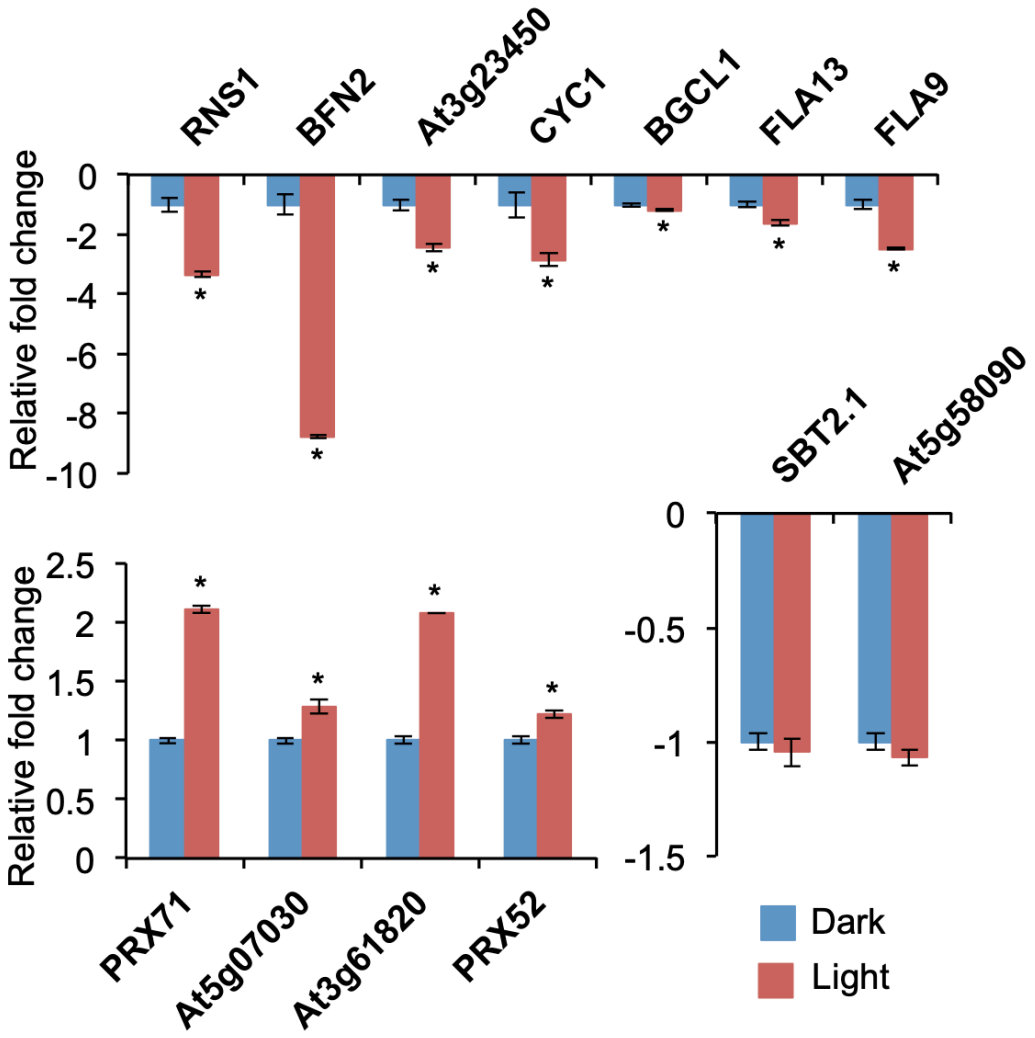

Figure 3.7. Effects of light on Arabidopsis gene expression of candidates selected by iTRAQ protein. RNA used for qRT-PCR analysis was obtained from 3-pooled biological replicate flasks of 3-days-old light- and dark-grown cell cultures. qRT-PCR values are an average of 3 technical replicates. Bars represent mean ± SD (n = 3). An asterisk indicates a significant difference between light and dark ($p \leq 0.05$). *ACTIN2* and *EIF4A* were used as constitutive reference control genes.

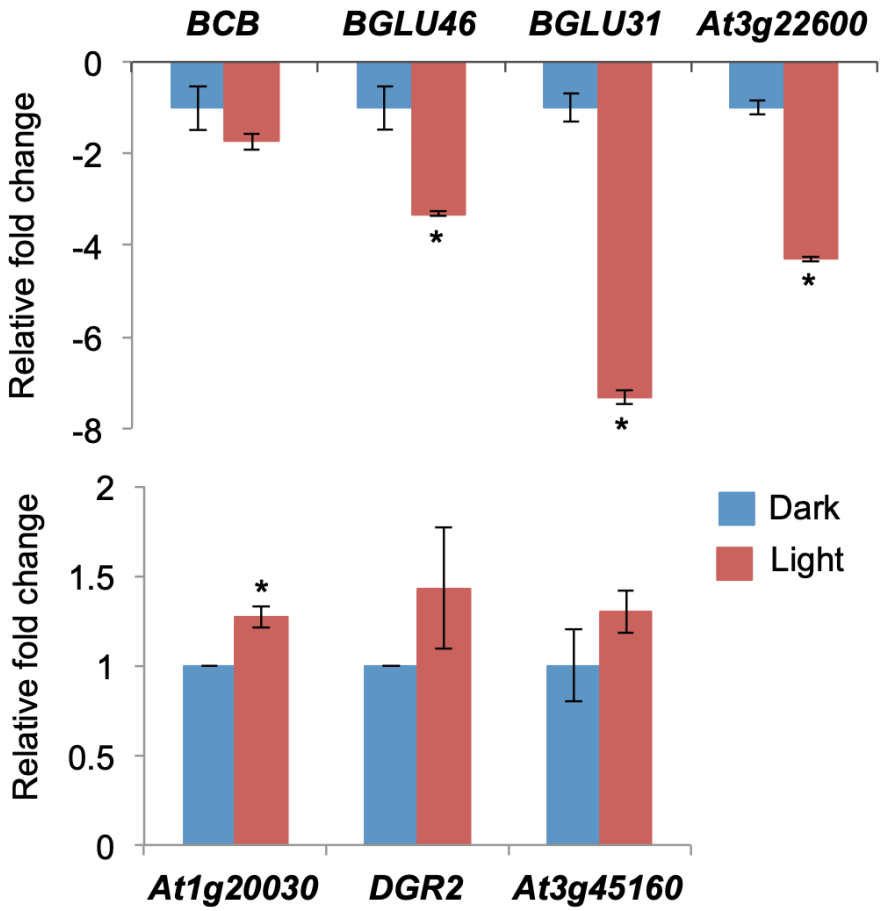

Figure 3.8. Effects of light on Arabidopsis gene expression of additional protein candidates. RNA used for qRT-PCR analysis was obtained from 3-pooled biological replicate flasks of 3-days-old light- and dark-grown cell cultures. qRT-PCR values are an average of 3 technical replicates. Bars represent mean ± SD (n = 3). An asterisk indicates a significant difference between light and dark ($p \leq 0.05$). *ACTIN2* and *EIF4A* were used as constitutive reference control genes.

3.7 Light-dependent gene expression in response to FB1

After selecting candidates that respond to light from the iTRAQ dataset, the next step was to determine whether these candidates also respond to FB1. For candidates responsive to FB1, it would also be crucial to establish if this response was regulated by light. Ideally, this should have been done using proteomic analysis, but the cost of iTRAQ experiments is prohibitive. Therefore, time-course experiments using gene expression analysis were a cheaper option. The purpose of this analysis was to further filter the list of proteins from the iTRAQ dataset to a selection of genes that respond to FB1 in a light-dependent manner. These genes will be ideal candidates to progress onto reverse genetic analysis.

Arabidopsis cell cultures, grown either in light or darkness, were treated with 1μM FB1 and cell samples were harvested at specific time-points up to 72 hours. Gene expression was performed by qRT-PCR analysis using gene-specific primers targeting selected candidates. Interestingly, many of the proteins that were originally showing lower expression in response to light, were expressed at very high levels in response to FB1 under light conditions. *RNS1, BFN2, CYC1, FLA13* and *FLA9* are all highly expressed under light conditions in response to FB1-treatment; however, this response was inhibited in the dark (Figure 3.9). *SBT2.1* and *BGCL1* are marginally expressed at higher levels in response to FB1 under light conditions, but did not appear to be expressed to the same extent as the other proteins (Figure 3.9). *PRX52, At3g61820, At5g07030* and *PRX71* were expressed at higher levels in response to light in untreated samples (Figure 3.7), but after treatment with FB1 they showed higher expression under dark conditions (Figure 3.9). However, *PRX71* showed slightly higher expression in response to light at later time points (Figure 3.9). *At5g58090* showed no significant response to either light-regulation or FB1 treatments (Figure 3.7 & 3.9). These results show a curious phenomenon where genes that were originally showing higher or lower expression in response to light in the absence of the toxin display a reverse trend upon FB1 treatment. Those that responded to light-regulation post FB1-treatment appeared to show a more dramatic response (maximum ~ 150 fold), whereas those that showed lower expression in response to light conditions were only marginally changing (maximum ~6 fold) (Figure 3.9).

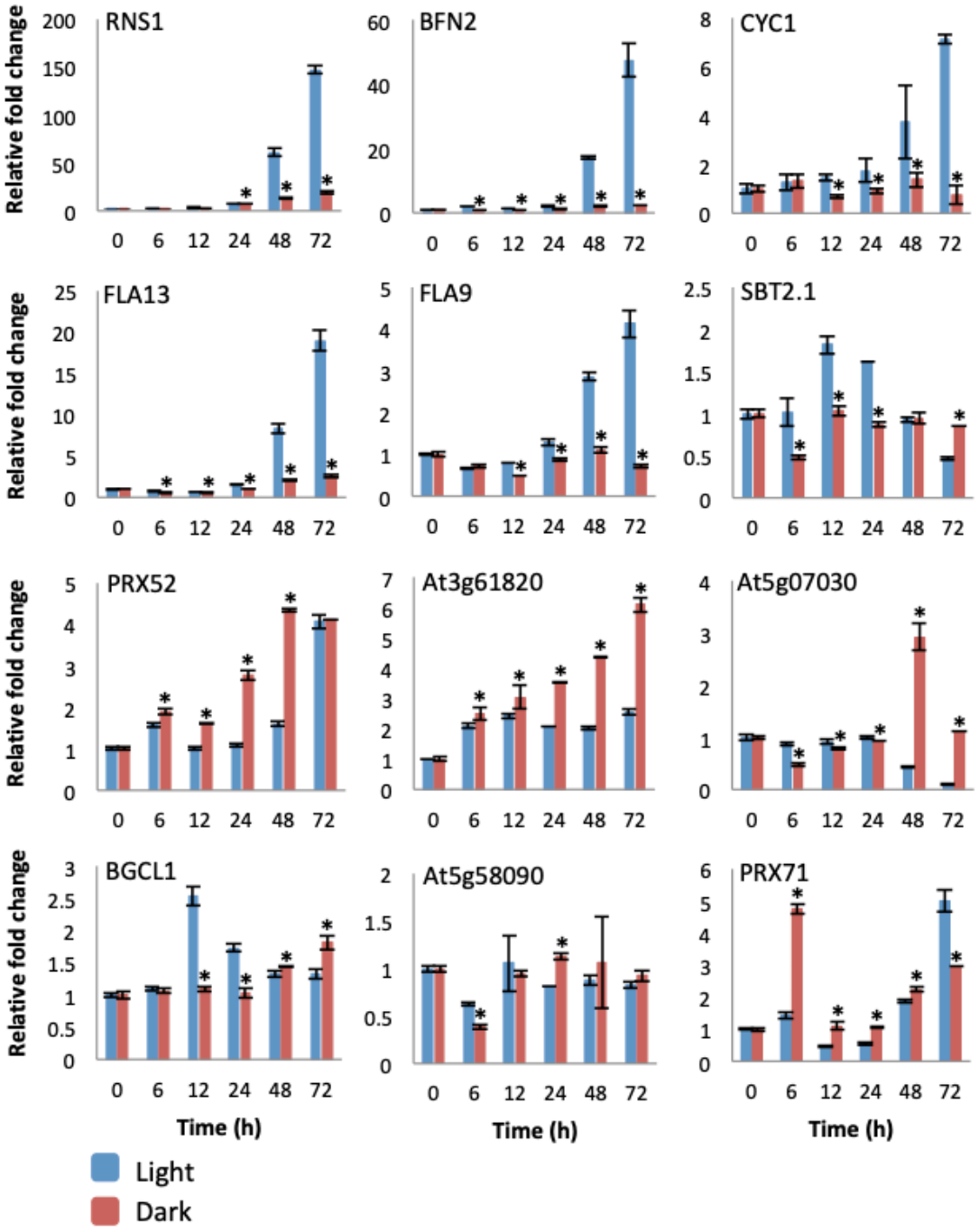

Figure 3.9. Effects of light on FB1-induced gene expression. Light- and dark-grown Arabidopsis cells were treated with 1μM FB1 and samples for RNA extraction harvested at the indicated time-points. RNA was extracted and transcript abundance analysed by qRT-PCR. qRT-PCR values are an average of 3 technical replicates. Bars are mean ± SD (n = 3). An asterisk indicates a significant difference between light and dark ($p \leq 0.05$).

I also chose to analyse the candidates that did not show a significant response to light in the iTRAQ screen, including those that were not identified at all. *BCB* showed no significant difference in response to light (without FB1), which explained why it was not identified as a significant protein by the iTRAQ. However, upon FB1 stimulation, *BCB* was highly expressed under light conditions and this response was inhibited under dark conditions (Figure 3.10). *BGLU46* and *BGLU31* showed the same pattern as *BCB* and yet were not identified at all in the iTRAQ, even in the total number of ECM proteins. *At3g22600* showed lower expression under light conditions and then higher expression in response to light upon FB1 stimulation (Figure 3.10). Although *At3g22600* was not as highly expressed in response to FB1 under dark conditions as it is in the light, it was not inhibited unlike *BCB*, *BGLU46* and *BGLU31*. *DGR2* showed no significant difference is response to light in the absence of FB1 (Figure 3.10), and did not respond at the protein level as well. However, after FB1 treatment, *DGR2* showed lower expression under light conditions when compared to the dark. Similar to the candidates from iTRAQ, genes showing lower expression under light conditions had marginal expression levels when compared to genes shower higher expression under light conditions. *At3g45160* was also initially non-responsive to only light. After stimulation with FB1, the gene showed lower expression under light conditions and returned to basal levels after 24 hours. Under dark conditions there was little discernable difference until it reached 12h, when the gene showed progressively lower espression. *At1g20030* showed no differences between light- and dark-incubated cells, and there was a very marginal response to FB1 treatment. These proteins not identified in the iTRAQ analysis clearly showed a similar pattern to some of the candidates within the iTRAQ dataset, in that proteins showing higher expression levels in response to light or dark conditions in untreated samples conform to a reverse pattern upon FB1 treatment. As stated previously, even though the response to FB1 at a transcript level is interesting, the final product is the protein. Therefore I chose to not continue with the genes that were not among the list of 172 proteins significantly identified from the iTRAQ.

The process of using light as a filter to discover proteins that respond to FB1 proved successful. The filter confirmed that light regulation plays an important role in FB1 detection and protein expression. The filter, comprising of proteomics and

transcriptomic analyses, provided a selection of genes that could be used for further analysis. The data from the iTRAQ also helped generate an in-house secretome database, which will be useful for future projects.

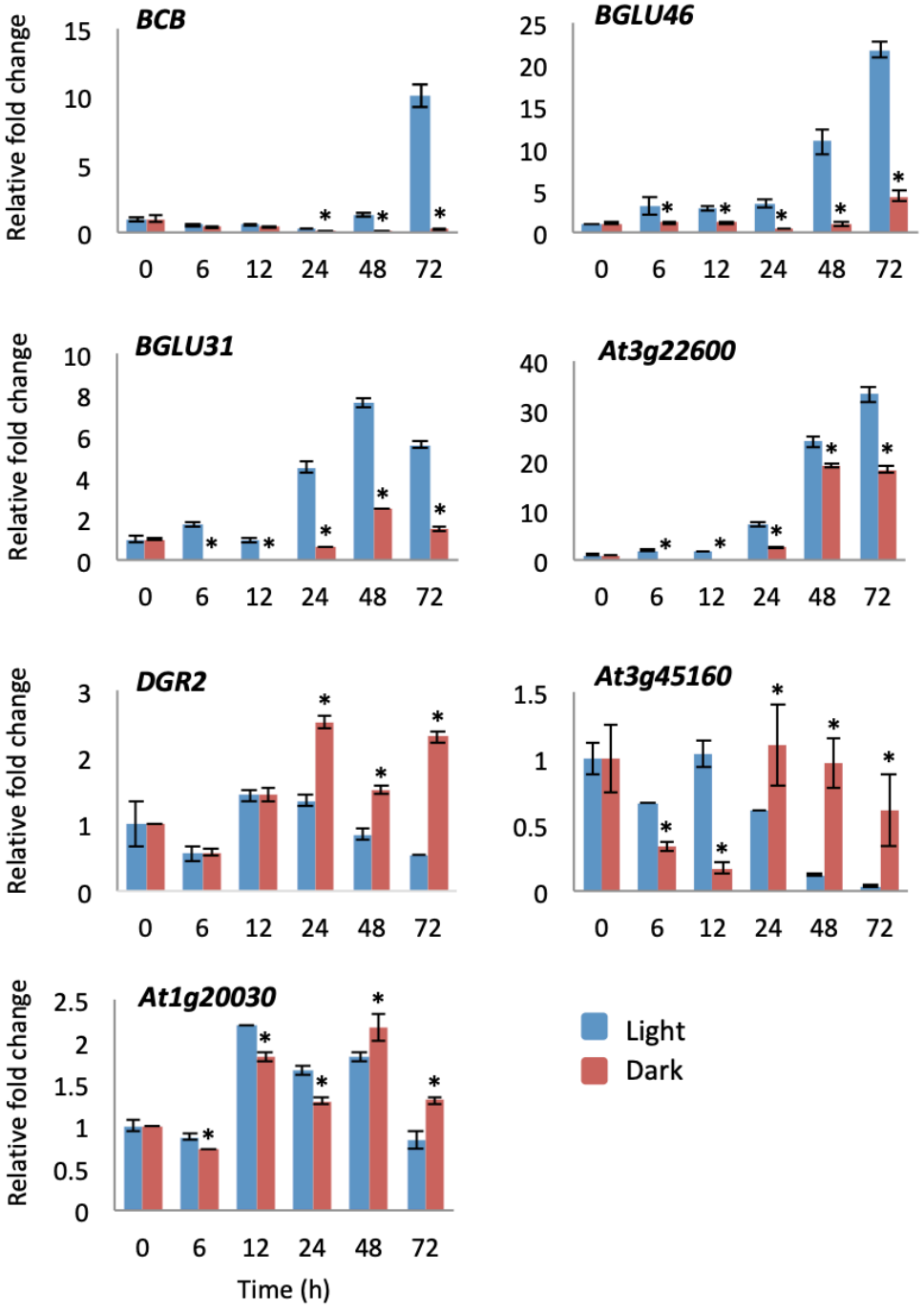

Figure 3.10. Gene expression analysis of additional proteins not identified by the iTRAQ screen. Light- and dark-grown Arabidopsis cells were treated with 1µM FB1 and samples for RNA extraction harvested at the indicated time-points. RNA was extracted and transcript abundance analysed by qRT-PCR. qRT-PCR values are an average of 3 technical replicates. Bars are mean ± SD (n = 3). An asterisk indicates a significant difference between light and dark ($p \leq 0.05$).

3.8. Potential role for PHYB in FB1-induced PCD

PHYB is the major photoreceptor for red/far-red light and mediates diverse light-dependent biological processes. Due to light-dependence of FB1-induced PCD, I wanted to investigate if the PHYB photoreceptor might play a role in this cell death response. I obtained T-DNA insertion gene knockout mutants, *phyb-1* (SALK_022035) *and phyb-2* (SALK_069700) from the SALK collection (Alonso *et al*., 2003). To begin with, I confirmed that both lines were indeed gene knockout lines with no *PHYB* transcripts, or that the transcript had a disruptive T-DNA insert. RT-PCR analysis, using primers spanning the T-DNA insertion positions, showed no transcript in the mutant lines, while an expected product was amplified in the Columbia-0 (Col-0) wildtype plants (Figure 3.11). This confirmed that these are loss-of-function mutants, with the previously reported phenotype of very long petioles (data not shown).

To evaluate the response to *phyb* loss-of-function mutants to FB1, leaves of 4-week-old plants were infiltrated with 3μM FB1. There was a significant reduction of FB1-induced PCD in the *phyb* lines in comparison to Col-0 plants (Figure 3.12). This suggests that photoreception through PHYB plays a dominant role in the development of FB1-induced PCD.

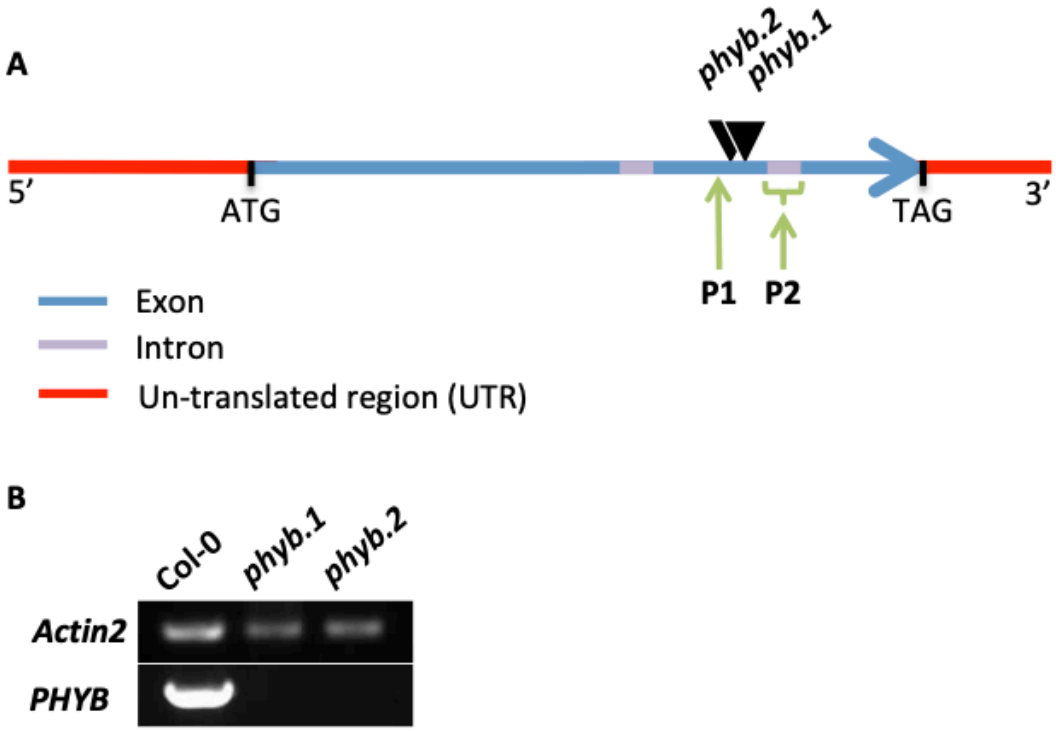

Figure 3.11. RT-PCR analysis of *phyb* knockout mutant plants. A) Schematic of the T-DNA insertion positions within the *PHYB* gene. **B)** Primers spanning the T-DNA insertion positions were used to show a transcript product in the Col-0 (P1 and P2 indicate primer positions). The two *phyb* lines did not produce the same transcript product, indicating that the lines have a T-DNA insertion. The *Actin2* served as a constitutive reference control gene.

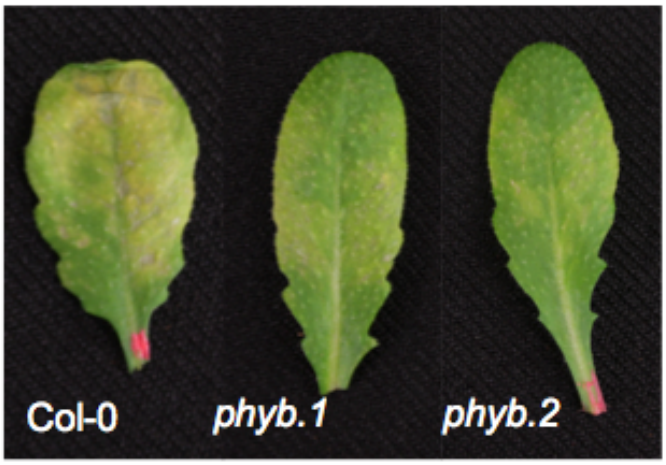

Figure 3.12. FB1-induced PCD is suppressed in loss-of-function *phyb* mutants. Arabidopsis wildtype (Col-0) and *phyb* knockout mutant plants were infiltrated with 3µM FB1. Leaves were detached from plants and photographed 3 days post infiltration.

Given that photoreception by PHYB plays a role in FB1-induced PCD, I next used the *phyb* knockout mutants to investigate if FB1 stimulation of gene expression is also dependent on PHYB signalling using selected candidates. *RNS1, ENDO2, PRX52* and *CYC1* were selected as they responded strongly to FB1 in a light-dependent manner. Four-week-old Arabidopsis plants (wild type and *phyb* mutants) were infiltrated with 3 μM FB1 and tissue for RNA extraction harvested every 24 h until 72h. The qRT-PCR analysis for each gene show a consistent trend of increased expression in the wild type which is inhibited or increased to a lesser extent in the *phyb* mutants (Figure 3.13). *RNS1* is up-regulated in the WT, peaking at around 14-fold at 12 hours, and then returning to lower levels from 24 hours (Figure 3.13). ENDO2 is marginally up-regulated to 2-fold in the WT, however the *phyb* mutants show consistent inhibition of this response among both of the lines (Figure 12). *PRX52* shows a gradual incline of gene expression in the wild type, however the maximal gene expression reaches an immense level of around 70-fold in the WT at 48 hours, and then begins to decline. The *phyb* mutants also show a gradual increase in gene expression, however this response is slower, with the highest peak at the last time point with an average fold change also around 70-fold between the two lines (Figure 3.13). *CYC1* shows a similar response to *PRX52* with a massive up-regulation in the WT, which is significantly lesser in the *phyb* mutants; but the transcription is not completely inhibited. The *phyb* mutants also eventually reach a similar abundance as WT at 72 hours (Figure 3.13).

The *phyb* knockout lines show an overall trend of inhibiting the transcription completely, or to a lesser extent, of these FB1-responsive genes. From the phenotypic response of the *phyb* lines, PHYB appears to be important in FB1-induced PCD. The PHYB protein also appears to have a substantial effect on FB1-responsive gene expression. However, the response to FB1 in some genes (*PRX52* and *CYC1*) is not completely inhibited in the *phyb* lines, suggesting that further light-dependent signalling pathways are resulting in the transcription of these genes in response to FB1.

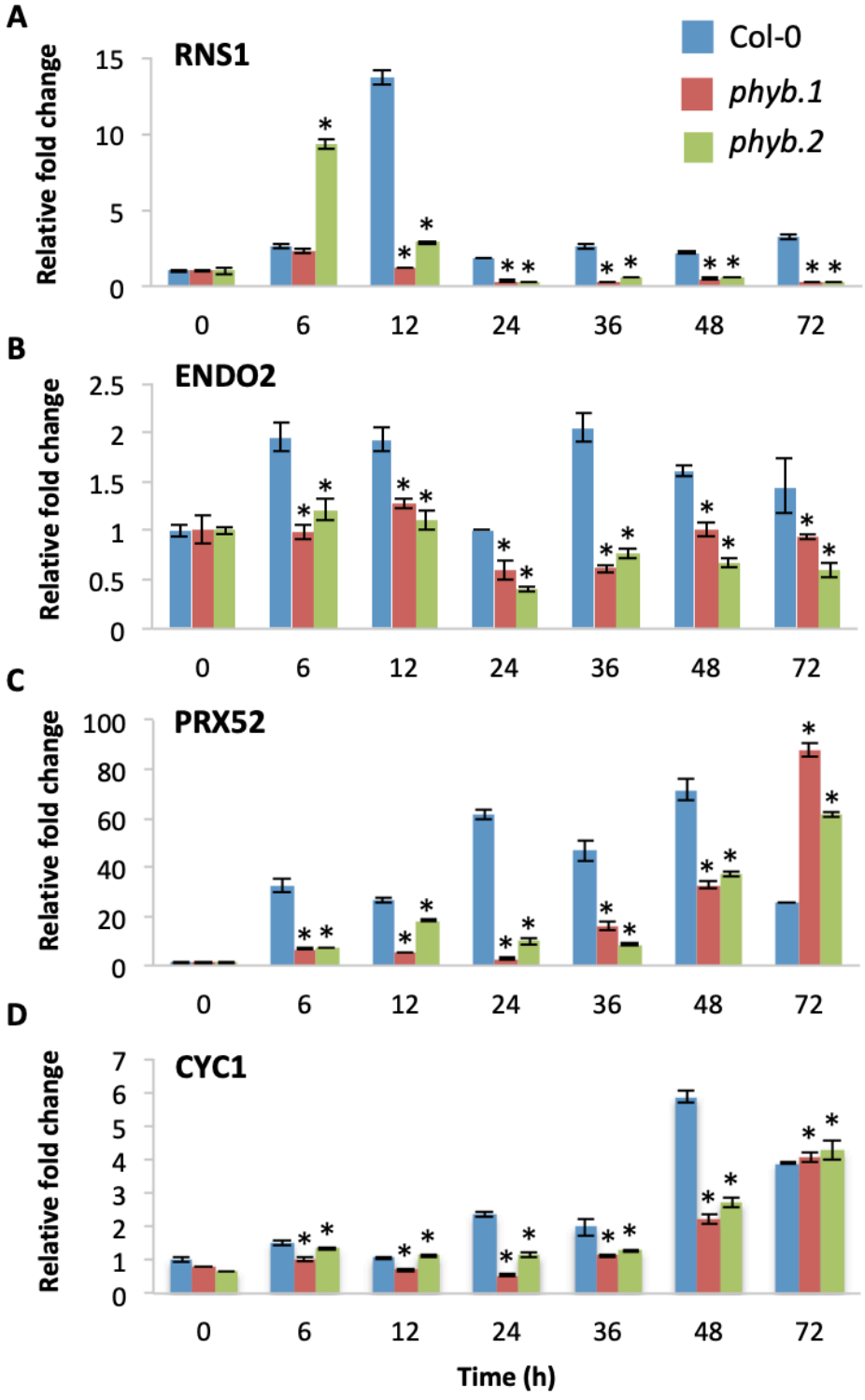

Figure 3.13. FB1-induced gene expression in loss-of-function *phyb* mutants. Leaves of wildtype and *phyb* mutant plants were infiltrated with 3µM FB1. RNA was extracted from 3 leaves, from 3 biological replicate plants, and harvested at indicated time-points. The RNA was analysed by qRT-PCR. qRT-PCR values are an average of 3 technical replicates. Bars represent mean ± SD (n = 3). Significant differences between wildtype and mutants are indicated by 1 ($p \leq 0.05$) or 2 ($p \leq 0.01$) asterisks.

3.9. Discussion

3.9.1. An *in vitro* cell culture system combined with proteomics is a powerful gene discovery tool

In order to gain new biological insights, it is sometimes necessary to focus experimental investigations on a particular subcellular compartment. Proteomics is useful in this regard as it combines protein fractionation, mass spectrometry and bioinformatics analysis. Previous studies have used proteomics to identify Arabidopsis proteins in a range of subcellular locations, such as: the nucleolus, chloroplast envelope membranes; leaf peroxisome, and mitochondria (Pendle *et al*., 2005; Bae *et al*., 2003; Ferro *et al*., 2003; Reuman *et al*., 2009; Millar *et al*., 2001). However, there are technical challenges to the isolation of protein fractions enriched for a particular compartment when using whole plants as the starting biological material. In this chapter, the use of cell suspension cultures was adopted, particularly because the mobile phase of the extracellular matrix can be isolated via simple filtration without tissue homogenisation. This provided protein fractions enriched for secreted proteins expressed in undifferentiated cells.

Treatments with FB1 demonstrated that cell death responses in this *in vitro* system mimics what happens in Arabidopsis plants, indicating that this system is suitable for studying plant cell death. Previous studies have similarly used plant cell culture systems as investigative tools to gain insights into complex physiological processes. For example, a role for a burst in reactive oxygen species in plant-pathogen interactions was revealed by experiments conducted using cell suspension cultures (Lamb & Dixon 1997; Mehdy *et al*., 1996). Cell culture systems were also instrumental in the discovery the role of extracellular ATP in FB1-induced cell death (Chivasa *et al*., 2005). Kaffarnik *et al*. (2009) also used Arabidopsis cell cultures and proteomics to identify ECM protein responses to different bacterial pathogens.

The main focus of this chapter was to develop a screen to identify proteins with a putative regulatory role in cell death triggered by the mycotoxin FB1. As FB1-triggered PCD response in Arabidopsis is light-dependent (Stone, *et al*. 2000; Asai. *et al*. 2000), I incorporated light in developing a screen to identify such proteins using cell cultures. In the course of these experiments, I made the unexpected

discovery that the culture medium contains light-induced secreted factors, which are powerful regulators of FB1 toxicity. Thus, the screen was then designed to focus on the ECM compartment and led to the identification of over 100 proteins. It is anticipated that some of the numerous proteins identified in this chapter will prove to have key PCD regulatory roles, particularly the subset of proteins whose response to FB1 is light-dependent.

3.9.2. Robustness of the screen for identifying PCD-regulatory protein targets

The first stage of the screen was to identify all proteins within the soluble phase of the ECM, which responded to light. Mass spectrometric analysis and database searches identified 363 proteins in these ECM fractions, with 172 of these showing a statistically significant response to light. The latter were considered to be potential candidates that could have a putative cell death-regulatory function. The second stage of the screen was to select candidates for gene expression analysis. The candidate selection process incorporated wide-ranging considerations, including preference for proteins showing high fold-changes in response to light; proteins representing the most abundant protein families appearing in the dataset (e.g. aspartyl proteases, flasciclin-like arabinogalactans, peroxidases); and also genes that have been previously linked with FB1-induced PCD from our research group (e.g. *CYCLASE1, BFN2, PRX52, RNS1*).

To test the effectiveness of the screen, some ECM proteins that had been excluded by the screen were selected for gene expression analysis. The genes were selected from previous ECM proteomics datasets and PCD-studies in the literature. This inquiry into the robustness of the screen showed two potential flaws. Firstly, a number of proteins excluded by the iTRAQ screen for lack of a statistically significant response to light (BCB, DGR2 and At3g45160), responded to FB1 in a light-dependent fashion, with a gene expression profile befitting candidates with a putative role in PCD control. This indicates that initially screening proteins based on light response, in the absence of FB1 stress; may result in exclusion of proteins that do not respond to light under optimal growth conditions, yet they significantly respond to PCD stimulation. Secondly, genes selected from alternative PCD investigations (BGLU46, BGLU31 and At3g22600), which were not detected by the screen, showed gene response profiles consistent with what would be expected of

cell death-regulatory candidates. In untreated cell cultures, there was a significant difference in transcript abundance between light and dark cell cultures (Figure 3.8). Furthermore, exposure to FB1 not only massively increased expression of all three genes in the light, but this response was significantly supressed under darkness (Figure 3.10). Failure to detect these proteins in the ECM protein fractions might indicate their extremely low abundance in primary undifferentiated cells. Therefore, protein abundance is a limiting factor to this screen. Taken together, these results suggest that to increase the effectiveness of the screen, an FB1 time-course proteomic analysis, plus or minus light, would be a more appropriate filter, rather than focusing on light-regulation prior to imposition of the PCD stimulus. An alternative iTRAQ analysis on light/dark cultures, including multiple time-points after FB1 treatments, is extremely costly to be feasible.

Notwithstanding these shortfalls, the screen identified proteins already known to regulate FB1-induced PCD. A previous publication from our group used iTRAQ analysis of the ECM proteome to identify a protein responsible for the negative regulation of cell death in Arabidopsis (Smith *et al*., 2015). In that study, treatments with salicylic acid (SA) and exogenous ATP led to the identification of 33 putative cell death-regulatory proteins. SA is a plant hormone commonly known for its promotion of PCD (Asai *et al*. 2000) and exogenous ATP has the ability of blocking FB1-induced PCD (Chivasa *et al*. 2005). The response of the 33 proteins to SA was attenuated by exogenous ATP, implicating these proteins in PCD regulation. One of these proteins was identified as CYCLASE1 (CYC1), which had no known function prior to this publication. Loss-of-function transfer-DNA (T-DNA) knock out mutants of CYC1 had increased sensitivity to FB1, displaying increased levels of PCD when exposed to FB1 treatments. Thus, CYC1 was identified through proteomic analysis of the culture filtrate of Arabidopsis, and then shown to play an essential role as a negative regulator of cell death (Smith *et al*. 2015).

CYC1 was identified in the iTRAQ dataset within this chapter as a protein that shows lower expression under light conditions. However, qRT-CPR analysis of cell cultures subjected to FB1 treatments under light or dark conditions shows that *CYC1* expression is dramatically increased in the light by FB1, with dark-incubation

inhibiting this response (Figure 3.9). The fact that CYC1 was captured by the screen developed in this chapter provides confidence in the dataset generated here.

3.9.3. A broad range of ECM protein families are implicated in plant PCD

The most abundant class of proteins in the iTRAQ were aspartyl proteases. Aspartic proteases use water, bound to an aspartate residue, to catalyse peptide hydrolysis. *At3g61820* and *At5g07030* are two aspartyl protease family proteins I selected for gene expression profiling. However the previous examples of aspartic proteases and their roles in PCD shows a strong precedence for this family of proteins in plant defence and possible defence-related PCD pathways. Transcripts and peptides of both genes were increased by light in the absence of stress. Upon FB1 treatment, both genes showed increased expression under light conditions, with continuous darkness suppressing this response (Figure 3.9). Although both proteins have not been directly linked with PCD, there is precedence for extracellular aspartyl protease function in plant defence and PCD responses. For example, CONSTITUTIVE DISEASE RESISTANCE 1 (CDR1) is an extracellular aspartic protease, which functions in salicylic-acid-dependent resistance to virulent *Pseudomonas Syringae* (Xia *et al*., 2004). Over-expression (OE) mutants resulted in hyper-activation of disease resistance. The OE mutant accumulated high levels of SA, increased transcription of SA marker genes (*PR1* and *PR2*), exhibited localized PCD, and oxidative bursts (Xia *et al*., 2004). Another extracellular aspartic protease plays a role in PCD during embryonic development. Loss-of-function mutants of PROMOTION OF CELL SURVIVAL (PCS1) have excessive cell death of developing embryos (Ge *et al*., 2005). Ectopic expression of PCS1 results in cell survival of septum and stomium cells in anther walls, resulting in male sterility (Ge *et al*., 2005).

Two of the candidates selected from the iTRAQ dataset were nucleases, ENDONUCLEASE2 (ENDO2/BFN2) and RIBONUCLEASE1 (RNS1). Endonucleases are enzymes that break down polynucleotide chains into shorter chains by cleaving the phosphodiester bond within the chain, and ribonucleases are similar to endonucleases, but are responsible specifically for the degradation of RNA. Endonucleases have been linked to PCD for many years, starting in mammalian systems. It was revealed that in mammalian lymphoid cells subjected to

glucocorticoid hormones, cell deletion occurred in a 'programmed' manner (Wyllie, 1980). This process was associated with endonuclease activity that removed nucleosome chains from nuclear chromatin (Wyllie, 1980). The concept of endonuclease responsibility for PCD in mammalian systems was also investigated in plants. In tobacco, detection of nuclear DNA degradation and an increase in activity of several endonucleases has been associated with Tobacco Mosaic Virus (TMV)-induced cell death (Mittler *et al*. 1995). Further investigations have shown that calcium-activated endonuclease cleavage of DNA induces a hypersensitive response after *Phytophthora infestans* infection in tomato (Wang *et al*. 1996). While these reports clearly show a role for nuclease enzymes in PCD-associated degradation of nucleic acids, how extracellular nuclease may participate in PCD is unclear.

Using GeneVestigator, I was able to determine whether ENDO2 and RNS1 have previously been implicated in light-regulation or PCD studies. RNS1 has shown higher expression in response to light and pathogen defence independently. However, RNS1 does not appear to be a focal point for light- or PCD-studies, and the light-dependence on PCD response in RNS1 has not been shown in previous literature. ENDO2 appears to have even less evidence from previous studies implicating the protein in light-regulation or PCD; and again there appears to be no specific link to a role in light-dependent PCD.

My iTRAQ results have shown lower expression of ENDO2 and RNS1 in response to light conditions, which was also observed at the transcript level. qRT-PCR analysis of the gene transcript, after FB1 treatment, shows *ENDO2* and *RNS1* expression to be massively increased, and this response is inhibited under dark conditions (Figure 3.9). This project is the first to recognise ENDO2 and RNS1 as FB1-responsive proteins, regulated by light.

Another group of proteins with a strong presence in the iTRAQ dataset are peroxidases. I identified a total of 13 peroxidases in the ECM, with 7 of these peroxidases significantly responding to light (Table 3.2). Peroxidases are a large family of antioxidant enzymes that catalyse the oxidation of numerous hydrogen donors in the presence of hydrogen peroxide or similar peroxides. In plants there are three different classes of peroxidases; intracellular class I, fungal-released class II, and secreted class III peroxidases (Welinder *et al*., 1992). Most of the peroxidases

identified in the iTRAQ data set come from the family of class III peroxidases (Prxs) found in higher plants. In Arabidopsis, this particular family consists of 73 heme-containing peroxidases (Welinder *et al*., 1992). Plant Prxs are glycoproteins that are easily detected through the whole lifespan of a plant, and have implications in a vast range of physiological functions; such as auxin metabolism, pathogen defence, lignin formation, cross-linking of cell wall components, metabolism of ROS and cellular growth (Liszkay *et al*, 2003). Plant Prx proteins play a vital role in plant defence, and belong to the PR-protein 9 subfamily of Pathogenesis-related (PR) proteins (van Loon *et al*., 2006). In plant defence, Prxs prevent infection spreading by reinforcing cellular structural barriers and generating ROS in order to create a toxic environment in which a pathogen is unable to survive.

Due to the secretory nature of Prx proteins and their well-recorded involvement in pathogen defence, I chose the top two Prx proteins from the iTRAQ for further analysis. PRX71 showed one of the highest fold changes in response to light in the iTRAQ dataset. Upon reflection of the transcriptomic analysis, the response to FB1 appears to be minimal. PRX71 shows a slight up-regulation in response to FB1 under dark conditions in the first 6 hours that returns to normal levels from 12 hours. Another slight up-regulation in response to light is seen at 72h. This shows that either, PRX71 shows a marginal up-regulation in response to FB1, and minimal differentiation in response to light; or that a longer time course is required to see a more substantial light-regulated response to FB1 in PRX71 (Figure 3.9). PRX52 shows an up-regulation in response to FB1 in both light and dark conditions, however the up-regulation is initiated quicker under light conditions (Figure 3.9).

The responses of PRX71 and PRX52 to FB1 show light dependence, which has not been reported in previous literature. Using GeneVestigator, PRX52 has shown to positively and independently respond to both light and defence-inducing treatments; however, previous literature has not focused on PRX52 in further developing the mechanisms of light regulation or defence gene induction. For PRX71, GeneVestigator shows the protein to be massively upregulated in response to various defense-inducing treatments, however there is little evidence for a light-responsive

regulation of PRX71, which coincides with the marginal light-responsiveness in Figure 3.9.

Further two candidate proteins showing similar transcript responses as *ENDO2, RNS1* and *CYC1*, were *FLA13* and *FLA9*. These candidates were selected to represent the multiple FASCICLIN-LIKE Arabinogalactan (FLA) proteins that were identified by iTRAQ. There are 21 FLA proteins identified in the *Arabidopsis thaliana* genome (Gasper *et al*., 2001; Schultz *et al*., 2002). Six of these were identified, with five being significantly regulated by light (Table 3.2). FLA proteins are a subclass of Arabinogalactan Proteins (AGPs) and are putative cell adhesion molecules (Johnson *et al*., 2003). AGPs are highly glycosylated, hydroxyproline-rich glycoproteins shown to play a role in various elements of plant growth and development (Showalter, 1993). AGPs are located in the extracellular space (Samson *et al*., 1984), and have been identified in the growth medium of cultured cells (Komalavilas *et al*., 1991), which supports the findings in this chapter. Some AGPs have also been located in the plasma membrane (Komalavilas *et al*., 1991), in the cell wall (Basile and Basile, 1987; Serpe and Nothnagel, 1994), and in multi-vesicular bodies (Herman and Lamb, 1992). A role for AGPs in cell death has been proposed on the basis of pharmacological experiments using (β-D-galactosyl)$_3$ Yariv phenylglycoside, a reagent that binds to AGPs in a non-covalent manner. When Yariv reagent is added to Arabidopsis cell suspension cultures, AGPs bind to the reagent and PCD is induced (Gao and Showalter, 1999). FLAs also precipitate with β-glucosyl Yariv reagent, which indicates that they have similar structural properties with AGPs (Johnson *et al*., 2003) and therefore may also induce PCD when bound to the Yariv reagent. The iTRAQ has provided new information that a large proportion of the FLA family proteins are light regulated; and in addition, I have used transciptomic analysis to confirm that at least FLA13 and FLA9 are also responsive to FB1 in a light-dependent manner. My data on light-dependent gene activation by FB1 together with previous pharmacological studies using Yariv reagent, lends further support to the possibility that the FLA protein family and other extracellular AGPs may have crucial roles in PCD regulation.

Further protein families highly represented in the dataset include: leucine-rich repeats; glucosidases; berberine bridge enzyme-like; SKU5 similar; galactosidases; pectinases; late-embryogeneises abundant; xylosidases; serine-carboxypeptidases; glycosyl hydrolases; isomerases; purple acid phosphatases; xyloglucan endotransglucosylases; early nodulin; and thioredoxin reductases. Some of these protein families have been implicated in PCD; such as the previously mentioned LeEix2 protein with an extracellular leucine-rich repeat. Isomerase proteins have also been linked to PCD during seed development. For example, protein disulfide isomerase 5 (PDI5) accumulates in the endothelium during PCD, which occurs during embryo development in Arabidopsis (Ondzighi *et al*., 2008). Loss-of-function mutants of PDI5 exhibit premature PCD and have immature seeds (Ondzighi *et al*., 2008). Similary to PDI5, another abundant family from the iTRAQ has been reported to manifest developmentally-initiated PCD. Furthermore, the serine carboxypeptidase protease protein, carboxypeptidase III (CPIII), initiates PCD during development of vascular tissue in wheat (Dominguez *et al*., 2002). Finding proteins within the iTRAQ dataset that come from families that have been implicated in PCD previously, supports the decision to focus on secreted proteins, and also shows the importance of light-regulation on a myriad of proteins.

3.9.4. Precedence for ECM control of signalling and PCD

The ECM is a dynamic zone that regulates cell-cell interactions. It is well documented that ECM proteins are involved in numerous biological processes and functions. Proteins inhabiting the ECM are responsible for processes such as turgor and cell expansion, cell-to-cell signalling, response to biotic and abiotic stress, and creating and maintaining the integrity of the ECM (Roberts, 1994; Seifert and Blaukopf, 2010; Brownlee, 2002). For example, CLAVATA3 is crucial for plant development and is localized to the apoplast and signals at the cell surface. The export of CLAVATA3 to the ECM is required for the activation of the CLAVATA1/CLAVATA2 receptor complex (Rojo *et al*., 2002). This process is required to restrict the amount of stem cells accumulating at the shoot apical meristems (SAM). Loss-of-function mutants of either of these genes, results in

overgrowth and extra flower production (Clark *et al*., 1993, 1995; Kayes and Clark, 1998).

The notion that extracellular proteins could be key regulators of plant cell death is not unprecedented. It is well documented that numerous proteins localized to the soluble phase of the ECM have been implicated in PCD regulation. For example, a xyloglucan-specific endo-β-1,4-glucanase inhibitor 1 (CaXEGIP1) protein from pepper (*Capscium annuum*) is highly induced in leaves when infected with avirulent *Xanthomonas campestris* pv. *vesicatoria* (Xcv). Over expression of *CaXEGIP1* in Arabidopsis promotes cell wall modifications, resulting in spontaneous cell death, independent of pathogen infection, and enhances resistance to downy mildew (Choi *et al*., 2012).

Another example of a PCD regulator is the cytosolic ascorbate peroxidase protein, cAPX (APX1). Previous studies have shown the importance of reactive oxygen species in PCD, especially hydrogen peroxide (H_2O_2) (Levine *et al*., 1994, 1996; Jabs *et al*., 1996; Mittler *et al*., 1996; Draper, 1997; Shirasu *et al*., 1997). The cAPX protein has been shown to be a key scavenger of H_2O_2, enabling the detoxification of free radicals in the cytoplasm, and resulting in reduced PCD. After viral induction of PCD in tobacco, cAPX expression is reduced. This process appears to occur post-transcriptionally, as a steady state of cAPX transcript is maintained; however the protein abundance declines. The suppression of the cAPX protein appears to reduce the ability of cells to scavenge H_2O_2, resulting in increased ROS in the ECM and the acceleration of PCD (Mittler., *et al*. 1998). Although cAPX has been identified as a cytosolic protein, and other locations include: golgi apparatus, cell wall, chloroplast and plasmodesma (Arabidopsis.org. 2018); cAPX was identified by my iTRAQ in the soluble phase of the ECM. The iTRAQ showed that, within the ECM, cAPX is expressed at lower levels in response to light (APX1: -1.33 fold) (Table 3.1).

Certain cell surface receptors in the plasma membrane have also been implicated in cell death induction. For example, a fungal ethylene-inducing xylanase (EIX) protein is a potent elicitor of programmed cell death by interacting with plasma membrane receptors in particular plant species (Fuchs *et al*., 1989; Bailey *et al*., 1993; Ron and

Avni, 2004; Elbaz *et al*., 2002). In tomato, the characterisation of the LeEix locus identified a novel gene cluster that encode such receptors. Two members from the gene clusters included LeEix1 and LeEix2. The two identified proteins each contained a Leu zipper; extracellular Leu-rich repeat domain (containing glycosylation signals); a transmembrane domain; and a c-terminal domain mirroring that of a mammalian endocytosis signal. The two receptors are capable of binding with the fungal EIX elicitor. Silencing of the two receptors resulted in the inability of EIX to bind to the cell, and therefore averting PCD. Overexpression of either of the receptors allowed binding of EIX to the cell, however; only LeEix2 could induce PCD (Ron and Avni, 2004). Further work has shown BAK1 to play an important role in this receptor complex and a potential model was hypothesized: LeEix1 is bound to BAK1 under normal conditions. Upon EIX detection, dissociation of the LeEix1/BAK1 complex occurs, and LeEix1 binds to LeEix2 resulting in the attenuation of EIX induced internalization and signalling of the LeEix2 receptor, preventing EIX sifganlling and PCD. LeEix1 expression decreases over time and reaches its normal endogenous levels, freeing LeEix2 to internalize EIX and induce HR, at a lower level (Bar *et al*., 2011).

My project has shown that the ECM is a complex and dynamic structure, and has expanded on previous studies by connecting light-regulated extracellular proteins with FB1-induced PCD. The secretome screen has identified proteins that have previously been implicated in PCD and plant defence, as well as identifying proteins with no previous link with PCD. The screen opens up new opportunities to focus on particular proteins, or protein families, for further PCD analysis, with the aim of understanding the pathways that ultimately result in PCD.

3.9.5 PHYB is crucial in regulating FB1 responses

As stated in chapter 1, light perception and regulation is achieved through photoreceptors, with phytochromes being at the centre of most studies. Phytochromes interact with PIFs (Phytochrome Interacting Factors), with PIF1, PIF3 and PIF6 showing a particularly strong affinity to PhyB (Toledo-Ortiz *et al*., 2003; Duek and Fankhauser, 2005). PIFs act as negative regulators of phytochrome activity, and are rapidly degraded in the presence of light (Al-Sady *et al*., 2006). PhyB has been implicated in plant immunity, particularly that of ROS production

and UV-induced cell death (Rusaczonek *et al*., 2015). Although there are various photoreceptors, due to the well-established nature of PhyB and its previous implications in plant immunity, I chose to investigate whether PhyB may regulate candidates selected from the screen developed here.

Phytochromes have not been implicated in FB1-induced cell death, however, by simply injecting FB1 into two independent *phyb* knockout mutant lines, a discernable difference in cell death response was demonstrated (Figure 3.12). This indicates that light perception via PHYB signalling is a potential positive regulator of cell death. Analysing the iTRAQ candidates in the *phyb* mutant background revealed that *RNS1, ENDO2, PRX52* and *CYC1* have altered gene transcription in response to FB1 compared to that of the wild type (WT).

First thing to note is the differing transcript profiles of each of the genes in response to cell culture treatments, compared with *in planta* experimentation. *RNS1, ENDO2* and *CYC1* show greater significance in the relative fold change of transcript abundance in cell cultures (Figure 3.8), rather than *in planta* (Figure 3.13). For *PRX52*, however, the opposite response is observed. The relative fold change in planta is drastically increased in FB1 treated leaf tissues against the untreated (Figure 3.13); this response is less significant in cell cultures (Figure 3.8). This is an interesting analysis and shows insight into how certain genes will respond more significantly in totipotent tissue, compared to specific tissue type (e.g. leaf tissue), and vice versa. For future investigation into further candidates from the iTRAQ analysis, analysis of the transcript abundance in both cell cultures and *in planta* should become routine.

The two independent *phyb* knock out lines show a similar trend of down-regulated transcription for each of the genes in comparison to the wild type. The *RNS1* transcription appears to be significantly regulated by PHYB to a greater extent than the other genes. *RNS1* peaks at 12 hours in the wild type and is then quickly down regulated. In the loss-of-function mutants, *RNS1* is completely inhibited in the knock out lines after 24 hours. In the WT, however, the expression after 24 hours is maintained marginally higher than the untreated time point. *ENDO2* shows a marginal level of up-regulation in response to FB1, however this response is completely inhibited in the mutants. *PRX52* and *CYC1* also show a general trend of

increased transcription in the wild type, which is stunted in the loss-of-function mutants; however, unlike *RNS1* and *ENDO2*, the transcription is not completely inhibited (Figure 3.13).

In conclusion, PHYB plays a pivotal role in gene regulation upon exposure to FB1 *in planta*. This response shows a complete inhibitory effect on RNS1 and ENDO2 transcription. For PRX52 and CYC1, although there is a prominent down regulation of gene transcription in the knockout mutants, the gene transcription is not completely inhibited. PHYB is a crucial protein in regulating FB1 responsive genes. For certain genes, PHYB is required for gene transcription (e.g. RNS1 and ENDO2). However, for other genes, PHYB appears to have an additive effect on gene transcription, and a PHYB-independent pathway is able to partially regulate their transcription (e.g. *PRX52* and *CYC1*). Although PHYB is clearly not the only receptor for FB1-induced gene regulation; plants are phenotypically affected by the loss of the PHYB protein. Also, key FB1-responsive genes are either partially, or completely, inhibited with loss of PHYB functionality.

3.9.6 Concluding remarks

ECM secretions play an incredibly significant role in FB1-induced PCD, and light is crucial in regulating this phenomenon. Using light-regulation as a screen for secreted proteins, which are responsible for FB1-induced PCD signalling, has been a success. The screen has produced a list of 172 proteins regulated by light, and from selecting a small number of proteins to analyse; I have found genes with significant transcriptional responses to FB1. Although the short-list of potential FB1-regulating genes has proved promising, the iTRAQ has much further potential for identifying many more FB1-responsive genes, regulated by light.

4
Ribonuclease 1 promotes FB1-induced cell death

4.1. Introduction

A regular forward genetics approach to elucidate signalling pathways underpinning a particular physiological process begins with creating mutant phenotypes via disruption or enhancement of an unknown gene(s). The mutation may have occurred naturally or through the induction of mutagenesis by chemicals, radiation or transposable elements. Subsequent back-crossing results in the isolation of individual mutants, which are then used for progeny ratio analysis (Griffiths *et al*., 2005). A more recent approach to genetic studies uses reverse genetics, which has only been made possible since the progress in recombinant DNA technology. In contrast to forward genetics, reverse genetics starts with a gene/protein, and works backwards towards the development of a mutagenized version of the gene. This ultimately provides a mutant phenotype, indicative of the disruption or loss of the gene-of-interest (Griffiths *et al*., 2005). The development of reverse genetics has been established in the Arabidopsis community through insertion mutant collections, along with the Arabidopsis genome initiative (Azpiroz-Leehan *et al*., 1997; Krysan *et al*., 1999; Speulman *et al*., 1999; Tissier *et al*., 1999; Parinov *et al*., 1999; Parinov and Sundaresan, 2000; Sussman *et al*., 2000; Sessions *et al*., 2002; Samson *et al*., 2002; Alonso *et al*., 2003; Kleinboelting *et al*., 2011; Arabidopsis Genome Initiative, 2000).

The proteomic screen in chapter 3 provided a list of proteins that may play a potential a role in the light-regulated Arabidopsis PCD in response to FB1 treatment. The objective in this chapter was to select a single candidate from the screen and obtain loss-of-function mutants and generate transgenic plants complemented with the native and mutant forms of the target protein. These plants would be used for investigating the potential role of the protein in FB1-induced cell death

4.2. Selection of protein targets for reverse genetics

In the screen described in chapter 3, ECM proteins with a putative cell death-regulatory function were identified. One of the objectives of the current chapter was

to select candidate proteins for functional validation using transgenic plants. The proteins were ranked in descending order of the modulus of the fold-change in response to light (Table 3.1). The top 8 proteins were selected as suitable candidates for further analysis (Table 4.1).

Proteins in this shortlist were used for bioinformatics analysis using WU-BLAST2 searches of the TAIR10 protein database (Arabidopsis.org. 2018; Altschul *et al*., 1990; Gish *et al*., 1994). The WU-BLAST search provided a list of proteins showing high sequence homology to the selected candidates (Table 4.1). This was used as a way to identify potential gene family members of each of the candidates within the entire Arabidopsis genome. An example of the WU-BLAST output for *At2g02990* (*RNS1*) can be viewed in Figure 4.1. The genes with the highest similarity score were the most closely related, as reflected by the highly significant probability value (P-value). For most of the proteins, the scores of related gene family members were high and very close to each other, with a sharp drop in both the score and statistical significance taken to indicate very little relatedness of the proteins under comparison (see red arrow in Figure 4.1). The genes below the drop in score were discarded and not considered likely gene family members. In the example given in Figure 4, 4 genes showed high homology to *RNS1* (Figure 4.1). Therefore, it is likely that *RNS1* belongs to an Arabidopsis family of 5 members, which are indicated by the asterisks in Figure 4.1. An accurate WU-BLAST protein score was attained for the majority of the selected proteins, however the BLAST pulled out more than 400 LRR kinases with apparently similar sequence homology to *At3g22800.* After carefully studying the list of LRR kinases, I discovered a number of genes that belonged to very different families, examples include BRI1, involved in brassinosteroid signaling (He *et al*., 2000; Li *et al*., 2002); EFR, a receptor for the bacterial PAMP, EF-Tu (Zipfel *et al*., 2006); and a protein kinase expressed in meristem cells, MRLK (Takmura *et al*., 1999). Therefore I determined that the BLAST search was inconclusive for At3g22800.

Since loss-of-function mutants were to be used for validation of gene function, priority was given to candidates from small gene families in which the likelihood of functional redundancy is low. On the basis of this selection criterion, *RNS1* and *At1g15270* emerged as the top candidates. *RNS1* was chosen as the first candidate for

further investigation because of its gene expression profile in response to FB1 treatment and light (Chapter 3). Furthermore, previous studies implicate ribonuclease activity in PCD (Castelli *et al*. 1998; Roiz *et al*. 2006).

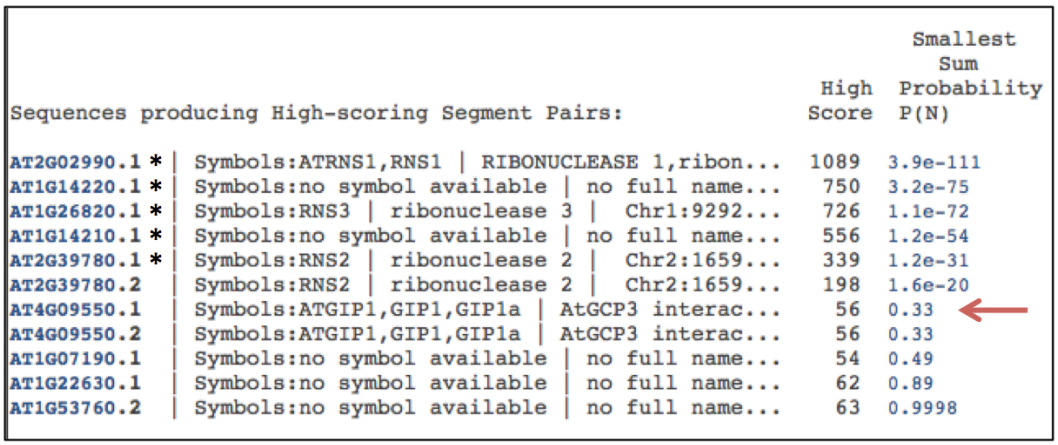

Sequences producing High-scoring Segment Pairs:			High Score	Smallest Sum Probability P(N)
AT2G02990.1 *	Symbols:ATRNS1,RNS1	RIBONUCLEASE 1,ribon...	1089	3.9e-111
AT1G14220.1 *	Symbols:no symbol available	no full name...	750	3.2e-75
AT1G26820.1 *	Symbols:RNS3	ribonuclease 3	Chr1:9292...	726	1.1e-72
AT1G14210.1 *	Symbols:no symbol available	no full name...	556	1.2e-54
AT2G39780.1 *	Symbols:RNS2	ribonuclease 2	Chr2:1659...	339	1.2e-31
AT2G39780.2	Symbols:RNS2	ribonuclease 2	Chr2:1659...	198	1.6e-20
AT4G09550.1	Symbols:ATGIP1,GIP1,GIP1a	AtGCP3 interac...	56	0.33
AT4G09550.2	Symbols:ATGIP1,GIP1,GIP1a	AtGCP3 interac...	56	0.33
AT1G07190.1	Symbols:no symbol available	no full name...	54	0.49
AT1G22630.1	Symbols:no symbol available	no full name...	62	0.89
AT1G53760.2	Symbols:no symbol available	no full name...	63	0.9998

Figure 4.1 WU-BLAST2 output after using RNS1 as the query sequence. The amino acid sequence of RNS1 (At2g02990) was used as query to search for highly homologous genes in the Arabidopsis genome database (TAIR10). A total of 9 individual genes were identified, but a sharp drop in the score and significance level can be seen between the proteins At2g39780 and At4g09550 (indicated by the red arrow). The red arrow indicates the cut-off point, and giving a total of 5 proteins (indicated with asterisks) in the RNS1 protein family.

Table 4.1. Predicted number of proteins in Arabidopsis protein families of selected candidates identified through iTRAQ

AGI[a]	*Symbol*[b]	*Protein name*	*Family size*[c]
At1g78850	MBL1	Curculin-like (Mannose-binding) lectin family protein	48
At5g19100	-	Eukaryotic aspartyl protease family protein	34
At4g12880	ENODL19	Early nodulin-like protein 19	43
At3g08030	-	DNA-directed RNA polymerase subunit beta	9
At2g02990	RNS1	Ribonuclease 1	5
At3g22800	-	Leucine-rich repeat extensin-like protein 6	N/A
At5g44130	FLA13	Fasciclin-like arabinogalactan protein 13	11
At1g15270	-	Translation machinery associated TMA7	2

[a]AGI (Arabidopsis Genome Initiative, 2000) code
[b]Gene symbol used in NCBI database
[c]Number of related proteins according to TAIR WU-BLAST2. A cut off probability score was set at $p < 0.05$

4.3. RNS1 is an ECM protein that responds to FB1

RNS1 was identified in the ECM of cell suspension cultures (see chapter 3). In accordance with its extracellular localization, *RNS1* possesses a signal peptide (Petersen *et al*., 2011) that targets it to the secretory pathway and no endoplasmic-retention motif, such as KDEL or HDEL (Sonnhammer *et al*., 1998; Krogh *et al*., 2001) (Figure 4.2). RNS1 has a P-loop, which is an ATP/GTP binding motif (Figure 4.2). This sequence is known as the Walker motif with a consensus sequence of GXXXXGK[T/S, where X stands for any amino acid (Saraste *et al*., 1990).

In chapter 3, the response of *RNS1* gene expression to FB1 was demonstrated using cell suspension cultures. Experiments to investigate if a similar response to FB1 exists in plant tissues were then conducted using *Arabidopsis thaliana* ecotype Columbia-0 (Col-0). Arabidopsis leaf discs were floated on either 3µM FB1 or water. The leaf discs were immediately incubated in complete darkness for 48 hours to allow maximal FB1 uptake, and then transferred to a 16 h-photoperiod. Samples were taken every 24 hours for analysis of gene expression through qRT-PCR. The

result in Figure 4.3 clearly shows that *RNS1* expression is strongly activated by FB1, particularly in the presence of light. This confirms the results from chapter 3 (Figure 3.9), showing light-dependent induction of *RNS1* expression by FB1 in cell cultures, is recapitulated in Arabidopsis plants tissues.

```
MKILLASLCLISLLVILPSVFSASSSSEDFDFFYFVQQWPGSYCDT
QKKCCYPNSGKPAADFGIHGLWPNYKDGTYPSNCDASKPFDSSTIS
DLLTSMKKSWPTLACPSGSGEAFWEHEWEKHGTCSESVIDQHEYFQ
TALNLKQKTNLLGALTKAGINPDGKSYSLESIRDSIKESIGFTPWV
ECNRDGSGNSQLYQVYLCVDRSGSGLIECPVFPHGKCGAEIEFPSF
```

Figure 4.2. The amino acid sequence of RNS1. The signal peptide sequence, highlighted in blue, targets RNS1 to the secretory pathway and there is no C-terminal H/KDEL motif, confirming that RNS1 is secreted to the extracellular matrix (ECM). The walker motif, which allows ATP-binding to RNS1, is highlighted in red.

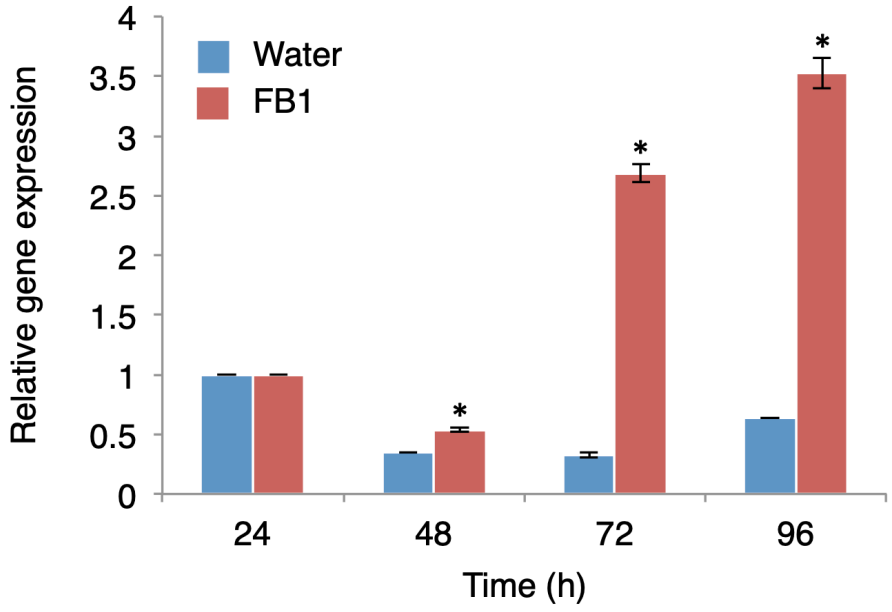

Figure 4.3. *RNS1* expression in response to FB1. Arabidopsis Col-0 leaf discs from 10 biological replicates were floated on either 3µM FB1 or water and incubated in the dark for 48h. They were then transferred to a 16/8 h light/dark cycle. Leaf discs for RNA extraction were harvested every 24 hours for and *RNS1* expression analysed by qRT-PCR using *ACTIN2* and *eIF4A* as constitutive reference control genes. qRT-PCR values are an average of 3 technical replicates. Bars represent mean fold-change ± SD (n = 3). An asterisk indicates a significant difference in the fold-change between control and FB1 samples ($p \leq 0.05$).

4.4. Generation of transgenic Arabidopsis lines with altered *RNS1* expression

T-DNA insertion knock out (KO) lines were obtained from INRA (Samson *et al*., 2002) GABI-Kat (Kleinboelting *et al*., 2011) and SALK (Alonso *et al*, 2003) collections. The INRA KO mutant (FLAG_566A08) is in the Wassilewskija (Ws) Arabidopsis ecotype, with the T-DNA insertion inside the final exon towards the 3' end of the gene sequence (Figure 4.4). Hereinafter the mutant line is referred to as *rns1.1*. The mutants SALK_087165 and GABI_760D11 (referred to as *rns1.2* and *rns1.3*, respectively) are in the Col-0 ecotype and have T-DNA insertions in the 5' un-translated region (UTR) (Figure 4.4). Finally, a transgenic line (as*RNS1*), expressing the full length *RNS1* antisence cDNA (Bariola *et al*., 1999), was included for comparison with the T-DNA KO mutants.

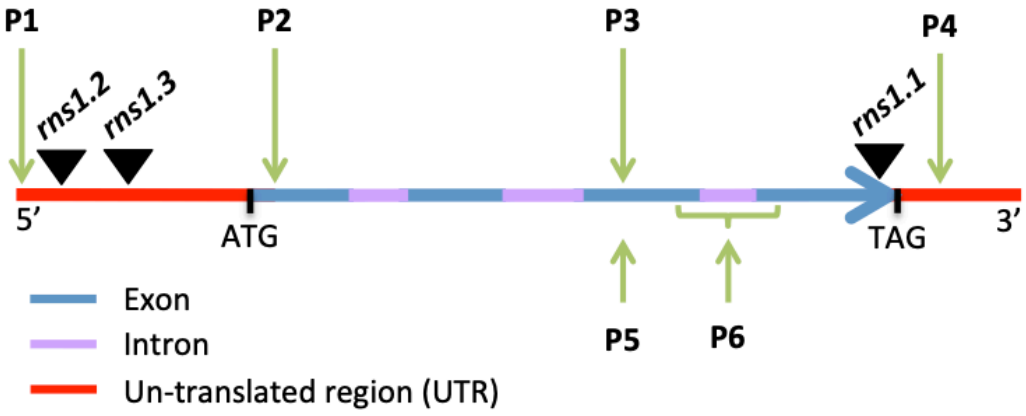

Figure 4.4. Location of T-DNA insertion mutants for *RNS1*. The *rns1.2* and *rns1.3* T-DNA insertion lines are located in the 5' un-translated region (UTR), and *rns1.1* is located in the final exon towards the 3' end.
P1 and P2 indicate the positions of primers used for confirmation of the *rns1.2* and *rns1.3* T-DNA insertions. P3 and P4 indicate the positions of primers used for confirmation of the *rns1.1* T-DNA insertion. P5 and P6 indicate the positions of primers used for qRT-PCR analysis.

To check if *RNS1* transcript accumulation had been impaired by the T-DNA insertions, qRT-PCR was used to analyse RNA samples from wildtype and the mutant plants (Figure 4.5). In addition to evaluating relative transcript abundance under normal growth conditions, activation of *RNS1* expression in response to wounding (LeBrasseur *et al*., 2002; Hillwig *et al*., 2008) was also determined, in case the T-DNA inserts only impaired *RNS1* stress response. In the Col-0 background, *rns1.2* and *rns1.3* expression is significantly down-regulated in comparison to the unwounded Col-0, whereas as*RNS1* is only marginally reduced and does not significantly change. In response to wounding, the Col-0 transcript is up-regulated, with similar expression profiles seen in *rns1.3* and as*RNS1*. This result suggests that *rns1.3* either does not contain a T-DNA insert, or that the insert has not altered the native transcription levels of RNS1. The as*RNS1* also does not appear to interfere with RNS1 transcription. The transcript abundance for wounded *rns1.2* remains lower than the unwounded Col-0. A similar response to wounding is seen in the Ws background, with *rns1.1* showing a reduction in RNS1 transcript in response to wounding (Figure 4.5.B). The unwounded conditions however show a higher transcript abundance in *rns1.1* compared to the Ws (Figure 4.5.B). Although *rns1.1* may prove to be a useful tool for investigating *RNS1* gene expression, the Ws background is naturally resistant to FB1 (Chivasa *et al*., unpublished data), and therefore this line could not be used in further experiments.

The results suggest that *rns1.2* is the most suitable knockout line for use in investigating a possible role for *RNS1* in Arabidopsis responses to FB1. Although *rns1.3* and as*RNS1* had similar *RNS1* transcript abundances to Col-0, at a protein level the alterations to the *RNS1* gene may result in an impaired protein.

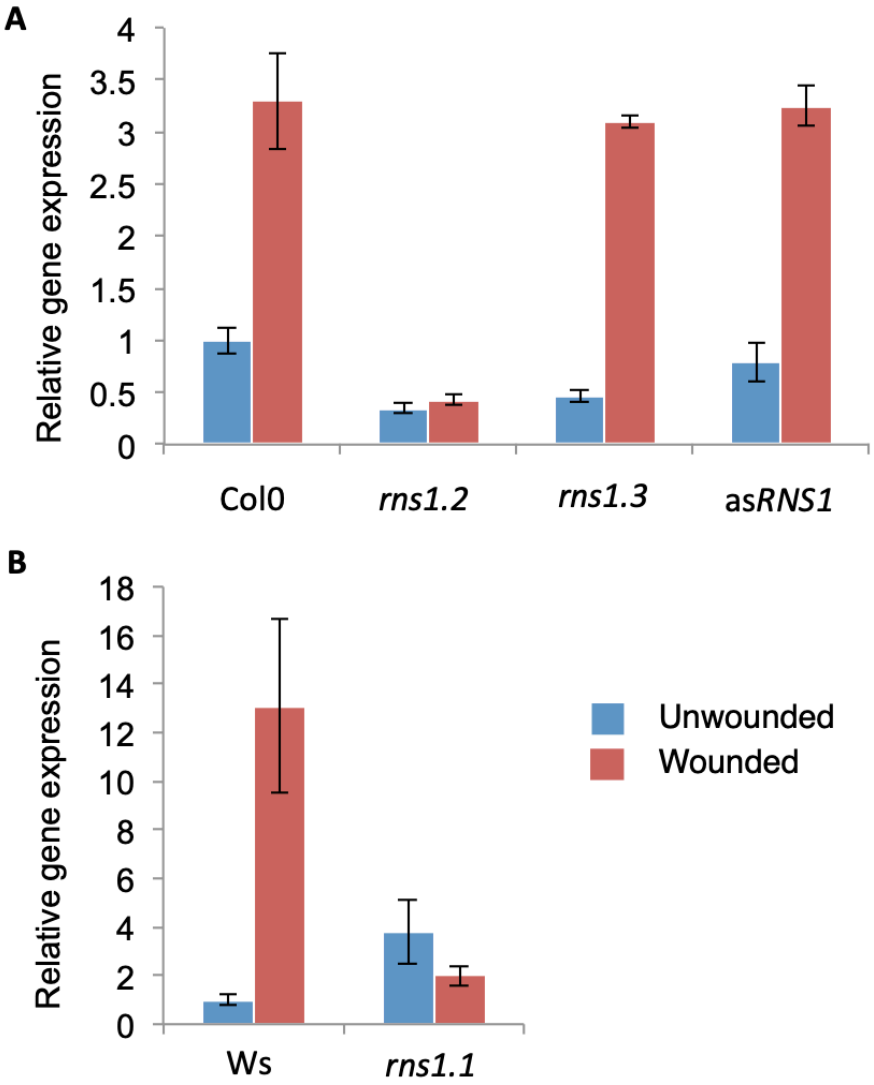

Figure 4.5 Analysis of *RNS1* gene expression in transgenic or mutant lines (A) Expression of *RNS1* before and 24 hours after wounding WT (Col-0) WT, *rns1.2*, *rns1.3* and as*RNS1* leaf tissue. All lines, besides *rns1.2,* responded to wounding, indicating that only *rns1.2* disrupted *RNS1* response to stress **(B)** Expression of *RNS1* before and 24 hours after wounding WT (Ws) and *rns1.1* leaves. The *RNS1* expression in *rns1.1* does not respond to wounding, but *RNS1* expression is not down-regulated further than basal levels of *RNS1* expression prior to wounding. *ACTIN2* and *eIF4A* were used as constitutive reference control genes in the qRT-PCR analysis. qRT-PCR values are an average of 3 technical replicates. Bars represent mean fold-change ± SD (n = 3).

To determine the functionality of the RNS1 protein in these mutant lines, an RNase activity assay was used. The RNase activity assay was originally developed by Yen and Green (1991) and subsequently modified by LeBrasseur *et al*. (2002). In these assays, visualization of RNS1 activity in gels is improved by wounding the leaf tissues prior to protein extraction, which activates *RNS1* gene transcription. Therefore, protein samples were extracted before and after wounding leaf tissues of Col-0, Ws-0, and mutant lines.. The protein samples were separated using non-denaturing SDS-PAGE in polyacrylamide gels infused with yeast RNA. The gels were stained with toluidine blue, which binds to nucleic acids, staining the entire background blue. Yeast RNA is degraded at all positions in the gel where active ribonuclease protein bands are located, resulting in a clear zone unstained with the dye (Figure 4.6.A). In Col-0 plants, two dominant ribonuclease bands were visible, with the lower molecular weight activity band (~20 kDa) representing RNS1 as indicated in Figure 4.5.A. Since the molecular weight of RNS1 is 24.5kDa, the lower molecular weight in native gels suggests the presence of disulphide bridges in the native RNS1 protein. A denatured and linearized protein runs at a higher molecular weight position than a globular folded protein. The RNS1 activity band does not appear in *rns1.2* sample, confirming that the mutant line does not accumulate significant RNS1 protein. However, the RNS1 activity band is clearly shown in *rns1.3* and *asRNS1*. Along with the RNS1 transcript abundance, the RNase activity confirms that both *rns1.3* T-DNA insertion line and the *asRNS1* are not successful in disrupting RNS1 expression. The Ws-0 wildtype shows a distinct RNS1 band, with a slightly lower abundance in comparison to the Col-0 wild type, and *rns1.1* shows reduced RNS1 activity. A second ribonuclease band appearing above the RNS1 band was unaffected by mutation or wounding across all lines, and therefore serves as a positive control.

Figure 4.5.B shows the same gel after complete removal of toluidine blue and re-staining with Coomassie Blue. Coomassie Brilliant Blue is a triphenylmethane dye that binds to proteins through an ionic interaction between the proteins positive amine group and the dye's sulfonic acid group (Groth *et al*., 1963). Coomassie staining was used to stain the proteins after the RNase assay to confirm that similar concentrations of protein had been accurately loaded into the gel for each sample.

Next I wanted to confirm that the *rns1.2* seed were homozygous for the T-DNA insert. PCR was used to amplify the genomic DNA of the *RNS1* transcript, with primers spanning the T-DNA insertion position (Figure 4.7.A). While a band was amplified in Col-0, no amplicon of similar size was present in PCR reactions with DNA derived from *rns1.2* plants. As the PCR reaction was performed for several plants, this confirms the presence of the T-DNA insert, and that it was homozygous.

Careful examination of the promoter region of *RNS1* and the insertion position of the T-DNA in *rns1.2* prompted consideration of the possibility that this mutant line could provide a unique genetic tool for investigations into the functionality of *RNS1*. The schematic diagram shown in Figure 4.7.B illustrates the relative positions of cis-acting elements upstream and downstream of the T-DNA insertion. Promoter binding elements positioned upstream of the T-DNA insertion point will be moved further upstream of the RNA polymerase II- binding site, thereby impeding their regulatory influence on gene expression. Promoter binding elements that may be crucial for activation of *RNS1* in response to external stimuli include a W-box binding site for WRKY18 and an ASF-1 binding site which is important for auxin and SA-induced gene expression (Xu *et al*., 2006; Schön *et al*., 2013; Niggeweg *et al*., 2000). These binding sites are upstream of the T-DNA insertion point and their regulatory control over *RNS1* is potentially impaired. If this is the case, it could lead to reduced SA sensitivity and defence against pathogens in this mutant (Chen and Chen, 2002. Niggeweg *et al*. 2000). Downstream of the T-DNA insertion is a binding site for the PHOSPHATE STARVATION RESPONSE 1 (PHIR1) protein, implying that *RNS1* transcription in response to inorganic phosphate starvation could be unaffected in the mutant. Overall, both qRT-PCR analysis and RNase activity assays confirm that *rns1.2* reduces *RNS1* transcript abundance and RNase activity, making this mutant suitable for studying the role of RNS1 in FB1-induced PCD. As only one T-DNA insertion line (*rns1.2*) was selected for use in further experiments, it is hereafter referred to just as *rns1*.

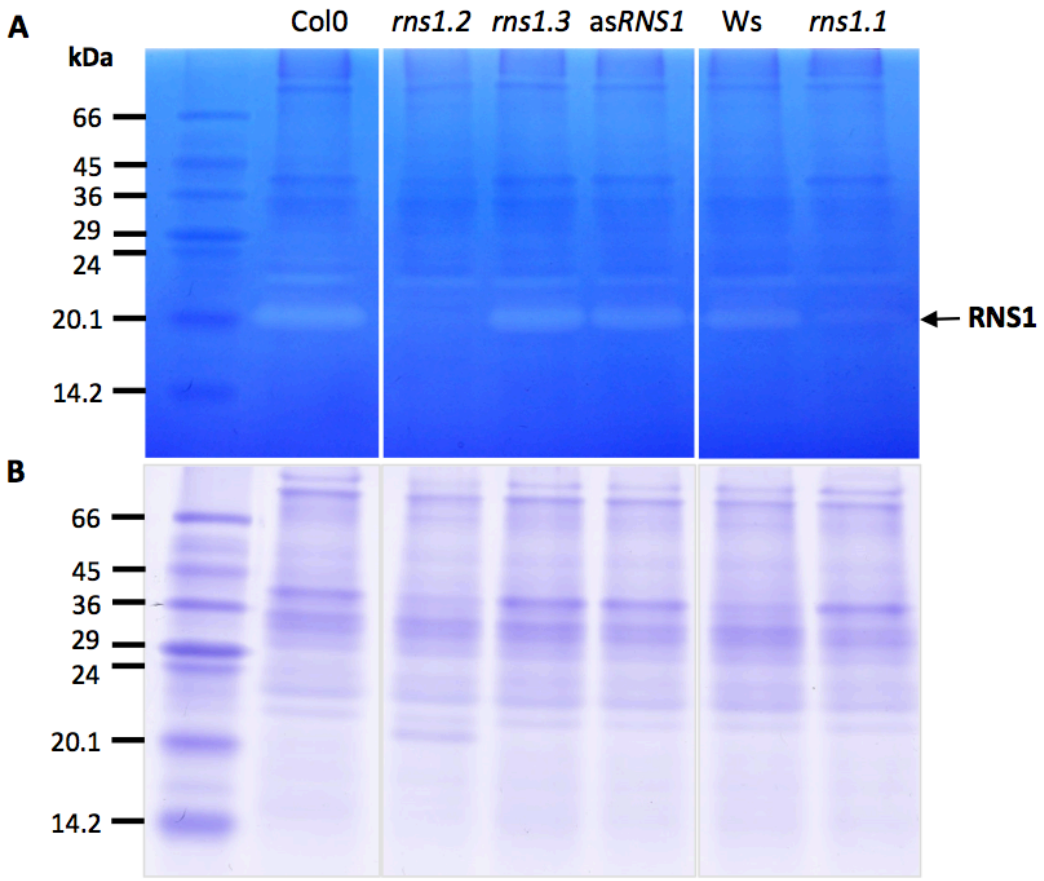

Figure 4.6. RNase activity assay gel. A) Proteins were extracted from wounded leaf tissue and 50µg of the protein was separated using native SDS-PAGE in an acrylamide gel containing yeast RNA. The gel was stained with toluidine blue, a nucleic acid stain. Ribonucleases are present in clear unstained bands where RNA had been degraded. The T-DNA insertion lines, *rns1.2* and *rns1.3*, along with the antisense line (*asRNS1*) are in the Colombia (Col0) ecotype background; whereas *rns1.1* is in the (Ws) background. The position of RNS1 is indicated by the arrow and is present in all lines, but *rns1.2*. The *rns1.1* T-DNA insertion line shows a faint band at the expected location for RNS1 **B)** Coomassie protein staining of the gel in A after removal of toluidine blue. The use of coomassie shows qualitative comparison of total protein present in each sample as a loading control.

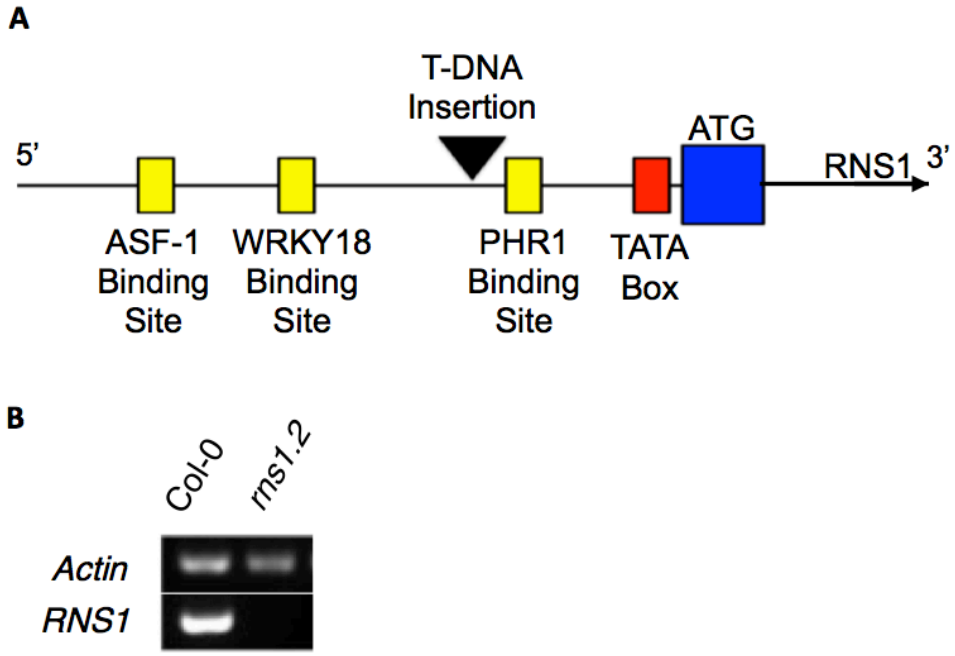

Figure 4.7. Analysis of *rns1.2* T-DNA insertion line. A) Schematic diagram showing T-DNA insertion position in the promoter region of *RNS1*. ASF-1 and WRKY18 binding sites are upstream of the insertion point, which is predicted to prevent *RNS1* expression in response to salicylic acid and pathogens; The TATA box and PHOSPHATE STARVATION RESPONSIVE 1 (PHIR1) are downstream of the T-DNA insertion. **B)** Amplification of the genomic DNA using primers straddling the insertion position of the T-DNA. In Col-0 the expected amplicon is present, which is absent from *rns1.2*. This indicates that *rns1.2* has the T-DNA insert. *ACTIN2* was used as a constitutive reference control gene.

To compensate for the inability to obtain a strong second T-DNA knockout line, gene constructs were generated for complementation of the *rns1* knockout mutant. The constructs were designed to investigate the role of RNS1 activity and suspected ATP-binding by the P-loop motif of the RNS1 protein. The first was a 35S CaMV promoter-driven *RNS1* construct for constitutive overexpression of the native RNS1 enzyme in the *rns1.2* background (Figure 4.8.A). The second construct had the same promoter driving expression of a catalytically inactive mutant of RNS1 in which two conserved active site histidine residues (at positions 65 and 123) are replaced with phenylalanine residues. Similar mutations in other organisms have been shown to knockout ribonuclease activity (Deshpande and Shankar, 2002; Acquati *et al*., 2005; Thompson and Parker, 2009). The final construct had a mutation of the ATP-binding

P-loop of RNS1, in which glycine and lysine residues at positions 162 and 163, respectively, were replaced by alanine residues (G162A and K163A mutations). Thus the following transgenic lines were generated:

1. Col-0::RNS1 transgenic Col-0 overexpressing native RNS1
2. Col::mRNS1 transgenic Col-0 overexpressing the RNS1 catalytic mutant
3. *rns1::RNS1* *rns1* knockout transformed with the native RNS1
4. *rns1*::m*RNS1* *rns1* knockout transformed with the RNS1 catalytic mutant
5. *rns1*::p*RNS1* *rns1* knockout transformed with RNS1 P-loop mutant

The process of gene synthesis, plasmid construction, and agrobacterium-mediated plant transformation was conducted by Dr Johan Kroon and Dr Stephen Chivasa (Durham University). I contributed to transformation of the *rns1* knockout plants and selection of homozygous transgenic lines. The gene construct had either a kanamycin-resistance gene or BASTA-resistance gene as a selection marker (Figure 4.8.A). After Arabidopsis transformation, thousands of T1 seeds were collected and sown in nurseries, which were sprayed with BASTA. After multiple treatments, a large proportion of the seedlings died but the T1 transformants were resistant to BASTA (Figure 4.8.B). Genomic DNA from the surviving T1 plants was analysed using qRT-PCR (Figure 4.8.C). The relative gene expression of the BASTA resistance gene was compared with a single-copy Arabidopsis gene encoding 4-hydroxyphenylpyruvate dioxygenase (At1g06570) as a reference. Heterozygous T1 plants were identified by a relative expression level of 0.5-fold for BASTA, indicating that the plant had a single insert in only one allele. T2 seeds were harvested from these heterozygous T1 plants and germinated on soil. The seedlings were again sprayed with BASTA to exclude any plants without the transgene. Surviving T2 plants consisted of heterozygotes and homozygotes. qRT-PCR analysis of genomic DNA led to the identification of transgenic homozygous plants with a relative expression ratio of 1 when compared to the endogenous single-copy gene, indicating a single insert in both alleles (Figure 4.8.C). The homozygous T3 seeds were bulked-up for use in experiments.

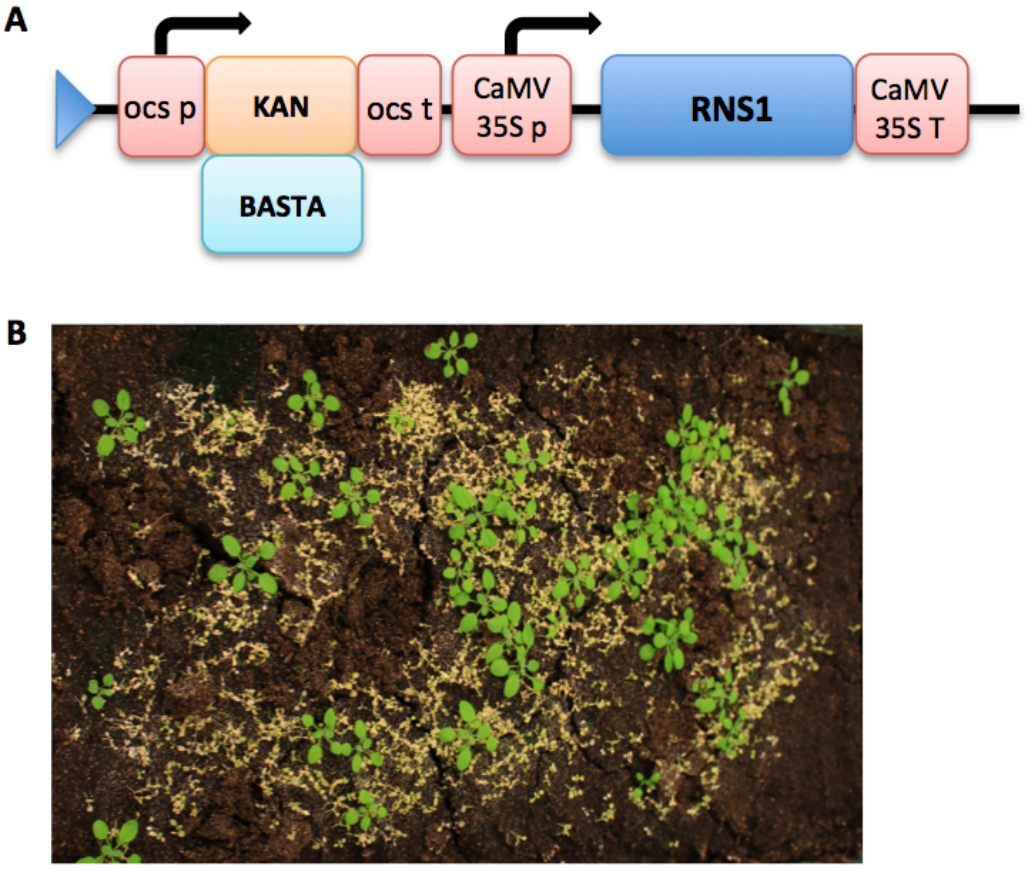

Figure 4.8. Generation of transgenic plants. (A) Schematic diagram of the gene constructs used for plant transformation. An Octopine synthase (oct) promoter-driven Kanamycin- or BASTA-resistance gene was used as a selection marker and RNS1 expression was under the constitutive CaMV 35S promoter. **(B)** BASTA selection of transformed plants. Transformed plants were grown to full maturity and T1 seeds were collected. The seeds were sown in nurseries and sprayed with BASTA at 1 week, and then a second spray at 2 weeks. The seedlings that survived BASTSA were analysed using qRT-PCR for transgene copy number analysis and plants with single inserts transplanted for T2 seed collection.

This project focused on using the complementation lines for *rns1*, but my project supervisor (Dr Stephen Chivasa, unpublished data) had generated the RNS1 overexpression lines in the Col-0 background (Figure 4.9). Initially, the steady-state RNS1 expression in the transgenic lines was compared to control Col-0 plants using qRT-PCR analysis. The selected transgenic lines had higher levels of gene expression, with the line transformed with native *RNS1* in Col-0 (Col-0::*RNS1*) showing a 10-fold increase in transcript while the line transformed with the mutated *RNS1* in Col-0 (Col-0::m*RNS1*) had nearly 50-fold transcript accumulation (Figure 4.9.A). The level of RNS1 activity was evaluated in these plants with an additional sample of wounded wildtype Col-0 plants included as a positive control (Figure 4.9.B). As with the previous RNase assay, wounding increased RNS1 activity in Col-0 plants. RNS1 activity is shown by an intense white band on a blue background at the 20k Da size position. The Col-0::*RNS1* showed a much brighter band than the wounded Col-0, which was to be expected and coincides with the high RNS1 expression seen in Figure 4.9.A. Although transcript accumulation was the highest in Col-0::m*RNS1* (Figure 4.9.A), no RNS1 activity band was observed, indicating that the mutation had successfully inhibited the ribonuclease activity of RNS1 (Figure 4.9.B) (Chivasa, Unpublished data). This confirmed that mutation of the conserved histidine residues disable Arabidopsis RNS1 activity.

The *rns1* complementation lines were similarly evaluated using the ribonuclease activity assays described above. The transgenic plants were verified to have been successfully transformed by the gene constructs. A simple genomic PCR-amplification of a region of the BASTA gene indicated the presence of the construct in each of the lines (Figure 4.10.A). The negative controls Col-0 and *rns1* showed no BASTA resistance gene as expected. This verified that the gene constructs had successfully integrated into the genome.

Next *RNS1* gene expression in each line was established using qRT-PCR analysis of wounded and unwounded tissues. *RNS1* transcript accumulation was expected to be higher in the three transgenic lines, when compared to Col-0, due to the 35S over-expressing promoter. This hypothesis was confirmed, however even at a transcript level, the lines showed alterations in transcript abundance, particularly in response to wounding (Figure 4.10.B). In the unwounded samples, *rns1*::p*RNS1* and

rns1::m*RNS1* showed the highest transcript abundances, followed by *rns1::RNS1*, when compared to the unwounded Col-0. In the wounded samples, *rns1* maintained a significantly reduced gene expression, and in the Col-0, *RNS1* expression significantly increased. The transgenic lines showed altered *RNS1* gene expression in response to wounding, with the *rns1::RNS1* showing the highest rate of *RNS1* expression. The *rns1*::m*RNS1* also increased *RNS1* gene expression in response to wounding but lagged behind the native RNS1 overexpressor. The *rns1*::p*RNS1*, which showed the highest relative *RNS1* gene expression in the unwounded samples, showed the lowest increase in response to wounding (Figure 4.10.B). Theoretically the transgenic lines should not have shown differing transcript abundances in response to wounding, as the transcription of the *RNS1* gene is driven by a 35S promoter, resulting in constitutive expression. A possible explanation for this phenomenon is that over expression of RNS1 may result in a cytotoxic effect and requires a mechanism to prevent excessive transcription under normal conditions. It is already known that under wounded conditions, the plant tissue is primed with cytotoxic components as a defensive measure to prevent infection through compromised tissue (Orozco-Cardenas *et al*., 1999, 2002; Maruta *et al*., 2012). This would suggest that mechanisms to hinder overexpression of cytotoxic components are inhibited. This is a possible hypothesis for the overexpression, and lack of regulation, of the transgenic lines under wounded conditions. Overall, the complementation lines of *RNS1* showed the expected overexpression of the target gene construct (Figure 4.10.B).

To determine whether the mutated transgenics had impacted the RNase activity of *rns1*, an RNase activity assay, as described above, was conducted (Figure 4.11). Tissue from wounded leaves was used for each of the transgenic lines, to show maximal RNase activity. The *rns1::RNS1* complementation line showed a much brighter RNS1 activity band, indicating high levels of enzyme activity as predicted. This demonstrated that the *rns1* line had been successfully complemented with the native *RNS1*. The *rns1*::*mRNS1* transgenic line showed no RNS1 activity, confirming the previous results from Figure 4.9.B, that the mutation disables the enzyme. The last complementation line, *rns1*::*pRNS1*, showed a faint white band, which indicated RNase activity was suppressed, but not completely blocked by altering two amino acid residues of the *RNS1* ATP-binding loop (Figure 4.11).

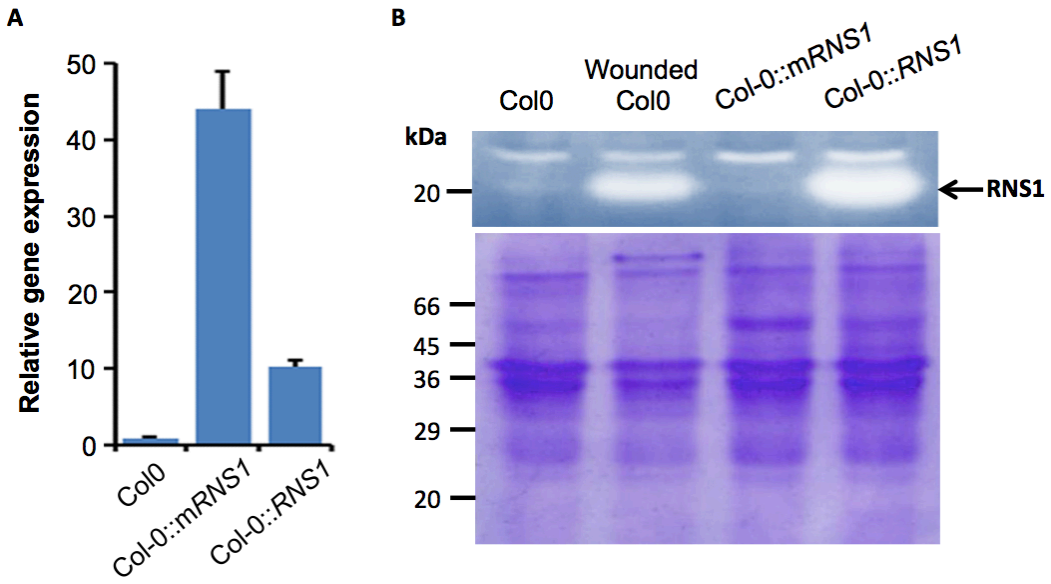

Figure 4.9. Evaluation of transgenic lines using qRT-PCR and RNase activity assay. A) qRT-PCR analysis confirms that the transgenic lines in the Col-0 background overexpress native or mutant *RNS1*.Bars represent mean fold-change ± SD (*n* = 3). **B)** RNase activity assay of protein samples extracted from leaf tissue. For each sample, 50µg of protein was used. A wounded Col-0 sample served as a positive control. Ribonucleases are visible as clear bands on a toluidine blue background, with RNS1 activity bands indicated by the arrow. The gel was completely de-stained and then stained with the Coomassie Blue protein stain to show the relative amounts of total protein in each sample. The Coomassie gel is below the activity gel.

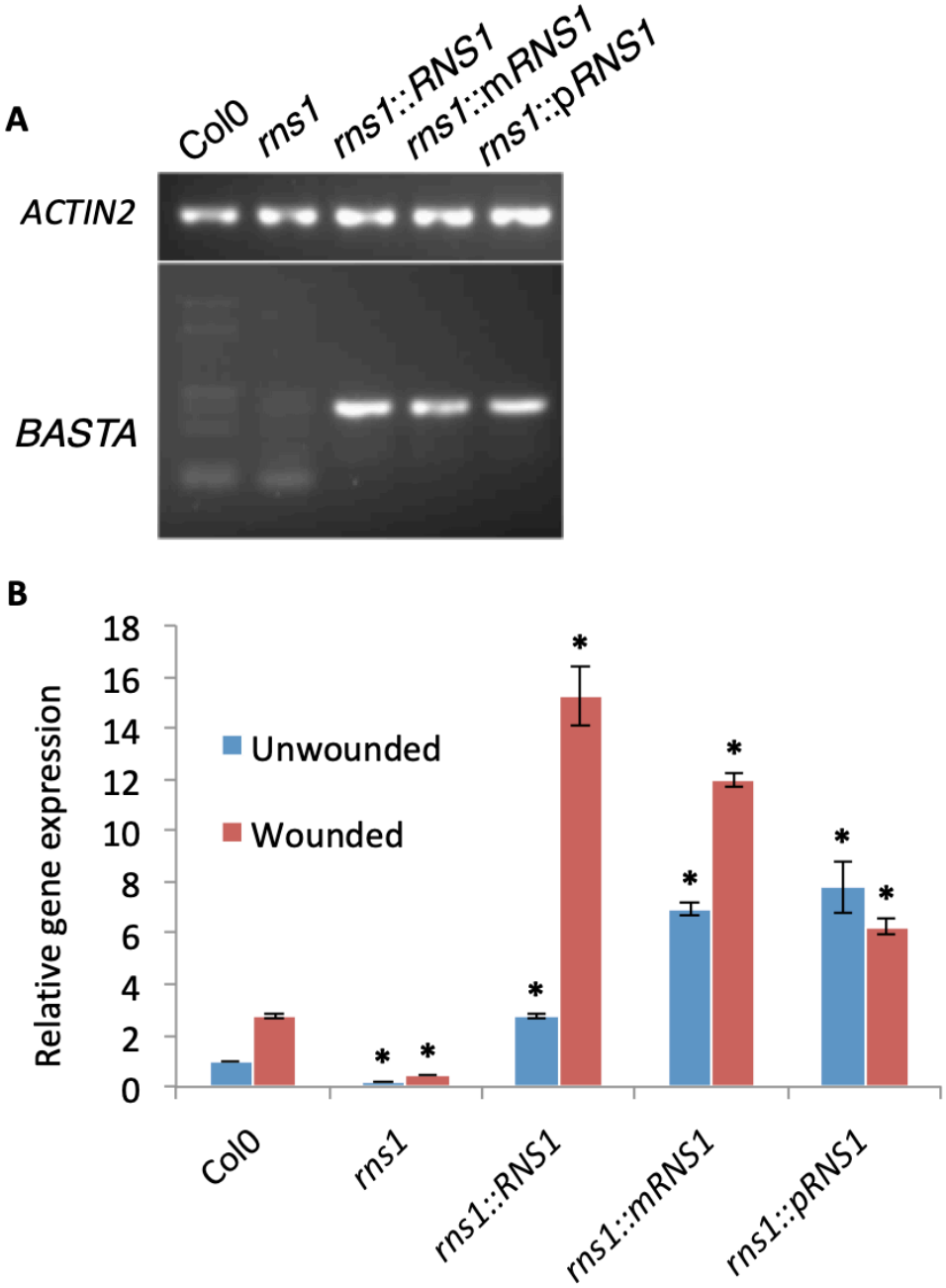

Figure 4.10 Analysis of RNS1 complementation lines. A) Amplification of genomic DNA with primers designed to amplify the BASTA resistance gene. The three complementation lines (*rns1::RNS1*; *rns1*::*mRNS1*; *rns1*::*pRNS1*) had the expected PCR product from the BASTA resistance gene, indicating that they are transformants. Col-0 and *rns1* served as negative controls. *ACTIN2* was used as a constitutive reference control gene. **B)** Analysis of *RNS1* gene expression using qRT-PCR. *ACTIN2* and *eIF4A* were used as constitutive reference control genes. qRT-PCR values are an average of 3 technical replicates. Bars represent mean fold-change ± SD (n = 3). An asterisk indicates a significant difference in the fold-change between the wildtype (Col-0) and *rns1* lines.

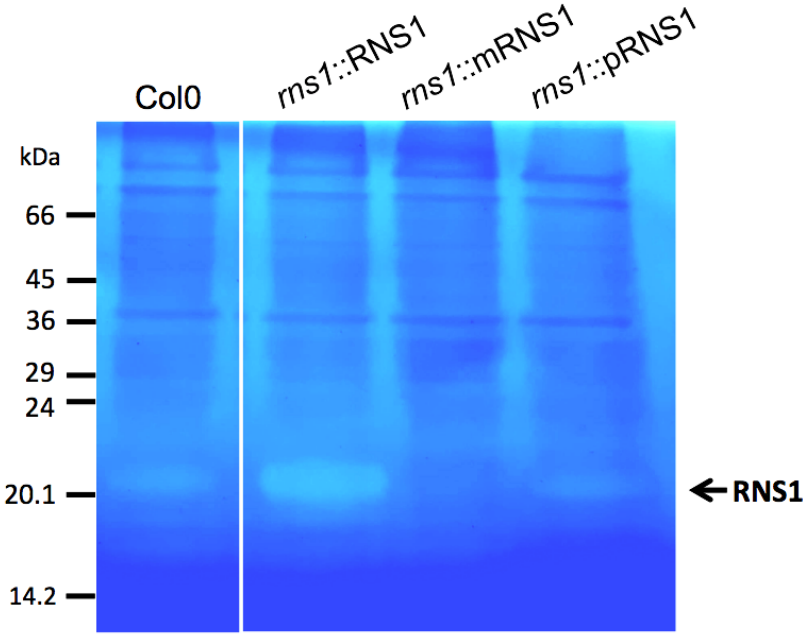

Figure 4.11. RNase activity assay gel. Proteins were extracted from wounded leaf tissue and separated using native SDS-PAGE in an acrylamide gel containing yeast RNA. The gel was incubated in toluidine blue, a nucleic acid stain. Ribonucleases are present in clear unstained bands. The Col-0 sample produced a white band, which signified RNase activity. The complementation line overexpressing the native *RNS1* (*rns1::RNS1*) produced an even brighter white band, indicative of a greater abundance of RNase activity. The complementation of *rns1* with the *RNS1* sequence mutated at the predicted site of RNase activity (*rns1*::m*RNS1*), successfully abolishes RNase activity. The complementation of *rns1* with the *RNS1* sequence mutated at the p-loop motif (*rns1*::p*RNS1*), produced a faint white band indicating that RNase activity was inhibited, but not abolished.

4.5 Characterisation of the cell death response in Arabidopsis complementation lines with altered *RNS1* expression

FB1-induced cell death was investigated via two approaches. In the first approach, FB1 was delivered into the leaf apoplast by syringe-infiltration. Development of cell death symptoms was monitored over 7 days. Chlorosis and bleaching of leaf tissues were used as visual markers of developing PCD symptoms. In conjunction with this, vital staining with microscopy allowed visualization of the cell death at the cellular level. The second approach relied on the uptake of the FB1 solution via the stomata of leaf tissues floating over FB1, with the abaxial surface in direct contact with the solution. Cell death was proportional to the increase in the conductance of the FB1 solution due to the breached integrity of the plasma membrane and ultimately cellular leakage of its contents. The electrolyte leakage assay provided a quantitative measure of cell death, while qualitative data was obtained from microscopy and visual assessments.

Leaf discs of 8mm diameter were cored from Arabidopsis leaves and floated on 3μM FB1 solution. The leaf discs were incubated in the dark for 48 hours before being introduced to a 16 h-photoperiod. To visualize the FB1-induced cell death, leaf discs were taken every 24 hours from the beginning of the experiment up until 96 hours. The discs were stained with Lactophenol blue staining (Rate *et al*., 1999). The lactophenol serves as a mounting fluid and allows the suspended leaf discs to stay intact, due to the high concentrations of phenol deactivating lytic cellular enzymes. The Trypan blue dye stains the cells that were dead prior to treatment, this includes xylem, along with cells that have succumbed to FB1. The discs were then assessed for cell death by light microscopy (Figure 4.12). The 24-hour and 48-hour samples had no cell death, except for the xylem used for water conduction, indicating that FB1-induced cell death does not begin until the leaf discs are exposed to the light. At 72- and 96-hour time points, there is a clear progression of cell death seen, as individual cells are stained blue.

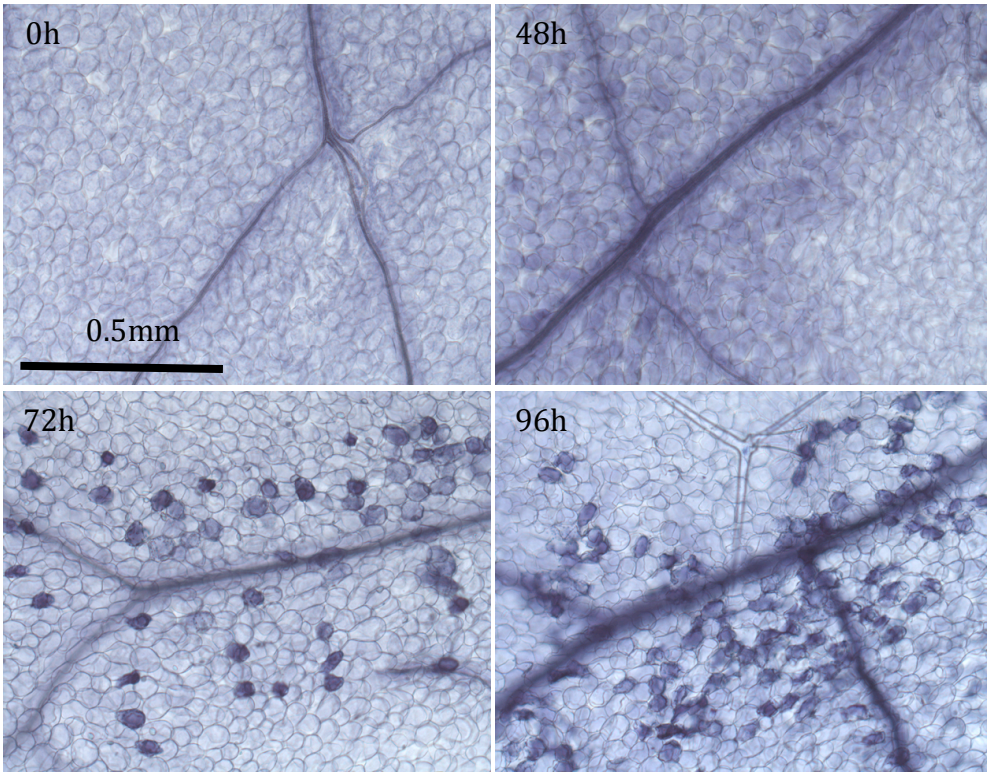

Figure 4.12. Response of Arabidopsis to FB1 treatment. (A) FB1-induced cell death observed through lactophenol-blue staining. Leaf discs from 4-week-old Arabidopsis plants (Col0) were floated on 3µM FB1. After 48 hours incubation in the dark, the floating discs were transferred to a light-dark cycle. Blue-stained dead cells can be seen in the72h and 96h samples.

Next the electrolyte leakage assay was performed. Leaf discs of 8mm diameter were cored from Arabidopsis leaves and floated on 5µM FB1 solution in 5-replicate petri dishes. The leaf discs were incubated in the dark for 48 hours before being transferred to a 16h-photoperiod. Conductivity measurements were taken starting at 48h and subsequently every 24 h. The initial experiment aimed at investigating the effects of plant age on susceptibility to FB1. For this, leaf discs were prepared from plants at 4, 5 and 6 weeks after sowing. The conductivity assay shows drastic differences in PCD of plants with different ages, with a reduction in cell death in older plants (Figure 4.13.A). The 4-week-old plants are much more susceptible to FB1 than the older plants. Photographs of PCD symptoms were taken at 72- and 96-hours after FB1 treatment (Figure 4.13.B). Chlorosis is more pronounced in the 4 weeks old tissues, while the older tissues have accumulation of anthocyanins (purple pigmentation), which is a defensive response. Therefore, for subsequent experiments, 4-week-old Arabidopsis plants were used.

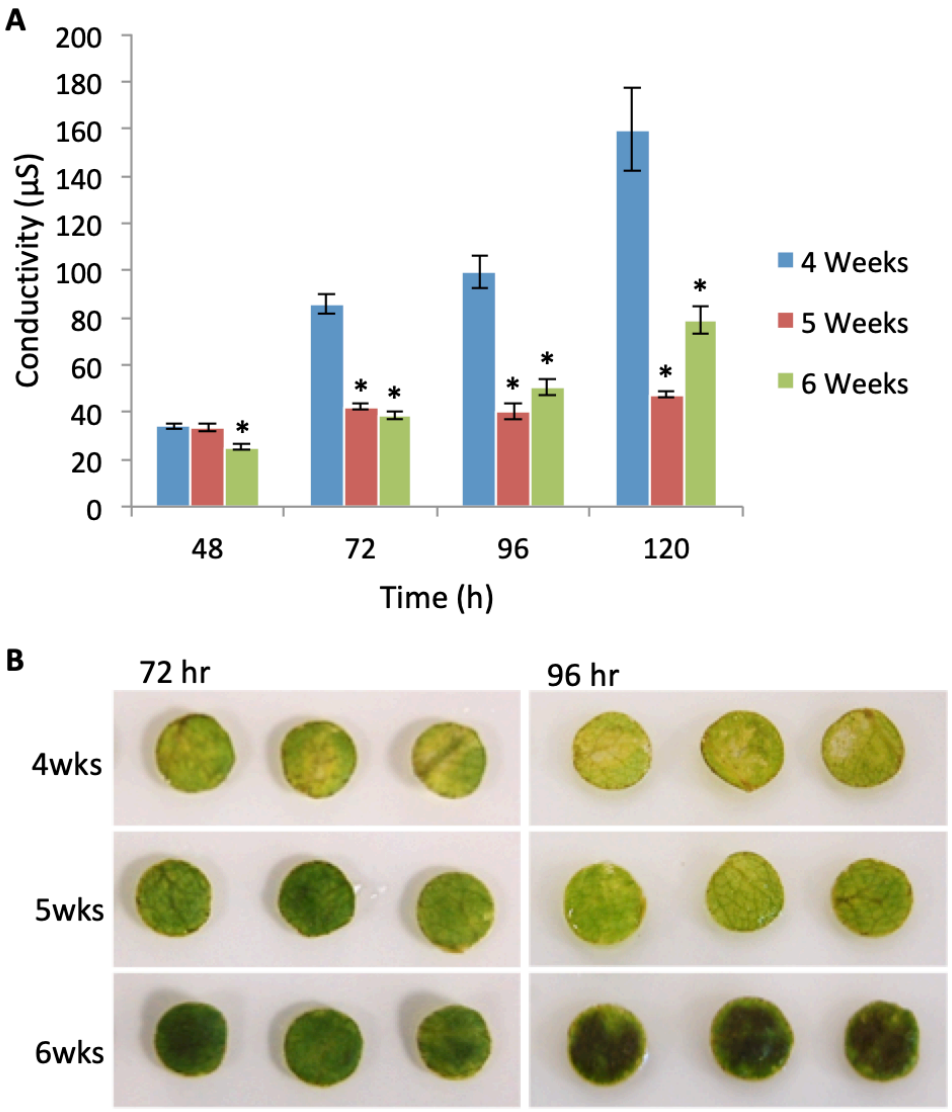

Figure 4.13. Response of Arabidopsis to FB1 treatment. (**A**) Electrolyte leakage assay showing the cell death response to FB1 treatment. **(B)** FB1-induced cell death in tissues of Arabidopsis plants at the indicated ages. Leaf discs from 4-, 5- and 6-week-old Arabidopsis plants (Col0) were floated on 5µM FB1. After 48 hours dark-incubation, the discs were transferred to light. Conductivity readings were taken at the indicated time points. **(C)** Photographs were taken at 72h and 96h alongside the conductivity readings. The plants grown for 4wks are more susceptible to FB1, showing more bleaching than older plants, and the conductivity shows the highest rate of ion leakage at in 4 weeks-old plants.

Using the complementation lines described above, the potential role of RNS1 in FB1-induced cell death was investigated via qualitative visual experiments and quantitative conductivity assays. Three leaves per plant, of at least 10 independent plants for each line, were syringe-infiltrated with 2.5μM FB1 (Figure 4.14). In such experiments, Col-0 leaves develop chlorotic specs ~3 days after infiltration. The specs expand, coalescing to form large patches of chlorotic tissues, which may or may not spread to the petiole. Chlorotic areas eventually die and, by 7 days, they become papery dry. However, there are still patches of green tissues within the leaves (Figure 4.14). The *rns1* knockout mutant was largely unaffected by FB1, exhibiting very few specs of chlorosis, but essentially the leaves survived. In contrast, complementing *rns1* with the native *RNS1* restored the cell death symptoms, and developed even further than in the wildtype. The *rns1::RNS1* leaves showed total cell death, which spread across the entire leaf and petiole. The *rns1*::*mRNS1* mutated line showed a similar phenotype to *rns1*, with marginal cell death symptoms appearing as small specs and patches towards the edge of the leaf. The *rns1*::*pRNS1* line showed patches of cell death but appeared healthier than the Col-0 and *rns1::RNS1* lines (Figure 4.14). Overall, these results show that the native *RNS1* can complement the loss-of-function mutation in *rns1*, while both catalytic and P-loop mutants fail to do so. The P-loop motif appears to be essential for RNS1 function, though evidence for direct involvement of ATP binding is still lacking.

The electrolyte leakage assay was then used to produce quantitative data of the response of the *rns1* complementation lines to FB1 treatment (Figure 4.15). A comparison of Col-0 to *rns1* corresponded with the differences in cell death observed in the infiltrated leaves (Figure 4.14). Col-0 plants had the characteristic profile of increasing cell death, which was suppressed in the *rns1* mutant (Figure 4.15). The mutated complementation lines also supported the symptomatic evidence of reduced cell death observed in infiltrated leaves (Figure 4.14). The conductivity assay showed that *rns1*::*mRNS1* showed an almost identical cell death profile to *rns1*, indicating the mutation to the catalytic region of RNS1 is crucial for the response of RNS1 to FB1 (Figure 4.15). The *rns1*::*pRNS1* reduced the rate of cell death even further than the absence of *RNS1* alone (Figure 4.15). Without the evidence to confirm that the p-loop mutation is affecting the direct interaction between ATP and

RNS1, we can only state that the mutated p-loop interferes with ribonuclease activity and the cell death response to FB1.

An surprising result was obtained for the plants complemented with the native RNS1over-expressor, *rns1::RNS1*. Although Figure 4.14 shows that complementation with native RNS1 resulted in severe cell death symptoms, the electrolyte leakage assay showed a contradictory phenotype – the cell death was the same as the *rns1* knockout plants. The rate of cell death is similar between *rns1* and *rns1*::*mRNS1* tissues (Figure 4.15). This unexpected discrepancy is likely accounted for by the differences between these two experiments. In the first experiment, FB1 was delivered into the apoplast by syringe-infiltration and cell death symptoms developed in leaves still attached to the plants (Figure 4.14). Thus, this is a whole plant experiment in which the plants show how they respond in their natural environment. The second is an *in vitro* experiment which relies on uptake of FB1 via passive diffusion through stomata and secretion of released electrolytes back into the bulk solution on which the discs are floating. If any gene mutation or overexpression affects stomatal responses, cuticular wax thickness, or other as yet unsuspected parameters relevant to uptake of solutes or release of ions, the resulting electrolyte leakage profile might cease to become a high fidelity proxy for the cell death response. This result implies that the leaf disc assay results will always need to be verified using direct application of FB1 instead of relying entirely on uptake by diffusion. Taken together, these results show that RNS1 promotes FB1-induced cell death.

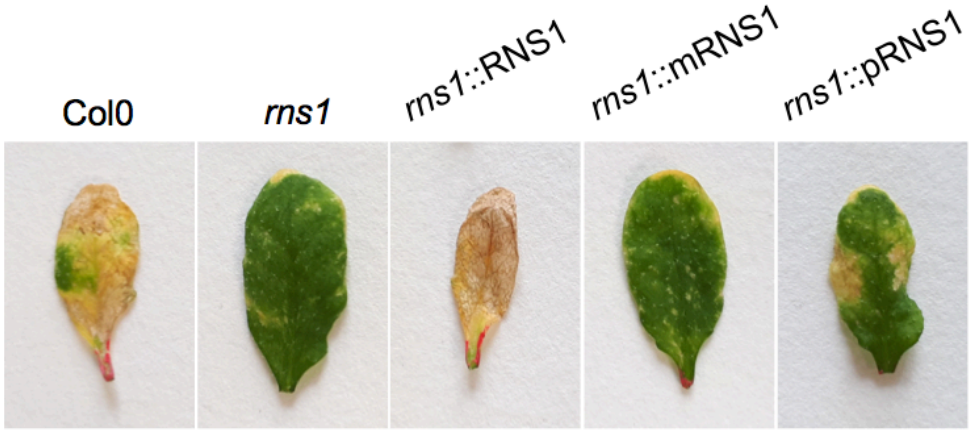

Figure 4.14. FB1-induced cell death in Arabidopsis with altered RNS1 levels. Intact leaves on plants were syringe-infiltrated with 2.5µM FB1 and symptom development was monitored over a 7-day period. Photographs of representative leaves were taken a week later. Each leaf is a representative of at least 10 similar leaves. This experiment was repeated twice and it gave similar results.

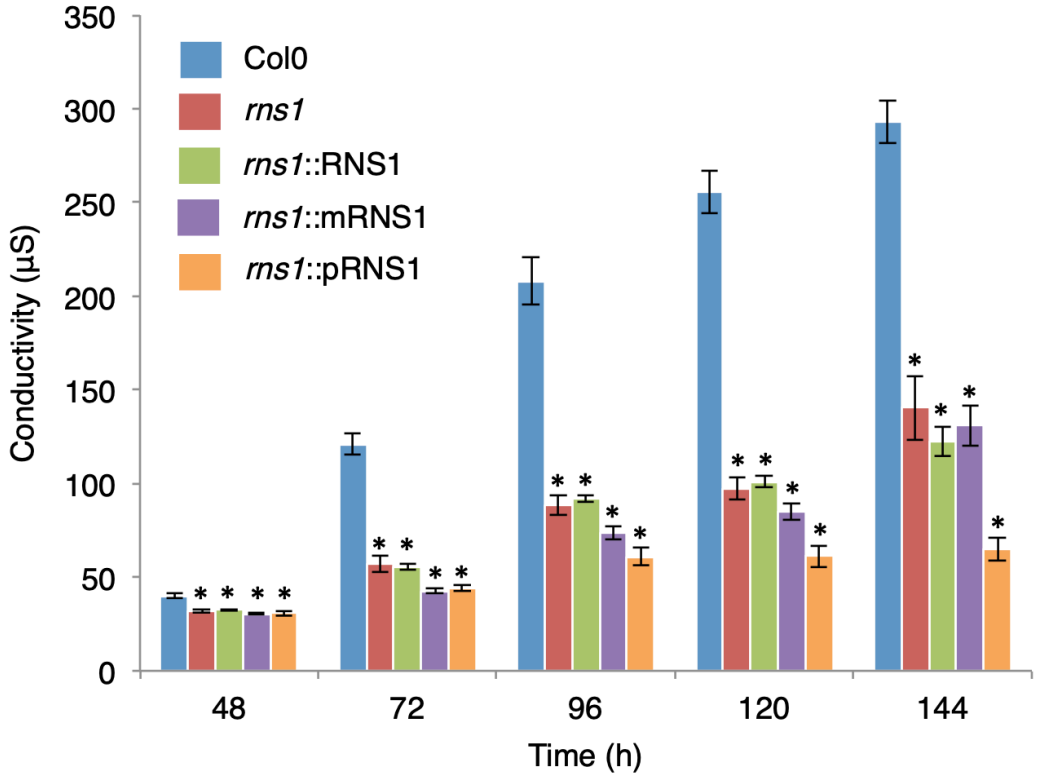

Figure 4.15. Ion leakage assay to evaluate FB1-induced cell death. Leaf discs from 4-week-old Arabidopsis plants of the indicated genotype were floated on 5µM FB1 and immediately incubated in the dark for 48h. The discs were transferred to a light/dark cycle and conductivity measured at the indicated time-points. Bars represent mean conductivity ± SE (n = 5). An asterisk indicates a significant difference in the fold-changes between the wildtype (Col-0) and the indicated mutant line ($p \leq 0.05$).

4.6. Analysis of RNS1 expression in *dorn1* knockout lines

At the beginning of my PhD, a plasma-membrane bound receptor for extracellular ATP (eATP) was discovered (Choi *et al*. 2014). DOES NOT RESPOND TO NUCLEOTIDES 1 (DORN1) is a lectin-receptor kinase (LecRK1.9) that binds ATP with a high affinity and initiates ATP-induced calcium influx into the cytosol (Choi *et al*., 2014). Though eATP receptors had been discovered in mammalian systems for some time; DORN1 is the first eATP receptor to be identified in plants. Considering eATP has been reported as a powerful regulator of FB1-induced cell death (Chivasa *et al*., 2005), I wanted to investigate if loss-of-function *dorn1* mutants affect FB1-induced cell death. Due to the ATP binding potential and extracellular location of RNS1, I also wanted to determine if RNS1 gene expression could also be affected by the loss of DONR1.

T-DNA knockout (KO) lines for DORN1, hereafter termed *dorn1.1* (SALK_042209) and *dorn1.2* (SALK_024581), were obtained from the SALK collection (Alonso *et al*., 2003). T-DNA in the two SALK lines is inserted towards the 5' end of the exon (Figure 4.16.A). The lines were confirmed to harbour a T-DNA insert in the DORN1 gene expression by RT-PCR, using primers specific to the DORN1 sequence. Figure 4.16.B shows a PCR-amplified fragment in the Col-0, which does not exist in both T-DNA insertion lines, confirming that both of the *dorn1* mutants contained a T-DNA insertion that disrupted *DORN1* gene expression.

Considering the putative P-loop in *RNS1*, which is known to bind ATP in other proteins (Walker *et al*., 1982), it is possible that exogenous ATP might actually influence *RNS1* gene expression as well as RNS1 protein activity. Two important questions were asked in this chapter. Does exogenous ATP activate *RNS1* gene expression? If so, does the removal of the eATP receptor, DORN1, affect this potential ATP-induced *RNS1* expression? To investigate this, ATP was infiltrated into the leaf apoplast of Col-0 and *dorn1.1* mutant plants. Tissues for RNA extraction were harvested at various time-points within 8h. Figure 4.17 shows the qRT-PCR analysis of gene expression results. ATP infiltration activated *RNS1* transcription in both Col-0 and *dorn1.1* plants. However, gene activation in the Col-0 was superseded by activation in the mutant. This suggests two things: (i) that exogenous ATP activates *RNS1* gene expression in the absence of DORN1 and (ii)

that DORN1 attenuates activation of *RNS1* expression by exogenous ATP. Whether this has any bearing on FB1-induced cell death is not clear from these experiments.

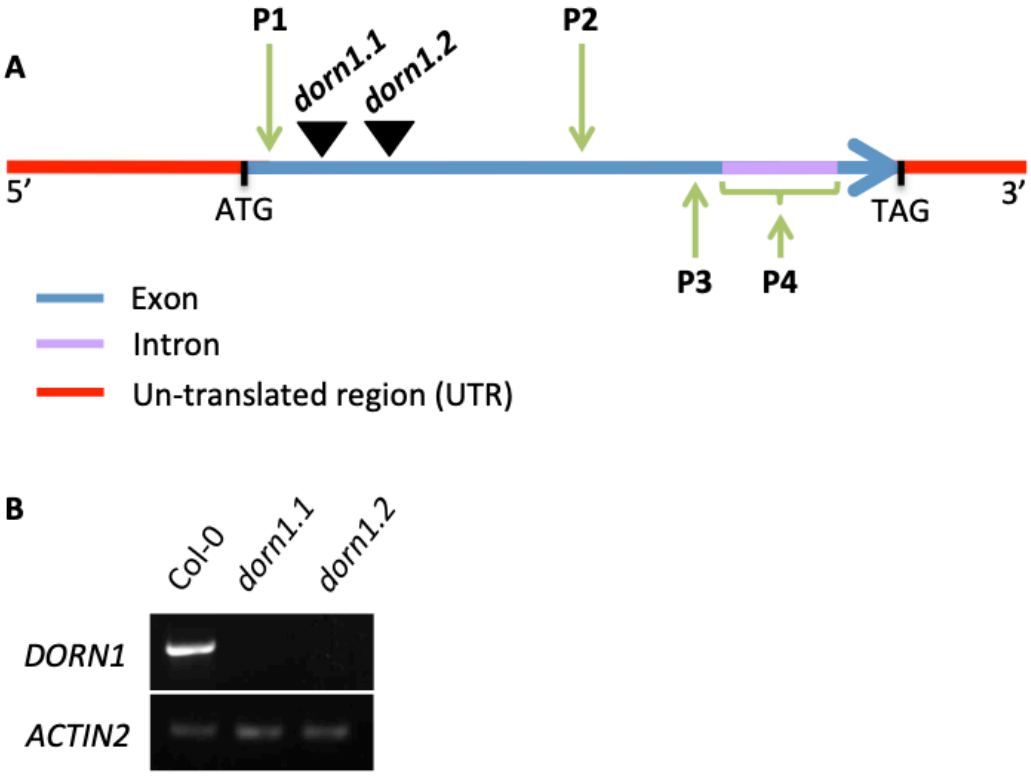

Figure 4.16. Analysis of *dorn1* T-DNA knockout plants. A) A schematic diagram of the insertion positions of *dorn1.1* and *dorn1.2* in the *DORN1* gene. P1 and P2 indicate position of primers used for RT-PCR confirmation of *dorn1* knockout mutants. P3 and P4 indicate position of primers used for qRT-PCR. **B)** RT-PCR analysis of *dorn1* knockout mutants. Primers specific to the DORN1 gene successfully amplified a PCR product in Col-0, whereas no product was present in the *dorn1.1* and *dorn1.2* mutants. *ACTIN2* was used as a constitutive reference control gene.

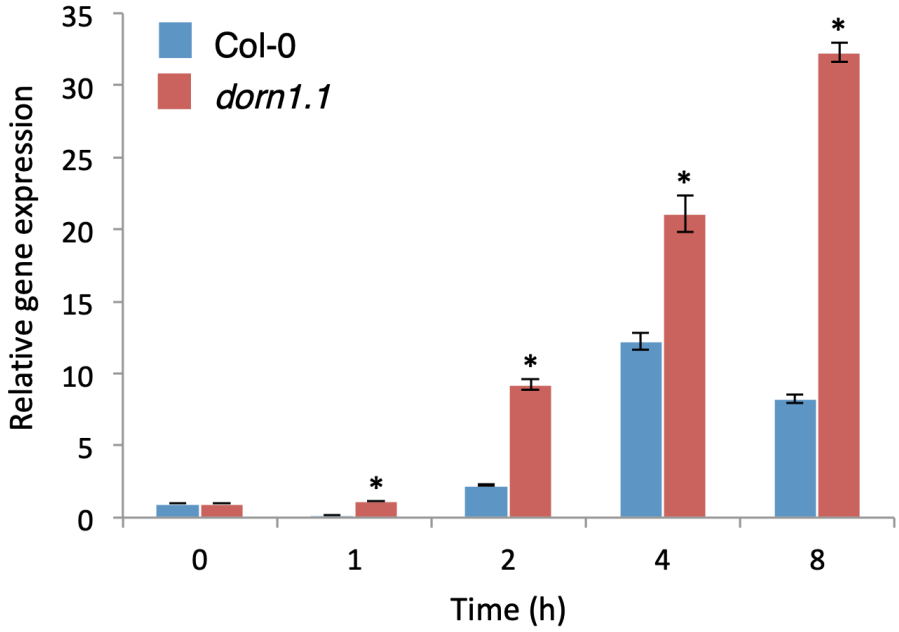

Figure 4.17. Exogenous ATP activation of *RNS1* gene expression. Arabidopsis plants with the indicated genoptypes were grown for 4 weeks and leaves infiltrated with 200µM ATP. Leaves were harvested at the indicated time-points for RNA extraction. *RNS1* gene expression was analysed using qRT-PCR. *ACTIN2* and *eIF4A* served as constitutive reference control genes. qRT-PCR values are an average of 3 technical replicates. Bars represent mean fold-change ± SD (n = 3). An asterisk indicates a significant difference in the fold-change between the wildtype (Col-0) and *dorn1.1* ($p \leq 0.05$).

A conductivity leaf disc assay using the *dorn1* knockout lines indicated a very modest, but significant reduction in ion leakage (Figure 4.18). In comparison with *rns1*, *dorn1* appears to have a lesser role in FB1-induced cell death. An important observation to note is the aggressiveness of the FB1 in the Col-0 lines. In Figure 4.15, Col-0 reaches almost 300µS/m at 144h, whereas in Figure 4.18 it only reaches 185µS. Both FB1 conductivity experiments used 5µM FB1, however I have observed that a number of factors can result in variation to the aggressiveness of FB1, specifically alterations in light intensity or duration. In particular, the plant growth room have several plant incubation bays. Although light intensity and airflow are strictly controlled via computerised systems, local variations around each bay may still exist depending on the age of different light bulbs and also the location of the bay in the growth room. This is the reason why each experiment incorporates a Col-0 control line that we use as a base-line for comparison. At 144h when the experiment was terminated, the *dorn1* knockout mutants had reduced conductivity (relative to

Col-0) by 26% (*dorn1.1*) and 41% (*dorn1.2*) (Figure 4.18). The *rns1* line showed a 52% reduction in conductivity (Figure 4.15). Although there were differences in the extent of FB1-induced cell death between these two experiments, by comparing the lines to their equivalent wild-type control, it can be concluded that RNS1 has a more crucial role in FB1-induced PCD regulation than DORN1.

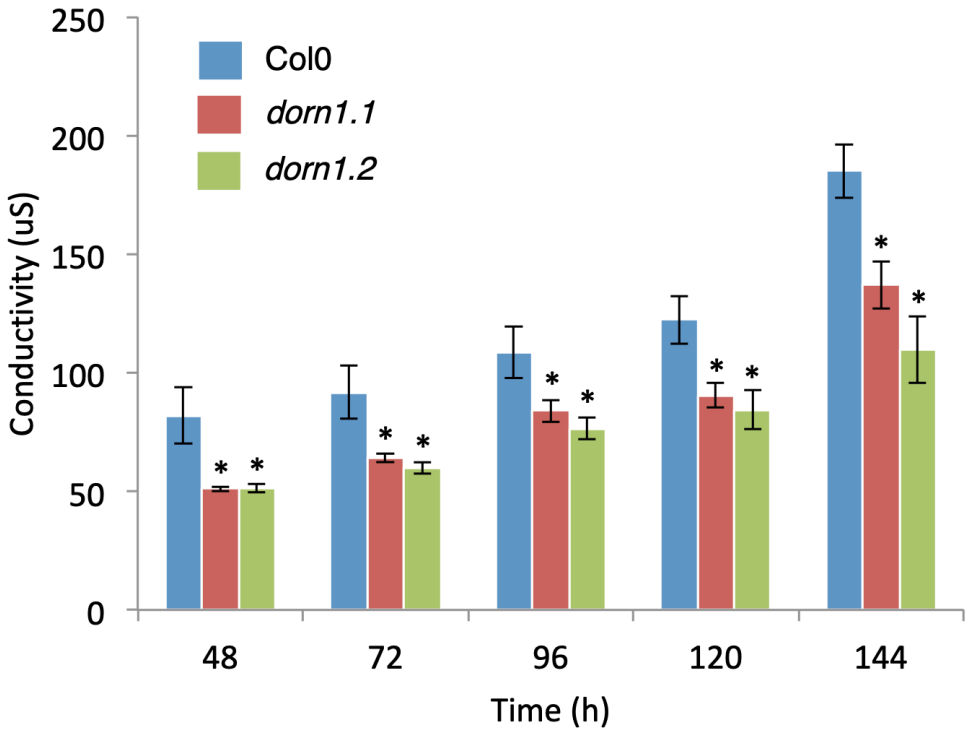

Figure 4.18. Leaf disc assay to evaluate FB1-induced cell death in *dorn1* knockout lines. Leaf discs of 8 mm diameter were cored from 4-week-old Arabidopsis plants (Col0) and floated on 5µM FB1. The leaf discs were incubated in the dark for 48h for maximal absorption of FB1 before being introduced to the light. The *dorn1* lines are less susceptible to FB1-induced PCD. Bars represent mean conductivity ± SE (n = 5). An asterisk indicates a significant difference in the fold-changes between the wildtype (Col-0) and the *dorn1* lines ($p \leq 0.05$).

Overall, the investigation in to RNS1 has highlighted a key molecular component in the response of *Arabidopsis thaliana* to FB1-induced cell death. Not only has RNS1 shown to be a positive regulator of cell death, but also by mutating the *RNS1* gene to inhibit RNase activity or potential ATP binding, suppression of the ability of RNS1 to induce cell death occurs. Furthermore, an induction in *RNS1* gene expression has been directly linked with exogenous ATP treatments, and this response to ATP is suppressed by the eATP receptor DORN1. Finally, DORN1 has shown to marginally regulate FB1-induced PCD, however DORN1 may not be as crucial a regulator as RNS1.

4.7. Discussion

The main focus of this chapter was to select a candidate from the iTRAQ screen in chapter 3, with the aim of investigating if it has a role in FB1-induced PCD. *RNS1* was selected due to its gene expression profile in response to FB1, as described in chapter 3 (Figure 3.8). *RNS1* was preferred over other candidate proteins because of the small number of proteins within its gene family in Arabidopsis (Table 4.1). As previously stated, the use of reverse genetics is likely to be more successful if the gene-of-interest comes from a small family of related proteins, as larger families might not result in a clear phenotype due to functional redundancy.

RNA-degrading enzymes, or more conveniently termed ribonucleases (RNases), have been studied in eukaryotic cells for a long time, with the first enzyme to be sequenced being the bovine pancreatic RNase A (Blackburn and Moore, 1982). There are three major families of RNases: RNaseA, RNaseT1, and RNase T2. T2 RNases have a wider distribution and are found in plants, animals, bacteria, protozoa and viruses (Deshpande *et al*., 2002). RNAse T1 only exists in bacterial and fungal systems, and RNaseA are only found in animals. Members of the T2 RNase family characteristically contain an archetypal signal sequence for entry into the secretory pathway; however, some inhabit internal compartments such as lysosome or vacuoles (Deshpande *et al*., 2002; Irie, 1999).

The first T2 RNases identified in plants, and those that make up the majority of the T2 family, are S-RNases. These RNases are glycoproteins located in the pistil of

self-incompatible (SI) Solanaceae, Rosaceae and Scrophulariaceae plants (Franklin-Tong and Franklin, 2003; Kao and Tsukamoto, 2004). The RNase activity is required for rejection of incompatible pollen (McClure *et al*., 1989; Huang *et al*., 1994). The T2 family is subdivided into S-RNases and S-like RNases. The latter are related to S-RNases, but do not play any role in SI and are expressed in various organs. S-like RNases are found in self-compatible plants and the expression is activated by specific stimuli. The S-like RNases have been implicated in various biological processes; however, an overall physiological function for the family remains unclear.

The expression of plant RNase genes has been observed to positively correlate with diverse physiological processes. Senescence is among the most prominent biological processes that influences S-like RNases, and this occurs in a number of plant species. During senescence, RNases are generally thought to have a role in the organised disassembly of the cells and redistribution of released materials, with particular emphasis on phosphate scavenging (McHale and Dove, 1967; Phillips *et al*., 1969; Löffler *et al*., 1993). S-like RNases expressed during senescence have been identified in Arabidopsis, *Atirrhinum* (AhSL28) and the Pomelo fruit, *Citrus grandis* Osbeck (CgSL2) (Liang *et al*., 2002; Chai *et al*., 2011).

The process of senescence and S-like RNase activity is linked with a phosphate starvation response. Phosphate limitation is a prominent condition in many soil types, therefore it would be useful for RNase gene products to scavenge phosphates from senescing tissues or dying organs for the benefit of growth and reproductive processes (Green, 1994). The first RNase implicated in phosphate starvation was the extracellular S-like RNaseLE of tomato (Nürnberger *et al*., 1990). Following this revelation, four other S-like RNases, localized to either the vacuole or endoplasmic reticulum, were also shown to respond to phosphate starvation in tomato cell suspension cultures (Löffler *et al*., 1992). The remobilisation of phosphates, particularly under limited phosphate conditions or senescence, has been linked with various other RNases, including AhSL28 from *Atirrhinum* (Liang *et al*., 2002; Nürnberger *et al*., 1990).

In Arabidopsis, there are 5 members of the S-like RNase family, RNS1 through to RNS5. Very little information is known about RNS4 and RNS5 and they remain uncharacterised. This was also confirmed by the inability of my laboratory group to

accumulate sufficient gene amplification using qRT-PCR (Chivasa, unpublished data). RNS1, RNS2 and RNS3 have been well characterised and successfully PCR-amplified (Taylor and Green, 1991; Bariola *et al*., 2007). Both RNS1 and RNS3 are extracellular RNases. They contain the archetypal signal peptide directing the RNases to the secretory pathway, as well as the absence of a HDEL/KDEL domain to retain the protein within the cell. RNS2 is also targeted to the secretory pathways but is retained to the vacuole (Taylor *et al*., 1993; Carter *et al*., 2004); this was confirmed via confocal microscopy with a cyan fluorescent protein (CFP) fusion to RNS2 (Hillwig *et al*., 2011). Immunolabeling also confirmed that RNS1 is secreted, whereas RNS2 is intracellular (Bariola *et al*., 1999).

There has been considerable interest in uncovering the function of the Arabidopsis S-like RNase genes. In Arabidopsis, RNS2 has been implicated as a senescence-induced ribonuclease, with RNS2 transcript increasing in senescing petals of intact Arabidopsis plants (Taylor *et al*., 1993). Expression of RNS3 and RNS1 is also induced during leaf senescence to a lesser extent (Taylor *et al*., 1993). Not unlike the previous RNases, Arabidopsis RNases have also been implicated in phosphate starvation. RNS1 has shown to be dramatically induced in response to phosphate starvation from a low basal level (Bariola *et al*., 1994). RNS2 showed a lesser induction in response to phosphate starvation, but already exhibited a high basal level (Bariola *et al*., 1994). Phosphate starvation had a minimal effect on RNS3 expression from a low basal level (Bariola *et al*., 1994). Although senescence and phosphate starvation appear to come hand-in-hand, the observation that RNS1 showed a modest response to senescence, but was massively induced in response to phosphate starvation, and vice versa with RNS2, indicates that the functionality of the S-like RNases differ. A possible explanation for the differing functionalities between the RNases, is that vacuolar RNases, such as RNS2, may be responsible for RNA decay during senescence. Vacuole lysis has been shown to occur prior to cell lysis (Matile, 1975) and therefore extracellular RNases will not interact with the components initiating vacuole lysis (Bariola *et al*., 1999), ergo RNS2 is likely to be at the forefront of senescence whereas extracellular RNases, such as RNS1 and RNS3, are likely to play a role in phosphate scavenging and remobilisation.

A characteristic response of phosphate starvation in plants is the accumulation of anthocyanins (Bariola *et al*., 1999), a type of flavonoid generating antioxidant effects. Anthocyanin production also coincides with the plants responses to UV, pathogen attack and nutrient stress (Stewart *et al*., 2001; Kliebenstein, 2004). Using antisense constructs of *RNS1* and *RNS2*, the accumulation of the native *RNS1* and *RNS2* was significantly inhibited. The resulting effect was the accumulation of abnormally high levels of anthocyanins. This indicates that although RNS1 and RNS2 may have differing localizations, together they have a distinct function in anthocyanin production (Bariola *et al*., 1999).

Another biological process extensively studied alongside RNases has been the wounding response in plants. The RNS1 protein from Arabidopsis shows a strong induction in response to wounding, both locally and systemically. The systemic response of RNS1 indicates a potential role in plant defence mechanisms, and this response has been confirmed to be independent of jasmonic acid and oligogalacturonide signalling, which are crucial regulators of systemic wound responses (LeBrasseur *et al*., 2002). Further investigations into RNS1 expression showed amplified induction in response to abscisic acid (ABA), however RNS1 can still be moderately induced by wounding, independent of ABA signalling (Hillwig *et al*., 2008). The RNaseLE from tomato has also shown to be induced in response to wounding, and unlike RNS1, does not accumulate systemically but remains local to the wounding site (Groß *et al*., 2004).

Alongside the apparent implication of RNS1 in phosphate starvation, anthocyanin production, and wounding; a recent proteomic study by Kaffarnick *et al*. showed RNS1 abundance to be down-regulated when Arabidopsis cell cultures were exposed to the virulent DC3000 strain of *Pseudomonas syringae pv*. tomato (Kaffarnick *et al*., 2009). In the proteomic study, RNS1 appeared alongside numerous genes responding to the bacteria, and no further work has investigated the role of RNS1 in plant bacterial immunity.

It appears that, unlike S-RNases, S-like RNases have not been defined by a clear biological function. Although there at biological functionalities that appear to correlate with the manipulation of S-like RNase abundance, a definitive role has not

been identified and the biological mechanism behind the role of S-like RNases remains elusive.

4.7.1 RNS1 is a positive regulator of FB1-induced PCD

The results in this chapter show that RNS1 promotes cell death. The loss-of function mutant, *rns1* showed significantly less cell death, in comparison with the wild type, in response to FB1. This was apparent in both direct infiltration of FB1 into the apoplast (Figure 4.14) and passive diffusion of FB1 through the stomata or wounds of cored leaf discs (Figure 4.15). The *rns1* phenotype was reversed by complementation with the native RNS1 (*rns1::RNS1*), showing severer symptoms of cell death compared to the wild type (Figure 4.14). Mutations of the *RNS1* amino acid sequence, targeting the RNase active site (*rns1*::m*RNS1*) or the P-loop (*rns1*::p*RNS1*) impaired the ability of RNS1 to reverse the phenotype of *rns1.2* knockout plants (Figure 4.14). The extent of cell death correlated with the ribonuclease activity displayed by the mutant proteins. The highest RNase activity, and the greatest intensity of cell death, was observed in the *rns1::RNS1* line, followed by the wild type (Figure 4.11; Figure 4.14). The *rns1*::p*RNS1* showed minimal RNase activity and a reduction in cell death (Figure 4.11; Figure 4.14). The *rns1*::m*RNS1* mimicked *rns1* with no RNase activity observed, and negligible symptoms of cell death (Figure 4.11; Figure 4.14).

The results imply that RNS1 functions as a pro-cell death protein, and that RNase activity is required for this process. Although the cell death-induction mechanism remains unclear, the concept of RNase involvement in PCD is not unprecedented. RNase proteins have been implicated in a diverse range of PCD pathways in mammalian systems. For example, inhibition of the mammalian protein RNase L in the 2-5A interferon pathway blocks apoptosis post-viral infection (Castelli *et al*. 1998). There has been strong precedence for RNases with anticarcinogenic and antiangiogenic properties. Ranpirnase (Constanzi *et al*., 2005), barnase (Edelweiss, 2008), binase (Zelenikhin *et al*., 2005) and ACTIBIND (Roiz *et al*., 2006) are all RNases that have shown to promote apoptosis within cancer cells. The involvement of RNases in PCD pathways is well established in mammalian systems, however there are a few examples in plants. The previously mentioned S-RNases promote self-pollen rejection through the cytotoxic effects of degrading pollen tube RNA, and

ultimately triggering actin depolymerisation and cell death (McClure *et al*., 1990; Franklin-Tong and Franklin, 2003; Takayama and Isogai, 2005). Another plant RNase involved in cell death is the rice probenazole-induced protein 1 (PBZ1), which has ribonuclease activity and activates PCD when expressed in Arabidopsis. PBZ1 also induces PCD when the recombinant protein is added to tobacco BY-2 cell suspension cultures or infiltrated into the leaf apoplast of tobacco plants (Kim *et al*., 2011). A further two examples of RNases that promote cell death, target ribosomal RNA. The cytotoxic lectin α-sacrin from *Aspergillus giganteus* is an RNase that targets 28S ribosomal RNA (Ackerman *et al*., 1988). Oconase is also a cytotoxic RNase from *Rana pipiens*, which also activates cell death by degradation of the 28S and 18S ribosomal RNA (Wu *et al*., 1993, Iordanov *et al*. 2000).

Although most examples indicate that RNases achieve cell death by RNA degradation, there are examples where the RNase activity is not required for cell death. ACTIBIND is a particularly interesting RNase as it is a fungal RNase protein from *Aspergillus niger* belonging to the T2 superfamily. In plants, ACTIBIND impedes the elongation and alters the orientation of pollen tubes by interfering with the intracellular actin network. This process is independent of RNase activity. ACTIBIND induces cross-linkage between actin filaments in pollen tubes and halts their elongation (Roiz *et al*., 1995a; 1995b; 2000). Furthermore, ACTIBIND has shown to inhibit angiogenesis and induce apoptosis of colonic tumours in rats (Roiz *et al*. 2006). ACTIBIND exerts antitumorigenic and antiangiogenic activities by competing with the ribonuclease angiogenin. The cytotoxic effect of ACTIBIND is not due the inhibition of protein synthesis via degradation of RNA, but it is internalized by melanoma cells and negatively competes with the angiogenic factor, angiogenin, in the nuclei of the cells (Schwartz *et al*., 2007). By blocking angiogenin signalling, angiogenesis is inhibited, resulting in the inhibition of the tumorigenic endothelial cell proliferation and blood vessel formation (Roiz *et al*., 2006; Schwarz *et al*., 2007).

It is clear that there is a strong precedence for RNase activity resulting in cell death. Many examples have shown that the mechanism for inducing cell death is the degradation of RNA and prevention of further protein synthesis, however sometimes

this is not simply the case and the resulting cell death occurs due to a complex signalling pathway involving the RNase protein.

A key question arising from these results is how a ribonuclease, located extracellularly, activates death via degradation of RNA? This requires RNS1 to enter the cytosol after exposure of tissue to FB1. Such a scenario has precedence in self-incompatibility. The S-RNase is secreted into the ECM from the pistil, and taken up by endocytosis into the pollen tube upon contact. If the pollen is incompatible, the S-RNase degrades RNA and triggers actin depolymerisation, resulting in pollen termination (McClure *et al*., 1990; Gray *et al*., 1991). Thus, S-RNase triggers pollen death via degradation of cellular RNA. Therefore, a role for plant ribonucleases in regulating cell death has precedence. Thus, I envision that localisation of RNS1 to the ECM acts as a means of sequestering a cytotoxic protein until its cytotoxicity is required in PCD.

4.7.2 DORN1 regulates ATP-induced *RNS1* activation

As stated in chapter 1, DORN1 is also referred to as LecRK1.9 (Choi *et al*., 2014). DORN1 is a membrane-bound lectin receptor kinase, with the lectin domain located on the extracellular side of the membrane, and the kinase domain on the intracellular side. The lectin domain has the ability to bind to extracellular ATP (Choi *et al*., 2014). Considering the role of eATP as a negative regulator of PCD (Chivasa *et al*., 2005; 2009), and the potential ATP-binding function of RNS1, I chose to investigate DORN1 alongside RNS1.

My investigation has shown that both RNS1 and DORN1 act as positive regulators of FB1-induced PCD. T-DNA insertion mutants for RNS1 and DORN1 have individually shown a reduction in cell death (RNS1 – Figure 4.14; Figure 4.15) (DORN1 – Figure 4.18). The extent of cell death reduction in the *dorn1* mutants is less dramatic than in *rns1*, indicating that RNS1 plays a more crucial role in FB1-induced cell death.

The possible connection between eATP-binding and both DORN1 and RNS1, led me to consider that the DORN1 receptor may directly or indirectly interact with the extracellular RNS1 to initiate an intracellular PCD signal. Injecting exogenous ATP

into wild type Arabidopsis leaves increases the expression of *RNS1*. In the *dorn1.1* mutant, the expression of *RNS1* is augmented. After reconsidering the experimental procedure to produce Figure 4.17, I realised that the increase in *RNS1* expression could be a wounding response, rather than a response to the ATP treatment. It is difficult to distinguish between wounding and ATP response for injecting tissues, as the wounding that occurs through injection will damage cells and cause ATP leakage into the apoplast. For a true representation of *RNS1* expression in response to eATP, I would propose using cell cultures and adding exogenous ATP to the culture medium. Unfortunately, due to time constraints, I was unable to begin the process of creating and maintaining cell cultures of *dorn1.1*. This would be a useful tool for future experimentation on *dorn1* mutants. For now, I can conclusively state that the transcriptional response of *RNS1* to wounding or exogenous ATP treatments is suppressed by DORN1.

4.7.3 Concluding remarks

My project has (i) developed a screen that uses light regulation to identify putative PCD regulatory proteins; (ii) selected RNS1 from the screen and found a positive regulatory role in FB1-induced PCD; and (iii) explored the link between this protein and the eATP receptor, DORN1.

5 Identification of EARP1 – a putative transcription factor regulating FB1-induced cell death

5.1. Introduction

Extracellular ATP (eATP) is a regulator of FB1-induced PCD as reported in the experiments of Chivasa *et al*. (2005). In these experiments, treatment of Arabidopsis cell cultures with FB1 activated gradual depletion of eATP starting from 16 h until no ATP was detectable in the culture medium by 40 h. Cell death, as measured by the breach in cell membrane integrity using Evans blue staining, commenced at 72 h after FB1 addition. This showed that depletion of eATP precedes the onset of cell death. Preventing eATP depletion by addition of exogenous ATP concurrently with FB1 prevented cell death (Chivasa *et al*., 2005). This suggested that eATP regulates FB1-induced cell death.

Subsequent experiments revealed that rescue of cells from cell death was possible only if exogenous ATP was added to the cultures concurrently with FB1 or at any time after until ~40 h. Added from 48 h onwards, exogenous ATP failed to rescue the cells from FB1-induced cell death, suggesting that beyond 40 h the cells are irreversibly committed to PCD. This suggests that between 40-48 h, there is an irreversible switch that commits cells to PCD (Figure 5.1). These results provided the basis for developing a screen using FB1 and ATP to identify genes with a critical role in FB1-induced cell death. Gene expression of cell cultures treated with FB1 can be compared to gene expression in cell cultures treated with both FB1 and ATP. Because ATP rescues the cells from PCD, genes whose response to FB1 is significantly changed by ATP may encode the protein network responsible for activation of cell death. Crucially, if the screen is confined to the 40-48 h time window, genes responsible for commitment to cell death could be identified.

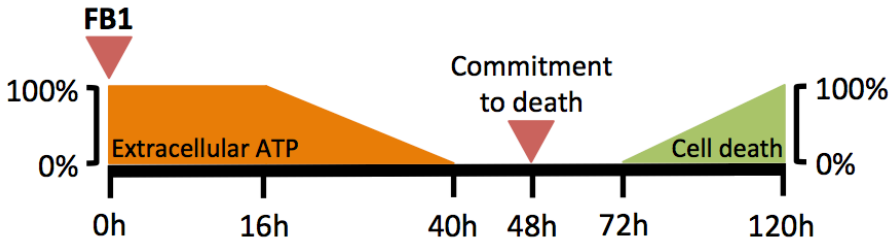

Figure 5.1. Schematic representation of FB1-induced cell death and the effects of extracellular ATP (eATP). The addition of FB1 to cell cultures results in gradual depletion of eATP starting at ~16 h. By 40 h, eATP is undetectable and cell death starts from 72 h. Cell death can be averted by replenishing the cell cultures with exogenous ATP at any point in the experiment up until 40 h. Between 40 – 48 h a commitment to cell death occurs, after which exogenous ATP is unable to prevent the initiation of cell death. Note that the decline of eATP from 100 – 0% and the increase of cell death from 0 –100% do not progress at rates indicated by the gradients on the diagram. (Chivasa *et al*., 2011).

5.2. Extracellular ATP and FB1 used to screen for putative PCD-regulatory genes

Prior to my PhD project, our group conducted a DNA microarray analysis to screen for FB1-responsive genes, which are impacted by exogenous ATP. Arabidopsis *Landsberg erecta* (Ler) cell cultures were exposed to FB1, and then further mock-treated or exogenous ATP-treated 40 h later. Cells were harvested at 41, 42, 44 and 48 h time-points. Out of a total of 7,258 genes responding to FB1, the response of 22% (1,656) of these genes was significantly ($p < 0.05$) altered by exogenous ATP. The gene list was filtered by excluding genes without a minimum threshold of 2-fold change in response to ATP on at least one of the time-points. This gave rise to a final list of 175 genes. As expected, gene ontology (GO) analysis of the 175 genes revealed an enrichment of stress responsive and defence-related genes (Figure 5.2.A). The GO analysis also determined the predominant localization of proteins encoded by these genes to be the plasma membrane and extracellular matrix (Figure 5.2.B). Among the 175 genes responsive to FB1 and ATP treatments are 13 putative transcription factors. The research group further analysed these 13 genes to ensure that the response to ATP seen in the cell culture *in vitro* system occurs in planta (Chivasa, unpublished data). The greatest change in response to ATP was seen in *At1g49900*, a zinc-finger protein in the C2H2 transcription factor family, which was duly named EXTRACELLULAR ATP-RESPONSIVE PROTEIN 1 (EARP1).

EARP1 expression was stimulated by FB1 treatment (Figure 5.3). Addition of exogenous ATP 40 h after FB1 treatment resulted in a rapid suppression of *EARP1* (Figure 5.3). This shows that *EARP1* expression is tightly controlled by ATP, which completely overrides the effects of FB1. The hypothesis of the screen was that the response of putative cell death-regulatory genes to FB1 would be reversed by exogenous ATP, which rescues cells from cell death. Due to the *EARP1* expression fitting the predicted profile of a key regulator of FB1-induced cell death, this gene was selected for further investigation.

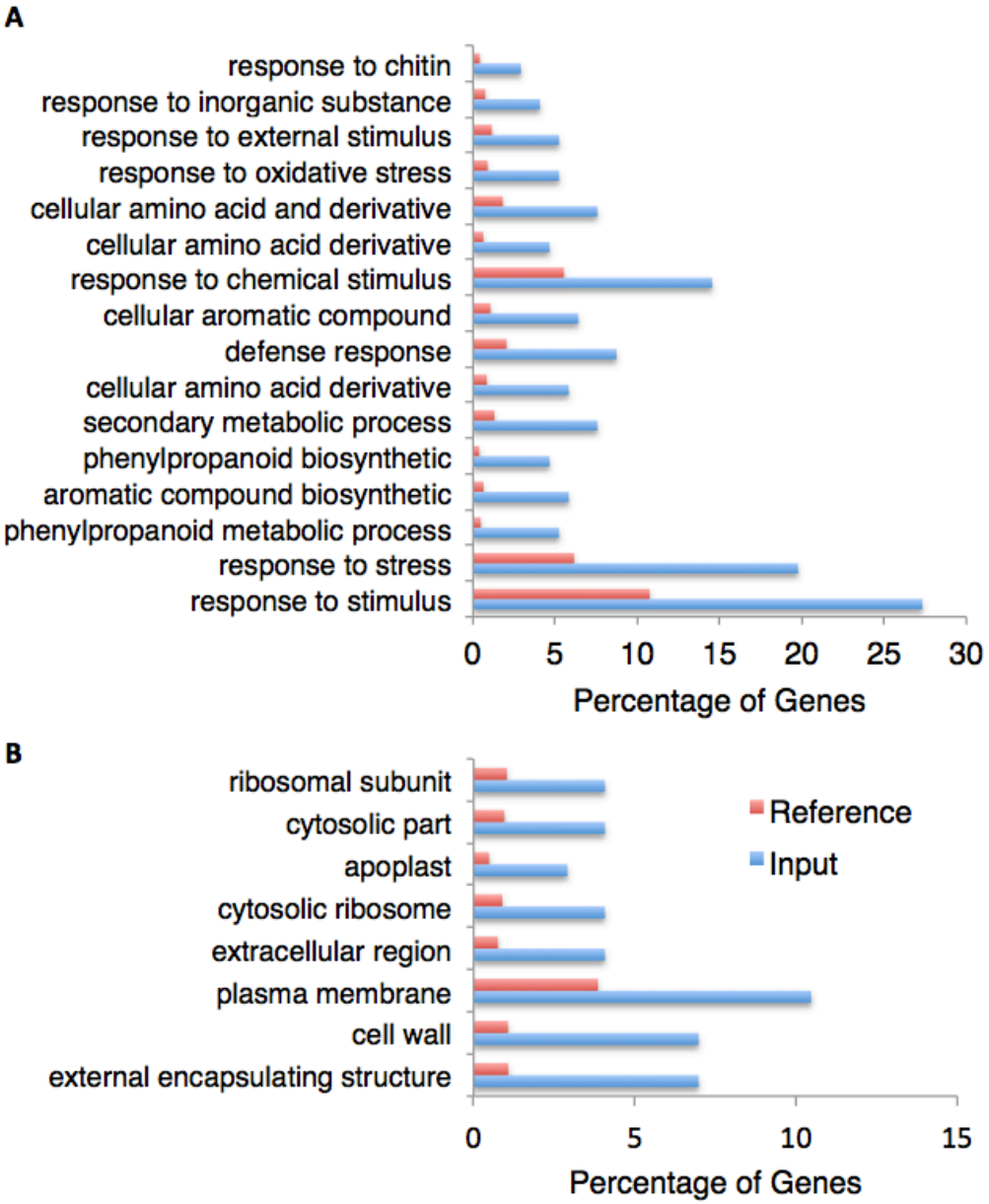

Figure 5.2. Gene Ontology analysis of the 175 genes responding to exogenous ATP, after FB1 treatment. A) The biological functions showing particular enrichment among the 175 genes identified. **B)** The localizations showing particular enrichment among the 175 genes identified.

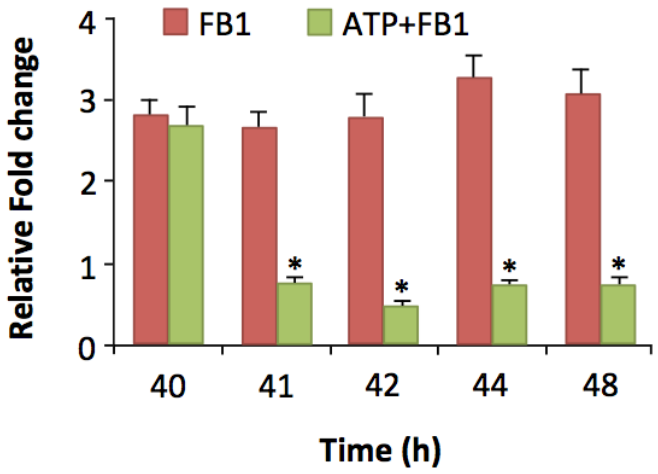

Figure 5.3. qRT-PCR analysis of *EARP1* expression in response to FB1 and exogenous ATP. Arabidopsis cell cultures were mock-treated or treated with FB1 alone, or ATP+FB1. Exogenous ATP was added at 40 h. Samples for RNA extraction were taken at the indicated time points and analysed by qRT-PCR. qRT-PCR values are an average of 3 technical replicates. Bars represent mean fold-change ± SD (n = 3). An asterisk indicates a significant difference in the fold-change between control and FB1 samples ($p \leq 0.05$).

5.3. EARP1 regulates FB1-induced PCD

Gene knockout mutants of were used in genetic experiment to investigate the potential role of EARP1 in FB1-induced cell death. The T-DNA insertion lines SALK_070432 and SALK_100396, hereafter referred to as *earp1.1* and *earp1.2*, were obtained from the SALK collection (Alonso *et al*, 2003). The location of the T-DNA inserts within the *EARP1* gene are shown in Figure 5.4.A. The *earp1.1* line contains a T-DNA insert in the first exon, towards the 5' end of the gene, whereas the *earp1.2* line has the insertion in the second exon, towards the 3' end of the gene. Confirmation of the T-DNA presence in the mutants is shown in Figure 5.4.B. Using primers straddling the T-DNA insertion sites, PCR amplified an *EARP1* genomic transcript in the wild type (Col-0), which was not present in both mutants, confirming disruption of the gene sequence by a T-DNA insert.

To evaluate the effects of EARP1 on FB1-induced cell death, leaf discs cored from Col-0, *earp1.1*, and *earp1.2* plants were floated on 5µM FB1 solutions. The leaf discs were incubated in the dark for 48 h before being exposed to the normal light-dark cycle. Conductivity of the FB1 solution was measured at 48 h and every 24 hours subsequent to this. The wildtype leaf discs initially developed patches of

chlorosis, which expanded to cover extensive areas. By about 5 days from the start of the experiment, the Col-0 discs showed extensive cell death characterized by patches of bleached transparent tissues. Both *earp1* knockout mutants showed very little signs of cell death. Representative leaf discs from Col-0 and earp1.1 were photographed and show typical symptoms (Figure 5.5.A).

Conductivity of the FB1 solutions upon which leaf discs were floated reflected the level of cell death within the plant tissues. While there was a steady rise over time in ion leakage from Col-0 tissues, both *earp1* knockout mutants significantly suppressed ion leakage in response to FB1 (Figure 5.5.B). Together, the suppression of ion leakage and the healthy appearance of *earp1* mutants leaf discs, indicate that loss of EARP1 impairs the development of FB1-induced cell death.

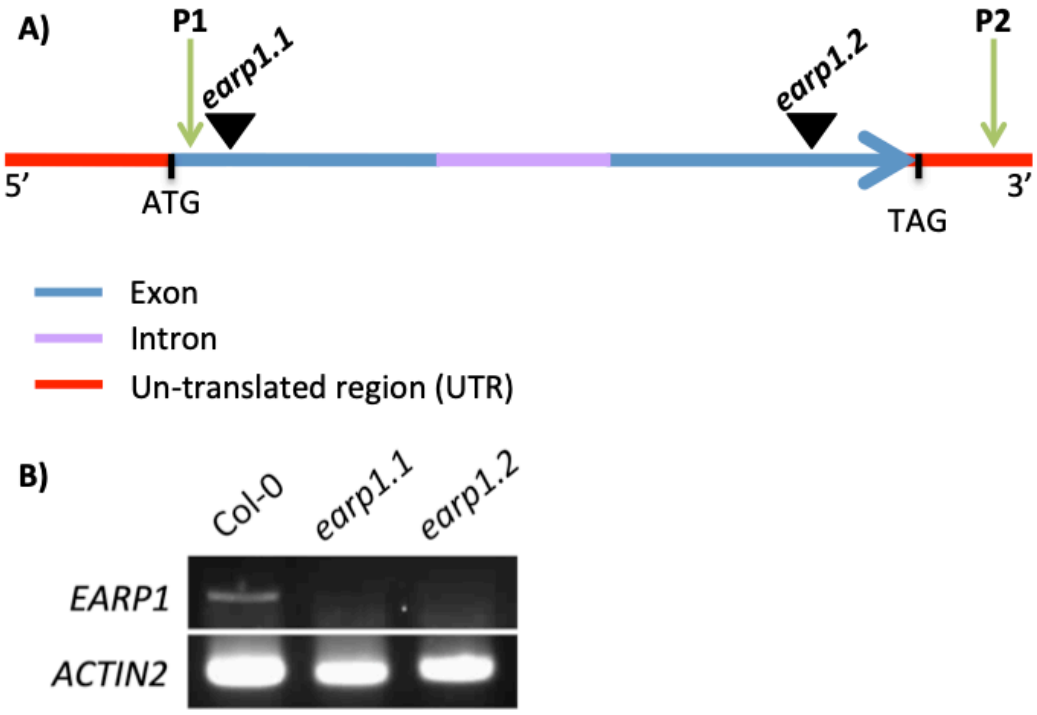

Figure 5.4. Confirmation of *EARP1* T-DNA insertion lines. A) Schematic representation of the *EARP1* gene showing the positions of T-DNA insertion. P1 and P2 indicate primer positions. **B)** Amplification of the genomic DNA using P1 and P2 primers straddling each of the T-DNA insertion positions. In Col-0 the expected amplicon is present, which is absent from *earp1.1* and *earp1.2*. This indicates that both mutant lines have the T-DNA insert. *ACTIN2* was used as a constitutive reference control gene.

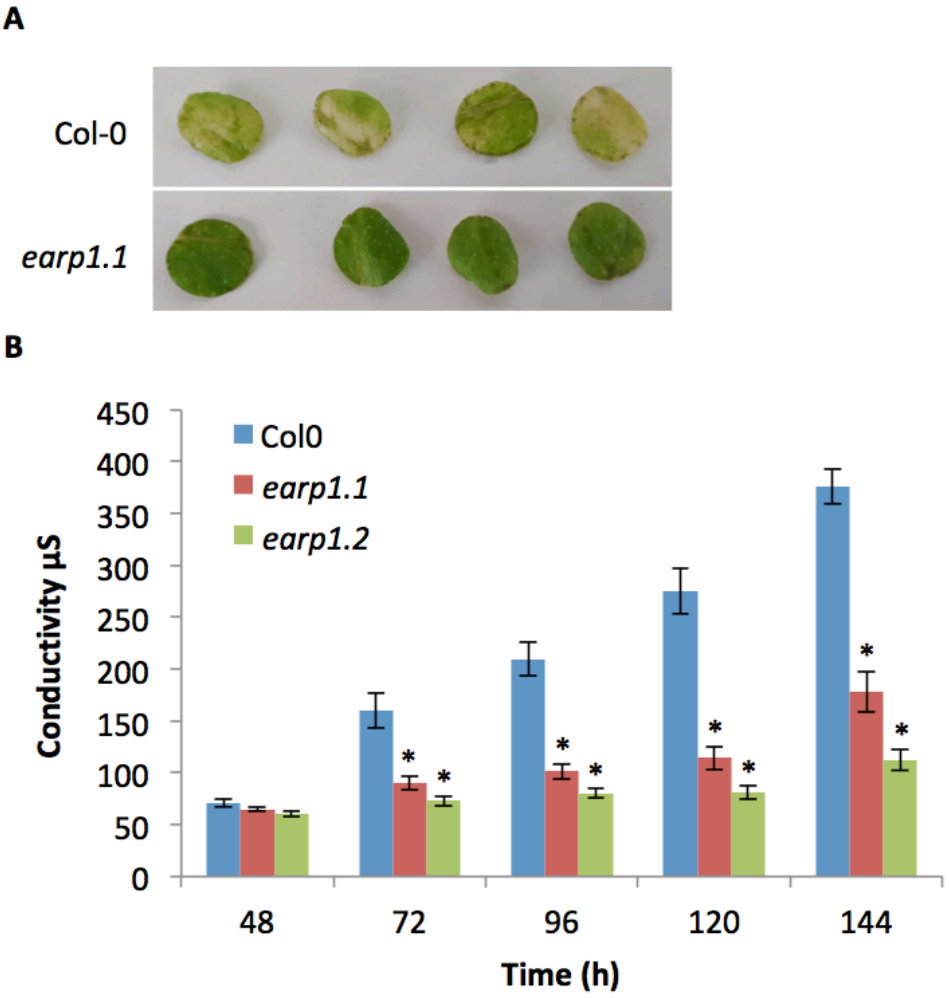

Figure 5.5. The response of *earp1* mutants to FB1. A) Leaf discs of 8mm diameter were floated on 5µM FB1. After a 48 h period of dark incubation at room temperature, the floating leaf discs were transferred to a 16 h-photoperiod. Photos were taken 5-days after treatment. **B)** Conductivity of the 5 µM FB1 solution on which leaf discs were floating was measured at 48 h and every 24 h after that. Asterisks indicate a significant difference between the *earp1* mutant and the wild type (Col-0) ($p \leq 0.05$). Bars are mean conductivity reading ±SD (n=5).

5.4 EARP1 mediates FB1-induced expression of some genes

Preceding results indicated that EARP1 is required for FB1-induced cell death. This provoked the question of whether FB1 requires EARP1 for activation of at least some of the FB1-induced genes. To investigate this, I selected *RNS1, BGLU46* and *PRX52* as FB1 marker genes previously shown to be responsive to FB1 (see chapter 3).

Col-0 and *earp1.1* leaf discs were floated on 5μM FB1 solution and incubated in the dark for 48 h. The discs were then transferred to a 16h-photoperiod. Samples for RNA extraction were harvested at the beginning of the experiment and every 24 h subsequent to this. Analysis of gene expression was quantified using qRT-PCR.

As expected, all 3 marker genes were up-regulated in response to FB1 in the Col-0 plants (Figure 5.6). Activation of *BGLU46* and *PRX52* was well-above 100-fold in comparison to the modest 10-fold increase in *RNS1*. However, activation of all marker genes was significantly suppressed in the *earp1.1* mutant. The suppression was more substantial in *BGLU46* and *PRX52* transcripts, while the *RNS1* was marginally suppressed. These results indicate that EARP1 mediates FB1-induced expression of certain genes, such as BGLU46 and PRX52, while its effects on others might be quite marginal. It is important to note that the disruption of EARP1 does not completely suppress gene expression of these markers, indicating some level of redundancy in the requirement of EARP1.

Overall, the cell death profile and marker gene analysis of EARP1 have shown that this putative transcription factor is an important regulatory protein of FB1-induced cell death, and appears to regulate someFB1-responsive genes. The extent to which EARP1 regulates FB1-induced gene expression requires a genome-wide analysis, such as DNA microarrays.

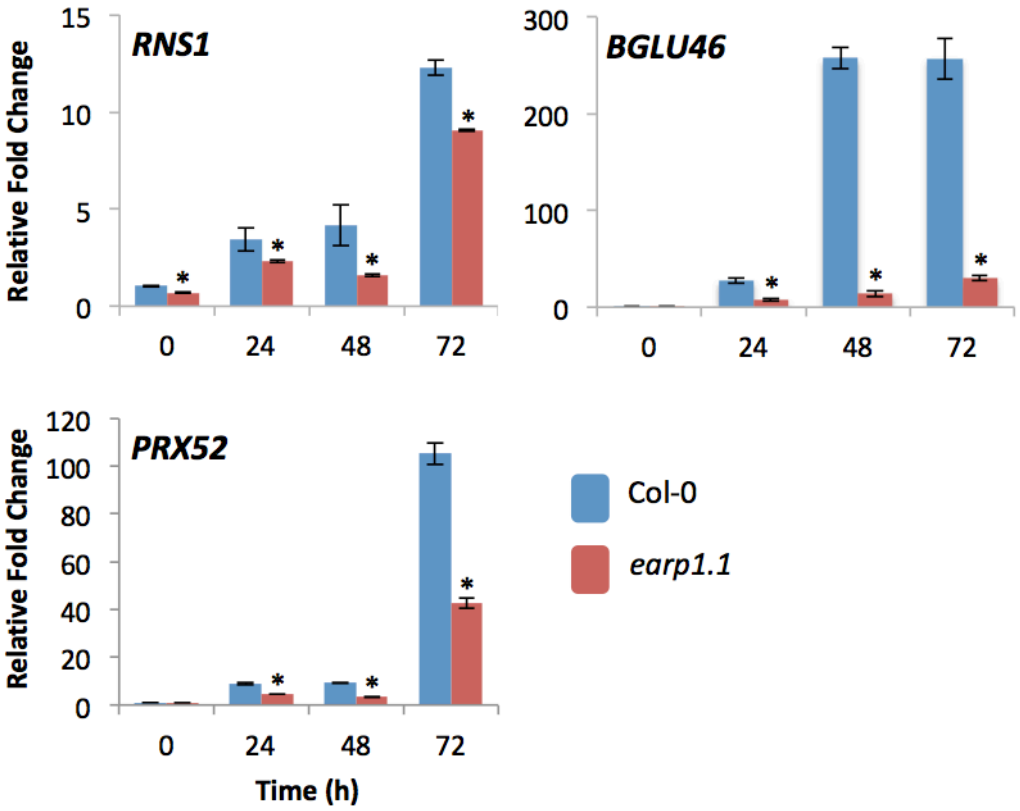

Figure 5.6. Effects of *earp1* knockout mutation on FB1-induced marker genes. 10 Leaf discs from 10 independent plants were floated on 5µM FB1 and incubated in the dark for 48 hours prior to transfer to a 16h-photoperiod. Samples were harvested at the indicated time points for RNA extraction and gene expression analysed using qRT-PCR. qRT-PCR values are an average of 3 technical replicates. Bars represent mean fold-change ± SD (n = 3). An asterisk indicates a significant difference in the fold-change between Col-0 and *earp1.1* samples ($p \leq 0.05$). *ACTIN2* and *EIF4A* were used as constitutive reference control genes.

5.5. Microarray analysis

Preceding results demonstrated that EARP1 is a regulator of cell death, which also controls FB1-induced gene expression. To further our understanding of this transcription factor and determine the extent of its influence on FB1gene activation, a whole-genome DNA microarray analysis was conducted on RNA samples extracted from FB1-treated Col-0 and *earp1.1* leaves. The aim of the experiment was to identify FB1-induced genes, which are downstream of EARP1. Some of these genes could have a putative role in FB1 signalling and FB1-induced PCD. Leaves of 5-week old Col-0 and *earp1.1* plants were injected with either 5µM FB1 or water. After 24 h, directly infiltrated leaf samples were harvested for RNA extraction. The RNA samples were processed through Oaklabs' ArrayXS (Oak-labs, Hennigsdorf, Germany). The microarray identified 7,733 genes significantly ($p < 0.05$) responding to FB1, irrespective of the genetic background. These genes had passed the response threshold of a minimum modulus Log_2 fold-change of 1. From the 7,733 genes, 53% were responsive in the Col-0 background, while 97% responded to FB1 in the *earp1.1* mutant. The total number of genes whose response to FB1 significantly ($p < 0.05$) differed between Col-0 and *earp1.1* was 5,389, which constitutes 70% of the FB1 responsive genes.

GO analysis was performed on the 5,389 genes showing a differential transcriptional response to FB1 between Col-0 and *earp1.1* (Figure 5.7). In this chapter I have highlighted the types of stimuli that induce a transcriptional response for a number of the 5,389 genes (Figure 5.7). The list of genes was enriched for chemical and stress-responsive genes, and in particular, genes responsive to the hormones: ABA, JA, ET and SA, which are key hormones in plant defence. With regards to plant defence, the list was particularly enriched for genes responding to chitin/fungi and bacteria (Figure 5.7). Further GO analysis also indicated that the functionality of the majority of genes was catalytic and binding activity, with particular emphasis on transferase activity, hydrolase activity and nucleotide binding. The predicted localization of the encoded proteins was predominantly intracellular and membrane-bound. The cytoplasm, plastid and chloroplast were prime locations for many of the genes.

Further filters were applied to the 5,389 genes to generate two priority lists of genes, which might have important functions in FB1 responses downstream of EARP1. The first list contained 53 genes that significantly responded to FB1 in Col-0, but showed no significant response in *earp1.1* (Table 5.1). Therefore, activation of these genes by FB1 is completely dependent on EARP1. The second list contains 527 genes that significantly responded to FB1 in *earp1.1*, but showed no significant response in Col-0. Therefore, the response of these genes to FB1 is suppressed by EARP1. The top 60 genes from the second list, showing the highest fold change in *earp1.1*, can be seen in Table 5.2. A heat map depicting the genes response to FB1, for each of the lists is shown in Figure 5.8. The heat map used red to indicate genes that were up-regulated in response to FB1, and green for those that were down-regulated. The lists show a mixture of up- and down-regulated genes, but the main focus is the dramatic difference between the Col-0 and *earp1.1*. Figure 5.8.A shows the list of 53 genes significantly responding to FB1 in Col-0, which is indicated by the majority of bright red or green bands. In the *earp1.1* background there are no bright bands with a large proportion completely black, which indicates no response to FB1. Figure 5.8.B shows the opposite results for the second list, with 527 genes significantly responding to FB1 in *earp1.1*, but not responding in the wild type. The heat map emphasises the dramatic effect of disrupting *EARP1* expression on Arabidopsis response to FB1. Although 5,389 genes have been identified as FB1-responsive and regulated by EARP1, the subset of 580 genes are likely to be of more critical importance in understanding the role of EARP1 in FB1-induced physiological responses, including cell death.

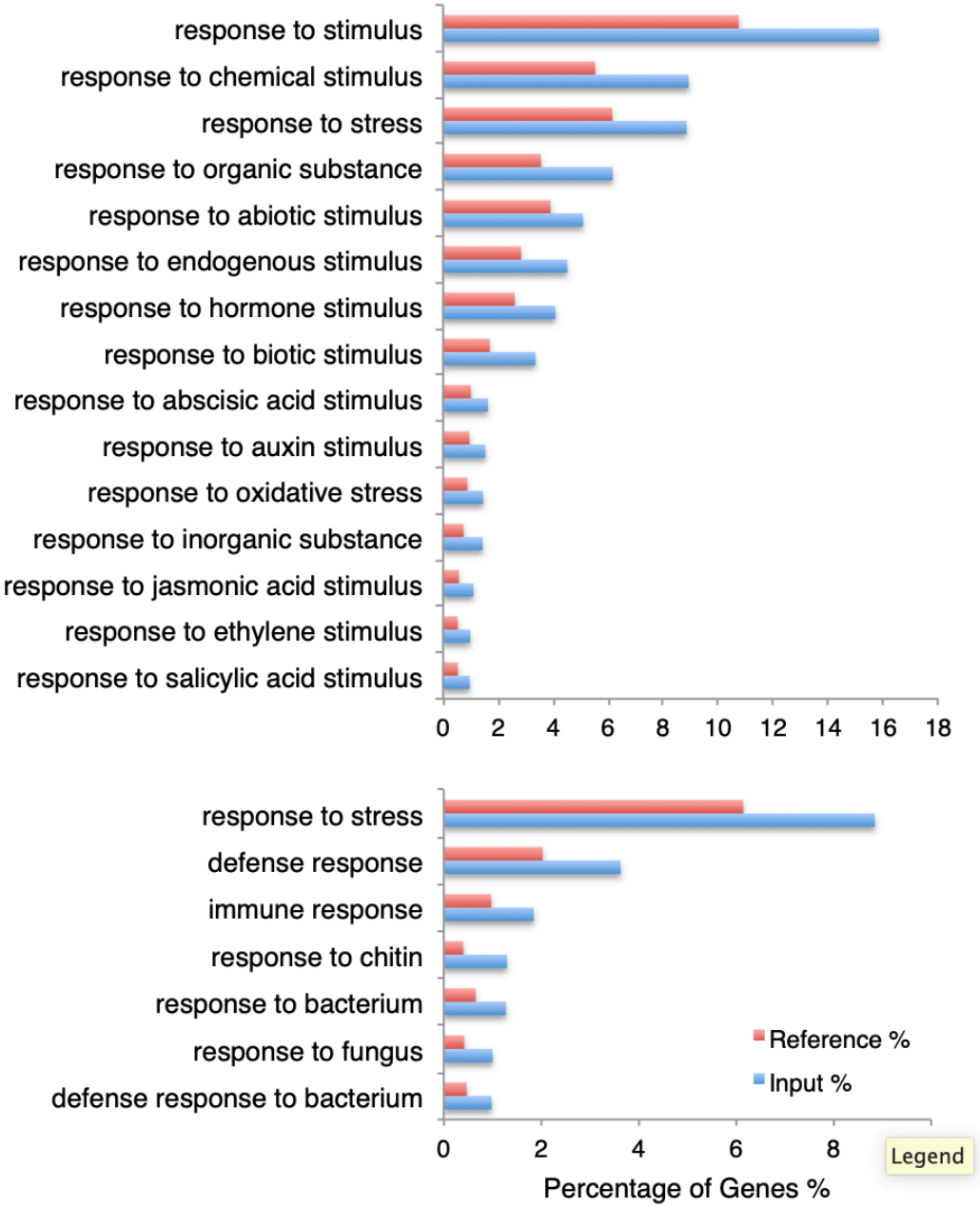

Figure 5.7. Gene Ontology analysis of 5,389 genes responding to FB1 in either the Col-0 or *earp1.1* background by a modulus of 1 (Log2) fold change. These genes showed a response to FB1 which was altered by the *earp1* mutation. The chart shows the biological processes that were particularly enriched within the list of genes. The 5,389 genes (Input %) were compared with the whole Arabidopsis genome (Reference %).

Table 5.1. FB1 responsive genes that are suppressed in *earp1.1*

Target Name[a]	Gene Symbol[b]	Col-0		*earp1.1*		Col-0/ *earp1.1*[e]
		F-C[c]	*p-value*[d]	F-C	*p-value*	*p-value*
AT2G20030		3.49	0.004	1.79	0.061	0.017
AT5G51990	CBF4	3.06	0.003	0.79	0.264	0.006
AT4G27890		2.81	0.05	-1.26	0.285	0.036
AT5G48000	CYP708A2	2.44	0.003	1.33	0.191	0.041
AT2G17723		2.16	0.008	0.76	0.395	0.028
AT3G59930		2.16	0.038	-0.2	0.774	0.036
AT3G28600		2	4.74E-06	0	0.996	0.00002
AT3G26200	CYP71B22	1.95	0.044	0.05	0.873	0.049
AT1G03940		1.87	0.00044	0.16	0.587	0.00024
AT5G54045		1.84	0.028	-0.83	0.158	0.012
AT5G24770	VSP2	1.7	0.00004	0.05	0.918	0.001
AT1G03495		1.66	0.006	0.19	0.473	0.007
AT5G60350		1.54	0.005	0.55	0.062	0.017
AT5G24780	VSP1	1.54	0.00002	0.33	0.436	0.001
AT5G42800	DFR	1.54	0.029	-0.41	0.445	0.012
AT4G22880	LDOX	1.46	0.025	-0.28	0.514	0.013
AT1G80580		1.45	0.00002	0.06	0.929	4.81E-06
AT1G56650	PAP1	1.43	0.002	0.17	0.569	0.002
AT4G11650	OSM34	1.37	0.014	-0.13	0.927	0.003
AT2G32830	PHT1;5	1.36	0.004	0.59	0.1	0.031
AT5G29054		1.3	0.012	0.23	0.573	0.037
AT5G35770	SAP	1.29	0.011	-0.18	0.755	0.013
AT5G59390		1.29	0.015	-0.38	0.357	0.003
AT2G37430		1.26	0.005	0.63	0.41	0.049
AT1G02405		1.23	0.006	0.45	0.221	0.039
AT4G25030		1.21	0.001	0.62	0.051	0.015
AT2G20880	ERF53	1.17	0.002	0.16	0.594	0.002
AT4G15210	BAM5	1.15	0.045	-0.41	0.444	0.024
AT2G39865		1.14	0.02	0.05	0.787	0.015
AT4G14090		1.09	0.013	-0.63	0.063	0.003
AT5G24370		1.08	0.04	-0.17	0.702	0.037
AT1G73330	DR4	1.08	0.006	-0.35	0.408	0.002
AT5G17220	GSTF12	1.07	0.028	-0.84	0.052	0.004
AT4G13120		1.05	0.024	-0.07	0.782	0.017
AT5G52670		1.01	0.049	-0.6	0.561	0.021
AT5G38895		1	0.03	0.25	0.628	0.04
AT5G49360	BXL1	-1.01	0.001	0.29	0.176	0.003
AT5G20870		-1.03	0.044	0.63	0.235	0.006
AT1G63230		-1.04	0.003	-2.28	0.084	0.00028

AT3G11560		-1.1	0.042	-0.39	0.162	0.009
AT3G31945		-1.15	0.042	0.01	0.319	1.15E-12
AT5G28080	WNK9	-1.17	0.002	-0.39	0.082	0.001
AT2G05914		-1.19	0.038	-0.18	0.516	0.02
AT2G31460		-1.21	0.002	-0.11	0.785	0.003
AT1G47490		-1.22	0.00008	-0.34	0.233	0.00006
AT3G50450	HR1	-1.33	0.003	-2.83	0.156	0.00004
AT3G29644		-1.34	0.005	-0.46	0.181	0.018
AT5G02200	FHL	-1.37	0.001	-0.27	0.415	0.012
AT5G44770		-1.39	0.046	-0.72	0.281	0.022
AT3G06080		-1.4	0.00027	-0.71	0.087	0.004
AT1G13770		-1.4	0.042	0.58	0.36	0.044
AT5G24510		-1.44	0.047	0.36	0.322	0.00023
AT2G23347	MIR844A	-1.67	0.044	-0.6	0.162	0.001

[a]AGI (Arabidopsis Genome Initiative, 2000) code
[b]Gene symbol used in NCBI database
[c]F-C is the $\log_2$ fold change gene expression in in response to FB1
[d]PComparison of FB1-induced gene expression between Col-0 and *earp1.1*

Table 5.2. The top 60 FB1 responsive genes that are activated in *earp1.1*

Target Name[a]	Gene Symbol[b]	Col-0		*earp1.1*		Col-0/ *earp1.1*[e]
		F-C[c]	*p-value*[d]	F-C	*p-value*	*p-value*
AT4G26260	MIOX4	0.69	0.181	4.97	0.02	0.022
AT5G38960		0.51	0.328	4.61	0.004	0.004
AT5G24205		-0.3	0.816	4.44	0.00047	0.00042
AT1G52900		0.82	0.102	4.35	3.60E-07	5.89E-07
AT2G45130	SPX3	1.11	0.059	4.19	0.023	0.03
AT1G60740		0.98	0.073	4.1	0.005	0.007
AT5G39180		1.07	0.126	3.97	0.024	0.033
AT5G19880		0.8	0.057	3.93	0.001	0.001
AT5G39100	GLP6	0.32	0.518	3.86	0.008	0.008
AT5G39110		0.74	0.152	3.83	0.007	0.009
AT1G53940	GLIP2	0.28	0.496	3.77	0.004	0.004
AT2G15780		0.66	0.313	3.75	0.008	0.01
AT2G26410	Iqd4	0.41	0.276	3.71	0.007	0.008
AT5G40990	GLIP1	0.04	0.906	3.66	0.006	0.006
AT5G59100		0.42	0.318	3.57	0.015	0.017
AT1G66852		0.57	0.107	3.55	0.001	0.001
AT3G14225	GLIP4	0.74	0.201	3.52	0.017	0.023
AT2G25090	CIPK16	0.48	0.149	3.51	0.001	0.001
AT4G17215		0.94	0.095	3.5	0.006	0.009
AT3G12910		0.52	0.089	3.48	0.00024	0.0003
AT1G26410		0.74	0.054	3.47	0.001	0.001
AT5G26310	UGT72E3	-0.25	0.54	3.46	0.001	0.001
AT1G09935		0.17	0.592	3.46	3.77E-06	3.00E-06
AT5G66690	UGT72E2	-0.28	0.474	3.46	0.002	0.002
AT3G44540	FAR4	-1.04	0.606	3.45	0.018	0.014
AT5G58840		0.37	0.412	3.43	0.019	0.022
AT4G33467		0.99	0.155	3.41	0.009	0.016
AT4G35380		0.4	0.213	3.35	0.001	0.001
AT2G04100		0.41	0.244	3.18	0.001	0.001
AT2G29100	GLR2.9	0.61	0.092	3.16	0.00043	0.001
AT1G26970		1.07	0.141	3.06	0.008	0.018
AT3G22620		0.36	0.26	3.05	0.0003	0.00033
AT5G53820		0.34	0.454	3.05	0.004	0.005
AT2G04090		0.39	0.28	3.04	0.001	0.002
AT1G64070	RLM1	0.61	0.256	3.02	0.006	0.008
AT3G57310		0.2	0.77	2.97	0.0001	0.00015
AT4G37030		0.45	0.239	2.95	0.003	0.004
AT4G19970		0.14	0.714	2.94	0.004	0.004
AT1G06137		0.97	0.1	2.94	0.00004	0.00026

AT5G24240		0.56	0.117	2.93	0.001	0.002
AT1G09400		0.68	0.099	2.92	0.001	0.002
AT1G62420		0.68	0.094	2.92	0.004	0.006
AT5G24090	CHIA	0.63	0.079	2.89	0.002	0.003
AT3G55150	EXO70H1	0.46	0.183	2.88	0.00004	0.00006
AT1G55240		0.89	0.106	2.83	0.011	0.023
AT1G55560	sks14	-0.03	0.966	2.82	0.046	0.046
AT2G22630	AGL17	0.68	0.062	2.82	0.017	0.025
AT1G68735		0.44	0.137	2.81	0.00037	0.00043
AT5G16230		0.56	0.067	2.79	0.001	0.001
AT1G60470	GolS4	0.48	0.271	2.78	0.005	0.007
AT5G37490		0.2	0.576	2.72	0.001	0.001
AT5G54700		0.46	0.386	2.72	0.00005	0.00007
AT5G56510	PUM12	0.61	0.053	2.71	0.013	0.019
AT5G52400	CYP715A1	1.46	0.057	2.71	0.00048	0.012
AT5G22560		0.32	0.181	2.7	0.001	0.001
AT5G26660	MYB86	0.79	0.056	2.67	0.005	0.01
AT5G65500		0.74	0.101	2.65	0.007	0.013
AT3G19690		1.33	0.12	2.63	0.002	0.031
AT4G11070	WRKY41	0.55	0.055	2.6	0.001	0.002
AT5G19930		0.6	0.286	2.55	0.002	0.005

[a]AGI (Arabidopsis Genome Initiative, 2000) code
[b]Gene symbol used in NCBI database
[c]F-C is the $\log_2$ fold change gene expression in in response to FB1
[d]PComparison of FB1-induced gene expression between Col-0 and *earp1.1*

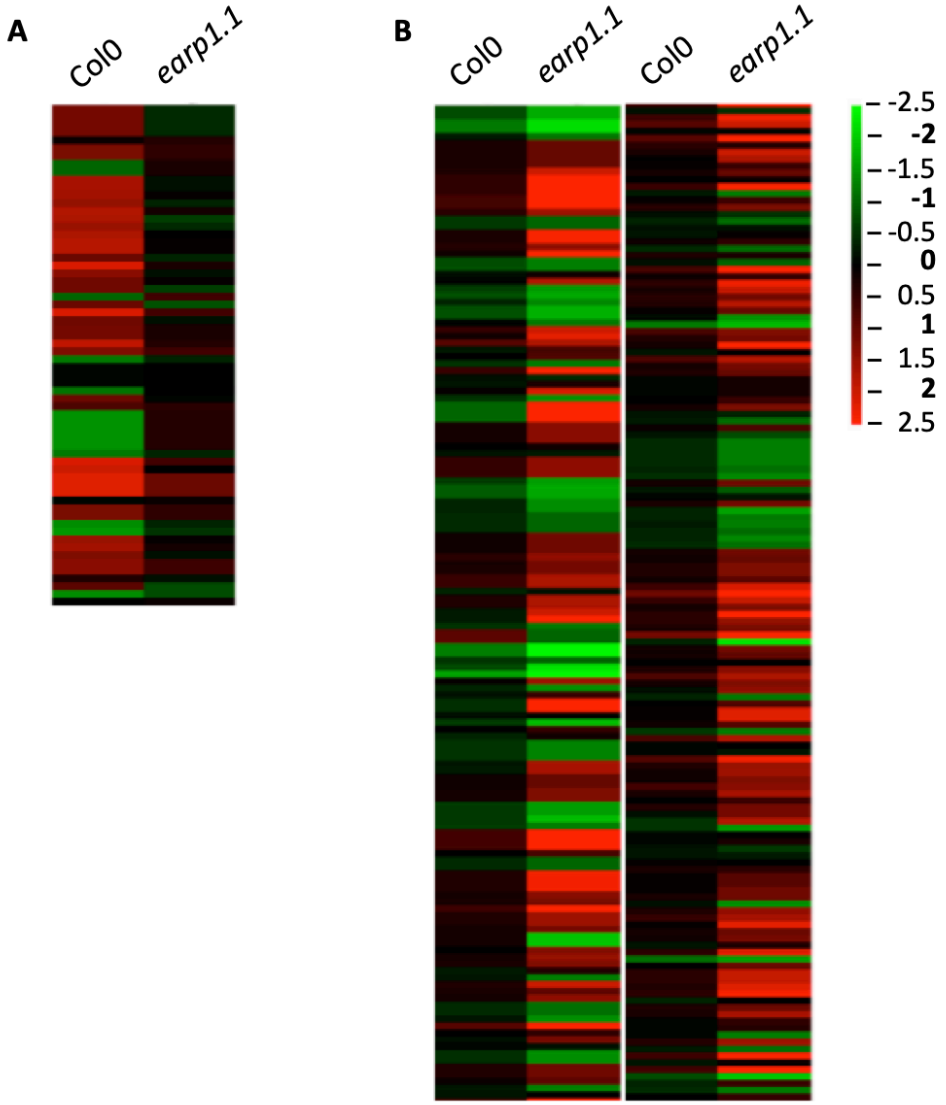

Figure 5.8. Heat map showing FB1-induced gene expression in Col-0 and *earp1.1*. The heat map uses red to indicate genes that were up-regulated in response to FB1, and green for those that were down-regulated, with black indicating no change in gene expression. The brightest red indicates a relative fold change >2.5 (Log_2Ratio). The brightest green indicates a fold change < -2.5 (Log_2Ratio). **A)** A visual representation of the gene expression for the list of 48 genes significantly responding to FB1 in Col-0, and not in *earp1.1*. **B)** A visual representation of the gene expression for the second list of 521 genes significantly responding to FB1 in *earp1.1*, but not responding in the wild type.

5.6. Effects of EARP1 on FB1-induced gene expression

The DNA microarray data provided a large number of genes differentially expressed in response to FB1 treatment. A few candidate genes were selected (Table 5.3) for analysis using an *in vitro* leaf disc assay. The majority of selected genes also feature in other datasets within this project, including Chapter 3 (Appendix 1) and Chapter 6 (Table 6.1).

In the leaf disc assays, leaf discs were floated on 5µM FB1 and incubated for 48h in the dark, after which they were placed in a 16 h-photoperiod. Samples for RNA extraction were harvested at the beginning and subsequently every 24h until 72h. This *in vitro* experimental system differs from the experiment conducted to generate samples for the DNA microarray in that the latter used infiltration of FB1 solutions into leaves left attached to the plants and harvested 24h later. In contrast, the *in vitro* experiments makes a ring wound around the tissues, places them in contact with the FB1 solution, and incubates them in continuous darkness for the first 48 h. However, because similar FB1 cell death symptoms are seen in the leaf disc assay as the whole plant experiments, the *in vitro* system is a rapid and useful tool for obtaining highly reproducible results.

A selection of qRT-PCR analysis results from the genes listed in Table 5.3 are shown in Figure 5.9. Each of the genes respond to FB1 in the Col-0, but each gene is down-regulated in the *earp1.1* line. Direct comparison between the qRT-PCR results to the DNA microarray data shows an apparent discrepancy between these results. For example, BGLU31 is highly responsive to FB1 in earp1.1 than Col-0 according to DNA microarray (Table 5.3), but it is the opposite in the qRT-PCR results (Figure 5.9). Because the DNA microarray results is from a single time-point, it may be that a time-course experiment could have revealed a different picture altogether. This is supported by the case of GSTU3, which has a higher response in *earp1.1* than in Col-0 at 24 h but the pattern reverses at 48 h and 72 h (Figure 5.9).

This paradox may be explained by a number of differences between the two experimental systems. Firstly, a major difference between the two systems is the use of intact leaves for the microarray, and excised leaf discs for the *in vitro* system. Secondly, the wounded leaf discs are compared to an unwounded control taken

immediately before the leaves were cored and floated on the FB1 solution, whereas the microarray samples are subjected to minimal wounding. Another key difference is the extended 48 h dark incubation of the leaf discs, which as previously stated was not applied to plants used for the microarray. Lastly, unlike the intact leaves for the microarray, the leaf discs were in a constant state of flooding, which is likely to influence gene expression. Although the *in vitro* system is less likely to indicate the most natural response to FB1, the system is highly controlled, through the size of the leaf discs and uptake of FB1. It is also an efficient method to take samples from multiple individual plants, at numerous time points.

An important point to note is that only one time point was taken for the microarray, as it is an expensive assay. This time point was taken at 24 hours. The *in vitro* system showed dramatic differences among a number of time points and this could be due to a number of reasons, including: response to FB1, response to light, response to flooding etc. Either way, the *in vitro* system has shown the expression for the majority of genes change drastically over a time period and therefore the microarray is only showing the response of these genes at one time point, therefore there may be genes that are not responding at 24 hours but respond earlier or later. Also you can observe in Figure 5.9, that the gene expression for *LTPG5, GSTU3* and *XTH10* appears to be up-regulated at 24 hours in *earp1.1* when compared to the Col-0; but at 48 hours, the gene expression is suppressed in *earp1.1*. This reiterates the importance of including multiple time points. Due to the drastic differences between each experimental system, it is important to analyse the data as two separate entities; however a conclusion that can be taken for both systems is that the genes selected from the microarray do indeed respond to FB1, and this response is regulated by the EARP1 transcription factor.

Table 5.3. A selection of candidates from the microarray analysis for further validation

Target Name[a]	*Gene Symbol*[b]	*Col-0 F-C*[c]	*earp1.1 F-C*	*Ratio of Col-0 to earp1.1*[d]	*Col-0/ earp1.1 p-value*[e]
AT1G15520	ABCG40	1.25	5.41	4.32	6.45E-04
AT3G13610	F6'H1	1.59	5.91	3.72	1.04E-03
AT3G22600	LTPG5	1.18	4.38	3.7	9.29E-04
AT3G28510	-	1.38	4.18	3.03	8.74E-06
AT2G29470	GSTU3	2.03	6.02	2.97	4.81E-03
AT5G24540	BGLU31	1.77	5.01	2.83	6.37E-06
AT5G59490	-	2.4	6.78	2.82	3.30E-07
AT5G07680	NAC080	0.41	1.14	2.74	0.0478
AT2G37770	ChlAKR	0.95	2.58	2.72	7.56E-05
AT2G14620	XTH10	2.79	7.05	2.53	3.33E-03
AT5G05340	PRX52	1.92	4.81	2.51	2.12E-03
AT2G42980	-	1.7	4.23	2.49	4.07E-03
AT5G64120	PRX71	0.89	2.18	2.47	5.19E-04
AT3G52430	PAD4	1.22	2.83	2.32	6.53E-04
AT2G45210	SAUR36	1.21	2.77	2.3	9.92E-04
AT1G77450	NAC032	1.14	2.01	1.76	1.92E-04
AT5G44570	-	2.54	3.98	1.57	1.81E-04
AT2G21370	XK-1	-1.29	-2.01	1.56	9.06E-03
AT4G15610	-	3.08	4.47	1.45	0.0165
AT2G37870	-	1.62	2.23	1.37	0.0498
AT3G49670	BAM2	-2.42	-3.23	1.34	0.045
AT2G26640	KCS11	-1.56	-2.03	1.3	0.0263
AT1G30040	GA2OX2	3.46	4.24	1.22	0.0402
AT1G08860	BON3	4.07	4.96	1.22	7.00E-03

[a]AGI (Arabidopsis Genome Initiative, 2000) code
[b]Gene symbol used in NCBI database
[c]F-C is the $\log_2$ fold change gene expression in in response to FB1
[d]Ratio of F-C between Col-0 and *earp1.1*
[e]PComparison of FB1-induced gene expression between Col-0 and *earp1.1*

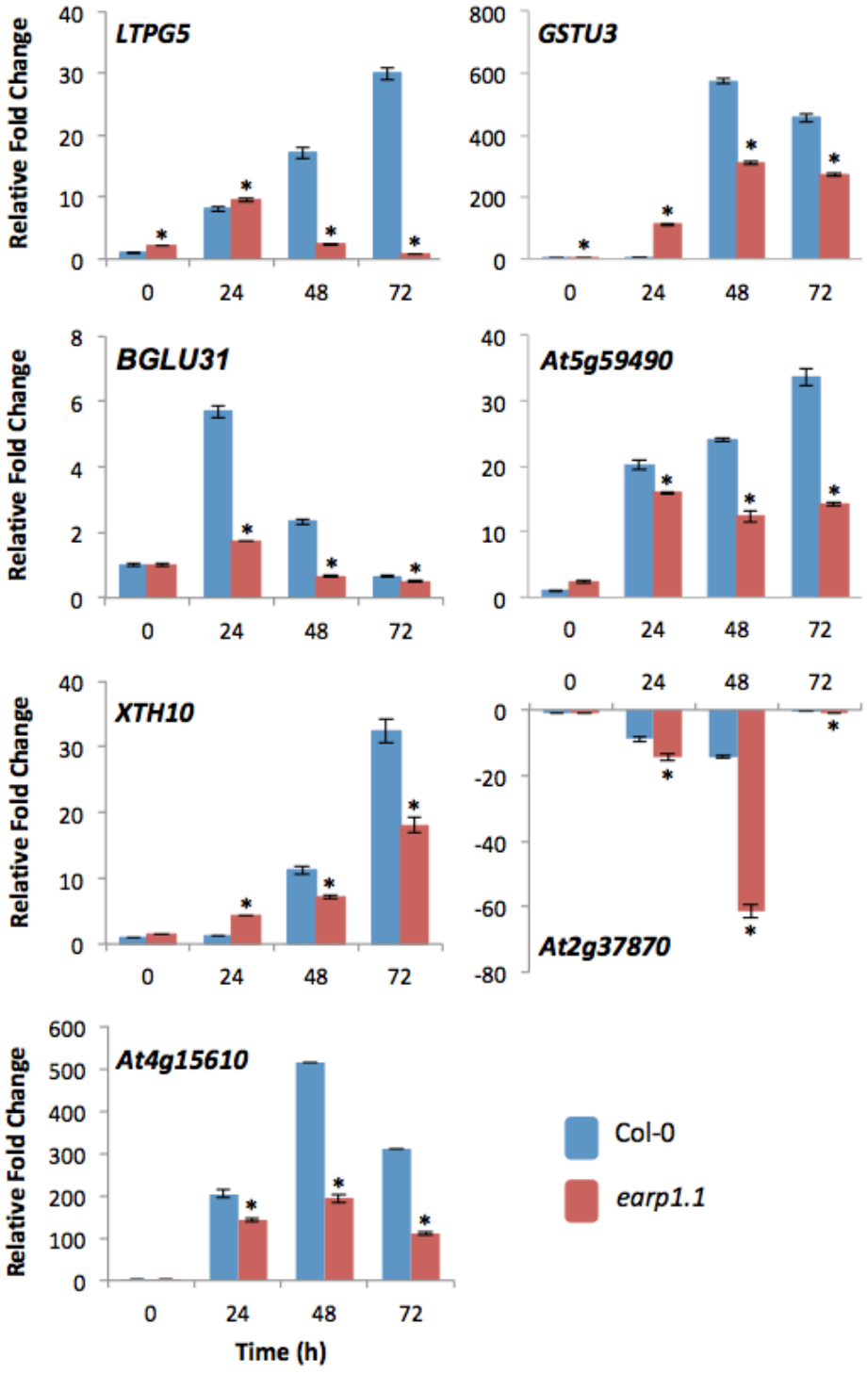

Figure 5.9. Gene expression in response to FB1. 10 leaf discs from 10 independent plants were floated on 5µM FB1. The leaf discs were incubated in the dark for 48 hours before being transferred to a 16h-photoperiod. Leaf discs were taken at the indicated time points and processed for RNA, and ultimately used for qRT-PCR. qRT-PCR values are an average of 3 technical replicates. Bars represent mean fold-change ± SD (n = 3). An asterisk indicates a significant difference in the fold-change between Col-0 and *earp1.1* samples ($p \leq 0.05$). *ACTIN2* and *EIF4A* were used as a constitutive reference control gene.

5.7. Comparison of the effects of EARP1 and light on FB1-induced gene expression

The absence of light blocks FB1-induced cell death in Arabidopsis (see Chapter 3), which phenocopies the response of *earp1* knockout mutants to FB1 (Figure 5.5). Because of this striking similarity, I was prompted to investigate if the effects of *earp1.1* knockout on FB1-induced gene expression could also resemble the effects of light on FB1-induced gene expression. Figure 5.10 compares the response of the same genes to FB1 in the cell culture system +/- light to the leaf disc *in vitro* assay in wildtype/*earp1.1* plants. The striking observation from this comparison is that suppression of FB1-induced gene expression by dark-incubation of cell cultures simulates the suppression of gene expression in response to FB1 by the *earp1.1* mutation. While a direct link between EARP1 and light cannot be made at this stage, the similar direction of response between these two systems could be a suggestion that the selected genes are high-fidelity marker genes prognostic of FB1-induced cell death.

Light regulation of FB1-induced gene expression shares a striking resemblance to EARP1 control of FB1-induced gene expression. Comparison of the 5,389 FB1-induced genes identified by the microarray (Chapter 5.5) against the FB1-induced gene expression regulated by light (Chapter 3.5) revealed an overlap of 57 proteins/genes between these two experiments. I also identified 7 genes that belonged to each of the three data sets (Table 5.4), indicating that the genes are regulated by light and EARP1, as well as responsive to FB1 and ATP. I expect that this list will produce useful candidates to further investigate FB1-induced cell death and the dependence on light.

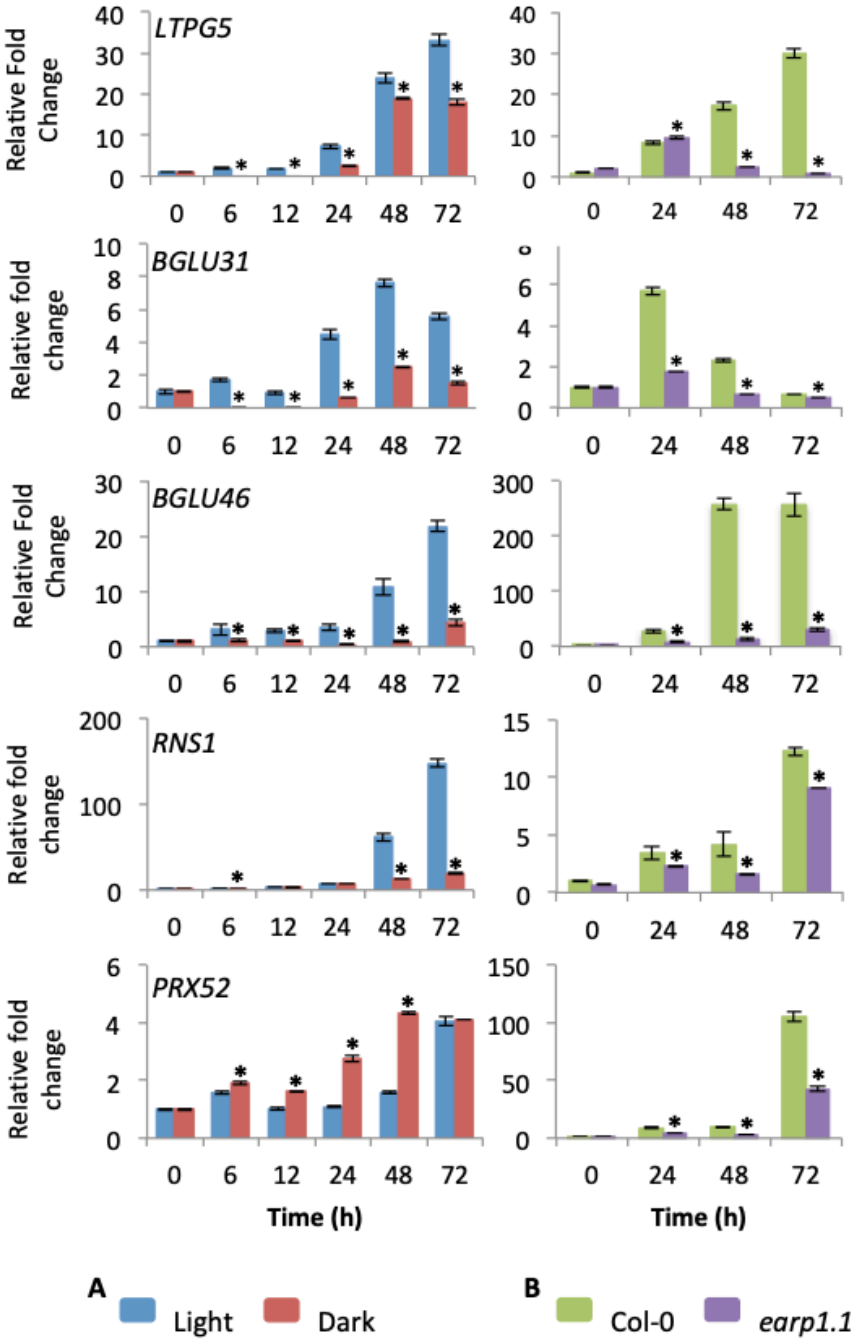

Figure 5.10. Gene expression analysis of FB1-responsive genes regulated by light and EARP1. **A)** Light- and dark-grown Arabidopsis cells were treated with 1µM FB1 and samples for RNA extraction harvested at the indicated time-points. RNA was extracted and transcript abundance analysed by qRT-PCR. **B)** 10 leaf discs from 10 independent plants were floated on 5µM FB1. The leaf discs were incubated in the dark for 48 hours before being transferred to a 16h-photoperiod. Leaf discs were taken at the indicated time points and processed for RNA, and ultimately used for qRT-PCR. qRT-PCR values are an average of 3 technical replicates. Bars represent mean fold-change ± SD (n = 3). An asterisk indicates a significant difference in the fold-change between Col-0 and *earp1.1* samples ($p \leq 0.05$). *ACTIN2* and *EIF4A* were used as a constitutive reference control gene.

Table 5.4. Light-regulated genes, downstream of EARP1, and responsive to FB1 and ATP

Target Name[a]	Gene Symbol[b]	Col-0 F-C[c]	*earp1.1* F-C	Col-0/earp1.1 p-value[d]
AT3G52470	-	1.073	1.555	0.00662
AT4G39830	-	0.678	2.644	0.00016
AT1G74000	SS3	0.937	1.354	0.01172
AT5G64120	-	0.885	2.182	0.00052
AT4G20830	-	1.007	3.021	0.00003
AT4G20860	-	1.206	2.59	0.00005
AT1G64760	HEB1	-0.675	-1.209	0.01101

[a]AGI (Arabidopsis Genome Initiative, 2000) code
[b]Gene symbol used in NCBI database
[c]F-C is the $\log_2$ fold change gene expression in in response to FB1
[d]PComparison of FB1-induced gene expression between Col-0 and *earp1.1*

5.8. Discussion

FB1 triggers diverse biochemical and physiological responses, some of which are dependent on the concentration of the mycotoxin used. At the biochemical level, it activates ROS production and accumulation (Stone *et al*., 2000; Shi *et al*., 2007), callose formation (Stone *et al*., 2000), and disruption of sphingolipid metabolism (Desai *et al*., 2002). At low concentration FB1 causes growth retardation (Abbas *et al*., 1988; Abbas *et al*., 1991; Abbas and Boyette. 1992; Stone *et al*., 2000), but activates cell death at higher concentration (Asai *et al*., 2000; Stone *et al*., 2000). These responses are likely to be driven by specific changes in gene expression as demonstrated in this chapter. Identification of FB1-responsive transcription factors reported in this chapter will help elucidate the gene networks underpinning FB1-induced Arabidopsis physiological responses.

Gene expression of 13 putative transcription factors identified here was significantly impacted by exogenous ATP during the 40-48 h time window when cell cultures exposed to FB1 undergo an irreversible cell death commitment step. This established the putative transcription factors as *bona fide* ATP-responsive genes as well, suggesting that they could also be important regulatory proteins in plant physiological responses activated by extracellular ATP. For example, eATP regulates pollen germination and pollen tube elongation (Reichler *et al*., 2009), root

gravitropism (Tang *et al*., 2003), stomatal opening (Clark *et al*., 2011; Hao *et al*., 2012; Chen *et al*., 2017), abiotic stress responses (Song *et al*., 2006; Kim *et al*., 2009; Weerasinghe *et al*., 2009; Dark *et al*., 2011;), biotic stress responses (Chivasa *et al*., 2009; Chen *et al*., 2017; Tripathi *et al*., 2018a, 2018b) and of course FB1-induced PCD (Chivasa *et al*., 2005). These identified transcription factors could be critical in either or both FB1- and eATP-mediated physiological responses.

5.8.1 EARP1 is a positive regulator of FB1-induced PCD

To begin with, it was demonstrated that FB1 activates *EARP1* gene-expression and that this response was suppressed by the additional treatment with exogenous ATP (Figure 5.3). Crucially, suppression of FB1-induced *EARP1* expression followed rapidly after addition of exogenous ATP and occurred within the 40-48 h time window in which critical events of commitment to cell death are activated. This expression profile is consistent with a gene having an important cell death regulatory role. A role for EARP1 in PCD was demonstrated by showing that progression of FB1-induced cell death is impaired in loss-of-function *earp1* mutants (Figure 5.5).

EARP1 belongs to the C2H2 zinc-finger family, which is one of the largest families of transcriptional regulators in plants, consisting of 176 members within *Arabidopsis thaliana* (Englbrecht *et al*., 2004). Zinc finger proteins have a diverse range of cellular functions. They are typically known for their activity as transcription factors and bind DNA in a sequence specific manner. However, there are examples of zinc finger proteins having alternative functions, such as RNA binding, protein-protein interactions and regulation of PCD (Choo & Klug, 1997; Takatsuji *et al*., 1992; Dietrich *et al*., 1997; Ciftci-Yilmaz and Mittler, 2008). There are several classification of zinc-finger proteins, with C2H2-type zinc finger proteins being the best studied. An *in silico* analysis estimated that roughly 0.7% of all Arabidopsis genes encode a C2H2-type zinc finger proteins (Englbrecht *et al*., 2004). The C2H2 motif uses 2 cysteine and 2 histidine residues, which tetrahedrally coordinate a central zinc ion, to stabilize the structure. The C2H2 domain interacts directly with the major groove of DNA, which is a distinguishing trait of transcription regulators. Transcriptional regulators ZAT12 and SUPERMAN, both have been implicated in response to abiotic stress signalling and normal plant development (Davletova *et al*., 2005; Bowman *et al*., 1992; Hiratsu *et al*., 2002). An archetypal characteristic among

zinc finger proteins is the specific amino acid sequence, QALGGH. This sequence is essential for DNA binding and likely to be a platform at the protein surface that directly interacts with DNA (Kubo *et al*., 1998; Takatsuji, 1999). Analysis of the *EARP1* sequence reveals four C2H2 domains, three QALGGH sequences, as well as an additional QSLGGH sequence that may also be responsible for DNA binding. As well as containing key DNA-binding regions within the amino acid sequence, the suspected transcriptional activation domains of *EARP1* contain the glutamine-rich and acidic regions typical of transcriptional activity. The *EARP1* sequence has 25% glutamine residues preceding the first and third zinc finger domain, as well as containing a highly acidic region (47%) between the second and third zinc finger.

EARP1 joins a group of transcription factors known to be key regulators of PCD. For example, AtSPL14 is a transcriptional regulator that has been identified as a positive regulator of FB1-induced cell death (Stone *et al*., 2005). Not only does ATSPL14 play a role in FB1 sensitivity, but it is also involved in maintaining normal plant architecture (Stone *et al*., 2005). Another example would be MYB30, which is a positive regulator of hypersensitive cell death (Daniel *et al*., 1999) and defence against bacterial and fungal pathogens (Vailleau *et al*., 2002). The overexpression of MYB30 results in the promotion and acceleration of cell death induced by an avirulent pathogen, ultimately increasing the plants resistance to the pathogen (Vailleau *et al*., 2002). The transcription factor, LSD1, has also been implicated in plant cell death and belongs to the zinc finger transcription factor family, C2C2 (Dietrich *et al*., 1997). The Arabidopsis *lsd1* mutant is hyper-responsive to cell death, indicating that LSD1 is a negative regulator of cell death. It was further demonstrated that EDS1 and PAD4 defence signalling genes are required for the runaway cell death profile of the *lsd1* mutant (Rustérucci *et al*., 2001).

Although there are well-established transcription factors that regulate PCD, EARP1 is the first transcription factor that links PCD with eATP signalling. Further investigation into the remaining 12 transcription factors, identified in this chapter, may give rise to a group of PCD regulators influenced by eATP signalling. Investigation into whether these transcription factors interact with one another to regulate PCD may be an interesting avenue for further research.

5.8.2. EARP1 regulates numerous genes, and is likely to be a 'hub-gene'

After confirming that EARP1 functions as a positive regulator of FB1-induced cell death, the next stage was to investigate how EARP1 impacts FB1-induced gene expression. This line of investigation was addressed by conducting a whole genome transcriptomic analysis using FB1 treatments of wildtype and *earp1.1* mutant plants in the entire experiment, a total of 7,733 genes responded to FB1 irrespective of the genotype. Of these genes, 5,389 showed an altered response to FB1 with the loss of EARP1. This shows that 70% of FB1-responsive genes are controlled by EARP1, suggesting that EARP1 is a Hub-gene in FB1-induced signalling.

The microarray data has provided a list of future targets for elucidating FB1 signalling across the different physiological responses it activates in plants. In order to condense the list down to key candidates that are likely to be critical components in PCD, the EARP1-regulated genes can be compared with similar experimental datasets from whole genome analysis. A comparison of gene responses between the cell culture FB1+/-ATP microarray study (Chapter 5.1) and the microarray experiment of FB1 treatment of Col-0/earp1.1 (Chapter 5.5) revealed an overlap of 62 genes. These should be high priority genes for reverse genetic analysis in the future. Comparison of the FB1-induced genes list with the DNA microarray data of Gechev *et al*. (2004) revealed an overlap of 74 genes. The Gechev study used the plant cell death-inducing fungal AAL-toxin instead of FB1 (Gechev *et al*., 2004).

6

Using the antagonistic relationship between salicylic acid and extracellular ATP to develop a screen to identify putative cell-death regulatory proteins

6.1. Introduction

Salicylic acid (SA) belongs to a diverse group of plant phenolics, characterised an aromatic ring bearing a hydroxyl group or another functional derivative. SA is plant hormone essential for a number of biological processes, such as plant growth (Rivas-San Vicente *et al*., 2011), lignin biosynthesis (Gallego-Giraldo *et al*., 2011), seed germination (Guan and Scandalios. 1995; Rajjou *et al*., 2006; Xie *et al*., 2007; Alonso-Ramirez *et al*., 2009), flowering (Lee and Skoog. 1965; Cleland and Ajami. 1974; Martinez *et al*., 2004), fruit ripening (Srivastava and Dwivedi, 2000), stomatal closure (Raskin *et al*., 1987) and influencing gene expression in response to abiotic and biotic stress. Abiotic stress responses influenced by SA signalling include drought (Munné-Bosch and Peñuelas, 2003; Chini *et al*., 2004), chilling (Janda *et al*., 1999; Kang and Saltveit 2002), heavy metal tolerance (Metwally *et al*., 2003; Yang *et al*., 2003; Freeman *et al*., 2005), heat (Larkindale and Knight, 2002; Larkindale *et al*., 2005) and osmotic stress (Borsani *et al*., 2001). The role SA plays in mediating signals in response to biotic stress, such as pests and pathogens, has been at the forefront of plant science research for many years.

Salicylic acid has been extensively studied as a signalling molecule in both local defences and systemic acquired resistance (SAR), as well as being a crucial regulator of disease symptom development (Malamy *et al*., 1990; Shah and Klessig, 1999; Dempsey *et al*., 1999; O'Donnell *et al*., 2003). The use of transgenic plants expressing the bacterial *nahG* gene, which encodes an enzyme that metabolises SA to catechol, displays reduced or no expression of pathogenesis-related (*PR)* genes, fails to induce SAR and is resistant to FB1-induced cell death (Gaffney *et al*., 1993; Delaney *et al*., 1994; Asai *et al*., 2000). Furthermore, Arabidopsis mutants devoid of either CPR1 or CPR6 accumulate high levels of SA, and in turn increase their

susceptibility to FB1 (Jirage *et al*., 2001; Clarke *et al*., 2001). Experimental studies such as these have shown that the phytohormone SA functions as a positive regulator of FB1-triggered PCD.

This chapter exploits the effects of SA on PCD, and the antagonistic impact of extracellular ATP (eATP), to develop a screen for identifying PCD genes. Treatment of tobacco cell suspension cultures with SA triggers depletion of eATP and concomitant treatment of the cell with SA and exogenous ATP blocks activation of PR-1 gene expression (Chivasa *et al*., 2009). Thus, ATP appears to antagonise some SA-induced responses. While SA promotes FB1-induced PCD (Jirage *et al*., 2001; Clarke *et al*., 2001), eATP suppresses it (Chivasa *et al*., 2005). This suggests that the effects of SA- and eATP-mediated signalling could be antagonistice in relation to FB1-induced PCD.

Smith *et al*. (2015) used the antagonistic relationship between SA and eATP to develop a screen adapted for identifying PCD regulatory proteins. Treatments of Arabidopsis cell cultures with SA alone or SA in combination with ATP were used to identify proteins, whose response to SA was blocked by ATP. The advantage of using agonist (SA) and antagonist (ATP) signals without inclusion of FB1 is the ability of detection of PCD-regulatory proteins without the background noise of cell death-related changes in protein expression. The hypothesis is that SA and ATP impact protein/gene expression in the same way regardless of FB1 presence/absence.

6.2. DNA microarray screening for PCD genes

A whole-genome DNA microarray analysis experiment was set-up using *Arabidopsis thaliana* ecotype Landsberg *erecta* (Ler) cell suspension cultures. The cultures were exposed to one of the following treatments: 200µM SA, 200µM SA plus 400µM ATP, or an equivalent volume of water as a control. Cells were harvested for RNA, in replicates of three, at 6, 8, 10, 12, and 24 h after treatment. The samples were submitted to NASC for analysis (Schena *et al*., 1995; Lockhart *et al*., 1996; Lipshutz *et al*., 1999). The top genes showing significant differences between their responses to SA only and SA+ATP across the time-series were identified, with the top 67 genes being selected for further analysis (Table 6.1). ATP significantly attenuates the response of these genes to SA on at least one of the time-points.

Due to the small sample size, GO analysis through AgriGO was inconclusive; therefore, I manually searched individual gene profiles from the NCBI database to determine the protein functionalities and family trends throughout the data set. Genes that have been implicated in defence-related biological functions account for 16% of the dataset, with 4% involved in PCD. A further 10% are known to be involved in ATP binding and synthesis. Genes responsive to phytohormones made up 12% of the dataset, with 6% responsive to SA. Interestingly, proteins involved in carbohydrate metabolism make up 12% of the dataset, with preference for beta-glucosidases (4%). Another biological processes with a number of representatives in the dataset belong to families involved in lipid metabolism (7%). Finally, 6% of the dataset was represented by serine/threonine protein phosphatases, particularly purple acid phosphatases (PAPs). The known localisations for the majority of proteins were intracellular (51%), and 33% belong to the extracellular region, including the plasma membrane. Of the intracellular proteins, 20% were localised to the chloroplast, 13% to the nucleus, and 6% to the mitochondria.

Table 6.1 SA and ATP responsive genes identified by the microarray

Target Name[a]	*Gene Symbol*[d]	*SA*[a]			*SA + ATP*[b]		
		6 h	*12 h*	*24 h*	*6 h*	*12 h*	*24 h**
At5g24540	BGLU31	5.318	5.445	6.465	4.575	1.905	3.567
At1g15520	ABCG40	5.655	5.113	5.401	3.641	3.193	4.416
At1g69880	TH8	4.398	4.522	3.944	5.124	6.287	5.638
At5g55460	-	4.105	3.756	4.349	3.416	1.755	2.328
At3g22600	LTPG5	3.153	3.502	4.267	2.345	1.06	1.627
At5g11930	-	3.155	3.863	3.761	2.144	2.219	2.654
At3g09940	-	2.756	2.939	3.731	2.102	1.125	1.648
At3g52430	PAD4	2.777	2.596	3.22	2.199	1.461	1.886
At2g37770	-	3.216	2.972	2.352	3.591	4.622	3.922
At5g24800	BZIP9	2.701	2.555	2.6	2.896	4.037	3.732
At3g22060	-	2.801	2.901	2.384	1.382	1.584	0.696
At5g03350	-	2.442	2.46	3.072	1.467	1.179	1.806
At5g45380	DUR3	2.497	3.028	2.66	2.701	3.787	3.692
At1g01680	PUB54	1.921	2.457	2.834	1.175	1.286	1.2
At5g22300	NIT4	2.671	2.296	1.74	3.38	4.412	3.347
At5g39670	-	1.729	2.127	2.653	1.68	0.837	0.722
At5g11940	-	1.587	2.218	2.633	0.049	0.013	0.48
At2g03290	-	2.156	1.543	2.3	1.178	0.69	1.074
At2g19190	FRK1	1.657	1.509	1.761	0.798	1.12	0.894
At4g15610	-	1.807	1.874	2.205	2.603	3.467	2.879
At4g33560	-	2.122	2.322	0.668	2.935	3.802	3.263
At1g05560	UGT75B1	2.215	2.344	1.435	2.535	3.977	3.607
At3g56710	SIB1	2.06	1.83	2.158	0.793	1.337	1.227
At5g61890	-	1.37	1.635	2.194	3.55	2.58	2.973
At5g08000	E13L3	-1.71	-2.16	-1.859	0.534	-0.602	0.172
At4g24040	TRE1	1.743	1.774	1.218	2.679	4.161	3.205
At1g35910	TPPD	1.651	1.443	2.078	1.763	0.169	0.677
At1g13750	-	2.056	1.787	1.954	0.903	0.05	0.422
At2g41480	-	-1.294	-1.376	-1.868	0.31	-0.373	-0.662
At3g28510	-	1.316	1.029	1.567	0.55	0.275	0.63
At4g24890	PAP24	-0.809	-1.988	-1.869	-2.762	-3.289	-3.599
At2g45210	SAUR36	1.529	1.465	1.159	2.047	2.324	2.174
At3g22620	-	1.109	1.638	1.475	0.786	0.368	0.081
At3g50660	DWF4	-1.29	-1.778	-1.191	-2.325	-2.906	-2.448
At3g47010	-	0.999	1.778	1.432	1.131	0.735	0.652
At2g45120	-	1.348	1.307	1.367	1.088	0.605	0.538
At2g46880	PAP14	-0.98	-1.743	-1.748	-2.33	-3.558	-3.617
At1g69080	-	-1.413	-1.656	-1.676	-3.919	-4.152	-4.515
At4g38660	-	-1.277	-1.615	-1.604	-1.82	-2.858	-2.474
At1g53660	-	1.433	0.983	1.676	0.72	-0.084	0.796
At1g77450	NAC032	1.356	0.802	0.942	1.501	2.19	2.317

At1g65730	YSL7	1.3	0.706	1.248	2.686	3.06	3.001
At4g30110	HMA2	-0.343	-1.553	-1.473	-1.611	-2.268	-2.455
At5g44570	-	0.876	0.893	1.521	0.64	0.365	0.275
At5g61820	-	1.432	1.179	1.216	2.016	2.546	2.538
At3g28050	UMAMIT41	-1.22	-0.954	-1.416	-0.718	-0.307	-0.268
At5g56530	-	-0.912	-1.407	-1.271	-1.608	-2.571	-1.977
At5g43380	TOPP6	-1.117	-1.217	-1.026	0.69	-0.556	-0.29
At3g49670	BAM2	-1.227	-1.105	-1.069	-1.694	-2.396	-2.066
At2g26640	KCS11	-0.924	-1.238	-0.824	-1.757	-2.634	-2.078
At2g37870	-	0.926	0.832	0.9	1.395	2.709	2.247
At5g15850	COL1	1.211	0.987	1.063	1.595	2.184	2.027
At1g48370	YSL8	0.909	0.879	1.031	0.358	-0.283	0.089
At4g17770	TPS5	-0.898	-1.124	-1.193	-1.608	-2.253	-1.885
At1g26560	BGLU40	-0.612	-1.042	-1.187	0.473	-0.188	0.251
At1g71830	SERK1	-1.174	-1.108	-0.764	-1.256	-2.167	-1.8
At2g21370	XK1	-0.805	-1.006	-0.76	-1.424	-2.03	-1.949
At5g21482	CKX7	0.678	0.569	1.171	0.141	0.196	0.054
At1g33700	-	-1.027	-1.166	-0.879	-0.039	0.177	0.288
At1g14780	-	0.843	1.082	1.101	2.65	2.319	1.848
At1g18250	ATLP-1	-0.757	-1.026	-0.954	-1.182	-2.099	-1.91
At1g50110	-	-0.801	-0.898	-0.978	-1.31	-2.044	-1.768
At3g18090	NRPD2B	-0.522	-1.014	-1.089	-1.577	-1.595	-1.523
At1g72490	-	-0.469	-1.073	-1.007	-0.811	-0.63	0.359
At3g22810	-	-0.776	-0.746	-1.054	-1.593	-1.979	-1.77
At1g70750	-	-1.04	-0.908	-0.821	-1.518	-2.035	-1.522
At1g52720	-	-1.037	-0.832	-1.021	-1.577	-1.492	-1.605

[a]AGI (Arabidopsis Genome Initiative, 2000) code and gene symbol
[b]Gene symbol used in NCBI database
[c]Gene expression in Arabidopsis cell cultures, in response to Salicylic Acid (SA)
[d]Gene expression in Arabidopsis cell cultures in response to SA and exogenous ATP
*Time points reduced to 6, 12 and 24 h

Using the original microarray RNA samples from Arabidopsis cell cultures, I selected a number of genes identified by the microarray for qRT-PCR analysis. The purpose of this experiment was to validate the microarray analysis. The selected genes ranged from those that showed the most dramatic response to SA+ATP antagonism; genes implicated in plant defence; genes of unknown function; and genes known to be responsive to SA, such as *PAD4* and *FRK1* (Table 6.2) (Glazebrook *et al*., 1996, 1997; Parker *et al*., 1996; Feys *et al*., 2001; Asai *et al*., 2002).

Table 6.2. Candidates selected from the microarray for further validation

		SA[c]			*SA + ATP*[d]		
AGI Code[a]	*Gene Symbol*[b]	*6 h*	*12 h*	*24 h*	*6 h*	*12 h*	*24 h**
At5g24540	BGLU31	5.318	5.445	6.465	4.575	1.905	3.567
At5g55460	-	4.105	3.756	4.349	3.416	1.755	2.328
At3g22600	LTPG5	3.153	3.502	4.267	2.345	1.06	1.627
At3g52430	PAD4	2.777	2.596	3.22	2.199	1.461	1.886
At5g24800	BZIP9	2.701	2.555	2.6	2.896	4.037	3.732
At2g19190	FRK1	1.657	1.509	1.761	0.798	1.12	0.894
At4g15610	-	1.807	1.874	2.205	2.603	3.467	2.879
At5g43380	TOPP6	-1.117	-1.217	-1.026	0.69	-0.556	-0.29
At2g37870	-	0.926	0.832	0.9	1.395	2.709	2.247
At2g21370	XK1	-0.805	-1.006	-0.76	-1.424	-2.03	-1.949
At2g14610	PR1	-	-	-	-	-	-
At4g34180	CYCLASE-1	-	-	-	-	-	-
At2g02990	RNS1	-	-	-	-	-	-

[a]AGI (Arabidopsis Genome Initiative, 2000) code and gene symbol
[b]Gene symbol used in NCBI database
[c]Gene expression in Arabidopsis cell cultures, in response to Salicylic Acid (SA)
[d]Gene expression in Arabidopsis cell cultures in response to SA and exogenous ATP
*Time points reduced to 6, 12 and 24 h

The genes *PR-1* and *CYCLASE-1* were selected for analysis as they are known to be up-regulated by SA, with exogenous ATP suppressing their activation by SA (Chivasa *et al*., 2009; Smith *et al*., 2015). The SA-induced defence marker gene *PR-1* gene expression increased over the duration of the experiment, with the steepest rise occurring between 12-24 h in the SA treatment (Figure 6.1). In accordance with previous results seen in tobacco (Chivasa *et al*., 2009) exogenous ATP completely inhibited activation of *PR-1* expression (Figure 6.1). *CYCLASE-1* showed the opposite response, with only a modest response to SA, but very high gene expression when ATP was mixed with SA.

An important observation was to compare the transcriptomic and proteomic information for *CYCLASE-1* (Smith *et al*., 2015). The first observation shows that both proteomic and transcriptomic data support the increased expression of *CYCLASE-1* in response to SA. An unexpected observation was the response of *CYCLASE-1* to the addition of ATP. The transcriptomic data consistently shows ATP

to enhance the response of *CYCLASE-1* to SA across the time course, whereas the proteomic data reports that the up-regulation of CYCLASE-1 to SA is suppressed by ATP. There are two possible explanations for this outcome. Firstly, the proteomic data comes from a single time point at 48 h, later than the transcriptomic time points that finish at 24 h. It is possible that between 24-48 h the expression of CYCLASE-1 was reversed. A more likely explanation is that for CYCLASE-1 expression, there appears to be a regulatory function occurring post-transcriptionally. Thus, even though CYCLASE-1 transcription is higher in ATP/SA treatment than in SA alone, the ATP might actually inhibit translation, leading to the suppression of protein expression seen by Smith *et al*. (2015). This unexpected observation highlights the importance of investigating genes at both transcriptomic and proteomic levels.

The *PR-1* marker gene shows that the experiment had the expected hallmarks of SA and ATP antagonism, though the *CYCLASE-1* results provide an important caveat to be considered when interpreting gene expression data. This suggests that genes, whose expression in response to SA is enhanced by exogenous ATP, could be crucial PCD regulators. This would have been counterintuitive on the basis of a simplistic linear correlation between transcript abundance and protein expression.

The qRT-PCR analysis for selected genes from the microarray analysis showed a significant difference between the response to SA alone and SA+ATP. Data from the entire analysis can be viewed in Appendix 2, but genes with the most significant responses are shown in Figure 6.2. *BGLU31, At5g55460* and *LTPG5* are up-regulated in response to SA, and this response is suppressed by the addition of ATP. The expression profiles for these genes are similar to that of *PR-1*. For *BZIP9*, *At4g15610, TOPP6* and *At2g37870,* gene expression was enhanced by exogenous ATP in the SA+ATP treatement, surpassing the response in SA alone. This response is similar to the profile of *CYCLASE-1* (Figure 6.2).

The data obtained for candidate genes selected for qRT-PCR analysis are in agreement with the microarray results. The screen has successfully identified genes responsive to SA, which are then suppressed or enhanced by ATP. Overall, these results provide a list of genes with a putative function in PCD regulation, though genetic experiments will be required to further filter the gene list.

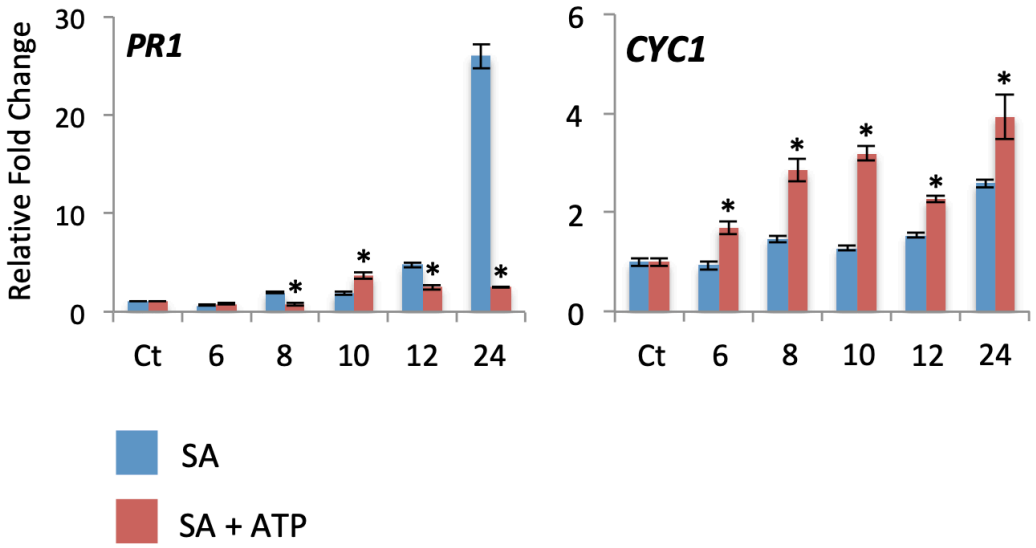

Figure 6.1 Gene expression profiles of SA-responsive marker genes. Cell cultures were treated with: 200µM SAalone or 200µM SA+400µM ATP. RNA was extracted from cells harvested at the indicated time-points and analysed via qRT-PCR. qRT-PCR values are an average of 3 technical replicates. Bars represent mean ± SD (n = 3). An asterisk indicates a significant difference between light and dark ($p \leq 0.05$). *ACTIN2* and *EIF4A* were used as constitutive reference control genes. Ct, control samples.

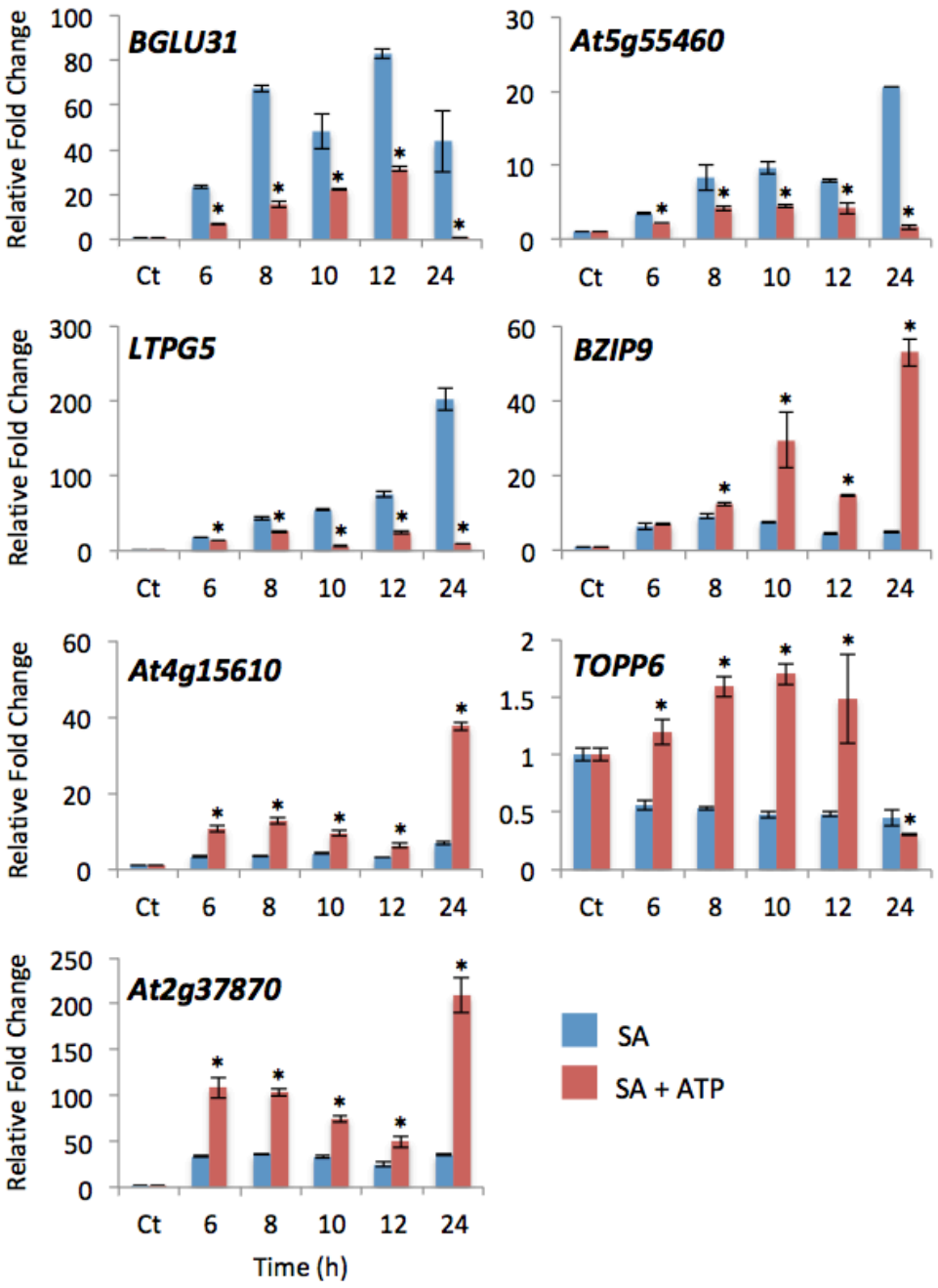

Figure 6.2 SA+/- ATP responses for candidates from the microarray. Cell cultures were exposed to one of the following treatments: 200µM SA, 200µM SA alongside 400µM ATP. RNA was harvested from the cells for qRT-PCR at 6, 8, 10, 12, and 24 h after treatment, including a 6 h water treated control. qRT-PCR values are an average of 3 technical replicates. Bars represent mean ± SD (n = 3). An asterisk indicates a significant difference between light and dark ($p \leq 0.05$). *ACTIN2* and *EIF4A* were used as constitutive reference control genes.

6.3. ICS1 is crucial protein for FB1-mediated cell death

Transgenic Arabidopsis plants expressing the *NahG* gene encoding bacterial salicylate hydroxylase fail to accumulate SA (Gaffney *et al*., 1993; Delaney *et al*., 1994). Salicylate hydroxylase-dependent SA degradation leads to FB1 resistance (Asai *et al*., 2000), while enhanced SA accumulation promotes FB1-induced cell death (Jirage *et al*., 2001; Clarke *et al*., 2001). In order to identify the major source of SA promoting FB1-induced cell death, experiments were conducted using a loss-of-function T-DNA insertion line in the *ICS1* gene. ICS1 is a key enzyme in the SA biosynthesis pathway responsible for pathogen-induced SA accumulation (Wildermuth *et al*., 2001). The line SALK_088254, hereafter referred to as *ics1*, which contains a T-DNA insert in the second intron within the *ICS1* gene (Figure 6.3.A), was obtained from the SALK collection (Alonso *et al*, 2003). Confirmation of the T-DNA presence in the mutant is shown in Figure 6.3.B. Primers straddling the T-DNA insertion sites were used to PCR-amplify a fragment of the *ICS1* genomic sequence in the wild type (Col-0), which was not present in the mutant plants, confirming disruption of the gene sequence by a T-DNA insert.

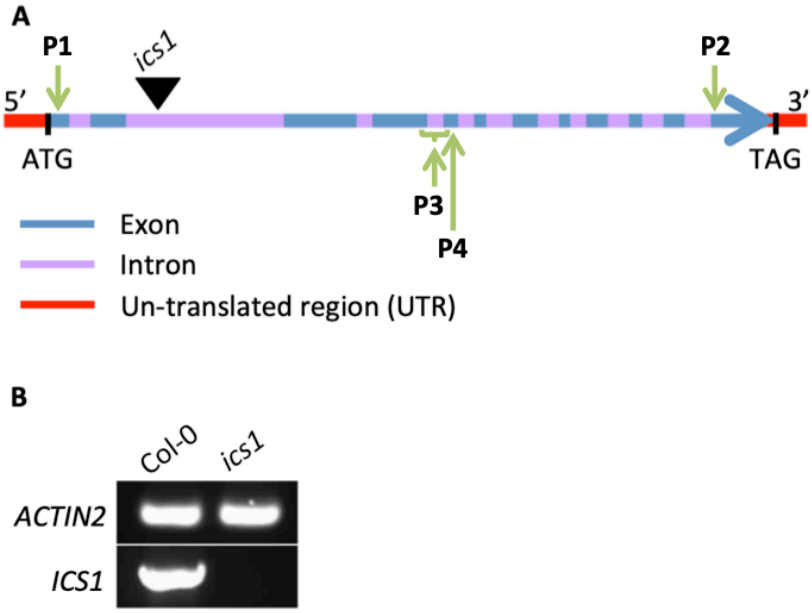

Figure 6.3. Confirmation of *ICS1* T-DNA insertion. A) Schematic representation of the *ICS1* gene showing the position of the T-DNA insertion. **B)** Amplification of the genomic DNA using primers straddling the T-DNA insertion position (P1 and P2 indicate primer positions). In Col-0 the expected amplicon is present, which is absent from *ics1*. This indicates that the mutant line has the T-DNA insert. *ACTIN2* was used as a constitutive reference control gene.
P3 and P4 indicate primer positions used for RT-PCR or q-RT-PCR analysis.

To evaluate the effects of ICS1 on FB1-induced cell death, leaf discs cored from 10 individual 4-week old Col-0 or *ics1* plants were floated on 5µM FB1. The leaf discs were incubated in the dark for 48 h before transfer to the normal 16 h-8 h light-dark cycle. Within 3 days of incubation in the light-dark cycle, Col-0 leaf discs developed patches of chlorosis, which expanded and coalesced to cover the entire tissue (Figure 6.4.A). By about 5 days from the start of the experiment, the Col-0 discs showed extensive cell death characterized by patches of bleached transparent tissues. The *ics1* mutant showed no signs of cell death. Representative leaf discs from Col-0 and *ics1* were photographed and show the typical symptoms (Figure 6.4.A).

In addition to determining the phenotypic response of if *ics1* to FB1, samples of leaf discs from the same experiment were harvested for RNA extraction and qRT-PCR analysis. Expression of *RNS1* as a marker gene for FB1 toxicity was evaluated. There was a very modest increase in *RNS1* expression in *ics1*, while gene expression was massively up-regulated in Col-0 plants (Figure 6.4.B). Differences in *RNS1* expression between FB1-treated Col-0 and *ics1* tissues became statistically significant from 48 h onwards (Figure 6.4.B). Therefore, these results suggest that ICS1-dependent SA accumulation plays a major role in FB1-induced gene expression and cell death.

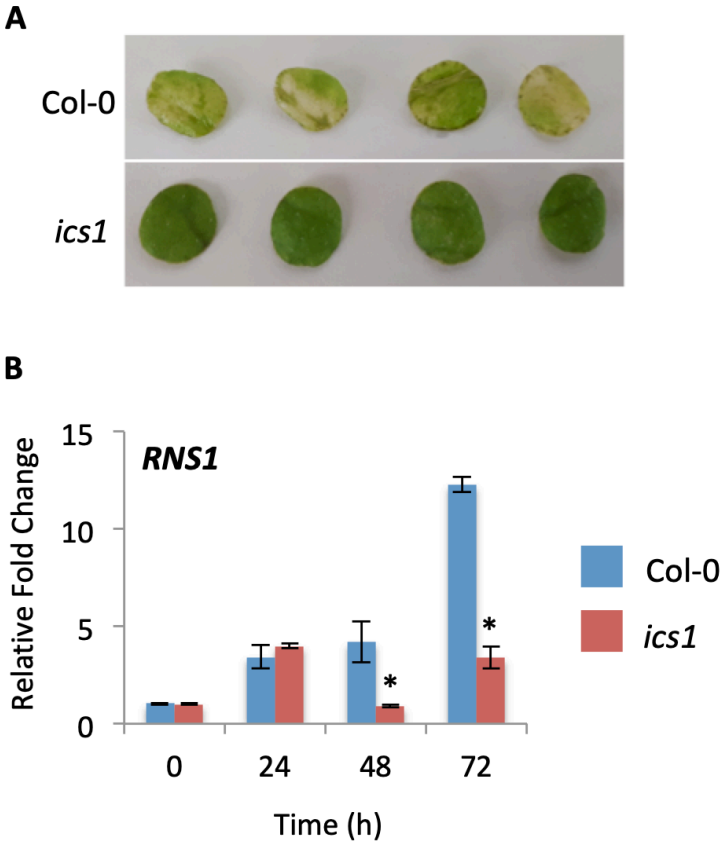

Figure 6.4. The response of *ics1* mutants to FB1. A) Leaf discs were floated on 5µM FB1. After a 48 h period of dark incubation, the tissues were transferred to a 16 h-photoperiod. Photos were taken 5-days after treatment. B) Samples were harvested from the same experiment at the indicated time points for RNA extraction and qRT-PCR analysis. qRT-PCR values are an average of 3 technical replicates. Bars represent mean fold-change ± SD (n = 3). An asterisk indicates a significant difference in the fold-change between Col-0 and *ics1* samples ($p \leq 0.05$). *ACTIN2* and *EIF4A* were used as constitutive reference control genes.

6.4. SA and ATP regulated genes are responsive to FB1

Considering that ICS1 enzyme is required for most of the SA produced in response to pathogens (Wildermuth *et al.*, 2001), the expectation is that FB1-induced expression of genes identified in the SA/ATP microarray experiment will most likely require ICS1 activity. To investigate this, a selection of genes identified in the microarray as differentially expressed in response to SA ±ATP were analysed using RNA from the FB1-treated Col-0 and *ics1* tissues (from section 6.3).

There were two main observations arising from this analysis. The first observation was that a number of the genes responded to SA (Figure 6.2) and to FB1 (Figure 6.5) with a similar profile. This suggests that FB1-induced expression is mediated via SA biosynthesis, as supported by attenuation of the response to FB1 of these genes in the *ics1* knockout mutants (Figure 6.5). Genes falling in this category are *SAUR36*, *At4g15610*, *KCS11* and *XK1* (Figure 6.5). Taken together with FB1 resistance of *ics1* mutants, this shows that ICS1-dependent SA biosynthesis is the predominant source of the phytohormone regulating Arabidopsis responses to this mycotoxin. The second unexpected observation is that the response of another group of genes (*BGLU31, LTPG5, At3g09940* and *At5g39670*) to FB1 seen in Col-0 was superseded by the response to FB1 in the *ics1* mutants (Figure 6.5). This result suggests that SA caps FB1-induced expression of some genes, given that disruption of SA biosynthesis triggers a greater enhancement of expression of these genes. These are likely to be genes involved in suppression of PCD, though such a conclusion can be fraught with problems given the unexpected lack of correlation between transcript abundance and protein expression of CYCLASE-1 described in section 6.2.

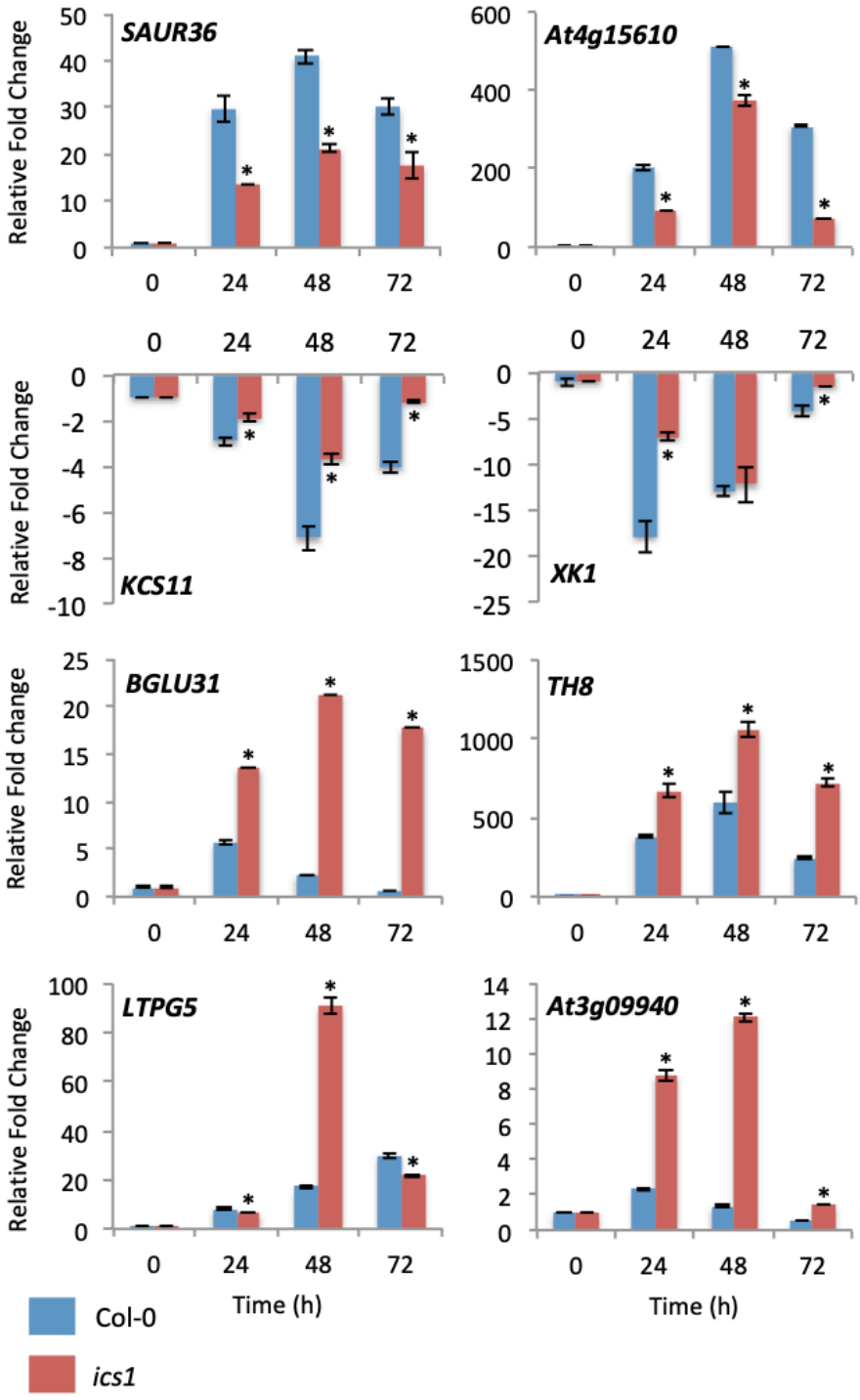

Figure 6.5 Effects of disrupting ICS1 activity on FB1-induced gene expression. 10 Leaf discs from 10 independent Col-0 and *ics1* mutant plants were floated on 5μM FB1 and incubated in the dark for 48 hours prior to transferring to a 16h-photoperiod. Samples were harvested at the indicated time points for RNA extraction and qRT-PCR analysis. qRT-PCR values are an average of 3 technical replicates. Bars represent mean fold-change ± SD (n = 3). An asterisk indicates a significant difference in the fold-change between Col-0 and *earp1.1* samples ($p \leq 0.05$). *ACTIN2* and *EIF4A* were used as constitutive reference control genes.

6.5. Discussion

In this chapter, an alternative screen for identifying PCD-regulatory genes was utilised to extend the number of candidate genes for future analysis. The screen used the phytohormone SA, which promotes FB1-induced cell death, and exogenous ATP as a cell death antagonist. The general antagonism between SA and ATP was demonstrated using the SA marker gene *PR-1*, whose activation by SA was blocked in the presence of exogenous ATP. This screen was previously used by Smith *et al*. (2015), who identified 33 proteins amongst which CYCLASE-1 was found to be a positive regulator of FB1-induced and pathogen-induced cell death. The Smith *et al*. (2015) study was limited to extracellular matrix proteins, whereas this chapter utilised a genome-wide microarray analysis.

6.5.1. The SA/ATP screen identifies new putative cell death-regulatory proteins

The SA/ATP screen identified numerous genes (Table 6.1) that may have a cell death-regulatory function. A number of genes identified by the microarray have previously been implicated in plant immunity and PCD. One such gene has previously been identified as a well-known SA-responsive protein, PHYTOALEXIN DEFICIENT 4 (PAD4). PAD4 works in conjunction with EDS1, a crucial protein to initiate the SA-induced defence signalling pathway (Glazebrook *et al*., 1996, 1997; Parker *et al*., 1996; Feys *et al*., 2001). PAD4 and EDS1 collaboration is required for ICS1 expression and SA accumulation, resulting in a feedback loop which further enhances the expression of EDS1, PAD4, and various other defence-related genes (Jirage *et al*., 1999; Feys *et al*., 2001; Vlot *et al*., 2009). The feedback loop generates increased SA levels sufficient for SA signalling and defence (Wiermer *et al*., 2005). Direct interactions between PAD4 and EDS1, along with SAG101, a well-known positive regulator of senescence, has also been confirmed (He & Gan, 2002; Rietz *et al*., 2011; Zhu *et al*., 2011). This triad of genes have proven to be a major barrier to infection to invasive biotropic and hemi-biotropic pathogens. EDS1 is essential for PAD4 and EDS1 accumulation, and appears to act as a kind of scaffold for PAD and SAG101. Double knockout mutants of *pad4/sag101* results in defective R-gene mediated resistance to avirulent pathogens and basal defence towards virulent pathogens (Wiermer *et al*., 2005)

PAD4 and EDS1 have been directly implicated in the regulatory switch of age-dependent cell death, which is associated with senescence. A study by Vogelmann and colleagues identified an E3 ubiquitin ligase gene, SAUL1, and mutants lacking this enzyme prematurely activated age-dependent cell death in young seedlings. The SA amplification loop promoted by PAD4 and EDS1 is crucial for cell death and senescence, increased SA content, and gene expression changes in *saul1* mutants challenged by low light (Vogelmann *et al*., 2012)

Furthermore it has been shown that PAD4 and EDS1 participate not only in resistance to pathogens and age-related senescence, but also in the transduction of photo-oxidative stress signals resulting in cell death and growth inhibition. Cell death and growth inhibition phenotypes of *lsd1*, *acd6-1*, *cpr1*, and *cpr6* mutants require PAD4 and EDS1, shown by the liberation of mutant phenotypes in double mutants with *pad4* or *eds1* (Jirage *et al*., 2001; Rustérucci *et al*., 2001; Mateo *et al*., 2004; Ochsenbein *et al*., 2006; Mühlenbock *et al*., 2008; Ng *et al*., 2011; Vogelmann *et al*., 2012).

Another defence-related protein identified by the microarray was FLG22-INDUCED RECEPTOR-LIKE KINASE (FRK1), a flagellin sensing protein and key player in PAMP-triggered immunity (PTI) (Asai *et al*., 2002). SOMATIC EMBRYOGENESIS RECEPTOR-LIKE KINASE 1 (SERK1) is another protein that was identified and has been implicated in a number of defence related biological functions. As well as being involved in floral development (Lewis *et al*., 2010), SERK1 has also been associated with resistance to aphids (Mantelin *et al*., 2011), brassinosteroid (BR) signalling (Karlova *et al*., 2006; Albrecht *et al*., 2008), and can form ligand-induced immune complexes with PRRs involved in PTI (He *et al*., 2007; Niehl *et al*., 2016).

The identification of known defence-related proteins supports the use of the SA/ATP relationship for identifying genes critical in plant immunity. The defence-related genes I have identified appear to be PTI and basal defence-related. In Chapter 1, I detailed the stages of plant immunity. To briefly recap, plants defend themselves from a variety of pathogenic microbes using a two-branched immune response system (Jones and Dangl. 2006). Pathogen Associated Molecular Proteins (PAMPs), such as flagellin, are flagged by the host plant by Pattern Recognition Receptors

(PRRs). This initiates a PAMP-triggered immune (PTI) response resulting in a cascade of defence responses such as ion fluxes, MAPK activation and ROS formation (Zipfel, 2009). If the pathogen is able to produce virulence factors (effectors) that effectively overcome the PTI, but are again recognized by the host plant, the host will initiate a more aggressive effector-triggered immune (ETI) response, which can ultimately result in the hypersensitive response and PCD. The SA/ATP screen has identified a number of PTI-related genes, and yet PCD occurs after ETI. If further investigation into these genes implicates them as PCD-regulatory proteins, I would suggest that the current model for plant-pathogen interaction is too simplistic and too linear. There has already been a number of reports criticising the simplicity of the PTI-ETI dichotomy. A review that particularly addressed this issue explained how PAMPs are considered as highly conserved throughout classes of microbes, whereas effectors are species-specific and generally effects a particular target. However, there have been cases where PAMPs are narrowly conserved and contribute to virulence, and effectors have had a broader target range. This is likely to propose that certain PAMPs can be equally defined as effectors, and vice versa (Thomma *et al*., 2011). This review on PAMPs and effectors supports my hypothesis that host defences will interact at varying levels of plant immunity, from PTI to ETI. Therefore it is possible that PTI-induced genes can also be activated during ETI, and more specifically with PCD.

Many genes identified from the microarray have not been associated with SA/ATP signalling, nor have they been implicated in plant immunity. This suggests that the screen has potentially identified genes with a novel function in plant immunity, and possibly PCD.

6.5.2 ICS1 is a positive regulator of FB1-induced cell death

The role of SA in FB1-induced PCD has been confirmed using the *cpr1* and *cpr6* mutants (Jirage *et al*., 2001; Clarke *et al*., 2001) and the transgenic plants expressing bacterial salicylate hydroxylase (Asai *et al*., 2000). Therefore, the pathway responsible for production of endogenous SA has regulatory control over FB1-induced cell death and so became a prime target for analysis. SA biosynthesis is dependent on the production of chorismate from shikimate pathway. Chorismate then serves as a substrate for the production of SA through two biosynthetic pathways.

The most predominant is the ISOCHORISMATE SYNTHASE (ICS) pathway, which converts chorismate to isochorismate using ICS1 and ICS2. Isochorismate is then converted to SA using pyruvate lyase, however this last step still remains unclear (Serino *et al*., 1995; Wildermuth *et al*., 2001). The second pathway, referred to as the PAL pathway, converts chorismate through a number of steps to phenyalanine, and then to cinnamic acid using phenylalanine ammonia lyase enzymes (PAL1-4). Cinnamic acid is then converted to benzoic acid before forming SA (Klambt, 1962; Leon *et al*., 1995).

Results in this chapter have revealed that FB1-induced SA biosynthesis occurs via the ICS pathway. The ICS pathway is also required for most of the SA produced in response to bacterial and fungal pathogens (Wildermuth *et al*., 2001). Therefore, ICS1 and other enzymes in the pathway define a novel class of Arabidopsis cell death regulatory proteins in FB1-induced PCD. While exogenous SA is a very good treatment simulating the surge in endogenous SA activated by pathogens or FB1, it lacks locality specificity and tight control between biosynthesis ad coversion to inactive SA-glycoside and other derivatives. The finding that ICS1 gene knockout provides a clear phenotypic response to FB1-induced cell death provides a better tool to filter the data obtained by the SA/ATP microarray screen, since it uses a more physiologically relevant system.

7
General Discussion

7.1 Overview of findings

The ECM is the main focal point of my PhD project. Simply put, the ECM consists of the apoplast, plasma membrane and cell wall. The ECM provides mechanical support and acts as a biochemical barrier, using an arsenal of proteins and polysaccharides. I picture the cell as military base, which requires constant surveillance in order detect an outside threat, along with the means to defend and protect the base from infiltration. This notion suggests that the ECM acts as an intimate interface between host and pathogen, and the ability for detection and action by the host's arsenal determines the outcome of the interaction.

The connection between light and cell death was observed by Asai *et al.,* (2000). The induction of cell death by FB1 requires light, and this response was consistent with the observations of HR against avirulent pathogens in Arabidopsis, which also requires light (Delaney et al., 1994). As the ECM is the compartment invaded prior to the infiltration of the cell, I proposed that the light-dependent components initiating cell death might inhabit the ECM. In Chapter 3, I confirmed the components within the soluble phase of the ECM induce light-dependent cell death in Arabidopsis cell cultures (Figure 3.1). Through this revelation I was able to devise a proteomic screen, focusing on light in the absence of FB1, with the aim of identifying putative PCD regulatory proteins within the soluble phase of the ECM. Among the proteins identified, this process successfully identified the ribonuclease protein RNS1, which was confirmed to be a pro-cell death regulator through reverse genetic experimentation and FB1 treatments.

Not only is FB1-induced cell death regulated by light, but also the interference of extracellular ATP utilization proceeds with the onset of cell death in a light dependent manner (Chivasa *et al*., 2005; Chivasa *et al*., 2009). Furthermore, FB1 treatments result in a dramtic collapse in apoplastic ATP prior to the onset of cell death, this determined that eATP signaling acts as a negative regulator of cell death (Chivasa et al., 2009; Chivasa et al., 2011).

In an effort to identify both extracellular and intracellular components in the cell death pathway, my laboratory group devised a whole-genome microarray analysis, using FB1 ± ATP. Through this screen, 13 transcription factors were identified, including EARP1. Reverse genetic analysis of EARP1 has concluded that EARP1 is a pro-cell death regulator of FB1-induced PCD.

To determine whether the novel eATP-responsive transcription factor influences a number of genes, another whole genome microarray analysis was developed using FB1 treatments on both wild type (Col-0) and an *earp1* knock-out line. Roughly 29% of genes within the Arabidopsis genome responded to FB1 treatment, and roughly 70% of these genes were altered through the removal of the EARP1 transcription factor. This has led me to believe that *EARP1* functions as a 'hub-gene', which interacts with a number of gene networks and is likely to play an important role in many biological processes.

In summary, the beginning of my project focused on the role of the ECM on FB1-induced cell death, and how light regulated this process. This advanced towards the role of eATP on FB1-induced cell death. The final chapter of my project focused on the role of the phytohormone, SA, on PCD. Asai and colleagues not only connected FB1-induced PCD with light regulation, but this process also resulted in an accumulation of SA. Further evidence for the role of SA was shown through the inability to induce cell death in the mutant Arabidopsis line, NahG, which expresses a bacterial protein that degrades SA (Asai et al., 2000).

In addition to the connection of SA with light-dependent FB1-induced cell death, Chivasa and colleagues showed that treatment of tobacco cell suspension cultures with SA triggers depletion of eATP. Furthermore, concomitant treatment of the cell with SA and exogenous ATP blocks activation of PR-1 gene expression (Chivasa *et al*., 2009). This indicated that ATP antagonises some SA-induced responses. This appeared to go hand-in-hand with the promotion of FB1-induced PCD via SA (Jirage *et al*., 2001; Clarke *et al*., 2001), and the suppressesion observed through treatments of exogenous ATP (Chivasa *et al*., 2005). This suggested that the effects of SA- and eATP-mediated signalling could be antagonistic in relation to FB1-induced PCD. Using the antagonistic relationship between SA and eATP, my laboratory group produced a proteomic screen that was adapted to identify PCD regulatory proteins

within the soluble phase of the ECM (Smith *et al*. 2015). Through this screen, CYCLASE1 was identified, and found to be a positive regulator of FB1-induced and pathogen-induced cell death (Smith et al., 2015). My project adopted the same concept, but applied the SA ± ATP system to whole genome microarray analysis. The screen identified a number of genes that have previously been implicated in SA-induced plant defence signalling (e.g. PAD4, FRK1); however, the screen also identified genes of either unknown function or have not been linked with either eATP- or SA-signalling. Furthermore, Arabidopsis plants treated with FB1 showed that a number of genes selected from the whole-genome analysis, showed altered expression levels in *ics1* knock out mutants. ICS1 is crucial for the synthesis of SA via the ICS pathway. Results in this chapter have revealed that FB1-induced SA biosynthesis occurs via the ICS pathway. The ICS pathway is also required for most of the SA produced in response to bacterial and fungal pathogens (Wildermuth *et al*., 2001). Therefore, ICS1 and other enzymes in the pathway define a novel class of Arabidopsis cell death regulatory proteins in FB1-induced PCD.

Each screen analysed within this thesis individually hones in on a fundamental aspect of FB1-induced PCD; whether that be light-regulation, response to eATP, response to SA/ATP antagonim, or regulation by the newly identified EARP1 transcription factor. Throughout the project, the screens have been analysed as separate entities in order to provide novel targets that may elucidate the mechanism behind FB1-induced PCD, and potentially other forms of PCD. Final comparisons between the datasets have provided a condensed list of target genes that are likely to be fundamental in FB1-signalling (Figure 7.1). A final list of 7 genes were identified as responsive to light, FB1, ATP and regulated by EARP1 (Table 7.1). I propose future projects to be developed with these genes in mind, beginning with reverse genetics and FB1 treatments to determine if the loss of these genes affects the progression of PCD.

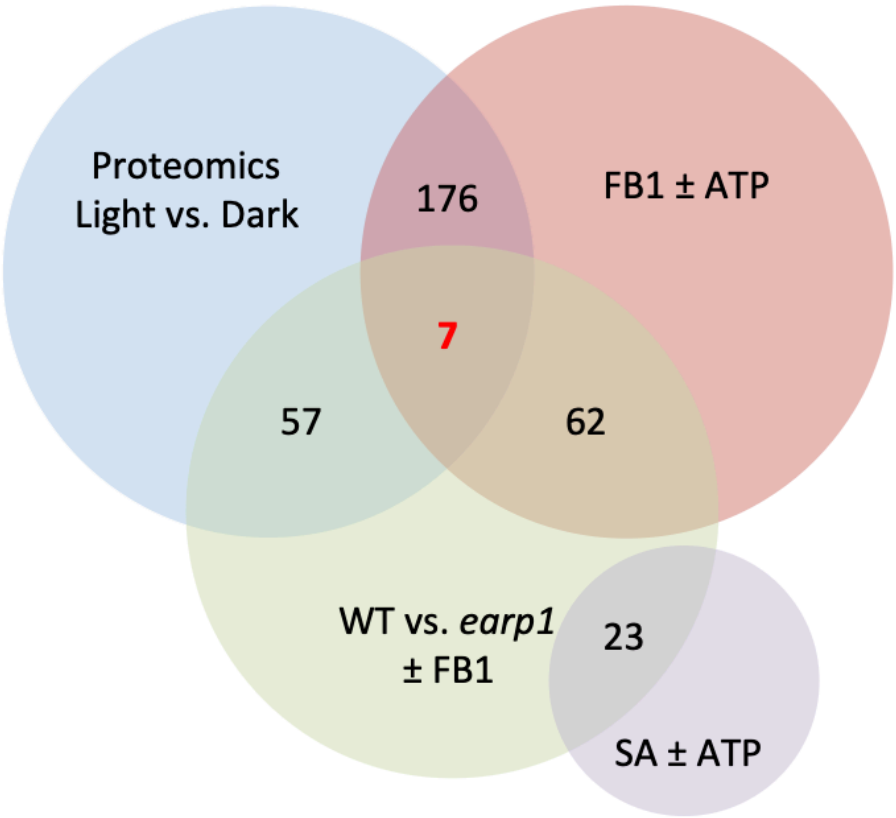

Figure 7.1. The number of genes identified across multiple screening platforms.

Table 7.1. Seven genes distributed among screens

AGI[a]	*Gene symbol*[b]	*Gene description*[c]
At3g52470	-	Late embryogenesis abundant (LEA) hydroxypoline-rich glycoprotein family
At4g39830	-	Cupredoxin superfamily protein
At1g74000	SS3	Strictosidine synthase 3
At4g20830	-	FAD-binding berberine family protein
At4g20860	BBE22	FAD-binding berberine family protein
At5g64120	PRX71	Peroxidase superfamily protein
At1g64760	ZET	O-Glycosyl hydrolases family 17 protein

[a]AGI (Arabidopsis Genome Initiative, 2000) code and gene symbol
[b]Gene symbol used in NCBI database
[c]Gene description used in NCBI database

7.2 Implications of this research

FB1 is a mycotoxin produced by *Fusarium verticillioides*, a fungal pathogen of maize. The findings of this research could provide new insights into how this pathogen suppresses plant host immunity and may form the basis for future strategies to combat this economically important plant disease affecting one of the world's top cereal crops.

7.2.1 FB1 is a virulence factor in plant disease

Together with rice and wheat, maize features in the top 3 cereal crops (Leff *et al*., 2004; FAO.org, 2019) of global importance in the human food chain. Great investment is being channelled into breeding efforts to generate maize cultivars resistant to *F. verticillioides* and in development of fungicides to control the pathogen after infection. However, application of certain fungicides has been reported to activate increased biosynthesis of fumonisin (Falcão *et al*., 2011), narrowing down available fungicides for use against this pathogen. Moreover, the high frequency of emergency of fungicide-resistance in pathogens (Ishii and Holloman, 2015; Frac.info. 2019) makes the chemical approach unsustainable. Thus, genetic resistance could offer a better option for controlling this pathogen. Better understanding of the molecular interactions between maize and this fungus could provide important clues for identifying key genetic targets. This research has begun to uncover key components in Arabidopsis.

F. verticillioides can infect maize at all growth stages, causing symptoms that have been classified as a number of diseases, including seedling blight, stalk rot, seed rot, root rot and kernel/ear rot (Kommedahl *et al*., 1981; Nelson *et al*., 1993). Infection in the early stages of maize development causes seedling blight, which is associated with stunted roots and shoots, and foliar lesions (Desjardins *et al*., 1998; 2002) ultimately causing severe yield losses. Infection at later stages of maize growth may be symptomless, with no impact on grain yield, but farmers still make 100% losses as their grain is condemned as not fit for human or livestock consumption due to mycotoxin contamination. Mycotoxins accumulating in maize include fumonisins, fusaric acid, and fusarin (Bacon *et al*., 2001; Fotso *et al*., 2002; Baldwin *et al*., 2014). Fumonisins are the most common mycotoxin and have the highest impact on

maize contamination. There are over 28 analogues of fumonsins, with Fumonsin B1 (FB1) being the most predominant and most toxicologically active, followed by FB2 and FB3 (Bartok *et al*., 2010).

Fumonisins are structurally similar to the free sphingoid bases, sphinganine and sphingosine. These structural similarities led to the discovery that fumonisins inhibit ceramide synthase, a key enzyme in sphingolipid biosynthesis (Wang *et al*., 1991). Sphingolipids are structural elements in the lipid bilayer and contribute to maintenance of membrane structure (Sperling *et al*., 2005). They have been further implicated in many cellular processes in yeast and animal cells, including signal transduction, cell-cell recognition (Hannun and Bell, 1989; Hakomori and Igarashi, 1995), apoptosis (Obeid *et al*., 1993; Smith *et al*., 2000) and senescence (Venable *et al*., 1995; Michaelson *et al*., 2016). Though the role of sphingolipids have been better defined in animal systems, they have been shown to be integral to a number of plant processes, such as pollen development (Teng *et al*., 2008; Rennie *et al*., 2014), signal transduction and responses to biotic and abiotic stress (Michaelson *et al*., 2016). The toxicity of fumonisins is thought to be a direct consequence of disrupted sphingolipid metabolism, resulting in the accumulation of toxic levels of sphingoid base metabolites and depletion of complex sphingolipids (Wang *et al*., 1991).

Although there is incontrovertible evidence for destabilisation of sphingolipid metabolism by FB1, the current project has demonstrated that in plants, the cell death is controlled by light-dependent factors secreted to the extracellular matrix. The fact that plant signals, controlling cell fate after exposure to FB1, are located in the compartment invaded by fungal hyphae might not be a mere coincidence. Fungal hyphae, which colonise the aploplast (extracellular matrix) would be expected to secrete FB1 within the same compartment. What is the role of FB1 in plant host-fungus interaction?

A role for FB1 in suppression of maize defences has been proposed on the basis of two key observations. The first observation is that development of seedling blight symptoms, such as reduced root weight, shoot stunting and leaf lesions, require FB1 production (Desjardins *et al*., 1998; 2002). The investigation into the role fumonisin production on enhancing the development of *F. verticillioides* infection has displayed varying results. Desjardins and colleagues stated that fumonisins appeared

to increase the virulence of *F. verticillioides* but was not necessary for disease development (Desjardins *et al*., 1995). On the contrary, Williams and colleagues (2006, 2007) reported a significant positive correlation between leaf lesion development on seedlings and the accumulation of FB1. This result was also paired with a reduction in root weight and stalk height, showing a negative correlation against FB1 accumulation (Williams *et al*., 2006, 2007). Further studies investigating this controversy supported Williams *et al*. by also demonstrating a positive correlation between FB1 production and disease development (Glenn *et al*., 2008).

The second observation came when a strain of *F. verticillioides* incapable of infecting maize, but pathogenic on banana, was identified (Hirata *et al*., 2001; Mirete *et al*., 2004; Moretti *et al*., 2004). This banana-infecting strain, subsequently named *F. musae*, does not produce fumonisins, unlike the maize-infecting *F. verticillioides*. A specific gene cluster required for fumonisin production, named FUM cluster, is absent from *F. musae*. FUM contains 16 sequential and co-expressed genes and loss-of-function fundal mutants are incapable of producing fumonisins (Proctor *et al*., 2003; Brown *et al*., 2007). Glenn and colleagues (2008) reported that the FUM cluster in the banana pathogen *F. musae* was deleted except for portions of *FUM21* and *FUM19*, which are terminal genes at either end of the cluster. Transformation of the banana strain with the entire FUM cluster produced fumonisin-producing transformants, which had acquired the ability to infect maize (Glenn *et al*., 2008). This demonstrates that fumonisins are virulence factors required by *F. verticillioides* to overcome maize defences. Therfore, focusing research on understanding the major components recruited in plant responses to FB1 could provide targets for controlling this pathogen. This project had identified numerous genes/proteins with expression profiles consistent with targets important in deciding plant cell fate after contact with FB1 has been made. However, the function of FB1-induced cell death in the fungus-plant interaction needs to be understood.

7.2.2 The functional relevance of FB1-induced cell death

F. verticillioides is an example of a facultative biotroph, which can switch between biotrophic and necrotrophic growth. This bimodal growth strategy is similar to *F. graminearum* Schwabe, a mycotoxin-producing fungus that causes fusarium head blight (FHB) disease of wheat. *F. graminearum* colonises wheat asymptomatically in

the initial biotrophic phase of infection and then switches to necrotrophic growth. The switch from biotrophic to nectrophic growth is associated with increased accumulation of the mycotoxin deoxynivalenol (DON) in host tissues (Bai and Shaner, 2004). Thus, increased mycotoxin production enables the fungus to kill host tissues by switching to necrotrophy. In fact treatment of Arabidopsis with DON triggers leaf chlorosis and cell death (Desmond *et al*., 2008) in a fashion similar to FB1 in Arabidopsis.

Therefore, the mycotoxin-induced cell death seen in Arabidopsis is equivalent to the maize or wheat necrosis activated when these pathogens switch to necrotrophy. In this vein, the mycotoxin-induced cell death represents total capitulation of the plant host to fungal invasion and a cue for the fungus to sporulate and spread. In light of this, FB1 or DON resistance could provide strong crop genetic resistance to fungal infection. This project has taken advantage of this link to identify an extensive list of potential gene targets that could be used to understand how the fungus overcomes host resistance for future development of genetic strategies to control Fusarium diseases.

7.3 Future prospects

As well as identifyting putative PCD-regulatory components, this project has conclusively identified several proteins important in regulating FB1-induced cell death, including ICS1, PHYB, EARP1, and RNS1. Since salicylic acid is an important defence protein and light perception is critical for plant development, both ICS1 and PHYB are not suitable candidates for genetic manipulation to alter plant sensitivity to mycotoxin and susceptibility to the fungal pathogens. However, Arabidopsis loss-of-function mutants without EARP1 or RNS1 did not have any obvious developmental or growth defects, making these ideal candidates for genetic manipulation. The Chivasa group previously identified CYCLASE1 and UDP-glucose pyrophosphorylase as enzymes that can be disrupted to enhance FB1 resistance. Pyramiding gene knockout of all these genes in the same mutant could provide a super FB1-resistant mutant. Future research could look into generating this multi-gene knockout mutant in Arabidopsis in the first instance to investigate if FB1 resistance is additive.

Identification of maize homologous proteins would be a key next step. These could be targeted for gene knockout using CRSPR technology. The CRISPR protein, Cas9, is an endonuclease that uses a guide sequence within an RNA duplex, tracrRNA:crRNA, to form base pairs with the targeted DNA sequence, allowing Cas9 to insert a site-specific double-strand breaks in the DNA. CRISPR-Cas9 technology has enabled remarkable developments in genome editing, whilst remaining cost effective and easy-to-use. The technology allows for easier design, high specificity, efficacy and it is compatible for high-throughput and multiplexed gene editing over a wide array of cells and organisms (Ran *et al*., 2014).

Even with ever progressing technologies, there are still a number of obstacles to overcome, such as determining the homologues from Arabidopsis in more complex genomes. Fortunately the maize genome has been mapped (Schnable *et al*., 2009), however searching for a homologues of a single Arabidopsis gene in a genome consisting of 10 chromosomes and 32,000 genes is difficult (Schnable *et al*., 2009), especially when a multitude of genes may be required for the functionality that one Arabidopsis gene provides. To identify homologues in maize I would use NCBI protein BLAST (Blast.ncbi.nlm.nih.gov. 2019). If the result showed very few homologous genes I would use CRISPR to knock out each of the genes. However, if a large number of homologues were identified, to begin with I would use Genevestigator (Hruz *et al*., 2008) to determine which genes are likely to be responsive to FB1 by searching for genes responding to light, salicylic acid and pathogens. Then I would select the homologues for CRISPR editing. The maize mutants could then be tested for susceptibility to *F. verticillioides* in both laboratory trials and field trials, should the legislative framework enable this. Successful outcomes of this future research will deliver impact in the way of better yields for farmers and prevention of mycotoxin contamination of maize grain. Although this is way in the future, this PhD project has provided the foundation for such translational work to begin.

Bibliography

A

Abbès, S., Ben Salah-Abbès, J., Jebali, R., Younes, R.B. and Oueslati, R., 2016. Interaction of aflatoxin B1 and fumonisin B1 in mice causes immunotoxicity and oxidative stress: Possible protective role using lactic acid bacteria. *Journal of immunotoxicology*, *13*(1), pp.46-54.

Abbracchio, M.P. and Burnstock, G., 1994. Purinoceptors: are there families of P2X and P2Y purinoceptors?. *Pharmacology & therapeutics*, *64*(3), pp.445-475.

Abramovitch, R.B., Anderson, J.C. and Martin, G.B., 2006. Bacterial elicitation and evasion of plant innate immunity. *Nature Reviews Molecular Cell Biology*, *7*(8), p.601.

Ackerman, E.J., Saxena, S.K. and Ulbrich, N., 1988. Alpha-sarcin causes a specific cut in 28 S rRNA when microinjected into Xenopus oocytes. *Journal of Biological Chemistry*, *263*(32), pp.17076-17083.

Acquati, F., Possati, L., Ferrante, L., Campomenosi, P., Talevi, S., Bardelli, S., Margiotta, C., Russo, A., Bortoletto, E., Rocchetti, R. and Calza, R., 2005. Tumor and metastasis suppression by the human RNASET2 gene. *International journal of oncology*, *26*(5), pp.1159-1168.

Ahmad, M. and Cashmore, A.R., 1993. HY4 gene of A. *thaliana* encodes a protein with characteristics of a blue-light photoreceptor. *Nature*, *366*(6451), p.162.

Al-Sady, B., Ni, W., Kircher, S., Schäfer, E. and Quail, P.H., 2006. Photoactivated phytochrome induces rapid PIF3 phosphorylation prior to proteasome-mediated degradation. *Molecular cell*, *23*(3), pp.439-446.

Albrecht, C., Russinova, E., Kemmerling, B., Kwaaitaal, M. and de Vries, S.C., 2008. Arabidopsis SOMATIC EMBRYOGENESIS RECEPTOR KINASE proteins serve brassinosteroid-dependent and-independent signaling pathways. *Plant physiology*, *148*(1), pp.611-619.

Alonso, J.M., Hirayama, T., Roman, G., Nourizadeh, S. and Ecker, J.R., 1999. EIN2, a bifunctional transducer of ethylene and stress responses in Arabidopsis. *Science*, *284*(5423), pp.2148-2152.

Alonso, J.M., Stepanova, A.N., Leisse, T.J., Kim, C.J., Chen, H., Shinn, P., Stevenson, D.K., Zimmerman, J., Barajas, P., Cheuk, R. and Gadrinab, C., 2003. Genome-wide insertional mutagenesis of *Arabidopsis thaliana*. *Science*, *301*(5633), pp.653-657.

Altschul, S.F., Gish, W., Miller, W., Myers, E.W. and Lipman, D.J., 1990. Basic local alignment search tool. *Journal of molecular biology*, *215*(3), pp.403-410

Alvarez, M.E., Pennell, R.I., Meijer, P.J., Ishikawa, A., Dixon, R.A. and Lamb, C., 1998. Reactive oxygen intermediates mediate a systemic signal network in the establishment of plant immunity. *Cell*, *92*(6), pp.773-784.

An, F., Zhao, Q., Ji, Y., Li, W., Jiang, Z., Yu, X., Zhang, C., Han, Y., He, W., Liu, Y. and Zhang, S., 2010. Ethylene-induced stabilization of ETHYLENE INSENSITIVE3 and EIN3-LIKE1 is mediated by proteasomal degradation of EIN3 binding F-box 1 and 2 that requires EIN2 in Arabidopsis. *The Plant Cell*, pp.tpc-110.

Arabidopsis.org. (2019). *TAIR - Home Page*. [online] Available at: http://www.Arabidopsis.org/index.jsp [Accessed 28 Mar. 2019

Arabidopsis Genome Initiative, 2000. Analysis of the genome sequence of the flowering plant *Arabidopsis thaliana*. *nature*, *408*(6814), p.796.

Asada, K., 2006. Production and scavenging of reactive oxygen species in chloroplasts and their functions. *Plant physiology*, *141*(2), pp.391-396.

Armstrong, W., 1980. Aeration in higher plants. In *Advances in botanical research* (Vol. 7, pp. 225-332). Academic Press.

Asai, T., Stone, J.M., Heard, J.E., Kovtun, Y., Yorgey, P., Sheen, J. and Ausubel, F.M., 2000. Fumonisin B1–induced cell death in Arabidopsis protoplasts requires jasmonate-, ethylene-, and salicylate-dependent signaling pathways. *The Plant Cell*, *12*(10), pp.1823-1835.

Asai, T., Tena, G., Plotnikova, J., Willmann, M.R., Chiu, W.L., Gomez-Gomez, L., Boller, T., Ausubel, F.M. and Sheen, J., 2002. MAP kinase signalling cascade in Arabidopsis innate immunity. *Nature*, *415*(6875), p.977.

Atkinson, M.M. and Baker, C.J., 1989. Role of the plasmalemma H+-ATPase in Pseudomonas syringae-induced K+/H+ exchange in suspension-cultured tobacco cells. *Plant physiology*, *91*(1), pp.298-303.

Azpiroz-Leehan, R. and Feldmann, K.A., 1997. T-DNA insertion mutagenesis in Arabidopsis: going back and forth. *Trends in Genetics*, *13*(4), pp.152-156.

B

Bacon, C.W., Yates, I.E., Hinton, D.M. and Meredith, F., 2001. Biological control of Fusarium moniliforme in maize. *Environmental Health Perspectives*, *109*(suppl 2), pp.325-332.

Bai, G.H., Chen, L.F. and Shaner, G.E., 1999. Breeding for resistance to head blight of wheat in China. *American Phytopathological Society Press*.

Bailey, Michael J., Johanna Buchert, and Liisa Viikari. "Effect of pH on production of xylanase by Trichoderma reesei on xylan-and cellulose-based media." *Applied microbiology and biotechnology* 40, no. 2-3 (1993): 224-229.

Baker, C.J. and Orlandi, E.W., 1995. Active oxygen in plant pathogenesis. *Annual review of phytopathology*, *33*(1), pp.299-321.

Balconi, C., Berardo, N., Locatelli, S., Lanzanova, C., Torri, A. and Redaelli, R., 2014. Evaluation of ear rot (Fusarium verticillioides) resistance and fumonisin accumulation in Italian maize inbred lines. *Phytopathologia Mediterranea*, pp.14-26.

Baldwin, T.T., Zitomer, N.C., Mitchell, T.R., Zimeri, A.M., Bacon, C.W., Riley, R.T. and Glenn, A.E., 2014. Maize seedling blight induced by Fusarium verticillioides: Accumulation of fumonisin B1 in leaves without colonization of the leaves. *Journal of agricultural and food chemistry*, *62*(9), pp.2118-2125.

Bar, M., Sharfman, M. and Avni, A., 2011. LeEix1 functions as a decoy receptor to attenuate LeEix2 signaling. *Plant signaling & behavior*, *6*(3), pp.455-457.

Bariola, P.A., Howard, C.J., Taylor, C.B., Verburg, M.T., Jaglan, V.D. and Green, P.J., 1994. The Arabidopsis ribonuclease gene RNS1 is tightly controlled in response to phosphate limitation. *The Plant Journal*, *6*(5), pp.673-685.

Bariola, P.A., MacIntosh, G.C. and Green, P.J., 1999. Regulation of S-like ribonuclease levels in Arabidopsis. Antisense inhibition of RNS1 orRNS2 elevates anthocyanin accumulation. *Plant Physiology*, *119*(1), pp.331-342.

Bartels, S., Lori, M., Mbengue, M., van Verk, M., Klauser, D., Hander, T., Böni, R., Robatzek, S. and Boller, T., 2013. The family of Peps and their precursors in Arabidopsis: differential expression and localization but similar induction of pattern-triggered immune responses. *Journal of experimental botany*, *64*(17), pp.5309-5321.

Bartók, T., Tölgyesi, L., Szekeres, A., Varga, M., Bartha, R., Szécsi, Á., Bartók, M. and Mesterházy, Á., 2010. Detection and characterization of twenty□eight isomers of fumonisin B1 (FB1) mycotoxin in a solid rice culture infected with Fusarium verticillioides by reversed□phase high□performance liquid chromatography/electrospray ionization time□of□flight and ion trap mass spectrometry. *Rapid Communications in Mass Spectrometry*, *24*(1), pp.35-42.

Basile, D.V. and Basile, M.R., 1987. The occurrence of cell wall-associated arabinogalactan proteins in the Hepaticae. *Bryologist*, pp.401-404.

Becker, B.A., Pace, L., Rottinghaus, G.E., Shelby, R., Misfeldt, M. and Ross, P.F., 1995. Effects of feeding fumonisin B1 in lactating sows and their suckling pigs. *American Journal of Veterinary Research*, *56*(9), pp.1253-1258.

Bendtsen, J.D., Nielsen, H., von Heijne, G. and Brunak, S., 2004. Improved prediction of signal peptides: SignalP 3.0. *Journal of molecular biology*, *340*(4), pp.783-795.

Berrocal-Lobo, M. and Molina, A., 2004. Ethylene response factor 1 mediates Arabidopsis resistance to the soilborne fungus Fusarium oxysporum. *Molecular plant-microbe interactions*, *17*(7), pp.763-770.

Bhandari, N. and Sharma, R.P., 2002. Fumonisin B1-induced alterations in cytokine expression and apoptosis signaling genes in mouse liver and kidney after an acute exposure. *Toxicology*, *172*(2), pp.81-92.

Bibikova, M., Beumer, K., Trautman, J.K. and Carroll, D., 2003. Enhancing gene targeting with designed zinc finger nucleases. *Science*, *300*(5620), pp.764-764.

Bienert, G.P., Schjoerring, J.K. and Jahn, T.P., 2006. Membrane transport of hydrogen peroxide. *Biochimica et Biophysica Acta (BBA)-Biomembranes*, *1758*(8), pp.994-1003.

Blackburn, P. and Moore, S., 1982. 12 Pancreatic Ribonuclease. In *The enzymes* (Vol. 15, pp. 317-433). Academic Press.

Bleecker, A.B., Estelle, M.A., Somerville, C. and Kende, H., 1988. Insensitivity to ethylene conferred by a dominant mutation in *Arabidopsis thaliana*. *Science*, *241*(4869), pp.1086-1089.

Boller, T. and Felix, G., 2009. A renaissance of elicitors: perception of microbe-associated molecular patterns and danger signals by pattern-recognition receptors. *Annual review of plant biology*, *60*, pp.379-406.

Bolwell, G.P., Bindschedler, L.V., Blee, K.A., Butt, V.S., Davies, D.R., Gardner, S.L., Gerrish, C. and Minibayeva, F., 2002. The apoplastic oxidative burst in response to biotic stress in plants: a three□component system. *Journal of experimental botany*, *53*(372), pp.1367-1376.

Borsani, O., Valpuesta, V. and Botella, M.A., 2001. Evidence for a role of salicylic acid in the oxidative damage generated by NaCl and osmotic stress in Arabidopsis seedlings. *Plant physiology*, *126*(3), pp.1024-1030.

Botto, J.F., Sanchez, R.A., Whitelam, G.C. and Casal, J.J., 1996. Phytochrome A mediates the promotion of seed germination by very low fluences of light and canopy shade light in Arabidopsis. *Plant Physiology*, *110*(2), pp.439-444.

Bowman, J.L., Sakai, H., Jack, T., Weigel, D., Mayer, U. and Meyerowitz, E.M., 1992. SUPERMAN, a regulator of floral homeotic genes in Arabidopsis. *Development*, *114*(3), pp.599-615.

Boyes, D.C., Nam, J. and Dangl, J.L., 1998. The *Arabidopsis thaliana* RPM1 disease resistance gene product is a peripheral plasma membrane protein that is degraded coincident with the hypersensitive response. *Proceedings of the National Academy of Sciences*, *95*(26), pp.15849-15854.

Brake, A.J., Wagenbach, M.J. and Julius, D., 1994. New structural motif for ligand-gated ion channels defined by an ionotropic ATP receptor. *Nature*, *371*(6497), p.519.

Briggs, W.R. and Christie, J.M., 2002. Phototropins 1 and 2: versatile plant blue-light receptors. *Trends in plant science*, *7*(5), pp.204-210.

Brooks, D.M., Bender, C.L. and Kunkel, B.N., 2005. The Pseudomonas syringae phytotoxin coronatine promotes virulence by overcoming salicylic acid□dependent defences in *Arabidopsis thaliana*. *Molecular plant pathology*, *6*(6), pp.629-639.

Brown, I., Trethowan, J., Kerry, M., Mansfield, J. and Bolwell, G.P., 1998. Localization of components of the oxidative cross□linking of glycoproteins and of callose synthesis in papillae formed during the interaction between non□pathogenic strains of Xanthomonas campestris and French bean mesophyll cells. *The Plant Journal*, *15*(3), pp.333-343.

Brown, R.L., Kazan, K., McGrath, K.C., Maclean, D.J. and Manners, J.M., 2003. A role for the GCC-box in jasmonate-mediated activation of the PDF1. 2 gene of Arabidopsis. *Plant physiology*, *132*(2), pp.1020-1032.

Brown, B.A., Cloix, C., Jiang, G.H., Kaiserli, E., Herzyk, P., Kliebenstein, D.J. and Jenkins, G.I., 2005. A UV-B-specific signaling component orchestrates plant UV protection. *Proceedings of the National Academy of Sciences*, *102*(50), pp.18225-18230.

Brown, D.W., Butchko, R.A., Busman, M. and Proctor, R.H., 2007. The Fusarium verticillioides FUM gene cluster encodes a Zn (II) 2Cys6 protein that affects FUM gene expression and fumonisin production. *Eukaryotic cell*, *6*(7), pp.1210-1218.

Brownlee, C., 2002. Role of the extracellular matrix in cell–cell signalling: paracrine paradigms. *Current opinion in plant biology*, *5*(5), pp.396-401.

Burnstock, G., 2001. Purine-mediated signalling in pain and visceral perception. *Trends in pharmacological sciences*, *22*(4), pp.182-188.

Bush, B.J., Carson, M.L., Cubeta, M.A., Hagler, W.M. and Payne, G.A., 2004. Infection and fumonisin production by Fusarium verticillioides in developing maize kernels. *Phytopathology*, *94*(1), pp.88-93.

C

Cao, Y., Liang, Y., Tanaka, K., Nguyen, C.T., Jedrzejczak, R.P., Joachimiak, A. and Stacey, G., 2014. The kinase LYK5 is a major chitin receptor in Arabidopsis and forms a chitin-induced complex with related kinase CERK1. *Elife*, *3*, p.e03766

Carlson, D.B., Williams, D.E., Spitsbergen, J.M., Ross, P.F., Bacon, C.W., Meredith, F.I. and Riley, R.T., 2001. Fumonisin B1 promotes aflatoxin B1 and N-methyl-N′-nitro-nitrosoguanidine-initiated liver tumors in rainbow trout. *Toxicology and applied pharmacology*, *172*(1), pp.29-36.

Carter, C., Pan, S., Zouhar, J., Avila, E.L., Girke, T. and Raikhel, N.V., 2004. The vegetative vacuole proteome of *Arabidopsis thaliana* reveals predicted and unexpected proteins. *The plant cell*, *16*(12), pp.3285-3303.

Casteel, S.W., Turk, J.R. and Rottinghaus, G.E., 1994. Chronic effects of dietary fumonisin on the heart and pulmonary vasculature of swine. *Fundamental and Applied Toxicology*, *23*(4), pp.518-524.

Castelli, J.C., Hassel, B.A., Maran, A., Paranjape, J., Hewitt, J.A., Li, X.L., Hsu, Y.T., Silverman, R.H. and Youle, R.J., 1998. The role of 2′-5′ oligoadenylate-activated ribonuclease L in apoptosis. *Cell death and differentiation*, *5*(4), p.313.

Castillon, A., Shen, H. and Huq, E., 2007. Phytochrome interacting factors: central players in phytochrome-mediated light signaling networks. *Trends in plant science*, *12*(11), pp.514-521.

Chai, L., Ge, X., Xu, Q. and Deng, X., 2011. CgSL2, an S-like RNase gene in 'Zigui shatian'pummelo (Citrus grandis Osbeck), is involved in ovary senescence. *Molecular biology reports*, *38*(1), pp.1-8.

Chai, T., Zhou, J., Liu, J. and Xing, D., 2015. LSD1 and HY5 antagonistically regulate red light induced-programmed cell death in Arabidopsis. *Frontiers in plant science*, *6*, p.292.

Chandra□Shekara, A.C., Gupte, M., Navarre, D., Raina, S., Raina, R., Klessig, D. and Kachroo, P., 2006. Light□dependent hypersensitive response and resistance signaling against Turnip Crinkle Virus in Arabidopsis. *The Plant Journal*, *45*(3), pp.320-334.

Chen, C.Y. and Heath, M.C., 1991. Cytological studies of the hypersensitive death of cowpea epidermal cells induced by basidiospore-derived infection by the cowpea rust fungus. *Canadian journal of botany*, *69*(6), pp.1199-1206.

Chen, W.P., Chen, P.D., Liu, D.J., Kynast, R., Friebe, B., Velazhahan, R., Muthukrishnan, S. and Gill, B.S., 1999. Development of wheat scab symptoms is delayed in transgenic wheat plants that constitutively express a rice thaumatin-like protein gene. *Theoretical and Applied Genetics*, *99*(5), pp.755-760.

Chen, H., Xue, L., Chintamanani, S., Germain, H., Lin, H., Cui, H., Cai, R., Zuo, J., Tang, X., Li, X. and Guo, H., 2009. ETHYLENE INSENSITIVE3 and ETHYLENE INSENSITIVE3-LIKE1 repress SALICYLIC ACID INDUCTION DEFICIENT2 expression to negatively regulate plant innate immunity in Arabidopsis. *The Plant Cell*, *21*(8), pp.2527-2540.

Chen, D., Cao, Y., Li, H., Kim, D., Ahsan, N., Thelen, J. and Stacey, G., 2017. Extracellular ATP elicits DORN1-mediated RBOHD phosphorylation to regulate stomatal aperture. *Nature communications*, *8*(1), p.2265.

Chini, A., Grant, J.J., Seki, M., Shinozaki, K. and Loake, G.J., 2004. Drought tolerance established by enhanced expression of the CC–NBS–LRR gene, ADR1, requires salicylic acid, EDS1 and ABI1. *The Plant Journal*, *38*(5), pp.810-822.

Chini, A., Fonseca, S., Fernandez, G., Adie, B., Chico, J.M., Lorenzo, O., Garcia-Casado, G., Lopez-Vidriero, I., Lozano, F.M., Ponce, M.R. and Micol, J.L., 2007. The JAZ family of repressors is the missing link in jasmonate signalling. *Nature*, *448*(7154), p.666.

Chivasa, S., Ndimba, B.K., Simon, W.J., Lindsey, K. and Slabas, A.R., 2005. Extracellular ATP functions as an endogenous external metabolite regulating plant cell viability. *The Plant Cell*, *17*(11), pp.3019-3034.

Chivasa, S., Murphy, A.M., Hamilton, J.M., Lindsey, K., Carr, J.P. and Slabas, A.R., 2009. Extracellular ATP is a regulator of pathogen defence in plants. *The Plant Journal*, *60*(3), pp.436-448.

Chivasa, S., Simon, W.J., Murphy, A.M., Lindsey, K., Carr, J.P. and Slabas, A.R., 2010. The effects of extracellular adenosine 5′□triphosphate on the tobacco proteome. *Proteomics*, *10*(2), pp.235-244.

Chivasa, S., Tome, D.F., Hamilton, J.M. and Slabas, A.R., 2011. Proteomic analysis of extracellular ATP-regulated proteins identifies ATP synthase β-subunit as a novel plant cell death regulator. *Molecular & Cellular Proteomics*, *10*(3), pp.M110-003905.

Choi, H.W., Kim, Y.J., Lee, S.C., Hong, J.K. and Hwang, B.K., 2007. Hydrogen peroxide generation by the pepper extracellular peroxidase CaPO2 activates local and systemic cell death and defense response to bacterial pathogens. *Plant physiology*, *145*(3), pp.890-904.

Choi, J., Tanaka, K., Liang, Y., Cao, Y., Lee, S.Y. and Stacey, G., 2014. Extracellular ATP, a danger signal, is recognized by DORN1 in Arabidopsis. *Biochemical Journal*, *463*(3), pp.429-437.

Choo, Y. and Klug, A., 1997. Physical basis of a protein-DNA recognition code. *Current opinion in structural biology*, *7*(1), pp.117-125.

Christian, M., Cermak, T., Doyle, E.L., Schmidt, C., Zhang, F., Hummel, A., Bogdanove, A.J. and Voytas, D.F., 2010. Targeting DNA double-strand breaks with TAL effector nucleases. *Genetics*, *186*(2), pp.757-761.

Christie, J.M., Reymond, P., Powell, G.K., Bernasconi, P., Raibekas, A.A., Liscum, E. and Briggs, W.R., 1998. Arabidopsis NPH1: a flavoprotein with the properties of a photoreceptor for phototropism. *Science*, *282*(5394), pp.1698-1701.

Christie, J.M., Salomon, M., Nozue, K., Wada, M. and Briggs, W.R., 1999. LOV (light, oxygen, or voltage) domains of the blue-light photoreceptor phototropin (nph1): binding sites for the chromophore flavin mononucleotide. *Proceedings of the National Academy of Sciences*, *96*(15), pp.8779-8783.

Chu, F.S. and Li, G.Y., 1994. Simultaneous occurrence of fumonisin B1 and other mycotoxins in moldy corn collected from the People's Republic of China in regions with high incidences of esophageal cancer. *Appl. Environ. Microbiol.*, *60*(3), pp.847-852.

Ciftci-Yilmaz, S. and Mittler, R., 2008. The zinc finger network of plants. *Cellular and Molecular Life Sciences*, *65*(7-8), pp.1150-1160.

Clack, T., Mathews, S. and Sharrock, R.A., 1994. The phytochrome apoprotein family in Arabidopsis is encoded by five genes: the sequences and expression of PHYD and PHYE. *Plant molecular biology*, *25*(3), pp.413-427.

Clark, K.L., Larsen, P.B., Wang, X. and Chang, C., 1998. Association of the Arabidopsis CTR1 Raf-like kinase with the ETR1 and ERS ethylene receptors. *Proceedings of the National Academy of Sciences*, *95*(9), pp.5401-5406.

Clark, G., Fraley, D., Steinebrunner, I., Cervantes, A., Onyirimba, J., Liu, A., Torres, J., Tang, W., Kim, J. and Roux, S.J., 2011. Extracellular nucleotides and apyrases regulate stomatal aperture in Arabidopsis. *Plant physiology*, *156*(4), pp.1740-1753.

Clarke, J.D., Aarts, N., Feys, B.J., Dong, X. and Parker, J.E., 2001. Constitutive disease resistance requires EDS1 in the Arabidopsis mutants cpr1 and cpr6 and is partially EDS1□dependent in cpr5. *The Plant Journal*, *26*(4), pp.409-420.

Cleland, C.F. and Ajami, A., 1974. Identification of the flower-inducing factor isolated from aphid honeydew as being salicylic acid. *Plant Physiology*, *54*(6), pp.904-906.

Clementi, E., Brown, G.C., Feelisch, M. and Moncada, S., 1998. Persistent inhibition of cell respiration by nitric oxide: crucial role of S-nitrosylation of mitochondrial complex I and protective action of glutathione. *Proceedings of the National Academy of Sciences*, *95*(13), pp.7631-7636.

Colvin, B.M. and Harrison, L.R., 1992. Fumonisin-induced pulmonary edema and hydrothorax in swine. *Mycopathologia*, *117*(1-2), pp.79-82.

Costanzi, J., Sidransky, D., Navon, A. and Goldsweig, H., 2005. Ribonucleases as a novel pro-apoptotic anticancer strategy: review of the preclinical and clinical data for ranpirnase. *Cancer investigation*, *23*(7), pp.643-650.

Curtis, R.W., 1984. Abscission-inducing properties of methyl jasmonate, ABA, and ABA-methyl ester and their interactions with ethephon, AgNO3, and malformin. *Journal of Plant Growth Regulation*, *3*(1-4), p.157.

D

D'Ovidio, R., Mattei, B., Roberti, S. and Bellincampi, D., 2004. Polygalacturonases, polygalacturonase-inhibiting proteins and pectic oligomers in plant–pathogen interactions. *Biochimica et Biophysica Acta (BBA)-Proteins and Proteomics*, *1696*(2), pp.237-244.

Dangl, J.L. and Jones, J.D., 2001. Plant pathogens and integrated defence responses to infection. *nature*, *411*(6839), p.826.

Dat, J.F., Lopez-Delgado, H., Foyer, C.H. and Scott, I.M., 2000. Effects of salicylic acid on oxidative stress and thermotolerance in tobacco. *Journal of Plant Physiology*, *156*(5-6), pp.659-665.

Dark, A., Demidchik, V., Richards, S.L., Shabala, S. and Davies, J.M., 2011. Release of extracellular purines from plant roots and effect on ion fluxes. *Plant signaling & behavior*, *6*(11), pp.1855-1857.

Dathe, W., Rönsch, H., Preiss, A., Schade, W., Sembdner, G. and Schreiber, K., 1981. Endogenous plant hormones of the broad bean, Vicia faba L.(-)-jasmonic acid, a plant growth inhibitor in pericarp. *Planta*, *153*(6), pp.530-535.

Davletova, S., Schlauch, K., Coutu, J. and Mittler, R., 2005. The zinc-finger protein Zat12 plays a central role in reactive oxygen and abiotic stress signaling in Arabidopsis. *Plant physiology*, *139*(2), pp.847-856.

De Torres Zabala, M., Bennett, M.H., Truman, W.H. and Grant, M.R., 2009. Antagonism between salicylic and abscisic acid reflects early host–pathogen conflict and moulds plant defence responses. *The Plant Journal*, *59*(3), pp.375-386.

De Vos, M., Van Oosten, V.R., Van Poecke, R.M., Van Pelt, J.A., Pozo, M.J., Mueller, M.J., Buchala, A.J., Métraux, J.P., Van Loon, L.C., Dicke, M. and Pieterse, C.M., 2005. Signal signature and transcriptome changes of Arabidopsis during pathogen and insect attack. *Molecular plant-microbe interactions*, *18*(9), pp.923-937.

Del Río, L.A. and López-Huertas, E., 2016. ROS generation in peroxisomes and its role in cell signaling. *Plant and Cell Physiology*, *57*(7), pp.1364-1376.

Delaney, T.P., Uknes, S., Vernooij, B., Friedrich, L., Weymann, K., Negrotto, D., Gaffney, T., Gut-Rella, M., Kessmann, H., Ward, E. and Ryals, J., 1994. A central role of salicylic acid in plant disease resistance. *Science*, *266*(5188), pp.1247-1250.

Demidchik, V., Shang, Z., Shin, R., Thompson, E., Rubio, L., Laohavisit, A., Mortimer, J.C., Chivasa, S., Slabas, A.R., Glover, B.J. and Schachtman, D.P., 2009. Plant extracellular ATP signalling by plasma membrane NADPH oxidase and Ca2+ channels. *The Plant Journal*, *58*(6), pp.903-913.

Dempsey, D.M.A., Shah, J. and Klessig, D.F., 1999. Salicylic acid and disease resistance in plants. *Critical Reviews in Plant Sciences*, *18*(4), pp.547-575.

Denecke, J., De Rycke, R. and Botterman, J., 1992. Plant and mammalian sorting signals for protein retention in the endoplasmic reticulum contain a conserved epitope. *The EMBO journal*, *11*(6), pp.2345-2355.

Desai, K., Sullards, M.C., Allegood, J., Wang, E., Schmelz, E.M., Hartl, M., Humpf, H.U., Liotta, D.C., Peng, Q. and Merrill Jr, A.H., 2002. Fumonisins and fumonisin analogs as inhibitors of ceramide synthase and inducers of apoptosis. *Biochimica et Biophysica Acta (BBA)-Molecular and Cell Biology of Lipids*, *1585*(2-3), pp.188-192.

Deshpande, R.A. and Shankar, V., 2002. Ribonucleases from T2 family. *Critical reviews in microbiology*, *28*(2), pp.79-122.

Desjardins, A.E., Plattner, R.D., Nelsen, T.C. and Leslie, J.F., 1995. Genetic analysis of fumonisin production and virulence of Gibberella fujikuroi mating population A (Fusarium moniliforme) on maize (Zea mays) seedlings. *Appl. Environ. Microbiol.*, *61*(1), pp.79-86.

Desjardins, A.E., Munkvold, G.P., Plattner, R.D. and Proctor, R.H., 2002. FUM1—a gene required for fumonisin biosynthesis but not for maize ear rot and ear infection by Gibberella moniliformis in field tests. *Molecular Plant-Microbe Interactions*, *15*(11), pp.1157-1164.

Desmond, O.J., Manners, J.M., Stephens, A.E., Maclean, D.J., Schenk, P.M., Gardiner, D.M., Munn, A.L. and Kazan, K., 2008. The Fusarium mycotoxin deoxynivalenol elicits hydrogen peroxide production, programmed cell death and defence responses in wheat. *Molecular Plant Pathology*, *9*(4), pp.435-445.

Díaz, J., Bernal, A., Pomar, F. and Merino, F., 2001. Induction of shikimate dehydrogenase and peroxidase in pepper (Capsicum annuum L.) seedlings in response to copper stress and its relation to lignification. *Plant Science*, *161*(1), pp.179-188.

Diepold, A. and Wagner, S., 2014. Assembly of the bacterial type III secretion machinery. *FEMS microbiology reviews*, *38*(4), pp.802-822.

Dietz, K.J., Baier, M. and Krämer, U., 1999. Free radicals and reactive oxygen species as mediators of heavy metal toxicity in plants. In *Heavy metal stress in plants* (pp. 73-97). Springer, Berlin, Heidelberg.

Dietrich, R.A., Richberg, M.H., Schmidt, R., Dean, C. and Dangl, J.L., 1997. A novel zinc finger protein is encoded by the Arabidopsis LSD1 gene and functions as a negative regulator of plant cell death. *Cell*, *88*(5), pp.685-694.

Dinesh-Kumar, S.P., Tham, W.H. and Baker, B.J., 2000. Structure–function analysis of the tobacco mosaic virus resistance gene N. *Proceedings of the National Academy of Sciences*, *97*(26), pp.14789-14794.

Ding, Y., Sun, T., Ao, K., Peng, Y., Zhang, Y., Li, X. and Zhang, Y., 2018. Opposite roles of salicylic acid receptors NPR1 and NPR3/NPR4 in transcriptional regulation of plant immunity. *Cell*, *173*(6), pp.1454-1467.

Domínguez, F., González, M. and Cejudo, F.J., 2002. A germination-related gene encoding a serine carboxypeptidase is expressed during the differentiation of the vascular tissue in wheat grains and seedlings. *Planta*, *215*(5), pp.727-734.

Du, Z., Zhou, X., Ling, Y., Zhang, Z. and Su, Z., 2010. agriGO: a GO analysis toolkit for the agricultural community. *Nucleic acids research*, *38*(suppl_2), pp.W64-W70.

Duek, P.D. and Fankhauser, C., 2005. bHLH class transcription factors take centre stage in phytochrome signalling. *Trends in plant science*, *10*(2), pp.51-54.

Dunning, F.M., Sun, W., Jansen, K.L., Helft, L. and Bent, A.F., 2007. Identification and mutational analysis of Arabidopsis FLS2 leucine-rich repeat domain residues that contribute to flagellin perception. *The Plant Cell*, *19*(10), pp.3297-3313

Durner, J., Wendehenne, D. and Klessig, D.F., 1998. Defense gene induction in tobacco by nitric oxide, cyclic GMP, and cyclic ADP-ribose. *Proceedings of the National Academy of Sciences*, *95*(17), pp.10328-10333.

Dutta, A.K., Okada, Y. and Sabirov, R.Z., 2002. Regulation of an ATP□conductive large□ conductance anion channel and swelling□induced ATP release by arachidonic acid. *The Journal of physiology*, *542*(3), pp.803-816.

E

Edelweiss, E., Balandin, T.G., Ivanova, J.L., Lutsenko, G.V., Leonova, O.G., Popenko, V.I., Sapozhnikov, A.M. and Deyev, S.M., 2008. Barnase as a new therapeutic agent triggering apoptosis in human cancer cells. *PloS one*, *3*(6), p.e2434.

Elbaz, M., Avni, A. and Weil, M., 2002. Constitutive caspase-like machinery executes programmed cell death in plant cells. *Cell death and differentiation*, *9*(7), p.726.

Ellis, R.E., Yuan, J. and Horvitz, H.R., 1991. Mechanisms and functions of cell death. *Annual review of cell biology*, *7*(1), pp.663-698.

Englbrecht, C.C., Schoof, H. and Böhm, S., 2004. Conservation, diversification and expansion of C2H2 zinc finger proteins in the *Arabidopsis thaliana* genome. *BMC genomics*, *5*(1), p.39.

F

Falcão, V.C.A., Ono, M.A., de Ávila Miguel, T., Vizoni, E., Hirooka, E.Y. and Ono, E.Y.S., 2011. Fusarium verticillioides: evaluation of fumonisin production and effect of fungicides on in vitro inhibition of mycelial growth. *Mycopathologia*, *171*(1), pp.77-84.

Falkenstein, E., Groth, B., Mithöfer, A. and Weiler, E.W., 1991. Methyljasmonate and α-linolenic acid are potent inducers of tendril coiling. *Planta*, *185*(3), pp.316-322.

Fao.org. (2019). *Cereals & Grains | Inpho | Food and Agriculture Organization of the United Nations*. [online] Available at: http://www.fao.org/in-action/inpho/crop-compendium/cereals-grains/en/ [Accessed 28 Mar. 2019].

Ferro, M., Salvi, D., Brugière, S., Miras, S., Kowalski, S., Louwagie, M., Garin, J., Joyard, J. and Rolland, N., 2003. Proteomics of the chloroplast envelope membranes from *Arabidopsis thaliana*. *Molecular & Cellular Proteomics*, *2*(5), pp.325-345.

Feys, B.J., Moisan, L.J., Newman, M.A. and Parker, J.E., 2001. Direct interaction between the Arabidopsis disease resistance signaling proteins, EDS1 and PAD4. *The EMBO journal*, *20*(19), pp.5400-5411.

Fields, K.A., Plano, G.V. and Straley, S.C., 1994. A low-Ca2+ response (LCR) secretion (ysc) locus lies within the lcrB region of the LCR plasmid in Yersinia pestis. *Journal of bacteriology*, *176*(3), pp.569-579.

Flors, V., Ton, J., Van Doorn, R., Jakab, G., García□Agustín, P. and Mauch□Mani, B., 2008. Interplay between JA, SA and ABA signalling during basal and induced resistance against Pseudomonas syringae and Alternaria brassicicola. *The Plant Journal*, *54*(1), pp.81-92.

Foreman, J., Demidchik, V., Bothwell, J.H., Mylona, P., Miedema, H., Torres, M.A., Linstead, P., Costa, S., Brownlee, C., Jones, J.D. and Davies, J.M., 2003. Reactive oxygen species produced by NADPH oxidase regulate plant cell growth. *Nature*, *422*(6930), p.442.

Foresi, N.P., Laxalt, A.M., Tonón, C.V., Casalongué, C.A. and Lamattina, L., 2007. Extracellular ATP induces nitric oxide production in tomato cell suspensions. *Plant Physiology*, *145*(3), pp.589-592.

Fotso, J., Leslie, J.F. and Smith, J.S., 2002. Production of beauvericin, moniliformin, fusaproliferin, and fumonisins B1, B2, and B3 by fifteen ex-type strains of Fusarium species. *Appl. Environ. Microbiol.*, *68*(10), pp.5195-5197.

Frac.info. (2019). *FRAC | Definition of fungicide resistance*. [online] Available at: http://www.frac.info/resistance-overview/what-is-resistance- [Accessed 28 Mar. 2019].

Franklin-Tong, N.V. and Franklin, F.C.H., 2003. Gametophytic self-incompatibility inhibits pollen tube growth using different mechanisms. *Trends in plant science*, *8*(12), pp.598-605.

Freeman, J.L., Garcia, D., Kim, D., Hopf, A. and Salt, D.E., 2005. Constitutively elevated salicylic acid signals glutathione-mediated nickel tolerance in Thlaspi nickel hyperaccumulators. *Plant physiology*, *137*(3), pp.1082-1091.

Freytag, S., Arabatzis, N., Hahlbrock, K. and Schmelzer, E., 1994. Reversible cytoplasmic rearrangements precede wall apposition, hypersensitive cell death and defense-related gene activation in potato/Phytophthora infestans interactions. *Planta*, *194*(1), pp.123-135.

Fu, Z.Q., Yan, S., Saleh, A., Wang, W., Ruble, J., Oka, N., Mohan, R., Spoel, S.H., Tada, Y., Zheng, N. and Dong, X., 2012. NPR3 and NPR4 are receptors for the immune signal salicylic acid in plants. *Nature*, *486*(7402), p.228.

Fuchs, Y., Saxena, A., Gamble, H.R. and Anderson, J.D., 1989. Ethylene biosynthesis-inducing protein from cellulysin is an endoxylanase. *Plant Physiology*, *89*(1), pp.138-143.

Furihata, T., Maruyama, K., Fujita, Y., Umezawa, T., Yoshida, R., Shinozaki, K. and Yamaguchi-Shinozaki, K., 2006. Abscisic acid-dependent multisite phosphorylation regulates the activity of a transcription activator AREB1. *Proceedings of the National Academy of Sciences*, *103*(6), pp.1988-1993.

Furuya, M., 1993. Phytochromes: their molecular species, gene families, and functions. *Annual review of plant biology*, *44*(1), pp.617-645.

Futerman, A.H., 1995. Inhibition of sphingolipid synthesis: effects on glycosphingolipid—GPI-anchored protein microdomains. *Trends in cell biology*, *5*(10), pp.377-380.

G

Gaffney, T., Friedrich, L., Vernooij, B., Negrotto, D., Nye, G., Uknes, S., Ward, E., Kessmann, H. and Ryals, J., 1993. Requirement of salicylic acid for the induction of systemic acquired resistance. *Science*, *261*(5122), pp.754-756.

Gallego-Giraldo, L., Escamilla-Trevino, L., Jackson, L.A. and Dixon, R.A., 2011. Salicylic acid mediates the reduced growth of lignin down-regulated plants. *Proceedings of the National Academy of Sciences*, *108*(51), pp.20814-20819.

Gao, M. and Showalter, A.M., 1999. Yariv reagent treatment induces programmed cell death in Arabidopsis cell cultures and implicates arabinogalactan protein involvement. *The Plant Journal*, *19*(3), pp.321-331.

Gao, Z., Sarsour, E.H., Kalen, A.L., Li, L., Kumar, M.G. and Goswami, P.C., 2008. Late ROS accumulation and radiosensitivity in SOD1-overexpressing human glioma cells. *Free Radical Biology and Medicine*, *45*(11), pp.1501-1509.

García-Mata, C. and Lamattina, L., 2001. Nitric oxide induces stomatal closure and enhances the adaptive plant responses against drought stress. *Plant Physiology*, *126*(3), pp.1196-1204.

Ge, X., Dietrich, C., Matsuno, M., Li, G., Berg, H. and Xia, Y., 2005. An Arabidopsis aspartic protease functions as an anti□cell□death component in reproduction and embryogenesis. *EMBO reports*, *6*(3), pp.282-288.

Gechev, T.S., Gadjev, I., Van Breusegem, F., Inzé, D., Dukiandjiev, S., Toneva, V. and Minkov, I., 2002. Hydrogen peroxide protects tobacco from oxidative stress by inducing a set of antioxidant enzymes. *Cellular and Molecular Life Sciences CMLS*, *59*(4), pp.708-714.

Gechev, T.S., Gadjev, I.Z. and Hille, J., 2004. An extensive microarray analysis of AAL-toxin-induced cell death in *Arabidopsis thaliana* brings new insights into the complexity of programmed cell death in plants. *Cellular and Molecular Life Sciences CMLS*, *61*(10), pp.1185-1197.

Gechev, T.S., Van Breusegem, F., Stone, J.M., Denev, I. and Laloi, C., 2006. Reactive oxygen species as signals that modulate plant stress responses and programmed cell death. *Bioessays*, *28*(11), pp.1091-1101.

Gelineau-van Waes, J., Starr, L., Maddox, J., Aleman, F., Voss, K.A., Wilberding, J. and Riley, R.T., 2005. Maternal fumonisin exposure and risk for neural tube defects: mechanisms in an in vivo mouse model. *Birth Defects Research Part A: Clinical and Molecular Teratology*, *73*(7), pp.487-497.

Geng, X., Shen, M., Kim, J.H. and Mackey, D., 2016. The Pseudomonas syringae type III effectors AvrRpm1 and AvrRpt2 promote virulence dependent on the F-box protein COI1. *Plant cell reports*, *35*(4), pp.921-932.

Genoud, T., Millar, A.J., Nishizawa, N., Kay, S.A., Schäfer, E., Nagatani, A. and Chua, N.H., 1998. An Arabidopsis mutant hypersensitive to red and far-red light signals. *The Plant Cell*, *10*(6), pp.889-904.

Genoud, T., Buchala, A.J., Chua, N.H. and Métraux, J.P., 2002. Phytochrome signalling modulates the SA-perceptive pathway in Arabidopsis. *The Plant Journal*, *31*(1), pp.87-95.

Gierasch, L.M., 1989. Signal sequences. *Biochemistry*, *28*(3), pp.923-930.

Gilchrist, D.G., Bostock, R.M. and Wang, H., 1995. Sphingosine-related mycotoxins in plant and animal diseases. *Canadian journal of botany*, *73*(S1), pp.459-467.

Gilchrist, D.G., 1997. Mycotoxins reveal connections between plants and animals in apoptosis and ceramide signaling. *Cell death and differentiation*, *4*(8), p.689.

Gish, W. and States, D.J., 1993. Identification of protein coding regions by database similarity search. *Nature genetics*, *3*(3), p.266.

Glazebrook, J. and Ausubel, F.M., 1994. Isolation of phytoalexin-deficient mutants of *Arabidopsis thaliana* and characterization of their interactions with bacterial pathogens. *Proceedings of the National Academy of Sciences*, *91*(19), pp.8955-8959.

Glazebrook, J., Rogers, E.E. and Ausubel, F.M., 1996. Isolation of Arabidopsis mutants with enhanced disease susceptibility by direct screening. *Genetics*, *143*(2), pp.973-982.

Glazebrook, J., Zook, M., Mert, F., Kagan, I., Rogers, E.E., Crute, I.R., Holub, E.B., Hammerschmidt, R. and Ausubel, F.M., 1997. Phytoalexin-deficient mutants of Arabidopsis reveal that PAD4 encodes a regulatory factor and that four PAD genes contribute to downy mildew resistance. *Genetics*, *146*(1), pp.381-392.

Glazebrook, J., Chen, W., Estes, B., Chang, H.S., Nawrath, C., Métraux, J.P., Zhu, T. and Katagiri, F., 2003. Topology of the network integrating salicylate and jasmonate signal transduction derived from global expression phenotyping. *The Plant Journal*, *34*(2), pp.217-228.

Glazebrook, J., 2005. Contrasting mechanisms of defense against biotrophic and necrotrophic pathogens. *Annu. Rev. Phytopathol.*, *43*, pp.205-227.

Glenn, A.E., Zitomer, N.C., Zimeri, A.M., Williams, L.D., Riley, R.T. and Proctor, R.H., 2008. Transformation-mediated complementation of a FUM gene cluster deletion in Fusarium verticillioides restores both fumonisin production and pathogenicity on maize seedlings. *Molecular plant-microbe interactions*, *21*(1), pp.87-97.

Gómez□Gómez, L., Felix, G. and Boller, T., 1999. A single locus determines sensitivity to bacterial flagellin in *Arabidopsis thaliana*. *The Plant Journal*, *18*(3), pp.277-284.

Gordon, J.L., 1986. Extracellular ATP: effects, sources and fate. *Biochemical Journal*, *233*(2), p.309.

Grant, J.J. and Loake, G.J., 2000. Role of reactive oxygen intermediates and cognate redox signaling in disease resistance. *Plant physiology*, *124*(1), pp.21-30.

Gray, J.E., McClure, B.A., Bonig, I., Anderson, M.A. and Clarke, A.E., 1991. Action of the style product of the self-incompatibility gene of Nicotiana alata (S-RNase) on in vitro-grown pollen tubes. *The Plant Cell*, *3*(3), pp.271-283.

Green, P.J., 1994. The ribonucleases of higher plants. *Annual review of plant biology*, *45*(1), pp.421-445.

Grennan, A.K., 2006. Genevestigator. Facilitating web-based gene-expression analysis. *Plant physiology*, *141*(4), pp.1164-1166.

Griebel, T. and Zeier, J., 2008. Light regulation and daytime dependency of inducible plant defenses in Arabidopsis: phytochrome signaling controls systemic acquired resistance rather than local defense. *Plant physiology*, *147*(2), pp.790-801.

Griffiths, A.J., Wessler, S.R., Lewontin, R.C., Gelbart, W.M., Suzuki, D.T. and Miller, J.H., 2005. *An introduction to genetic analysis*. Macmillan.

Groß, N., Wasternack, C. and Köck, M., 2004. Wound-induced RNaseLE expression is jasmonate and systemin independent and occurs only locally in tomato (Lycopersicon esculentum cv. Lukullus). *Phytochemistry*, *65*(10), pp.1343-1350.

Groth, S.F.D.S., Webster, R.G. and Datyner, A., 1963. Two new staining procedures for quantitative estimation of proteins on electrophoretic strips. *Biochimica et biophysica acta*, *71*, pp.377-391.

Guan, L. and Scandalios, J.G., 1995. Developmentally related responses of maize catalase genes to salicylic acid. *Proceedings of the National Academy of Sciences*, *92*(13), pp.5930-5934.

Guo, X. and Stotz, H.U., 2010. ABA signaling inhibits oxalate-induced production of reactive oxygen species and protects against Sclerotinia sclerotiorum in *Arabidopsis thaliana*. *European journal of plant pathology*, *128*(1), pp.7-19.

H

Hakomori, S.I. and Igarashi, Y., 1995. Functional role of glycosphingolipids in cell recognition and signaling. *The journal of biochemistry*, *118*(6), pp.1091-1103.

Halliwell, B., 2006. Oxidative stress and neurodegeneration: where are we now?. *Journal of neurochemistry*, *97*(6), pp.1634-1658.

Hameed, A., Goher, M. and Iqbal, N., 2013. Drought induced programmed cell death and associated changes in antioxidants, proteases, and lipid peroxidation in wheat leaves. *Biologia plantarum*, *57*(2), pp.370-374.

Hannun, Y.A. and Bell, R.M., 1989. Functions of sphingolipids and sphingolipid breakdown products in cellular regulation. *Science*, *243*(4890), pp.500-507.

Hao, D., Chao, M., Yin, Z. and Yu, D., 2012. Genome-wide association analysis detecting significant single nucleotide polymorphisms for chlorophyll and chlorophyll fluorescence parameters in soybean (Glycine max) landraces. *Euphytica*, *186*(3), pp.919-931.

He, Z., Wang, Z.Y., Li, J., Zhu, Q., Lamb, C., Ronald, P. and Chory, J., 2000. Perception of brassinosteroids by the extracellular domain of the receptor kinase BRI1. *Science*, *288*(5475), pp.2360-2363.

He, Y., Fukushige, H., Hildebrand, D.F. and Gan, S., 2002. Evidence supporting a role of jasmonic acid in Arabidopsis leaf senescence. *Plant physiology*, *128*(3), pp.876-884.

He, Y. and Gan, S., 2002. A gene encoding an acyl hydrolase is involved in leaf senescence in Arabidopsis. *The Plant Cell*, *14*(4), pp.805-815.

He, K., Gou, X., Yuan, T., Lin, H., Asami, T., Yoshida, S., Russell, S.D. and Li, J., 2007. BAK1 and BKK1 regulate brassinosteroid-dependent growth and brassinosteroid-independent cell-death pathways. *Current Biology*, *17*(13), pp.1109-1115.

Heath, M.C., 2000. Hypersensitive response-related death. In *Programmed cell death in higher plants* (pp. 77-90). Springer, Dordrecht.

Henzler, T. and Steudle, E., 2000. Transport and metabolic degradation of hydrogen peroxide in Chara corallina: model calculations and measurements with the pressure probe suggest transport of H2O2 across water channels. *Journal of experimental botany*, *51*(353), pp.2053-2066.

Herman, E.M. and Lamb, C.J., 1992. Arabinogalactan-rich glycoproteins are localized on the cell surface and in intravacuolar multivesicular bodies. *Plant Physiology*, *98*(1), pp.264-272.

Herrmann, K.M. and Weaver, L.M., 1999. The shikimate pathway. *Annual review of plant biology*, *50*(1), pp.473-503.

Hervé, C., Serres, J., Dabos, P., Canut, H., Barre, A., Rougé, P. and Lescure, B., 1999. Characterization of the Arabidopsis lecRK-a genes: members of a superfamily encoding putative receptors with an extracellular domain homologous to legume lectins. *Plant molecular biology*, *39*(4), pp.671-682.

Hillwig, M.S., LeBrasseur, N.D., Green, P.J. and MacIntosh, G.C., 2008. Impact of transcriptional, ABA-dependent, and ABA-independent pathways on wounding regulation of RNS1 expression. *Molecular Genetics and Genomics*, *280*(3), p.249.

Hillwig, M.S., Contento, A.L., Meyer, A., Ebany, D., Bassham, D.C. and MacIntosh, G.C., 2011. RNS2, a conserved member of the RNase T2 family, is necessary for ribosomal RNA decay in plants. *Proceedings of the National Academy of Sciences*, *108*(3), pp.1093-1098.

Hirata, T., Kimishima, E., Aoki, T., Nirenberg, H.I. and O'Donnell, K., 2001. Morphological and molecular characterization of Fusarium verticillioides from rotten banana imported into Japan. *Mycoscience*, *42*(2), pp.155-166.

Hiratsu, K., Ohta, M., Matsui, K. and Ohme-Takagi, M., 2002. The SUPERMAN protein is an active repressor whose carboxy□terminal repression domain is required for the development of normal flowers. *FEBS letters*, *514*(2-3), pp.351-354.

Horton, P., 1989. Interactions between electron transport and carbon assimilation: regulation of light-harvesting and photochemistry. *Plant biology (USA)*.

Howe, G.A. and Jander, G., 2008. Plant immunity to insect herbivores. *Annu. Rev. Plant Biol.*, *59*, pp.41-66.

Hruz, T., Laule, O., Szabo, G., Wessendorp, F., Bleuler, S., Oertle, L., Widmayer, P., Gruissem, W. and Zimmermann, P., 2008. Genevestigator v3: a reference expression database for the meta-analysis of transcriptomes. *Advances in bioinformatics*, *2008*.

Hua, J. and Meyerowitz, E.M., 1998. Ethylene responses are negatively regulated by a receptor gene family in *Arabidopsis thaliana*. *Cell*, *94*(2), pp.261-271.

Huala, E., Oeller, P.W., Liscum, E., Han, I.S., Larsen, E. and Briggs, W.R., 1997. Arabidopsis NPH1: a protein kinase with a putative redox-sensing domain. *Science*, *278*(5346), pp.2120-2123.

Huang, S., Lee, H.S., Karunanandaa, B. and Kao, T.H., 1994. Ribonuclease activity of Petunia inflata S proteins is essential for rejection of self-pollen. *The Plant Cell*, *6*(7), pp.1021-1028.

Hueck, C.J., 1998. Type III protein secretion systems in bacterial pathogens of animals and plants. *Microbiology and molecular biology reviews*, *62*(2), pp.379-433.

Huffaker, A. and Ryan, C.A., 2007. Endogenous peptide defense signals in Arabidopsis differentially amplify signaling for the innate immune response. *Proceedings of the National Academy of Sciences*, *104*(25), pp.10732-10736

Huffaker, A., Pearce, G. and Ryan, C.A., 2006. An endogenous peptide signal in Arabidopsis activates components of the innate immune response. *Proceedings of the National Academy of Sciences*, *103*(26), pp.10098-10103

Huq, E., Al-Sady, B., Hudson, M., Kim, C., Apel, K. and Quail, P.H., 2004. Phytochrome-interacting factor 1 is a critical bHLH regulator of chlorophyll biosynthesis. *Science*, *305*(5692), pp.1937-1941.

Huq, E. and Quail, P.H., 2002. PIF4, a phytochrome□interacting bHLH factor, functions as a negative regulator of phytochrome B signaling in Arabidopsis. *The EMBO journal*, *21*(10), pp.2441-2450.

Hyde, S.C., Emsley, P., Hartshorn, M.J., Mimmack, M.M., Gileadi, U., Pearce, S.R., Gallagher, M.P., Gill, D.R., Hubbard, R.E. and Higgins, C.F., 1990. Structural model of ATP-binding proteing associated with cystic fibrosis, multidrug resistance and bacterial transport. *Nature*, *346*(6282), p.362.

I

Imeson, A., 2012. *Desertification, land degradation and sustainability*. John Wiley & Sons.

Innes, R., 2018. The Positives and Negatives of NPR: A Unifying Model for Salicylic Acid Signaling in Plants. *Cell*, *173*(6), pp.1314-1315.

Iordanov, M.S., Ryabinina, O.P., Wong, J., Dinh, T.H., Newton, D.L., Rybak, S.M. and Magun, B.E., 2000. Molecular determinants of apoptosis induced by the cytotoxic ribonuclease onconase: evidence for cytotoxic mechanisms different from inhibition of protein synthesis. *Cancer Research*, *60*(7), pp.1983-1994.

Irie, M., 1999. Structure-function relationships of acid ribonucleases: lysosomal, vacuolar, and periplasmic enzymes. *Pharmacology & therapeutics*, *81*(2), pp.77-89.

Ishii, H. and Holloman, D.W., 2015. Fungicide resistance in plant pathogens. *Tokyo: Springer, doi*, *10*, pp.978-4.

J

Janda, T., Szalai, G., Tari, I. and Paldi, E., 1999. Hydroponic treatment with salicylic acid decreases the effects of chilling injury in maize (Zea mays L.) plants. *Planta*, *208*(2), pp.175-180.

Jirage, D., Zhou, N., Cooper, B., Clarke, J.D., Dong, X. and Glazebrook, J., 2001. Constitutive salicylic acid□dependent signaling in cpr1 and cpr6 mutants requires PAD4. *The Plant Journal*, *26*(4), pp.395-407.

Jones, J.D. and Dangl, J.L., 2006. The plant immune system. *Nature*, *444*(7117), p.323.

Johnson, K.L., Jones, B.J., Bacic, A. and Schultz, C.J., 2003. The fasciclin-like arabinogalactan proteins of Arabidopsis. A multigene family of putative cell adhesion molecules. *Plant physiology*, *133*(4), pp.1911-1925.

Ju, C., Yoon, G.M., Shemansky, J.M., Lin, D.Y., Ying, Z.I., Chang, J., Garrett, W.M., Kessenbrock, M., Groth, G., Tucker, M.L. and Cooper, B., 2012. CTR1 phosphorylates the central regulator EIN2 to control ethylene hormone signaling from the ER membrane to the nucleus in Arabidopsis. *Proceedings of the National Academy of Sciences*, *109*(47), pp.19486-19491.

K

Kaffarnik, F.A., Jones, A.M., Rathjen, J.P. and Peck, S.C., 2009. Effector proteins of the bacterial pathogen Pseudomonas syringae alter the extracellular proteome of the host plant, *Arabidopsis thaliana*. *Molecular & cellular proteomics*, *8*(1), pp.145-156.

Kaliff, M., Staal, J., Myrenås, M. and Dixelius, C., 2007. ABA is required for Leptosphaeria maculans resistance via ABI1-and ABI4-dependent signaling. *Molecular plant-microbe interactions*, *20*(4), pp.335-345.

Kang, H.M. and Saltveit, M.E., 2002. Effect of chilling on antioxidant enzymes and DPPH□radical scavenging activity of high□and low□vigour cucumber seedling radicles. *Plant, Cell & Environment*, *25*(10), pp.1233-1238.

Karlova, R., Boeren, S., Russinova, E., Aker, J., Vervoort, J. and de Vries, S., 2006. The Arabidopsis somatic embryogenesis receptor-like kinase1 protein complex includes brassinosteroid-insensitive1. *The Plant Cell*, *18*(3), pp.626-638.

Karpinski, S., Reynolds, H., Karpinska, B., Wingsle, G., Creissen, G. and Mullineaux, P., 1999. Systemic signaling and acclimation in response to excess excitation energy in Arabidopsis. *Science*, *284*(5414), pp.654-657.

Karpinski, S., Szechynska-hebda, Magdalena, Wituszynska, W. and Burdiak, P., 2013. Light acclimation, retrograde signalling, cell death and immune defences in plants. *Plant, cell & environment*, *36*(4), pp.736-744.

Kauss, H., Fauth, M., Merten, A. and Jeblick, W., 1999. Cucumber hypocotyls respond to cutin monomers via both an inducible and a constitutive H2O2-generating system. *Plant physiology*, *120*(4), pp.1175-1182

Kawasaki, T., Henmi, K., Ono, E., Hatakeyama, S., Iwano, M., Satoh, H. and Shimamoto, K., 1999. The small GTP-binding protein Rac is a regulator of cell death in plants. *Proceedings of the National Academy of Sciences*, *96*(19), pp.10922-10926.

Kayes, J.M. and Clark, S.E., 1998. CLAVATA2, a regulator of meristem and organ development in Arabidopsis. *Development*, *125*(19), pp.3843-3851.

Keller, T., Damude, H.G., Werner, D., Doerner, P., Dixon, R.A. and Lamb, C., 1998. A plant homolog of the neutrophil NADPH oxidase gp91phox subunit gene encodes a plasma membrane protein with Ca2+ binding motifs. *The Plant Cell*, *10*(2), pp.255-266.

Kennedy, C. and Burnstock, G., 1985. ATP produces vasodilation via P1 purinoceptors and vasoconstriction via P2 purinoceptors in the isolated rabbit central ear artery. *Journal of Vascular Research*, *22*(3), pp.145-155.

Khakh, B.S. and North, R.A., 2006. P2X receptors as cell-surface ATP sensors in health and disease. *Nature*, *442*(7102), p.527.

Khanna, R., Huq, E., Kikis, E.A., Al-Sady, B., Lanzatella, C. and Quail, P.H., 2004. A novel molecular recognition motif necessary for targeting photoactivated phytochrome signaling to specific basic helix-loop-helix transcription factors. *The Plant Cell*, *16*(11), pp.3033-3044.

Kieber, J.J., Rothenberg, M., Roman, G., Feldmann, K.A. and Ecker, J.R., 1993. CTR1, a negative regulator of the ethylene response pathway in Arabidopsis, encodes a member of the raf family of protein kinases. *Cell*, *72*(3), pp.427-441.

Kim, W.Y., Fujiwara, S., Suh, S.S., Kim, J., Kim, Y., Han, L., David, K., Putterill, J., Nam, H.G. and Somers, D.E., 2007. ZEITLUPE is a circadian photoreceptor stabilized by GIGANTEA in blue light. *Nature*, *449*(7160), p.356.

Kim, S.H., Yang, S.H., Kim, T.J., Han, J.S. and Suh, J.W., 2009. Hypertonic stress increased extracellular ATP levels and the expression of stress-responsive genes in *Arabidopsis thaliana* seedlings. *Bioscience, biotechnology, and biochemistry*, *73*(6), pp.1252-1256.

Kim, S.G., Kim, S.T., Wang, Y., Yu, S., Choi, I.S., Kim, Y.C., Kim, W.T., Agrawal, G.K., Rakwal, R. and Kang, K.Y., 2011. The RNase activity of rice probenazole-induced protein1 (PBZ1) plays a key role in cell death in plants. *Molecules and cells*, *31*(1), pp.25-31.

Klämbt, H.D., 1962. Conversion in plants of benzoic acid to salicylic acid and its βd-glucoside. *Nature*, *196*(4853), p.491.

Kliebenstein, D.J., 2004. Secondary metabolites and plant/environment interactions: a view through *Arabidopsis thaliana* tinged glasses. *Plant, Cell & Environment*, *27*(6), pp.675-684.

Kleinboelting, N., Huep, G., Kloetgen, A., Viehoever, P. and Weisshaar, B., 2011. GABI-Kat SimpleSearch: new features of the *Arabidopsis thaliana* T-DNA mutant database. *Nucleic acids research*, *40*(D1), pp.D1211-D1215.

Komalavilas, P.A.D.M.I.N.I., Zhu, J.K. and Nothnagel, E.A., 1991. Arabinogalactan-proteins from the suspension culture medium and plasma membrane of rose cells. *Journal of Biological Chemistry*, *266*(24), pp.15956-15965.

Kombrink, A., Sánchez-Vallet, A. and Thomma, B.P., 2011. The role of chitin detection in plant–pathogen interactions. *Microbes and infection*, *13*(14-15), pp.1168-1176.

Kommedahl, T. and Windels, C.E., 1981. Root-, stalk-, and ear-infecting Fusarium species on corn in the USA. *Fusarium: diseases, biology and taxonomy*, *94*, p.103.

Knogge, W., 1996. Fungal infection of plants. *The Plant Cell*, *8*(10), p.1711

Krogh, A., Larsson, B., Von Heijne, G. and Sonnhammer, E.L., 2001. Predicting transmembrane protein topology with a hidden Markov model: application to complete genomes. *Journal of molecular biology*, *305*(3), pp.567-580.

Krysan, P.J., Young, J.C. and Sussman, M.R., 1999. T-DNA as an insertional mutagen in Arabidopsis. *The Plant Cell*, *11*(12), pp.2283-2290.

Kubo, K.I., Sakamoto, A., Kobayashi, A., Rybka, Z., Kanno, Y., Nakagawa, H., Nishino, T. and Takatsuji, H., 1998. Cys2/His2 zinc-finger protein family of petunia: evolution and general mechanism of target-sequence recognition. *Nucleic acids research*, *26*(2), pp.608-615.

Kwak, J.M., Mori, I.C., Pei, Z.M., Leonhardt, N., Torres, M.A., Dangl, J.L., Bloom, R.E., Bodde, S., Jones, J.D. and Schroeder, J.I., 2003. NADPH oxidase AtrbohD and AtrbohF genes function in ROS□ dependent ABA signaling in Arabidopsis. *The EMBO journal*, *22*(11), pp.2623-2633.

L

Laloi, C., Przybyla, D. and Apel, K., 2006. A genetic approach towards elucidating the biological activity of different reactive oxygen species in *Arabidopsis thaliana*. *Journal of Experimental Botany*, *57*(8), pp.1719-1724.

Lam, E., Kato, N. and Lawton, M., 2001. Programmed cell death, mitochondria and the plant hypersensitive response. *Nature*, *411*(6839), p.848.

Lamb, C. and Dixon, R.A., 1997. The oxidative burst in plant disease resistance. *Annual review of plant biology*, *48*(1), pp.251-275.

Lambeth, J.D., 2004. NOX enzymes and the biology of reactive oxygen. *Nature Reviews Immunology*, *4*(3), p.181.

Lardy, H.A. and Wellman, H., 1952. Oxidative phosphorylations: role of inorganic phosphate and acceptor systems in control of metabolic rates. *Journal of Biological Chemistry*, *195*(1), pp.215-224.

Larkindale, J. and Knight, M.R., 2002. Protection against heat stress-induced oxidative damage in Arabidopsis involves calcium, abscisic acid, ethylene, and salicylic acid. *Plant physiology*, *128*(2), pp.682-695.

Larkindale, J., Hall, J.D., Knight, M.R. and Vierling, E., 2005. Heat stress phenotypes of Arabidopsis mutants implicate multiple signaling pathways in the acquisition of thermotolerance. *Plant physiology*, *138*(2), pp.882-897.

Laxalt, A.M., Raho, N., ten Have, A. and Lamattina, L., 2007. Nitric oxide is critical for inducing phosphatidic acid accumulation in xylanase-elicited tomato cells. *Journal of Biological Chemistry*, *282*(29), pp.21160-21168.

LeBrasseur, N.D., MacIntosh, G.C., Pérez□Amador, M.A., Saitoh, M. and Green, P.J., 2002. Local and systemic wound□induction of RNase and nuclease activities in Arabidopsis: RNS1 as a marker for a JA□independent systemic signaling pathway. *The Plant Journal*, *29*(4), pp.393-403.

Leff, B., Ramankutty, N. and Foley, J.A., 2004. Geographic distribution of major crops across the world. *Global Biogeochemical Cycles*, *18*(1).

Leon, J., Lawton, M.A. and Raskin, I., 1995. Hydrogen peroxide stimulates salicylic acid biosynthesis in tobacco. *Plant Physiology*, *108*(4), pp.1673-1678.

Les Erickson, F., Holzberg, S., Calderon□Urrea, A., Handley, V., Axtell, M., Corr, C. and Baker, B., 1999. The helicase domain of the TMV replicase proteins induces the N□mediated defence response in tobacco. *The Plant Journal*, *18*(1), pp.67-75.

Lewis, M.W., Leslie, M.E., Fulcher, E.H., Darnielle, L., Healy, P.N., Youn, J.Y. and Liljegren, S.J., 2010. The SERK1 receptor□like kinase regulates organ separation in Arabidopsis flowers. *The Plant Journal*, *62*(5), pp.817-828.

Levine, A., Tenhaken, R., Dixon, R. and Lamb, C., 1994. H2O2 from the oxidative burst orchestrates the plant hypersensitive disease resistance response. *Cell*, *79*(4), pp.583-593.

Levine, A., Pennell, R.I., Alvarez, M.E., Palmer, R. and Lamb, C., 1996. Calcium-mediated apoptosis in a plant hypersensitive disease resistance response. *Current Biology*, *6*(4), pp.427-437.

Li, J., Wen, J., Lease, K.A., Doke, J.T., Tax, F.E. and Walker, J.C., 2002. BAK1, an Arabidopsis LRR receptor-like protein kinase, interacts with BRI1 and modulates brassinosteroid signaling. *Cell*, *110*(2), pp.213-222.

Liang, L., Lai, Z., Ma, W., Zhang, Y. and Xue, Y., 2002. AhSL28, a senescence-and phosphate starvation-induced S-like RNase gene in Antirrhinum. *Biochimica et Biophysica Acta (BBA)-Gene Structure and Expression*, *1579*(1), pp.64-71.

Lipshutz, R.J., Fodor, S.P., Gingeras, T.R. and Lockhart, D.J., 1999. High density synthetic oligonucleotide arrays. *Nature genetics*, *21*(1s), p.20.

Liszkay, A., Kenk, B. and Schopfer, P., 2003. Evidence for the involvement of cell wall peroxidase in the generation of hydroxyl radicals mediating extension growth. *Planta*, *217*(4), pp.658-667.

Liu, J., Elmore, J.M., Lin, Z.J.D. and Coaker, G., 2011. A receptor-like cytoplasmic kinase phosphorylates the host target RIN4, leading to the activation of a plant innate immune receptor. *Cell host & microbe*, *9*(2), pp.137-146.

Lo Presti, L., Lanver, D., Schweizer, G., Tanaka, S., Liang, L., Tollot, M., Zuccaro, A., Reissmann, S. and Kahmann, R., 2015. Fungal effectors and plant susceptibility. *Annual review of plant biology*, *66*, pp.513-545.

Lockhart, D.J., Dong, H., Byrne, M.C., Follettie, M.T., Gallo, M.V., Chee, M.S., Mittmann, M., Wang, C., Kobayashi, M., Norton, H. and Brown, E.L., 1996. Expression monitoring by hybridization to high-density oligonucleotide arrays. *Nature biotechnology*, *14*(13), p.1675.

Löffler, A., Glund, K. and Irie, M., 1993. Amino acid sequence of an intracellular, phosphate□starvation□induced ribonuclease from cultured tomato (Lycopersicon esculentum) cells. *European journal of biochemistry*, *214*(3), pp.627-633.

Lopez-Delgado, H., Dat, J.F., Foyer, C.H. and Scott, I.M., 1998. Induction of thermotolerance in potato microplants by acetylsalicylic acid and H2O2. *Journal of experimental botany*, *49*(321), pp.713-720.

Lorenzo, O., Piqueras, R., Sánchez-Serrano, J.J. and Solano, R., 2003. ETHYLENE RESPONSE FACTOR1 integrates signals from ethylene and jasmonate pathways in plant defense. *The Plant Cell*, *15*(1), pp.165-178.

M

Ma, Y., Szostkiewicz, I., Korte, A., Moes, D., Yang, Y., Christmann, A. and Grill, E., 2009. Regulators of PP2C phosphatase activity function as abscisic acid sensors. *Science*, *324*(5930), pp.1064-1068.

Malamy, J., Carr, J.P., Klessig, D.F. and Raskin, I., 1990. Salicylic acid: a likely endogenous signal in the resistance response of tobacco to viral infection. *Science*, *250*(4983), pp.1002-1004.

Mantelin, S., Peng, H.C., Li, B., Atamian, H.S., Takken, F.L. and Kaloshian, I., 2011. The receptor□ like kinase SlSERK1 is required for Mi□1□mediated resistance to potato aphids in tomato. *The Plant Journal*, *67*(3), pp.459-471.

May, M.J., Hammond-Kosack, K.E. and Jones, J.D., 1996. Involvement of reactive oxygen species, glutathione metabolism, and lipid peroxidation in the Cf-gene-dependent defense response of tomato cotyledons induced by race-specific elicitors of Cladosporium fulvum. *Plant Physiology*, *110*(4), pp.1367-1379.

Mandadi, K.K. and Scholthof, K.B.G., 2013. Plant immune responses against viruses: how does a virus cause disease?. *The plant cell*, pp.tpc-113.

Maruta, T., Inoue, T., Noshi, M., Tamoi, M., Yabuta, Y., Yoshimura, K., Ishikawa, T. and Shigeoka, S., 2012. Cytosolic ascorbate peroxidase 1 protects organelles against oxidative stress by wounding- and jasmonate-induced H2O2 in Arabidopsis plants. *Biochimica et Biophysica Acta (BBA)-General Subjects*, *1820*(12), pp.1901-1907.

Matile, P., 2012. *The lytic compartment of plant cells* (Vol. 1). Springer Science & Business Media.

Martínez, C., Pons, E., Prats, G. and León, J., 2004. Salicylic acid regulates flowering time and links defence responses and reproductive development. *The Plant Journal*, *37*(2), pp.209-217.

Mateo, A., Mühlenbock, P., Rustérucci, C., Chang, C.C.C., Miszalski, Z., Karpinska, B., Parker, J.E., Mullineaux, P.M. and Karpinski, S., 2004. LESION SIMULATING DISEASE 1 is required for acclimation to conditions that promote excess excitation energy. *Plant Physiology*, *136*(1), pp.2818-2830.

Mathews, S. and Sharrock, R.A., 1997. Phytochrome gene diversity. *Plant, cell & environment*, *20*(6), pp.666-671.

Mazzella, M.A., Alconada Magliano, T.M. and Casal, J.J., 1997. Dual effect of phytochrome A on hypocotyl growth under continuous red light. *Plant, Cell & Environment*, *20*(2), pp.261-267.

McClure, B.A., Haring, V., Ebert, P.R., Anderson, M.A., Simpson, R.J., Sakiyama, F. and Clarke, A.E., 1989. Style self-incompatibility gene products of Nicotlana alata are ribonucleases. *Nature*, *342*(6252), p.955.

McClure, B.A., Gray, J.E., Anderson, M.A. and Clarke, A.E., 1990. Self-incompatibility in Nicotiana alata involves degradation of pollen rRNA. *Nature*, *347*(6295), p.757.

McHale, J.S. and Dove, L.D., 1968. Ribonuclease activity in tomato leaves as related to development and senescence. *New Phytologist*, *67*(3), pp.505-515.

Mehdy, M.C., Sharma, Y.K., Sathasivan, K. and Bays, N.W., 1996. The role of activated oxygen species in plant disease resistance. *Physiologia Plantarum*, *98*(2), pp.365-374.

Métraux, J.P. and Raskin, I., 1993. Role of phenolics in plant disease resistance.

Metwally, A., Finkemeier, I., Georgi, M. and Dietz, K.J., 2003. Salicylic acid alleviates the cadmium toxicity in barley seedlings. *Plant physiology*, *132*(1), pp.272-281.

Michaelson, L.V., Napier, J.A., Molino, D. and Faure, J.D., 2016. Plant sphingolipids: Their importance in cellular organization and adaption. *Biochimica et Biophysica Acta (BBA)-Molecular and Cell Biology of Lipids*, *1861*(9), pp.1329-1335.

Millar, A.H., 2007. The plant mitochondrial proteome. In *Plant Proteomics* (pp. 226-246). Springer, Berlin, Heidelberg.

Mirete, S., Vázquez, C., Mulè, G., Jurado, M. and González-Jaén, M.T., 2004. Differentiation of Fusarium verticillioides from banana fruits by IGS and EF-1α sequence analyses. In *Molecular Diversity and PCR-detection of Toxigenic Fusarium Species and Ochratoxigenic Fungi* (pp. 515-523). Springer, Dordrecht.

Mittler, R. and Lam, E., 1995. Identification, characterization, and purification of a tobacco endonuclease activity induced upon hypersensitive response cell death. *The Plant Cell*, *7*(11), pp.1951-1962.

Mittler, R., Shulaev, V., Seskar, M. and Lam, E., 1996. Inhibition of Programmed Cell Death in Tobacco Plants during a Pathogen-Induced Hypersensitive Response at Low Oxygen Pressure. *The Plant Cell*, *8*(11), pp.1991-2001.

Mittler, R., Simon, L. and Lam, E., 1997. Pathogen-induced programmed cell death in tobacco. *Journal of Cell Science*, *110*(11), pp.1333-1344.

Mittler, R., Feng, X. and Cohen, M., 1998. Post-transcriptional suppression of cytosolic ascorbate peroxidase expression during pathogen-induced programmed cell death in tobacco. *The Plant Cell*, *10*(3), pp.461-473.

Mittler, R., Vanderauwera, S., Gollery, M. and Van Breusegem, F., 2004. Reactive oxygen gene network of plants. *Trends in plant science*, *9*(10), pp.490-498.

Møller, I.M., 2001. Plant mitochondria and oxidative stress: electron transport, NADPH turnover, and metabolism of reactive oxygen species. *Annual review of plant biology*, *52*(1), pp.561-591.

Montoya, T., Nomura, T., Farrar, K., Kaneta, T., Yokota, T. and Bishop, G.J., 2002. Cloning the tomato curl3 gene highlights the putative dual role of the leucine-rich repeat receptor kinase tBRI1/SR160 in plant steroid hormone and peptide hormone signaling. *The PlantCell*, *14*(12), pp.3163-3176.

Morel, J.B. and Dangl, J.L., 1997. The hypersensitive response and the induction of cell death in plants. *Cell death and differentiation*, *4*(8), p.671.

Mori, I.C., Pinontoan, R., Kawano, T. and Muto, S., 2001. Involvement of superoxide generation in salicylic acid-induced stomatal closure in Vicia faba. *Plant and Cell Physiology*, *42*(12), pp.1383-1388.

Moretti, A., Mulè, G., Susca, A., González-Jaén, M.T. and Logrieco, A., 2004. Toxin profile, fertility and AFLP analysis of Fusarium verticillioides from banana fruits. In *Molecular Diversity and PCR-detection of Toxigenic Fusarium Species and Ochratoxigenic Fungi* (pp. 601-609). Springer, Dordrecht.

Mosmann, T., 1983. Rapid colorimetric assay for cellular growth and survival: application to proliferation and cytotoxicity assays. *Journal of immunological methods*, *65*(1-2), pp.55-63.

Mühlenbock, P., Szechyńska-Hebda, M., Płaszczyca, M., Baudo, M., Mateo, A., Mullineaux, P.M., Parker, J.E., Karpińska, B. and Karpiński, S., 2008. Chloroplast signaling and LESION SIMULATING DISEASE1 regulate crosstalk between light acclimation and immunity in Arabidopsis. *The Plant Cell*, *20*(9), pp.2339-2356.

Munné-Bosch, S. and Peñuelas, J., 2004. Drought-induced oxidative stress in strawberry tree (Arbutus unedo L.) growing in Mediterranean field conditions. *Plant Science*, *166*(4), pp.1105-1110.

Munro, S. and Pelham, H.R., 1987. A C-terminal signal prevents secretion of luminal ER proteins. *Cell*, *48*(5), pp.899-907.

N

Napier, R.M., Fowke, L.C., Hawes, C.H.R.I.S., Lewis, M.I.K.E. and Pelham, H.R., 1992. Immunological evidence that plants use both HDEL and KDEL for targeting proteins to the endoplasmic reticulum. *Journal of Cell Science*, *102*(2), pp.261-271.

Nawrath, C. and Métraux, J.P., 1999. Salicylic acid induction–deficient mutants of Arabidopsis express PR-2 and PR-5 and accumulate high levels of camalexin after pathogen inoculation. *The Plant Cell*, *11*(8), pp.1393-1404.

Nawrath, C., Heck, S., Parinthawong, N. and Métraux, J.P., 2002. EDS5, an essential component of salicylic acid–dependent signaling for disease resistance in Arabidopsis, is a member of the MATE transporter family. *The Plant Cell*, *14*(1), pp.275-286.

Neill, S.J., Desikan, R., Clarke, A. and Hancock, J.T., 2002. Nitric oxide is a novel component of abscisic acid signaling in stomatal guard cells. *Plant physiology*, *128*(1), pp.13-16.

Nelson, P.E., Desjardins, A.E. and Plattner, R.D., 1993. Fumonisins, mycotoxins produced by Fusarium species: biology, chemistry, and significance. *Annual review of phytopathology*, *31*(1), pp.233-252.

Ndamukong, I., Abdallat, A.A., Thurow, C., Fode, B., Zander, M., Weigel, R. and Gatz, C., 2007. SA□inducible Arabidopsis glutaredoxin interacts with TGA factors and suppresses JA□responsive PDF1. 2 transcription. *The Plant Journal*, *50*(1), pp.128-139.

Ng, G., Seabolt, S., Zhang, C., Salimian, S., Watkins, T.A. and Lu, H., 2011. Genetic dissection of salicylic acid-mediated defense signaling networks in Arabidopsis. *Genetics*, *189*(3), pp.851-859.

Ni, M., Tepperman, J.M. and Quail, P.H., 1999. Binding of phytochrome B to its nuclear signalling partner PIF3 is reversibly induced by light. *Nature*, *400*(6746), p.781.

Niehl, A., Wyrsch, I., Boller, T. and Heinlein, M., 2016. Double□stranded RNA s induce a pattern□ triggered immune signaling pathway in plants. *New Phytologist*, *211*(3), pp.1008-1019.

Nielsen, H., 1999. SignalP, a server for predicting the presence and location of signal cleavage sites in amino acid sequences. *SCIENTIST-PHILADELPHIA-*, *13*, pp.8-8.

Niggeweg, R., Thurow, C., Kegler, C. and Gatz, C., 2000. Tobacco transcription factor TGA2. 2 is the main component of as-1-binding factor ASF-1 and is involved in salicylic acid-and auxin-inducible expression of as-1-containing target promoters. *Journal of Biological Chemistry*, *275*(26), pp.19897-19905.

Nürnberger, T., Abel, S., Jost, W. and Glund, K., 1990. Induction of an extracellular ribonuclease in cultured tomato cells upon phosphate starvation. *Plant Physiology*, *92*(4), pp.970-976.

O

Obeid, L.M., Linardic, C.M., Karolak, L.A. and Hannun, Y.A., 1993. Programmed cell death induced by ceramide. *Science*, *259*(5102), pp.1769-1771.

Ochsenbein, C., Przybyla, D., Danon, A., Landgraf, F., Göbel, C., Imboden, A., Feussner, I. and Apel, K., 2006. The role of EDS1 (enhanced disease susceptibility) during singlet oxygen□mediated stress responses of Arabidopsis. *The Plant Journal*, *47*(3), pp.445-456.

O'donnell, P.J., Schmelz, E.A., Moussatche, P., Lund, S.T., Jones, J.B. and Klee, H.J., 2003. Susceptible to intolerance–a range of hormonal actions in a susceptible Arabidopsis pathogen response. *The Plant Journal*, *33*(2), pp.245-257.

Oerke, E.C., 2006. Crop losses to pests. *The Journal of Agricultural Science*, *144*(1), pp.31-43.

Ogawa, D., Nakajima, N., Sano, T., Tamaoki, M., Aono, M., Kubo, A., Kanna, M., Ioki, M., Kamada, H. and Saji, H., 2005. Salicylic acid accumulation under O3 exposure is regulated by ethylene in tobacco plants. *Plant and cell physiology*, *46*(7), pp.1062-1072.

Oh, E., Yamaguchi, S., Hu, J., Yusuke, J., Jung, B., Paik, I., Lee, H.S., Sun, T.P., Kamiya, Y. and Choi, G., 2007. PIL5, a phytochrome-interacting bHLH protein, regulates gibberellin responsiveness by binding directly to the GAI and RGA promoters in Arabidopsis seeds. *The Plant Cell*, *19*(4), pp.1192-1208.

Ohnishi, N., Allakhverdiev, S.I., Takahashi, S., Higashi, S., Watanabe, M., Nishiyama, Y. and Murata, N., 2005. Two-step mechanism of photodamage to photosystem II: step 1 occurs at the oxygen-evolving complex and step 2 occurs at the photochemical reaction center. *Biochemistry*, *44*(23), pp.8494-8499.

Ondzighi, C.A., Christopher, D.A., Cho, E.J., Chang, S.C. and Staehelin, L.A., 2008. Arabidopsis protein disulfide isomerase-5 inhibits cysteine proteases during trafficking to vacuoles before programmed cell death of the endothelium in developing seeds. *The Plant Cell*, *20*(8), pp.2205-2220.

Orozco-Cardenas, M. and Ryan, C.A., 1999. Hydrogen peroxide is generated systemically in plant leaves by wounding and systemin via the octadecanoid pathway. *Proceedings of the National Academy of Sciences*, *96*(11), pp.6553-6557.

Orozco-Cárdenas, M.L., Narváez-Vásquez, J. and Ryan, C.A., 2001. Hydrogen peroxide acts as a second messenger for the induction of defense genes in tomato plants in response to wounding, systemin, and methyl jasmonate. *The Plant Cell*, *13*(1), pp.179-191.

Orozco-Cárdenas, M.L. and Ryan, C.A., 2002. Nitric oxide negatively modulates wound signaling in tomato plants. *Plant physiology*, *130*(1), pp.487-493.

Overmyer, K., Brosché, M. and Kangasjärvi, J., 2003. Reactive oxygen species and hormonal control of cell death. *Trends in plant science*, *8*(7), pp.335-342.

P

Park, S.Y., Fung, P., Nishimura, N., Jensen, D.R., Fujii, H., Zhao, Y., Lumba, S., Santiago, J., Rodrigues, A., Tsz-fung, F.C. and Alfred, S.E., 2009. Abscisic acid inhibits type 2C protein phosphatases via the PYR/PYL family of START proteins. *science*, *324*(5930), pp.1068-1071.

Parinov, S. and Sundaresan, V., 2000. Functional genomics in Arabidopsis: large-scale insertional mutagenesis complements the genome sequencing project. *Current Opinion in Biotechnology*, *11*(2), pp.157-161.

Parinov, S., Sevugan, M., Ye, D., Yang, W.C., Kumaran, M. and Sundaresan, V., 1999. Analysis of flanking sequences from dissociation insertion lines: a database for reverse genetics in Arabidopsis. *The Plant Cell*, *11*(12), pp.2263-2270.

Parker, J.E., Holub, E.B., Frost, L.N., Falk, A., Gunn, N.D. and Daniels, M.J., 1996. Characterization of eds1, a mutation in Arabidopsis suppressing resistance to Peronospora parasitica specified by several different RPP genes. *The Plant Cell*, *8*(11), pp.2033-2046.

Pearce, G., Strydom, D., Johnson, S. and Ryan, C.A., 1991. A polypeptide from tomato leaves induces wound-inducible proteinase inhibitor proteins. *Science*, *253*(5022), pp.895-897.

Peever, T.L. and Higgins, V.J., 1989. Electrolyte leakage, lipoxygenase, and lipid peroxidation induced in tomato leaf tissue by specific and nonspecific elicitors from Cladosporium fulvum. *Plant Physiology*, *90*(3), pp.867-875.

Pelham, H.R., 1990. The retention signal for soluble proteins of the endoplasmic reticulum. *Trends in biochemical sciences*, *15*(12), pp.483-486.

Pendle, A.F., Clark, G.P., Boon, R., Lewandowska, D., Lam, Y.W., Andersen, J., Mann, M., Lamond, A.I., Brown, J.W. and Shaw, P.J., 2005. Proteomic analysis of the Arabidopsis nucleolus suggests novel nucleolar functions. *Molecular biology of the cell*, *16*(1), pp.260-269.

Penninckx, I.A., Thomma, B.P., Buchala, A., Métraux, J.P. and Broekaert, W.F., 1998. Concomitant activation of jasmonate and ethylene response pathways is required for induction of a plant defensin gene in Arabidopsis. *The Plant Cell*, *10*(12), pp.2103-2113.

Petersen, T.N., Brunak, S., von Heijne, G. and Nielsen, H., 2011. SignalP 4.0: discriminating signal peptides from transmembrane regions. *Nature methods*, *8*(10), p.785.

Pfaffl, M.W., 2001. A new mathematical model for relative quantification in real-time RT–PCR. *Nucleic acids research*, *29*(9), pp.e45-e45.

Pfaffl, M.W., Horgan, G.W. and Dempfle, L., 2002. Relative expression software tool (REST©) for group-wise comparison and statistical analysis of relative expression results in real-time PCR. *Nucleic acids research*, *30*(9), pp.e36-e36.

Phillips, D.R., Horton, R.F. and Fletcher, R.A., 1969. Ribonuclease and chlorophyllase activities in senescing leaves. *Physiologia plantarum*, *22*(5), pp.1050-1054.

Prasad, T.K., Anderson, M.D., Martin, B.A. and Stewart, C.R., 1994. Evidence for chilling-induced oxidative stress in maize seedlings and a regulatory role for hydrogen peroxide. *The Plant Cell*, *6*(1), pp.65-74.

Pré, M., Atallah, M., Champion, A., De Vos, M., Pieterse, C.M. and Memelink, J., 2008. The AP2/ERF domain transcription factor ORA59 integrates jasmonic acid and ethylene signals in plant defense. *Plant physiology*, *147*(3), pp.1347-1357.

Proctor, R.H., Brown, D.W., Plattner, R.D. and Desjardins, A.E., 2003. Co-expression of 15 contiguous genes delineates a fumonisin biosynthetic gene cluster in Gibberella moniliformis. *Fungal Genetics and Biology*, *38*(2), pp.237-249.

Q

Qiao, H., Shen, Z., Huang, S.S.C., Schmitz, R.J., Urich, M.A., Briggs, S.P. and Ecker, J.R., 2012. Processing and subcellular trafficking of ER-tethered EIN2 control response to ethylene gas. *Science*, p.1224344.

Quail, P.H., 1991. Phytochrome: a light-activated molecular switch that regulates plant gene expression. *Annual review of genetics*, *25*(1), pp.389-409.

Quail, P.H., 1994. Phytochrome genes and their expression. In *Photomorphogenesis in plants* (pp. 71-104). Springer, Dordrecht.

Quail, P.H., Boylan, M.T., Parks, B.M., Short, T.W., Xu, Y. and Wagner, D., 1995. Phytochromes: photosensory perception and signal transduction. *Science*, *268*(5211), pp.675-680.

R

Rajjou, L., Belghazi, M., Huguet, R., Robin, C., Moreau, A., Job, C. and Job, D., 2006. Proteomic investigation of the effect of salicylic acid on Arabidopsis seed germination and establishment of early defense mechanisms. *Plant physiology*, *141*(3), pp.910-923.

Ran, F.A., Hsu, P.D., Wright, J., Agarwala, V., Scott, D.A. and Zhang, F., 2013. Genome engineering using the CRISPR-Cas9 system. *Nature protocols*, *8*(11), p.2281.

Rapoport, T.A., 1992. Transport of proteins across the endoplasmic reticulum membrane. *Science*, *258*(5084), pp.931-936.

Raskin, I. and Ladyman, J.A., 1988. Isolation and characterization of a barley mutant with abscisic-acid-insensitive stomata. *Planta*, *173*(1), pp.73-78.

Rate, D.N., Cuenca, J.V., Bowman, G.R., Guttman, D.S. and Greenberg, J.T., 1999. The gain-of-function Arabidopsis acd6 mutant reveals novel regulation and function of the salicylic acid signaling pathway in controlling cell death, defenses, and cell growth. *The Plant Cell*, *11*(9), pp.1695-1708.

Reichler, S.A., Torres, J., Rivera, A.L., Cintolesi, V.A., Clark, G. and Roux, S.J., 2009. Intersection of two signalling pathways: extracellular nucleotides regulate pollen germination and pollen tube growth via nitric oxide. *Journal of experimental botany*, *60*(7), pp.2129-2138.

Rennie, E.A., Ebert, B., Miles, G.P., Cahoon, R.E., Christiansen, K.M., Stonebloom, S., Khatab, H., Twell, D., Petzold, C.J., Adams, P.D. and Dupree, P., 2014. Identification of a sphingolipid α-glucuronosyltransferase that is essential for pollen function in Arabidopsis. *The Plant Cell*, *26*(8), pp.3314-3325.

Reumann, S., Quan, S., Aung, K., Yang, P., Manandhar-Shrestha, K., Holbrook, D., Linka, N., Switzenberg, R., Wilkerson, C.G., Weber, A.P. and Olsen, L.J., 2009. In-depth proteome analysis of Arabidopsis leaf peroxisomes combined with in vivo subcellular targeting verification indicates novel metabolic and regulatory functions of peroxisomes. *Plant Physiology*, *150*(1), pp.125-143.

Rietz, S., Stamm, A., Malonek, S., Wagner, S., Becker, D., Medina□Escobar, N., Vlot, A.C., Feys, B.J., Niefind, K. and Parker, J.E., 2011. Different roles of Enhanced Disease Susceptibility1 (EDS1) bound to and dissociated from Phytoalexin Deficient4 (PAD4) in Arabidopsis immunity. *New Phytologist*, *191*(1), pp.107-119.

Riley, R.T., Torres, O., Matute, J., Gregory, S.G., Ashley□Koch, A.E., Showker, J.L., Mitchell, T., Voss, K.A., Maddox, J.R. and Gelineau□van Waes, J.B., 2015. Evidence for fumonisin inhibition of ceramide synthase in humans consuming maize□based foods and living in high exposure communities in Guatemala. *Molecular nutrition & food research*, *59*(11), pp.2209-2224.

Rivas-San Vicente, M. and Plasencia, J., 2011. Salicylic acid beyond defence: its role in plant growth and development. *Journal of experimental botany*, *62*(10), pp.3321-3338.

Rizzini, L., Favory, J.J., Cloix, C., Faggionato, D., O'Hara, A., Kaiserli, E., Baumeister, R., Schäfer, E., Nagy, F., Jenkins, G.I. and Ulm, R., 2011. Perception of UV-B by the Arabidopsis UVR8 protein. *Science*, *332*(6025), pp.103-106.

Roberts, K., 1994. The plant extracellular matrix: in a new expansive mood. *Current opinion in cell biology*, *6*(5), pp.688-694.

Robson, C.A. and Vanlerberghe, G.C., 2002. Transgenic plant cells lacking mitochondrial alternative oxidase have increased susceptibility to mitochondria-dependent and-independent pathways of programmed cell death. *Plant Physiology*, *129*(4), pp.1908-1920.

Robson, P.R., Whitelam, G.C. and Smith, H., 1993. Selected components of the shade-avoidance syndrome are displayed in a normal manner in mutants of *Arabidopsis thaliana* and Brassica rapa deficient in phytochrome B. *Plant Physiology*, *102*(4), pp.1179-1184.

Roden, L.C. and Ingle, R.A., 2009. Lights, rhythms, infection: the role of light and the circadian clock in determining the outcome of plant–pathogen interactions. *The Plant Cell*, *21*(9), pp.2546-2552.

Roiz, L. and Shoseyov, O., 1995. Stigmatic RNase in self-compatible peach (Prunus persica). *International journal of plant sciences*, *156*(1), pp.37-41.

Roiz, L., Goren, R. and Shoseyov, O., 1995. Stigmatic RNase in calamondin (Citrus reticulata var. austera x Fortunella sp.). *Physiologia Plantarum*, *94*(4), pp.585-590.

Roiz, L., Ozeri, U., Goren, R. and Shoseyov, O., 2000. Characterization of Aspergillus niger B-1 RNase and its inhibitory effect on pollen germination and pollen tube growth in selected tree fruit. *Journal of the American Society for Horticultural Science*, *125*(1), pp.9-14.

Roiz, L., Smirnoff, P., Bar□Eli, M., Schwartz, B. and Shoseyov, O., 2006. ACTIBIND, an actin□binding fungal T2□RNase with antiangiogenic and anticarcinogenic characteristics. *Cancer*, *106*(10), pp.2295-2308.

Rojo, E., Sharma, V.K., Kovaleva, V., Raikhel, N.V. and Fletcher, J.C., 2002. CLV3 is localized to the extracellular space, where it activates the Arabidopsis CLAVATA stem cell signaling pathway. *The Plant Cell*, *14*(5), pp.969-977.

Ron, M. and Avni, A., 2004. The receptor for the fungal elicitor ethylene-inducing xylanase is a member of a resistance-like gene family in tomato. *The Plant Cell*, *16*(6), pp.1604-1615.

Rusaczonek, A., Czarnocka, W., Kacprzak, S., Witoń, D., Ślesak, I., Szechyńska-Hebda, M., Gawroński, P. and Karpiński, S., 2015. Role of phytochromes A and B in the regulation of cell death and acclimatory responses to UV stress in *Arabidopsis thaliana*. *Journal of experimental botany*, *66*(21), pp.6679-6695.

Rustérucci, C., Aviv, D.H., Holt, B.F., Dangl, J.L. and Parker, J.E., 2001. The disease resistance signaling components EDS1 and PAD4 are essential regulators of the cell death pathway controlled by LSD1 in Arabidopsis. *The Plant Cell*, *13*(10), pp.2211-2224.

Ryerson, D.E. and Heath, M.C., 1996. Cleavage of nuclear DNA into oligonucleosomal fragments during cell death induced by fungal infection or by abiotic treatments. *The Plant Cell*, *8*(3), pp.393-402.

S

Samson, F., Brunaud, V., Balzergue, S., Dubreucq, B., Lepiniec, L., Pelletier, G., Caboche, M. and Lecharny, A., 2002. FLAGdb/FST: a database of mapped flanking insertion sites (FSTs) of *Arabidopsis thaliana* T-DNA transformants. *Nucleic acids research*, *30*(1), pp.94-97.

Samson, M.R., Jongeneel, R. and Klis, F.M., 1984. Arabinogalactan protein in the extracellular space of Phaseolus vulgaris hypocotyls. *Phytochemistry*, *23*(3), pp.493-496.

Schön, M., Töller, A., Diezel, C., Roth, C., Westphal, L., Wiermer, M. and Somssich, I.E., 2013. Analyses of wrky18 wrky40 plants reveal critical roles of SA/EDS1 signaling and indole-glucosinolate biosynthesis for Golovinomyces orontii resistance and a loss-of resistance towards Pseudomonas syringae pv. tomato AvrRPS4. *Molecular Plant-Microbe Interactions*, *26*(7), pp.758-767.

Sato, M., Tsuda, K., Wang, L., Coller, J., Watanabe, Y., Glazebrook, J. and Katagiri, F., 2010. Network modeling reveals prevalent negative regulatory relationships between signaling sectors in Arabidopsis immune signaling. *PLoS pathogens*, *6*(7), p.e1001011.

Schena, M., Shalon, D., Davis, R.W. and Brown, P.O., 1995. Quantitative monitoring of gene expression patterns with a complementary DNA microarray. *Science*, *270*(5235), pp.467-470.

Scheer, J.M. and Ryan, C.A., 2002. The systemin receptor SR160 from Lycopersicon peruvianum is a member of the LRR receptor kinase family. *Proceedings of the National Academy of Sciences*, *99*(14), pp.9585-9590.

Schnable, P.S., Ware, D., Fulton, R.S., Stein, J.C., Wei, F., Pasternak, S., Liang, C., Zhang, J., Fulton, L., Graves, T.A. and Minx, P., 2009. The B73 maize genome: complexity, diversity, and dynamics. *science*, *326*(5956), pp.1112-1115.

Schön, M., Töller, A., Diezel, C., Roth, C., Westphal, L., Wiermer, M. and Somssich, I.E., 2013. Analyses of wrky18 wrky40 plants reveal critical roles of SA/EDS1 signaling and indole-glucosinolate biosynthesis for Golovinomyces orontii resistance and a loss-of resistance towards Pseudomonas syringae pv. tomato AvrRPS4. *Molecular Plant-Microbe Interactions*, *26*(7), pp.758-767.

Schroeder, J.I., Kwak, J.M. and Allen, G.J., 2001. Guard cell abscisic acid signalling and engineering drought hardiness in plants. *Nature*, *410*(6826), p.327.

Schwartz, B., Shoseyov, O., Melnikova, V.O., McCarty, M., Leslie, M., Roiz, L., Smirnoff, P., Hu, G.F., Lev, D. and Bar-Eli, M., 2007. ACTIBIND, a T2 RNase, competes with angiogenin and inhibits human melanoma growth, angiogenesis, and metastasis. *Cancer research*, *67*(11), pp.5258-5266.

Schweitzer, E., 1987. Coordinated release of ATP and ACh from cholinergic synaptosomes and its inhibition by calmodulin antagonists. *Journal of Neuroscience*, *7*(9), pp.2948-2956.Scott *et al*., 1994

Seifert, G.J. and Blaukopf, C., 2010. Irritable walls: the plant extracellular matrix and signaling. *Plant Physiology*, *153*(2), pp.467-478.

Serino, L., Reimmann, C., Baur, H., Beyeler, M., Visca, P. and Haas, D., 1995. Structural genes for salicylate biosynthesis from chorismate in Pseudomonas aeruginosa. *Molecular and General Genetics MGG*, *249*(2), pp.217-228.

Serpe, M.D. and Nothnagel, E.A., 1994. Effects of Yariv phenylglycosides onRosa cell suspensions: Evidence for the involvement of arabinogalactan-proteins in cell proliferation. *Planta*, *193*(4), pp.542-550.

Sessions, A., Burke, E., Presting, G., Aux, G., McElver, J., Patton, D., Dietrich, B., Ho, P., Bacwaden, J., Ko, C. and Clarke, J.D., 2002. A high-throughput Arabidopsis reverse genetics system. *The Plant Cell*, *14*(12), pp.2985-2994.

Shah, J., Tsui, F. and Klessig, D.F., 1997. Characterization of a salicylic acid-insensitive mutant (sai1) of *Arabidopsis thaliana*, identified in a selective screen utilizing the SA-inducible expression of the tms2 gene. *Molecular Plant-Microbe Interactions*, *10*(1), pp.69-78.

Shah, J. and Klessig, D.F., 1999. Salicylic acid: signal perception and transduction. InBiochemistry and Molecular Biology of Plant Hormones, vol. 33, eds K. Libbenga, M. Hall and PJJ Hooykaas.

Shan, Q., Wang, Y., Li, J., Zhang, Y., Chen, K., Liang, Z., Zhang, K., Liu, J., Xi, J.J., Qiu, J.L. and Gao, C., 2013. Targeted genome modification of crop plants using a CRISPR-Cas system. *Nature biotechnology*, *31*(8), p.686.

Shaw, B.P., Sahu, S.K. and Mishra, R.K., 2004. Heavy metal induced oxidative damage in terrestrial plants. In *Heavy metal stress in plants* (pp. 84-126). Springer, Berlin, Heidelberg.

Shi, L., Bielawski, J., Mu, J., Dong, H., Teng, C., Zhang, J., Yang, X., Tomishige, N., Hanada, K., Hannun, Y.A. and Zuo, J., 2007. Involvement of sphingoid bases in mediating reactive oxygen intermediate production and programmed cell death in Arabidopsis. *Cell research*, *17*(12), p.1030.

Shimizu-Sato, S., Huq, E., Tepperman, J.M. and Quail, P.H., 2002. A light-switchable gene promoter system. *Nature biotechnology*, *20*(10), p.1041.

Showalter, A.M., 1993. Structure and function of plant cell wall proteins. *The Plant Cell*, *5*(1), p.9.

Simon□Plas, F., Elmayan, T. and Blein, J.P., 2002. The plasma membrane oxidase NtrbohD is responsible for AOS production in elicited tobacco cells. *The Plant Journal*, *31*(2), pp.137-147.

Small, I.M., Flett, B.C., Marasas, W.F.O., McLeod, A., Stander, M.A. and Viljoen, A., 2012. Resistance in maize inbred lines to Fusarium verticillioides and fumonisin accumulation in South Africa. *Plant disease*, *96*(6), pp.881-888.

Smith, H., 1995. Physiological and ecological function within the phytochrome family. *Annual review of plant biology*, *46*(1), pp.289-315.

Smith, H. and Whitelam, G.C., 1997. The shade avoidance syndrome: multiple responses mediated by multiple phytochromes. *Plant, Cell & Environment*, *20*(6), pp.840-844.

Smith, E.R., Merrill, A.H., Obeid, L.M. and Hannun, Y.A., 2000. Effects of sphingosine and other sphingolipids on protein kinase C. *Methods in enzymology*, *312*, pp.361-373.

Smith, S.J., Kroon, J.T., Simon, W.J., Slabas, A.R. and Chivasa, S., 2015. A novel function for Arabidopsis CYCLASE1 in programmed cell death revealed by isobaric tags for relative and absolute quantitation (iTRAQ) analysis of extracellular matrix proteins. *Molecular & Cellular Proteomics*, *14*(6), pp.1556-1568.

Solano, R., Stepanova, A., Chao, Q. and Ecker, J.R., 1998. Nuclear events in ethylene signaling: a transcriptional cascade mediated by ETHYLENE-INSENSITIVE3 and ETHYLENE-RESPONSE-FACTOR1. *Genes & development*, *12*(23), pp.3703-3714.

Song, C.J., Steinebrunner, I., Wang, X., Stout, S.C. and Roux, S.J., 2006. Extracellular ATP induces the accumulation of superoxide via NADPH oxidases in Arabidopsis. *Plant physiology*, *140*(4), pp.1222-1232.

Sonnhammer, E.L., Von Heijne, G. and Krogh, A., 1998, July. A hidden Markov model for predicting transmembrane helices in protein sequences. In *Ismb* (Vol. 6, pp. 175-182).

Sperling, P., Franke, S., Lüthje, S. and Heinz, E., 2005. Are glucocerebrosides the predominant sphingolipids in plant plasma membranes? *Plant Physiology and Biochemistry*, *43*(12), pp.1031-1038.

Speulman, E., Metz, P.L., van Arkel, G., te Lintel Hekkert, B., Stiekema, W.J. and Pereira, A., 1999. A two-component enhancer-inhibitor transposon mutagenesis system for functional analysis of the Arabidopsis genome. *The Plant Cell*, *11*(10), pp.1853-1866.

Spiegel, S. and Merrill Jr, A.H., 1996. Sphingolipid metabolism and cell growth regulation. *The FASEB Journal*, *10*(12), pp.1388-1397.

Spoel, S.H. and Dong, X., 2012. How do plants achieve immunity? Defence without specialized immune cells. *Nature reviews immunology*, *12*(2), p.89.

Srivastava, M.K. and Dwivedi, U.N., 2000. Delayed ripening of banana fruit by salicylic acid. *Plant Science*, *158*(1-2), pp.87-96.

Staswick, P.E., Su, W. and Howell, S.H., 1992. Methyl jasmonate inhibition of root growth and induction of a leaf protein are decreased in an *Arabidopsis thaliana* mutant. *Proceedings of the National Academy of Sciences*, *89*(15), pp.6837-6840.

Stewart, A.J., Chapman, W., Jenkins, G.I., Graham, I., Martin, T. and Crozier, A., 2001. The effect of nitrogen and phosphorus deficiency on flavonol accumulation in plant tissues. *Plant, Cell & Environment*, *24*(11), pp.1189-1197.

Stintzi, A., Heitz, T., Prasad, V., Wiedemann-Merdinoglu, S., Kauffmann, S., Geoffroy, P., Legrand, M. and Fritig, B., 1993. Plant 'pathogenesis-related'proteins and their role in defense against pathogens. *Biochimie*, *75*(8), pp.687-706.

Stone, J.M., Heard, J.E., Asai, T. and Ausubel, F.M., 2000. Simulation of fungal-mediated cell death by fumonisin B1 and selection of fumonisin B1–resistant (fbr) Arabidopsis mutants. *The Plant Cell*, *12*(10), pp.1811-1822.

Stone, J.M., Liang, X., Nekl, E.R. and Stiers, J.J., 2005. Arabidopsis AtSPL14, a plant□specific SBP□domain transcription factor, participates in plant development and sensitivity to fumonisin B1. *The Plant Journal*, *41*(5), pp.744-754.

Sun, W., Dunning, F.M., Pfund, C., Weingarten, R. and Bent, A.F., 2006. Within-species flagellin polymorphism in Xanthomonas campestris pv campestris and its impact on elicitation of Arabidopsis FLAGELLIN SENSING2–dependent defenses. *The Plant Cell*, *18*(3), pp.764-779.

Sun, G., Wang, S., Hu, X., Su, J., Huang, T., Yu, J., Tang, L., Gao, W. and Wang, J.S., 2007. Fumonisin B1 contamination of home-grown corn in high-risk areas for esophageal and liver cancer in China. *Food additives and contaminants*, *24*(2), pp.181-185.

Sussman, M.R., Amasino, R.M., Young, J.C., Krysan, P.J. and Austin-Phillips, S., 2000. The Arabidopsis knockout facility at the University of Wisconsin–Madison. *Plant Physiology*, *124*(4), pp.1465-1467.

T

Takatsuji, H., Mori, M., Benfey, P.N., Ren, L. and Chua, N.H., 1992. Characterization of a zinc finger DNA□binding protein expressed specifically in Petunia petals and seedlings. *The EMBO journal*, *11*(1), pp.241-249.

Takatsuji, H., 1999. Zinc-finger proteins: the classical zinc finger emerges in contemporary plant science. *Plant molecular biology*, *39*(6), pp.1073-1078.

Takayama, S. and Isogai, A., 2005. Self-incompatibility in plants. *Annu. Rev. Plant Biol.*, *56*, pp.467-489.

Tampakaki, A.P., Fadouloglou, V.E., Gazi, A.D., Panopoulos, N.J. and Kokkinidis, M., 2004. Conserved features of type III secretion. *Cellular microbiology*, *6*(9), pp.805-816.

Tanaka, K., Gilroy, S., Jones, A.M. and Stacey, G., 2010. Extracellular ATP signaling in plants. *Trends in cell biology*, *20*(10), pp.601-608.

Tanaka, K., Choi, J., Cao, Y. and Stacey, G., 2014. Extracellular ATP acts as a damage-associated molecular pattern (DAMP) signal in plants. *Frontiers in plant science*, *5*, p.446.

Tang, W., Brady, S.R., Sun, Y., Muday, G.K. and Roux, S.J., 2003. Extracellular ATP inhibits root gravitropism at concentrations that inhibit polar auxin transport. *Plant Physiology*, *131*(1), pp.147-154.

Taylor, C.B. and Green, P.J., 1991. Genes with homology to fungal and S-gene RNases are expressed in *Arabidopsis thaliana*. *Plant Physiology*, *96*(3), pp.980-984.

Taylor, C.B., Bariola, P.A., Raines, R.T. and Green, P.J., 1993. RNS2: a senescence-associated RNase of Arabidopsis that diverged from the S-RNases before speciation. *Proceedings of the National Academy of Sciences*, *90*(11), pp.5118-5122.

Teng, C., Dong, H., Shi, L., Deng, Y., Mu, J., Zhang, J., Yang, X. and Zuo, J., 2008. Serine palmitoyltransferase, a key enzyme for de novo synthesis of sphingolipids, is essential for male gametophyte development in Arabidopsis. *Plant physiology*, *146*(3), pp.1322-1332.

Testerink, C. and Munnik, T., 2005. Phosphatidic acid: a multifunctional stress signaling lipid in plants. *Trends in plant science*, *10*(8), pp.368-375.

Thilmony, R., Underwood, W. and He, S.Y., 2006. Genome□wide transcriptional analysis of the *Arabidopsis thaliana* interaction with the plant pathogen Pseudomonas syringae pv. tomato DC3000 and the human pathogen Escherichia coli O157: H7. *The Plant Journal*, *46*(1), pp.34-53.

Thines, B., Katsir, L., Melotto, M., Niu, Y., Mandaokar, A., Liu, G., Nomura, K., He, S.Y., Howe, G.A. and Browse, J., 2007. JAZ repressor proteins are targets of the SCF COI1 complex during jasmonate signalling. *Nature*, *448*(7154), p.661.

Thomma, B.P., Nürnberger, T. and Joosten, M.H., 2011. Of PAMPs and effectors: the blurred PTI-ETI dichotomy. *The plant cell*, *23*(1), pp.4-15.

Thompson, D.M. and Parker, R., 2009. The RNase Rny1p cleaves tRNAs and promotes cell death during oxidative stress in Saccharomyces cerevisiae. *The Journal of cell biology*, *185*(1), pp.43-50.

Tian, T., Liu, Y., Yan, H., You, Q., Yi, X., Du, Z., Xu, W. and Su, Z., 2017. agriGO v2. 0: a GO analysis toolkit for the agricultural community, 2017 update. *Nucleic acids research*, *45*(W1), pp.W122-W129.

Tissier, A.F., Marillonnet, S., Klimyuk, V., Patel, K., Torres, M.A., Murphy, G. and Jones, J.D., 1999. Multiple independent defective suppressor-mutator transposon insertions in Arabidopsis: a tool for functional genomics. *The Plant Cell*, *11*(10), pp.1841-1852.

Toledo-Ortiz, G., Huq, E. and Quail, P.H., 2003. The Arabidopsis basic/helix-loop-helix transcription factor family. *The Plant Cell*, *15*(8), pp.1749-1770.

Tolleson, W.H., Dooley, K.L., Sheldon, W.G., Thurman, J.D., Bucci, T.J. and Howard, P.C., 1996. The mycotoxin fumonisin induces apoptosis in cultured human cells and in livers and kidneys of rats. In *Fumonisins in Food* (pp. 237-250). Springer, Boston, MA.

Tonón, C., Terrile, M.C., Iglesias, M.J., Lamattina, L. and Casalongué, C., 2010. Extracellular ATP, nitric oxide and superoxide act coordinately to regulate hypocotyl growth in etiolated Arabidopsis seedlings. *Journal of plant physiology*, *167*(7), pp.540-546.

Torres, M.A. and Dangl, J.L., 2005. Functions of the respiratory burst oxidase in biotic interactions, abiotic stress and development. *Current opinion in plant biology*, *8*(4), pp.397-403.

Torres, M.A., Onouchi, H., Hamada, S., Machida, C., Hammond□Kosack, K.E. and Jones, J.D., 1998. Six *Arabidopsis thaliana* homologues of the human respiratory burst oxidase (gp91phox). *The Plant Journal*, *14*(3), pp.365-370.

Torres, M.A., Dangl, J.L. and Jones, J.D., 2002. Arabidopsis gp91phox homologues AtrbohD and AtrbohF are required for accumulation of reactive oxygen intermediates in the plant defense response. *Proceedings of the National Academy of Sciences*, *99*(1), pp.517-522. Torres *et al*., 2005

Torres, M.A., Jones, J.D. and Dangl, J.L., 2006. Reactive oxygen species signaling in response to pathogens. *Plant physiology*, *141*(2), pp.373-378.

Torres, O., Matute, J., Gelineau-van Waes, J., Maddox, J.R., Gregory, S.G., Ashley-Koch, A.E., Showker, J.L., Voss, K.A. and Riley, R.T., 2014. Human health implications from co-exposure to aflatoxins and fumonisins in maize-based foods in Latin America: Guatemala as a case study. *World Mycotoxin Journal*, *8*(2), pp.143-159.

Traw, M.B. and Bergelson, J., 2003. Interactive effects of jasmonic acid, salicylic acid, and gibberellin on induction of trichomes in Arabidopsis. *Plant Physiology*, *133*(3), pp.1367-1375.

Tripathi, D., Zhang, T., Koo, A.J., Stacey, G. and Tanaka, K., 2018. Extracellular ATP acts on jasmonate signaling to reinforce plant defense. *Plant physiology*, *176*(1), pp.511-523.

Tripathi, D. and Tanaka, K., 2018. A crosstalk between extracellular ATP and jasmonate signaling pathways for plant defense. *Plant signaling & behavior*, *13*(5), pp.511-523.

U

Ueda, J. and Kato, J., 1982. Inhibition of cytokinin□induced plant growth by jasmonic acid and its methyl ester. *Physiologia Plantarum*, *54*(3), pp.249-252.

Usadel, B., Poree, F., Nagel, A., Lohse, M., CZEDIK□EYSENBERG, A.N.G.E.L.I.K.A. and Stitt, M., 2009. A guide to using MapMan to visualize and compare Omics data in plants: a case study in the crop species, Maize. *Plant, cell & environment*, *32*(9), pp.1211-1229.

V

Vailleau, F., Daniel, X., Tronchet, M., Montillet, J.L., Triantaphylides, C. and Roby, D., 2002. A R2R3-MYB gene, AtMYB30, acts as a positive regulator of the hypersensitive cell death program in

plants in response to pathogen attack. *Proceedings of the National Academy of Sciences*, *99*(15), pp.10179-10184.

Van Baarlen, P., Woltering, E.J., Staats, M. and van Kan, J.A., 2007. Histochemical and genetic analysis of host and non□host interactions of Arabidopsis with three Botrytis species: an important role for cell death control. *Molecular Plant Pathology*, *8*(1), pp.41-54.

Van der Does, D., Leon-Reyes, A., Koornneef, A., Van Verk, M.C., Rodenburg, N., Pauwels, L., Goossens, A., Körbes, A.P., Memelink, J., Ritsema, T. and Van Wees, S.C., 2013. Salicylic acid suppresses jasmonic acid signaling downstream of SCFCOI1-JAZ by targeting GCC promoter motifs via transcription factor ORA59. *The Plant Cell*, *25*(2), pp.744-761.

Van Doorn, W.G., 2011. Classes of programmed cell death in plants, compared to those in animals. *Journal of experimental botany*, *62*(14), pp.4749-4761.

Van Gijsegem, F., Gough, C., Zischek, C., Niqueux, E., Arlat, M., Genin, S., Barberis, P., German, S., Castello, P. and Boucher, C., 1995. The hrp gene locus of Pseudomonas solanacearum, which controls the production of a type III secretion system, encodes eight proteins related to components of the bacterial flagellar biogenesis complex. *Molecular microbiology*, *15*(6), pp.1095-1114.

Van Loon, L.C. and Van Strien, E.A., 1999. The families of pathogenesis-related proteins, their activities, and comparative analysis of PR-1 type proteins. *Physiological and molecular plant pathology*, *55*(2), pp.85-97.

Van Loon, L.C., Rep, M. and Pieterse, C.M., 2006. Significance of inducible defense-related proteins in infected plants. *Annu. Rev. Phytopathol.*, *44*, pp.135-162.

Van Verk, M.C., Bol, J.F. and Linthorst, H.J., 2011. WRKY transcription factors involved in activation of SA biosynthesis genes. *BMC plant biology*, *11*(1), p.89.

Van Wees, S.C., Chang, H.S., Zhu, T. and Glazebrook, J., 2003. Characterization of the early response of Arabidopsis to Alternaria brassicicola infection using expression profiling. *Plant physiology*, *132*(2), pp.606-617.

Venable, M.E., Lee, J.Y., Smyth, M.J., Bielawska, A. and Obeid, L.M., 1995. Role of ceramide in cellular senescence. *Journal of Biological Chemistry*, *270*(51), pp.30701-30708.

Vogelmann, K., Drechsel, G., Bergler, J., Subert, C., Philippar, K., Soll, J., Engelmann, J.C., Engelsdorf, T., Voll, L.M. and Hoth, S., 2012. Early senescence and cell death in Arabidopsis saul1 mutants involves the PAD4-dependent salicylic acid pathway. *Plant physiology*, *159*(4), pp.1477-1487.

Von Heijne, G., 1990. The signal peptide. *Journal of Membrane Biology*, *115*(3), pp.195-201.

Vos, I.A., Verhage, A., Schuurink, R.C., Watt, L.G., Pieterse, C.M. and Van Wees, S., 2013. Onset of herbivore-induced resistance in systemic tissue primed for jasmonate-dependent defenses is activated by abscisic acid. *Frontiers in Plant Science*, *4*, p.539.

Voss, K.A., Riley, R.T., Norred, W.P., Bacon, C.W., Meredith, F.I., Howard, P.C., Plattner, R.D., Collins, T.F., Hansen, D.K. and Porter, J.K., 2001. An overview of rodent toxicities: liver and kidney effects of fumonisins and Fusarium moniliforme. *Environmental Health Perspectives*, *109*(suppl 2), pp.259-266.

Vranová, E., Inzé, D. and Van Breusegem, F., 2002. Signal transduction during oxidative stress. *Journal of experimental botany*, *53*(372), pp.1227-1236.

W

Wada, M. and Iino, M. eds., 2005. *Light sensing in plants*. Tokyo, Japan: Springer.

Walker, J.E., Saraste, M., Runswick, M.J. and Gay, N.J., 1982. Distantly related sequences in the alpha□and beta□subunits of ATP synthase, myosin, kinases and other ATP□requiring enzymes and a common nucleotide binding fold. *The EMBO journal*, *1*(8), pp.945-951.

Wang, E., Norred, W.P., Bacon, C.W., Riley, R.T. and Merrill, A.H., 1991. Inhibition of sphingolipid biosynthesis by fumonisins. Implications for diseases associated with Fusarium moniliforme. *Journal of Biological Chemistry*, *266*(22), pp.14486-14490.

Wang, H., Li, J., Bostock, R.M. and Gilchrist, D.G., 1996. Apoptosis: a functional paradigm for programmed plant cell death induced by a host-selective phytotoxin and invoked during development. *The Plant Cell*, *8*(3), pp.375-391.

Wang, W., Jones, C., Ciacci-Zanella, J., Holt, T., Gilchrist, D.G. and Dickman, M.B., 1996. Fumonisins and Alternaria alternata lycopersici toxins: sphinganine analog mycotoxins induce apoptosis in monkey kidney cells. *Proceedings of the National Academy of Sciences*, *93*(8), pp.3461-3465.

Weerasinghe, R.R., Swanson, S.J., Okada, S.F., Garrett, M.B., Kim, S.Y., Stacey, G., Boucher, R.C., Gilroy, S. and Jones, A.M., 2009. Touch induces ATP release in Arabidopsis roots that is modulated by the heterotrimeric G-protein complex. *Febs Letters*, *583*(15), pp.2521-2526.

Welinder, K.G., 1992. Superfamily of plant, fungal and bacterial peroxidases. *Current Opinion in Structural Biology*, *2*(3), pp.388-393.

Whitelam, G.C. and Smith, H., 1991. Retention of phytochrome-mediated shade avoidance responses in phytochrome-deficient mutants of Arabidopsis, cucumber and tomato. *Journal of Plant Physiology*, *139*(1), pp.119-125.

Who.int. (2019). *WHO | Climate change and human health - risks and responses. Summary.*. [online] Available at: https://www.who.int/globalchange/climate/summary/en/index5.html [Accessed 28 Mar. 2019].

Wiermer, M., Feys, B.J. and Parker, J.E., 2005. Plant immunity: the EDS1 regulatory node. *Current opinion in plant biology*, *8*(4), pp.383-389.

Wildermuth, M.C., Dewdney, J., Wu, G. and Ausubel, F.M., 2001. Isochorismate synthase is required to synthesize salicylic acid for plant defence. *Nature*, *414*(6863), p.562.

Williams, L.D., Glenn, A.E., Bacon, C.W., Smith, M.A. and Riley, R.T., 2006. Fumonisin production and bioavailability to maize seedlings grown from seeds inoculated with Fusarium verticillioides and grown in natural soils. *Journal of agricultural and food chemistry*, *54*(15), pp.5694-5700.

Williams, L.D., Glenn, A.E., Zimeri, A.M., Bacon, C.W., Smith, M.A. and Riley, R.T., 2007. Fumonisin disruption of ceramide biosynthesis in maize roots and the effects on plant development and Fusarium verticillioides-induced seedling disease. *Journal of agricultural and food chemistry*, *55*(8), pp.2937-2946.

Woestyn, S., Allaoui, A., Wattiau, P. and Cornelis, G.R., 1994. YscN, the putative energizer of the Yersinia Yop secretion machinery. *Journal of bacteriology*, *176*(6), pp.1561-1569.

World Health Organisation, 2018

World Population Prospects, *United Nations*. 2018

Wu, W.S., Wu, J.R. and Hu, C.T., 2008. Signal cross talks for sustained MAPK activation and cell migration: the potential role of reactive oxygen species. *Cancer and Metastasis Reviews*, *27*(2), pp.303-314.

Wu, S.J., Liu, Y.S. and Wu, J.Y., 2008. The signaling role of extracellular ATP and its dependence on Ca2+ flux in elicitation of Salvia miltiorrhiza hairy root cultures. *Plant and cell physiology*, *49*(4), pp.617-624.

Wu, Y., Zhang, D., Chu, J.Y., Boyle, P., Wang, Y., Brindle, I.D., De Luca, V. and Després, C., 2012. The Arabidopsis NPR1 protein is a receptor for the plant defense hormone salicylic acid. *Cell reports*, *1*(6), pp.639-647.

X

Xia, Y., Suzuki, H., Borevitz, J., Blount, J., Guo, Z., Patel, K., Dixon, R.A. and Lamb, C., 2004. An extracellular aspartic protease functions in Arabidopsis disease resistance signaling. *The EMBO journal*, *23*(4), pp.980-988.

Xie, D.X., Feys, B.F., James, S., Nieto-Rostro, M. and Turner, J.G., 1998. COI1: an Arabidopsis gene required for jasmonate-regulated defense and fertility. *Science*, *280*(5366), pp.1091-1094.

Xie, Z., Zhang, Z.L., Hanzlik, S., Cook, E. and Shen, Q.J., 2007. Salicylic acid inhibits gibberellin-induced alpha-amylase expression and seed germination via a pathway involving an abscisic-acid-inducible WRKY gene. *Plant molecular biology*, *64*(3), pp.293-303.

Xu, X., Chen, C., Fan, B. and Chen, Z., 2006. Physical and functional interactions between pathogen-induced Arabidopsis WRKY18, WRKY40, and WRKY60 transcription factors. *The Plant Cell*, *18*(5), pp.1310-1326.

Y

Yaeno, T. and Iba, K., 2008. BAH1/NLA, a RING-type ubiquitin E3 ligase, regulates the accumulation of salicylic acid and immune responses to Pseudomonas syringae DC3000. *Plant physiology*, *148*(2), pp.1032-1041.

Yamaguchi-Shinozaki, K. and Shinozaki, K., 2006. Transcriptional regulatory networks in cellular responses and tolerance to dehydration and cold stresses. *Annu. Rev. Plant Biol.*, *57*, pp.781-803.

Yamane, H., Sugawara, J., Suzuki, Y., Shimamura, E. and Takahashi, N., 1980. Syntheses of jasmonic acid related compounds and their structure-activity relationships on the growth of rice seedings. *Agricultural and Biological Chemistry*, *44*(12), pp.2857-2864.

Yang, Z.M., Wang, J., Wang, S.H. and Xu, L.L., 2003. Salicylic acid-induced aluminum tolerance by modulation of citrate efflux from roots of Cassia tora L. *Planta*, *217*(1), pp.168-174.

Ye, J., Coulouris, G., Zaretskaya, I., Cutcutache, I., Rozen, S. and Madden, T.L., 2012. Primer-BLAST: a tool to design target-specific primers for polymerase chain reaction. *BMC bioinformatics*, *13*(1), p.134.

Yoo, H.S., Norred, W.P., Showker, J. and Riley, R.T., 1996. Elevated sphingoid bases and complex sphingolipid depletion as contributing factors in fumonisin-induced cytotoxicity. *Toxicology and applied pharmacology*, *138*(2), pp.211-218.

Yoshida, R., Hobo, T., Ichimura, K., Mizoguchi, T., Takahashi, F., Aronso, J., Ecker, J.R. and Shinozaki, K., 2002. ABA-activated SnRK2 protein kinase is required for dehydration stress signaling in Arabidopsis. *Plant and Cell Physiology*, *43*(12), pp.1473-1483.

Yoshida, R., Umezawa, T., Mizoguchi, T., Takahashi, S., Takahashi, F. and Shinozaki, K., 2006a. The regulatory domain of SRK2E/OST1/SnRK2. 6 interacts with ABI1 and integrates abscisic acid (ABA) and osmotic stress signals controlling stomatal closure in Arabidopsis. *Journal of Biological Chemistry*, *281*(8), pp.5310-5318.

Yoshida, T., Nishimura, N., Kitahata, N., Kuromori, T., Ito, T., Asami, T., Shinozaki, K. and Hirayama, T., 2006b. ABA-hypersensitive germination3 encodes a protein phosphatase 2C (AtPP2CA) that strongly regulates abscisic acid signaling during germination among Arabidopsis protein phosphatase 2Cs. *Plant physiology*, *140*(1), pp.115-126.

Yoshida, Y., Sano, R., Wada, T., Takabayashi, J. and Okada, K., 2009. Jasmonic acid control of GLABRA3 links inducible defense and trichome patterning in Arabidopsis. *Development*, *136*(6), pp.1039-1048.

Yoshioka, H., Numata, N., Nakajima, K., Katou, S., Kawakita, K., Rowland, O., Jones, J.D. and Doke, N., 2003. Nicotiana benthamiana gp91phox homologs NbrbohA and NbrbohB participate in H2O2 accumulation and resistance to Phytophthora infestans. *The Plant Cell*, *15*(3), pp.706-718.

Yoshizawa, T., Yamashita, A. and Luo, Y., 1994. Fumonisin occurrence in corn from high-and low-risk areas for human esophageal cancer in China. *Appl. Environ. Microbiol.*, *60*(5), pp.1626-1629.

Z

Zander, M., Thurow, C. and Gatz, C., 2014. TGA transcription factors activate the salicylic acid-suppressible branch of the ethylene-induced defense program by regulating ORA59 expression. *Plant physiology*, *165*(4), pp.1671-1683.

Zarei, A., Körbes, A.P., Younessi, P., Montiel, G., Champion, A. and Memelink, J., 2011. Two GCC boxes and AP2/ERF-domain transcription factor ORA59 in jasmonate/ethylene-mediated activation of the PDF1. 2 promoter in Arabidopsis. *Plant molecular biology*, *75*(4-5), pp.321-331.

Zeier, J., Pink, B., Mueller, M.J. and Berger, S., 2004. Light conditions influence specific defence responses in incompatible plant–pathogen interactions: uncoupling systemic resistance from salicylic acid and PR-1 accumulation. *Planta*, *219*(4), pp.673-683.

Zelenikhin, P.V., Kolpakov, A.I., Cherepnev, G.V. and Ilinskaya, O.I., 2005. Induction of apoptosis in tumor cells by binase. *Molecular Biology*, *39*(3), pp.404-409.

Zhang, Y., Fan, W., Kinkema, M., Li, X. and Dong, X., 1999. Interaction of NPR1 with basic leucine zipper protein transcription factors that bind sequences required for salicylic acid induction of the PR-1 gene. *Proceedings of the National Academy of Sciences*, *96*(11), pp.6523-6528.

Zhang, Y., Xu, S., Ding, P., Wang, D., Cheng, Y.T., He, J., Gao, M., Xu, F., Li, Y., Zhu, Z. and Li, X., 2010. Control of salicylic acid synthesis and systemic acquired resistance by two members of a plant-specific family of transcription factors. *Proceedings of the National Academy of Sciences*, *107*(42), pp.18220-18225.

Zhang, X. and Cai, X., 2011. Climate change impacts on global agricultural land availability. *Environmental Research Letters*, *6*(1), p.014014.

Zhao, Y., Thilmony, R., Bender, C.L., Schaller, A., He, S.Y. and Howe, G.A., 2003. Virulence systems of Pseudomonas syringae pv. tomato promote bacterial speck disease in tomato by targeting the jasmonate signaling pathway. *The Plant Journal*, *36*(4), pp.485-499.

Zhu, Y., Tepperman, J.M., Fairchild, C.D. and Quail, P.H., 2000. Phytochrome B binds with greater apparent affinity than phytochrome A to the basic helix–loop–helix factor PIF3 in a reaction requiring the PAS domain of PIF3. *Proceedings of the National Academy of Sciences*, *97*(24), pp.13419-13424.

Zhu, S., Jeong, R.D., Venugopal, S.C., Lapchyk, L., Navarre, D., Kachroo, A. and Kachroo, P., 2011. SAG101 forms a ternary complex with EDS1 and PAD4 and is required for resistance signaling against turnip crinkle virus. *PLoS pathogens*, *7*(11), p.e1002318.

Zipfel, C., Kunze, G., Chinchilla, D., Caniard, A., Jones, J.D., Boller, T. and Felix, G., 2006. Perception of the bacterial PAMP EF-Tu by the receptor EFR restricts Agrobacterium-mediated transformation. *Cell*, *125*(4), pp.749-760.

Zipfel, C., 2009. Early molecular events in PAMP-triggered immunity. *Current opinion in plant biology*, *12*(4), pp.414-420

Zimmermann, P., Hirsch-Hoffmann, M., Hennig, L. and Gruissem, W., 2004. GENEVESTIGATOR. Arabidopsis microarray database and analysis toolbox. *Plant physiology*, *136*(1), pp.2621-2632.

Appendix

Appendix 1. Protein analysis using isobaric tags for relative and absolute quantitation (iTRAQ)

Arabidopsis proteins up-regulated in response to light.

AGI	*Gene symbol*	*F-C*	*P-value*	*Protein score*	*%Cov (95)*	*Peptides (95%)*
At5g19100	-	2.18	3.49E-04	26.42	36.06	18
AT3G08030	-	2.12	5.77E-06	19.38	33.97	12
AT5G44130	FLA13	1.92	5.03E-06	7.49	16.6	4
AT1G15270	-	1.85	3.09E-05	3.04	32.81	2
AT5G64120	PRX71	1.84	1.74E-05	22.4	52.13	29
At5g44390	BBE25	1.81	1.01E-04	40.97	38.56	24
AT1G49750	-	1.79	2.45E-04	8.2	9.312	6
At2g13820	XYP2	1.75	0.015	2.39	7.692	2
At5g07030	-	1.69	2.29E-05	13.22	21.76	9
AT4G12910	SCPL20	1.65	2.50E-06	21.71	24.95	13
AT1G44130	-	1.65	1.45E-04	9.16	16.3	11
AT1G71380	CEL3	1.65	1.56E-05	17.24	35.33	22
AT1G03870	FLA9	1.63	5.24E-05	2.27	12.96	7
At2g47010	-	1.62	1.14E-06	9.3	10.14	5
AT3g54400	-	1.61	0.002	11.94	24.24	10
AT3G45970	EXPL1	1.6	9.06E-06	12.4	30.19	14
At3g18280	TED4	1.59	0.004	2.07	6.667	2
AT3G45600	TET3	1.57	4.40E-05	6.09	12.28	6
AT5G06870	PGIP2	1.55	0.001	27.47	53.33	41
AT5G64570	BXL4 XYL4	1.53	1.07E-06	24.55	20.66	18
AT3G61820	-	1.51	0.001	16.91	25.47	16
AT5G05340	PRX52	1.48	0.007	22.87	58.95	118
At1g64760	ZET	1.43	5.15E-07	21.66	28.9	17
AT2G46880	PAP14	1.43	1.06E-05	7.64	9.476	4
AT5G08380	AGAL1	1.43	1.02E-06	14.46	24.15	10
AT4G38400	EXPL2 EXLA2	1.42	6.63E-05	9.22	18.11	5
AT3G54200	-	1.39	1.74E-04	6	17.45	3
At4g38670	-	1.39	0.001	2.94	14.95	3
At1g28600	-	1.38	0.022	6	13.23	4
AT5G42240	SCPL42	1.37	2.17E-05	12.68	17.12	9
AT5G06720	PRX53	1.37	7.12E-06	12.17	21.49	26
AT1G41830	SKS6	1.37	0.036	13.07	25.46	19
AT4G34870	ROC5 CYP1 EXGT-A1 EXT	1.35	0.001	7.48	29.65	5
AT2G06850	XTH4	1.35	4.82E-06	14.01	27.7	9
AT3G52400	SYP122	1.34	8.85E-05	5.68	9.091	3
AT1G32960	SBT3.3	1.32	4.52E-05	23.54	20.59	14
At2g27260	-	1.32	2.00E-04	3.33	9.465	3
At5g20950	-	1.31	0.003	29.43	29.49	22
AT3G52470	-	1.29	6.43E-05	10.83	31.73	8
AT1G09070	SRC2	1.29	0.019	4.01	6.79	2
AT3G49220	PME34	1.29	7.34E-05	3.33	3.679	2
AT4G19410	PAE7	1.28	1.05E-04	5.75	17.39	8
AT2G45470	FLA8	1.27	6.19E-05	19.48	29.05	15
At4g20840	ATBBE21	1.27	0.001	13.2	18.18	13
At5g58090	-	1.26	8.84E-06	14.43	31.03	15

AT1G61250	SC3	1.26	3.65E-04	7.36	17.3	4
AT4G34260	FUC95A	1.26	6.10E-05	36.06	22.06	18
AT3G12145	FLR1	1.26	8.96E-05	6.11	12.62	4
AT4G23820	-	1.25	0.002	4.74	12.16	3
At4g22010	SKS4	1.25	0.032	9.24	14.6	7
At4g20830	-	1.24	0.021	43.33	38.07	30
At5g55180	-	1.23	2.61E-03	23.89	39.78	32
AT4G38740	ROC1	1.23	0.01	2.75	12.79	2
AT2G17760	-	1.23	0.002	5.21	8.967	7
AT5G46700	TRN2 TET1	1.23	0.018	4.72	9.665	3
At5g67130	-	1.21	1.86E-03	12.02	19.95	9
AT1G78060	-	1.21	0.002	29.73	23.08	23
AT3G55430	-	1.21	0.007	8.17	18.04	6
At3g25290	-	1.2	0.004	9.57	19.34	10
AT4G31840	ENODL15	1.2	4.98E-04	7.52	34.46	9
AT5G62890	-	1.2	4.61E-06	2.09	4.323	3
At2g01080	-	1.19	0.032	2.05	13.42	2
AT4G12700	FLA2	1.19	0.02	7.68	13.4	4
AT1G68560	XYL1	1.18	6.76E-04	50.87	32.02	49
AT5g66920	SKS17	1.18	0.003	23.32	34.43	24
AT2G28470	BGAL8	1.18	2.17E-04	18.72	19.25	11
AT1G49740	-	1.17	2.56E-04	8.62	18.66	6
At5g23400	-	1.17	0.003	11.62	13.58	7
AT2G44610	RAB6	1.17	0.007	2.21	12.02	2
AT5G11540	GULLO3	1.17	0.003	14.86	17.44	10
AT4G20860	BBE22	1.17	8.83E-04	27.09	26.98	20
At5g18470	-	1.16	7.07E-04	9.46	15.74	5
AT5G06320	NHL3	1.16	0.012	7.42	21.65	6
AT1G21670	-	1.16	9.82E-04	10.48	11.1	6
AT2G34070	TBL37	1.16	0.019	5.2	8.312	3
At2g38010	-	1.15	0.012	19.5	15.72	10
At1g65240	-	1.14	0.018	7	11.68	4
At4g34480	-	1.14	2.40E-03	26.95	52.18	73
AT4G25240	SKS1	1.14	4.08E-04	10.55	15.45	12
AT4G25720	ATQC QCT	1.13	0.02	5.5	12.19	3
At3g16530	-	1.13	0.037	3.07	27.9	11
At4g31140	-	1.12	2.46E-03	14.62	22.52	11
AT1G26630	ELF5A FBR12	1.12	0.022	2.57	12.58	2
AT4G11600	ATGPX6	1.11	0.03	4.12	6.466	2
At4g39830	-	1.11	0.021	15.62	19.93	10
AT3G13750	BGAL1	1.11	0.019	7.98	7.438	5
AT5G48450	SKS3 SKU5	1.1	0.037	4.05	7.085	6
AT1G78380	GSTU19	1.1	0.017	2.61	9.589	2
At5g07830	GUS2	1.08	0.025	9.85	11.97	5
At4g24780	PLL19	1.08	0.04	4.41	7.353	4
AT1G74020	SS2	1.08	0.044	12.47	30.15	10
At1g65240	A39	1.04	0.029	7.68	12.21	4

Arabidopsis proteins down-regulated in response to light

AGI	*Gene symbol*	*Fold change*	*T-test (2-tailed)*	*Protein score*	*%Cov (95)*	*Peptides (95%)*
At5g07360	-	-1.07	8.93E-04	17.67	18.82	14
AT5G13690	CYL1 NAGLU	-1.08	1.86E-03	24.4	18.98	16
AT2G28100	FUC1	-1.09	0.016	24.48	26.09	12

At3g26380	APSE	-1.09	0.018	14.38	12.36	8
AT4g34180	CYCLASE1	-1.1	0.015	16.65	37.65	14
At5g14450	-	-1.11	9.67E-04	28.86	38.56	22
AT2G44450	BGLU15	-1.11	6.49E-03	35.89	52.17	44
At1g05840	-	-1.12	3.45E-04	12.4	19.18	8
AT1G74000	SSL11	-1.12	0.015	9.36	24.32	7
AT4G24890	PAP24	-1.12	0.014	6.57	6.829	5
AT1G30600	SBT2.1	-1.12	0.017	11.99	10.22	9
At5g44400	BBE26	-1.13	0.015	11.62	15.08	9
AT4G09320	NDK1	-1.13	0.047	4.67	16.78	2
At3g23450	-	-1.13	0.037	6.28	50.88	3
AT3G20390	RIDA	-1.14	5.30E-04	7.17	27.27	6
AT1G56070	LOS1	-1.14	0.024	21.9	18.51	15
AT3G07320	-	-1.14	0.013	9.05	14.57	7
AT3G56370	-	-1.14	3.71E-03	17.95	12.03	12
At3g14920	-	-1.15	5.02E-06	13.11	11.99	12
AT4G15940	-	-1.15	0.024	4.4	15.32	3
AT4G16500	-	-1.15	8.45E-03	6.62	42.74	5
AT4G36360	BGAL3	-1.16	5.18E-03	12.62	11.8	8
AT3G04120	GAPC1	-1.16	0.023	17.26	36.69	10
AT3G02740	-	-1.16	7.00E-03	6	8.713	3
At2g05790	-	-1.16	6.48E-03	16.43	21.61	11
At5g57330	-	-1.16	5.82E-03	13.65	25.32	8
AT4G37800	XTH7	-1.16	9.46E-03	8.17	20.14	5
At1g28580	-	-1.17	8.71E-03	4.76	11.79	4
AT5G10560	BXL6	-1.17	6.78E-04	18.53	14.52	10
AT4G03210	XTH9	-1.18	0.026	4.98	16.9	4
AT1G28290	AGP31	-1.18	0.034	3.49	8.078	3
At5g21105	-	-1.18	0.029	25.17	30.44	35
At5g16450	-	-1.19	0.017	4.97	24.1	4
AT2G37130	PER21	-1.19	1.73E-03	5.45	13.15	4
AT5G56030	HSP90.2	-1.2	1.69E-03	11.77	8.727	7
AT5G17820	PER57	-1.2	4.67E-03	9.17	22.04	5
AT2G17420	NTR2	-1.2	0.016	4.03	7.311	2
AT5G17920	ATMS1	-1.21	0.032	7.83	9.673	4
AT1G11840	GLX1	-1.21	2.45E-03	10.2	18.01	5
AT3G24480	-	-1.21	6.77E-03	13.61	14.17	15
At5g13980	-	-1.22	4.15E-04	32.76	22.36	19
At5g25090	ENODL13	-1.23	2.01E-04	10	31.72	6
At3g52500	-	-1.23	7.81E-04	15.5	25.8	10
At1g79720	-	-1.23	1.02E-03	4.57	8.471	3
AT5G55480	SVL1	-1.23	8.08E-06	16.18	11.75	11
AT5G42980	TRX3	-1.25	1.80E-03	6.23	34.75	5
AT1G13750	PAP1	-1.25	0.028	2.02	2.121	3
At5g21090	-	-1.25	4.29E-03	6.79	24.31	7
AT5G56600	PRF3	-1.26	0.028	4.16	25.19	3
AT3G10850	GLX2.2 GLY2	-1.27	0.02	2.97	13.95	4
AT4G12420	SKU5	-1.27	1.20E-04	20.69	21.81	15
AT3G18490	ASPG1	-1.27	2.95E-04	21.28	34.2	35
At5g44380	-	-1.29	2.00E-03	2.8	6.285	5
AT5G08260	SCPL35	-1.3	3.44E-03	6.07	13.12	4
AT1G19570	DHAR5	-1.32	9.35E-04	5.44	18.31	4
AT2G17120	LYM2	-1.33	1.25E-04	5.12	8.571	5
AT1G07890	APX1	-1.33	0.023	3.54	9.6	2
AT2G22420	PER17	-1.33	3.86E-05	7.66	14.89	4

At5g19120	-	-1.35	1.68E-05	24.04	44.56	32
At4g29360	-	-1.35	1.86E-05	12.23	13.48	10
At5g41870	-	-1.37	3.72E-05	15.12	24.05	12
AT5G15650	RGP2	-1.37	3.30E-03	12.7	22.5	7
At2g19780	-	-1.38	7.63E-03	7.75	12.69	6
At4g22730	-	-1.38	1.77E-03	3.83	3.343	2
AT3G45010	SCPL48	-1.39	2.12E-05	11.4	19.41	11
AT1G03230	-	-1.39	2.01E+04	12	22.58	11
AT3G62060	PAE6	-1.41	0.012	3.46	10.98	5
AT3G12700	NANA	-1.44	9.02E-05	10.97	15.18	7
At1g03820	-	-1.45	5.87E-03	2.34	7.658	2
AT4G25900	-	-1.48	2.24E-05	21.63	43.4	17
AT1G19730	ATH4	-1.48	0.034	4	17.65	2
AT1G68290	BFN2 ENDO2	-1.63	1.57E-04	6.49	21.38	6
AT2G47320	-	-1.64	1.23E-06	11.02	31.3	10
AT3G15356	FLA1	-1.7	1.56E-05	16.63	42.8	35
AT1G03220	-	-1.9	4.91E-05	19.28	35.33	23
AT2G16060	AHB1 GLB1 HB1	-1.92	4.22E-06	8.43	35.62	5
AT3G22800	-	-1.98	2.40E-07	6.02	8.723	4
At2g02990	RNS1	-2.1	5.14E-05	7.81	27.39	8
At4g12880	ENODL19	-2.14	5.12E-06	4.2	13.48	2
AT1G78850	MBL1	-2.35	1.50E-07	29.37	38.55	46

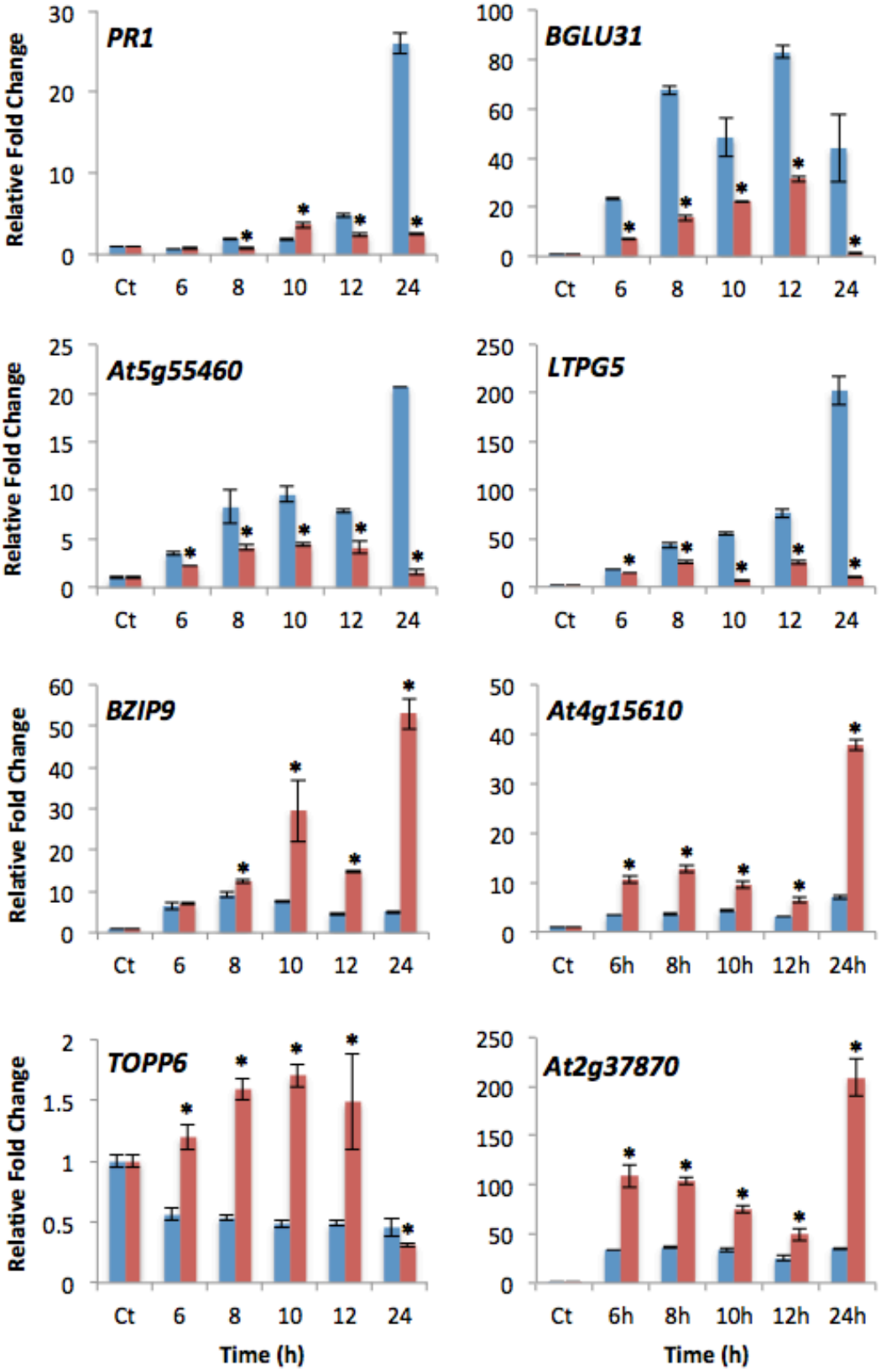
PR1
BGLU31
At5g55460
LTPG5
BZIP9
At4g15610
TOPP6
At2g37870
Relative Fold Change
Ct
6
8
10
12
24
6h
8h
10h
12h
24h
Time (h)

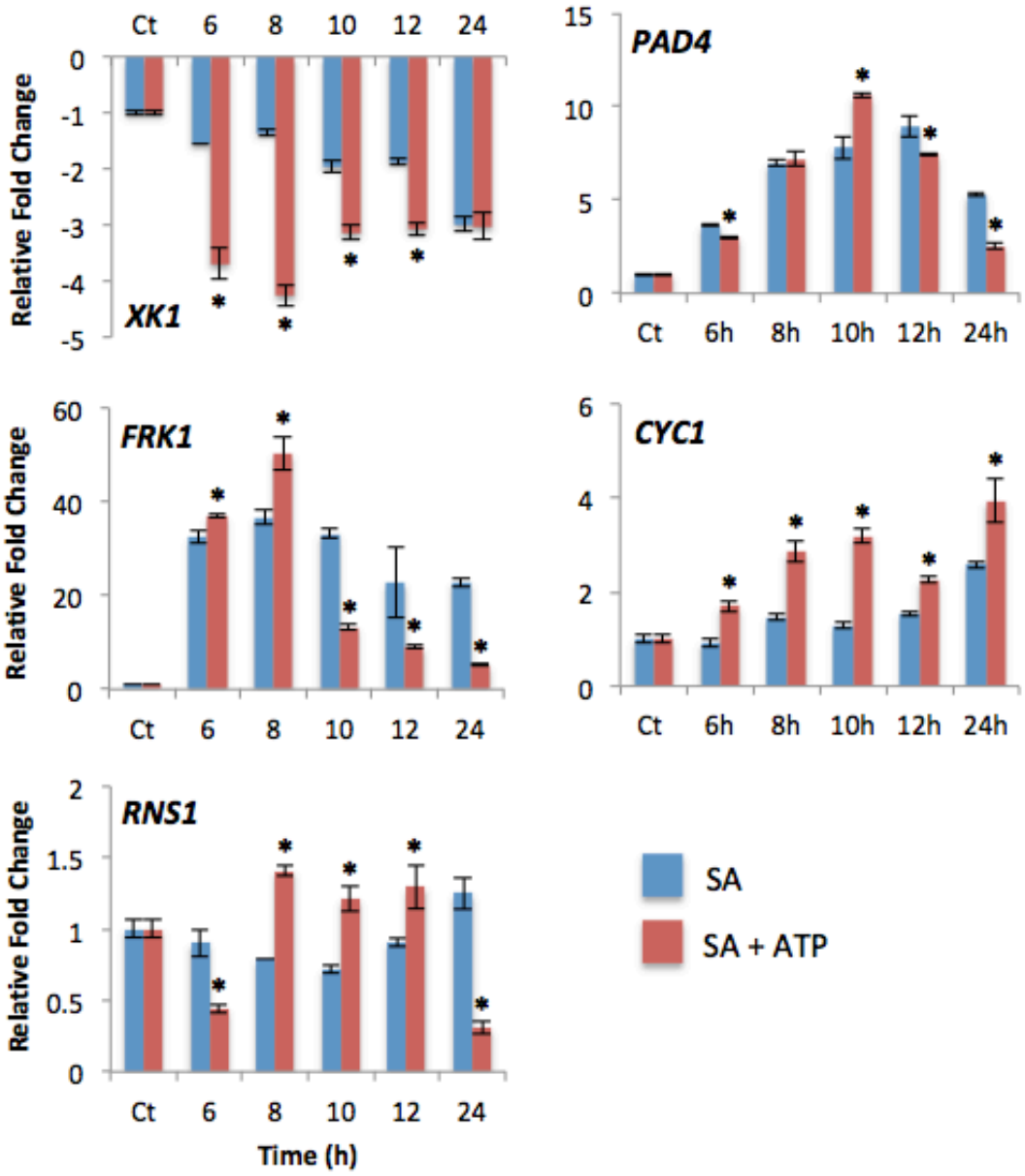

Appendix 2. SA+/- ATP response for candidates from the microarray. Cell cultures were exposed to one of the following treatments: 200µM SA, 200µM SA alongside 400µM ATP. RNA was harvested from the cells for qRT-PCR at 6, 8, 10, 12, and 24 h after treatment, including a 6 h water treated control. Bars represent mean ± SD (n = 3). An asterisk indicates a significant difference between light and dark ($p \leq 0.05$). *ACTIN2* and *EIF4A* were used as constitutive reference control genes.

AGI	Gene name	Forward Primer	Reverse Primer	Function
At1g49900	*EARP1*	CGTTGCGCCTCCTAGGTTTA	TGTCGAACCTCCAAAAGCTC	Genotyping
At2g02990	*RNS1*	CGTTTTGGGAGCACGAATGG	ATCCCGGCTTTGGTTAGAGC	qRT-PCR
At2g02990	*RNS1*	CGTTTTGGGAGCACGAATGG	AGATCGATGCCGGTTCAAGAG	Genotyping
At2g02990	*RNS1*	ATTGGGCCGTTACGTGCATA	TGATCAAACACAATGATGCTAGAAG	Genotyping
At1g68290	*BFN2*	CGTCTCAGACTAGGTTGGATGA	ACGATCAGCCCCAAAAGACACA	qRT-PCR
AT3G23450	-	CGGCGGTATCGGTAAAGGT	CCAATTCCACCGCCAACA	qRT-PCR
At4g34180	*CYCLASE1*	AACCCGTTAACCGGCGACCC	GCATTCAGAGGCTTCTCCTTGGTGC	qRT-PCR
At5g20950	*BGCL1*	GTATGGCGCCACCATTTTCC	CAAACTGCAATACACGGGGC	qRT-PCR
At5g44130	*FLA13*	TAGCACCAACAGACAACGCT	CACCAACGTCTCGACCTGAA	qRT-PCR
At1g03870	*FLA9*	CACCGGCCAAACAAACCAAA	AACTGCGAGAGGACGTTGTT	qRT-PCR
At5g64120	*PRX71*	TTCTCACTCAAGGAACAGGC	AGCATTCGAAGCCAAAGAAAC	qRT-PCR
At5g07030	_	GAAAGTCGTCGATTTACCGC	GTTGAGTCGAAGATGGT	qRT-PCR
At5g05240	*PRX52*	GCTTTGTCAACGGATGCGAC	CTGAATTGCGGTTTGGAGCC	qRT-PCR
At1g30600	*SBT2.1*	GGTCATCGCCTTGGAAATGC	CATCTTGAGCCGCCTGATCT	qRT-PCR
At5g58090	_	CATCTCCACCGACAACGTCA	TGGATGTTCCTAACGCAGG	qRT-PCR
At5g20230	*BCB*	CTTCGCGGAGGACTACGATG	AAATTCGAGCTCGTCGCCTA	qRT-PCR
At1g61820	*BGLU46*	CCCCAAAATCGCAATGATGC	GCACCTTCATACTGGAAAGCAG	qRT-PCR
At5g24540	*BGLU31*	GCTGAATGTTTAGCATGTCGTTGA	GCTGAATGTTTAGCATGTCGTTGA	qRT-PCR
At3g22600	*LTPG5*	CTCTCCTGCAGAATCACCAAA	CCGCGGAGAAGAAGGCAATA	qRT-PCR
At1g20030	_	GTCCTTCTCCCAACACCAGC	CCGGAACTTGGACTTGTCGT	qRT-PCR
At5g25460	*DGR2*	TGGTGTTGAGGAAGATCCAGC	ACGGTGGGATCAAAACTCCA	qRT-PCR
At3g45160	_	GCTCATGTTTGGCTGCAAGG	GCTGCTTCTTGGGTGCTCTA	qRT-PCR
At3g61820	_	TGACGACTGTGAAGGTTCCG	TCCCCATAGTTCCGGCAAAC	qRT-PCR
At2g18790	*PHYB*	GCAGCAAGCTTTAGCAGTCC	TGGTCGCTTTCGAGGTACAG	qRT-PCR
At2g18790	*PHYB*	AGGATTCAACAGCTCCTGGC	ACGACCATTCTGAATTCTGTGC	Genotyping
At5g60300	*DORN1*	ACCACTCACCTTACGCTTGG	GGCTGGACTCTCTGACTGC	qRT-PCR
At5g60300	*DORN1*	TGCAGTTGACAAATGCTTCAG	TTCAGACATCTCATGCTCACG	Genotyping
At2g29470	*GSTU3*	AAGTCACAATGATAGGGCTCAGG	ACTTCTTCGATTGCAACGTCA	qRT-PCR
At5g59490	_	CCGGTCTTAAGGCGGTAGGT	CGGGTCCGGTTTAAGGTTTTC	qRT-PCR
At2g14620	*XTH10*	TCCTACCCACGTTAACACCT	TGGAAGAAAAAGAAGCTCCAGA	qRT-PCR
At4g15610	_	CGGTGATGGTGGGGATAGTG	TAGGAGGAGGAGGACAACCG	qRT-PCR
At2g14610	*PR1*	TTAGCCTGGGGTAGCGGTGAC	GTTACACCTCACTTTGGCACATC	qRT-PCR
At5g55460	_	GTGGCCTGACAACAATCCCT	TGCAGGACAAGTTCGAGTGA	qRT-PCR
At5g24800	*BZIP9*	CACAGTCCTCAATCTGCGAG	CTCGGCATCTTCGTCATCAGA	qRT-PCR
At5g43380	*TOPP6*	TGTTAGAGGTTGGGGGCCTA	TCATCGCACCTGCATTGTCA	qRT-PCR
At1g74710	*ICS1/ SID2*	ACAAGGTTGTTCTTGCTCGT	TGCTAGCCAAGCAATGGGAT	qRT-PCR
At1g74710	*ICS1/ SID2*	TCTTCTCAGTTTCTGGGCTCAA	TGAGAACCCCTTATCCCCCA	Genotyping
At2g45210	*SAUR36*	GGCCAACGTCTCAAGCAAAG	CAGTCGCCGTCTTTTTGACC	qRT-PCR
At2g26640	*KCS11*	TCGACCACGTCCTGTCTACT	GTAAGTCGATTCCCCGAGCC	qRT-PCR
At2g21370	*XK1*	ATGATTGCATTGTCTGCACCG	ACCATTTGTCATCCAGGCGG	qRT-PCR
At3g09940	_	TACGCGGCGAGAGAGTTTAG	GCTCAAAAGGAGGCACTGGT	qRT-PCR
At3g18780	*ACTN2*	GTGGTCGTACAACCGGTATTG	TCACGTCCAGACCGGTCAAG	qRT-PCR
At3g18780	*ACTIN2*	GGATCGGTGGTTCCATTCTTCG	AGAGTTTGTCACACACAAGTGCA	Genotyping
At3g13920	*EIF4A*	ATGAGAGGATGCTCTGCCTTCG	GCAGAGCAAACACAGCAAGGG	qRT-PCR

Appendix 3. Primer sequences